NUEVOS PROCESOS DE CURADO CLICK CON TIOLES Y SU APLICACIÓN A LA PREPARACIÓN DE MATERIALES BASADOS EN EUGENOL

Dailyn Guzmán Meneses

UNIVERSITAT ROVIRA I VIRGILI
NUEVOS PROCESOS DE CURADO CLICK CON TIOLES Y SU APLICACIÓN A LA PREPARACIÓN DE MATERIALES BASADOS EN EUGENOL
Dailyn Guzmán Meneses

UNIVERSITAT ROVIRA I VIRGILI
NUEVOS PROCESOS DE CURADO CLICK CON TIOLES Y SU APLICACIÓN A LA PREPARACIÓN DE MATERIALES BASADOS EN EUGENOL
Dailyn Guzmán Meneses

DAILYN GUZMÁN MENESES

Nuevos procesos de curado *click* con tioles y su aplicación a la preparación de materiales basados en eugenol

Tesis doctoral

Supervisada por: Prof. Àngels Serra i Albet

y Prof. Xavier Ramis Juan

Departament de

Química Analítica i Química Orgànica

UNIVERSITAT ROVIRA I VIRGILI

Tarragona, España

2017

UNIVERSITAT ROVIRA I VIRGILI
NUEVOS PROCESOS DE CURADO CLICK CON TIOLES Y SU APLICACIÓN A LA PREPARACIÓN DE MATERIALES BASADOS EN EUGENOL
Dailyn Guzmán Meneses

DEPARTAMENT DE QUÍMICA ANALÍTICA i QUÍMICA ORGÀNICA

Campus Sescelades

Carrer Marcel·lí Domingo s/n

43007 Tarragona

Àngels Serra i Albet del departamento de Química Analítica i Química Orgànica de la Universitat Rovira i Virgili y Xavier Ramis Juan del Departament de Màquines i Motors Tèrmics de la ETSEIB de la Universidad Politècnica de Catalunya,

CERTIFiCAN:

Que la tesis doctoral titulada: "Nuevos procesos de curado *click* con tioles y su aplicación a la preparación de materiales basados en eugenol", presentada por Dailyn Guzmán Meneses con el fin de obtener el título de Doctor, se ha llevado ha llevado a cabo bajo su supervisión en el Departament de Química Analítica y Química Orgànica de la Universitat Rovira i Virgili y todos los resultados recogidos en esta tesis se obtuvieron a partir de experimentos realizados por la mencionada estudiante de doctorado.

Tarragona, 22 de junio, 2017

Prof. Àngels Serra i Albet

Prof. Xavier Ramis Juan

UNIVERSITAT ROVIRA I VIRGILI
NUEVOS PROCESOS DE CURADO CLICK CON TIOLES Y SU APLICACIÓN A LA PREPARACIÓN DE MATERIALES BASADOS EN EUGENOL
Dailyn Guzmán Meneses

Quiero empezar agradeciendo a Dios por permitirme recorrer este camino, que no ha sido fácil pero que ha valido la pena cada esfuerzo.

A mis directores de tesis: Angels Serra y Xavier Ramis. Gracias por la oportunidad que me han brindado, por toda la paciencia que han tenido conmigo, pero sobre todo gracias por todo el apoyo a nivel profesional y personal.

A Xavier Fernández, gracias por toda tu colaboración durante la tesis. Eres una de las piezas importantes de este trabajo.

A Silvia de la Flor, gracias por tu colaboración, por dedicarme tu tiempo, por tus palabras de aliento.

A Francesc Ferrando, gracias por tu disposición de ayudarme siempre.

A Ramón Guerrero, gracias por tu dedicación, siempre dispuesto a ayudar a los demás. Gracias por todo ese optimismo que siempre reflejas.

A mis profes María Dolores y María Jesús, sin su apoyo hoy esto no sería posible. Gracias por creer en mí.

Quiero agradecer también a Marta, Toni y Sergio Castillo por siempre ser tan amables y cordiales.

A las secretarias y a los técnicos del Departamento de Química Anaítica y Química Orgánica.

A todos mis compañeros del laboratorio 330, los que se han ido ya y los que aún siguen. Asta, Cristina Mas, Marjorie, Adrian, Surya. Quiero agradecer especialmente a Cristina Acebo, Xavier Montané, Alberto, Isaac, Gianmarco, Mimmo, Rita, Rubén, David, Blai, Oleksandra y Ulpiano No tengo palabras para agradecerles por todo su apoyo, sus atenciones, sus muestras de solidaridad, por los buenos momentos compartidos. Creo que he tenido mucha suerte al coincidir con ustedes. ¡Simplemente gracias!

A mis compañeros del grupo de SUCRES y de SUSPOL, pero sobre todo a Zeynep, Alev y Camilo.

Durante toda esta etapa he tenido la suerte de contar con personas excepcionales que me han ayudado en mi crecimiento personal. Nuevamente tengo que agradecer a mi profe Angels Serra, de quien he aprendido la valiosa lección de la fortaleza y la constancia. ¡Gracias por ayudarme a levantarme una y otra vez!

A mis amigas Judith, Yonhara, Maryluz, Nibadita, Carmencita quienes han sido ejemplo de lucha, coraje, perseverancia y solidaridad. Hemos compartido muchas risas y lágrimas. Gracias por estar para mí en todo momento. ¡A mi mamita Isaura, Gracias por estar allí!

A mis amigas Arneida y Neudys, Todo empezó con ustedes. Son un claro ejemplo de que cuando se quiere se puede. Las admiro y quiero agradecerles por todo el apoyo que me han dado durante muchos años.

A mi querido Krzysztof, fuiste uno de mis grandes apoyos durante toda la tesis. En los momentos difíciles siempre estuviste allí dándome apoyo. Eres la persona más amable que he conocido en toda mi vida. Espero que no cambies esa bonita virtud.

A Javi, Magda, Sandrita, Miriam, Jorgito, Mariola, Edwin, Lourdes y Mónica.

¡Gracias a todos por ayudarme a ser cada día una mejor persona!

¡A mi familia! Quienes siempre han sido el motor que me ha impulsado y de donde saco la fortaleza necesaria para seguir adelante día tras día.

A la familia Estela Redondo, gracias por todo el apoyo y el esfuerzo por hacerme sentir en casa.

A mi novio Adrián Estela. Gracias por tener paciencia de santo, sobre todo en estos últimos meses, gracias por todo tu apoyo, tu ayuda, tus palabras de aliento cuando sentía que ya no podía más. ¡Una y mil veces gracias!

UNIVERSITAT ROVIRA I VIRGILI
NUEVOS PROCESOS DE CURADO CLICK CON TIOLES Y SU APLICACIÓN A LA PREPARACIÓN DE MATERIALES BASADOS EN EUGENOL
Dailyn Guzmán Meneses

UNIVERSITAT ROVIRA I VIRGILI
NUEVOS PROCESOS DE CURADO CLICK CON TIOLES Y SU APLICACIÓN A LA PREPARACIÓN DE MATERIALES BASADOS EN EUGENOL
Dailyn Guzmán Meneses

"Dios concede la victoria a la constancia"

Simón Bolívar

UNIVERSITAT ROVIRA I VIRGILI
NUEVOS PROCESOS DE CURADO CLICK CON TIOLES Y SU APLICACIÓN A LA PREPARACIÓN DE MATERIALES BASADOS EN EUGENOL
Dailyn Guzmán Meneses

UNIVERSITAT ROVIRA I VIRGILI
NUEVOS PROCESOS DE CURADO CLICK CON TIOLES Y SU APLICACIÓN A LA PREPARACIÓN DE MATERIALES BASADOS EN EUGENOL
Dailyn Guzmán Meneses

UNIVERSITAT ROVIRA I VIRGILI
NUEVOS PROCESOS DE CURADO CLICK CON TIOLES Y SU APLICACIÓN A LA PREPARACIÓN DE MATERIALES BASADOS EN EUGENOL
Dailyn Guzmán Meneses

Tabla de contenidos

UNIVERSITAT ROVIRA I VIRGILI
NUEVOS PROCESOS DE CURADO CLICK CON TIOLES Y SU APLICACIÓN A LA PREPARACIÓN DE MATERIALES BASADOS EN EUGENOL
Dailyn Guzmán Meneses

UNIVERSITAT ROVIRA I VIRGILI
NUEVOS PROCESOS DE CURADO CLICK CON TIOLES Y SU APLICACIÓN A LA PREPARACIÓN DE MATERIALES BASADOS EN EUGENOL
Dailyn Guzmán Meneses

CAPÍTULO 1

Introducción general

UNIVERSITAT ROVIRA I VIRGILI
NUEVOS PROCESOS DE CURADO CLICK CON TIOLES Y SU APLICACIÓN A LA PREPARACIÓN DE MATERIALES BASADOS EN EUGENOL
Dailyn Guzmán Meneses

1.1. Materiales termoestables

1.1.1. Aspectos generales

En la actualidad existe una gran demanda de materiales termoestables gracias a sus excelentes propiedades térmicas, químicas y mecánicas.[1] El inicio de estos materiales se remonta al año 1909 con el desarrollo de las resinas fenólicas por Leo Baekeland, sin embargo, el descubrimiento de la vulcanización por Goodyear es considerado como el primer paso en la producción de termoestables. Baekeland no solo produjo el primer polímero sintético entrecruzado (baquelita) sino que también desarrolló el proceso de moldeo para producir artículos comerciales.[2] Hoy en día estos materiales tienen una gran presencia y se encuentran en diferentes aplicaciones que van desde el campo de la medicina hasta la industria aeroespacial.[1]

Los termoestables pueden ser definidos como polímeros reticulados que forman una red tridimensional después de un proceso de polimerización irreversible, conocido como curado. Estos polímeros se caracterizan por ser infusibles e insolubles en cualquier disolvente orgánico.

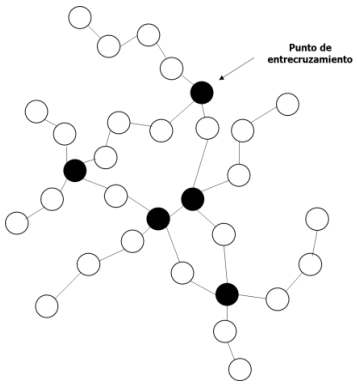

Figura 1.1. Estructura conceptual de los polímeros termoestables

Los termoestables son materiales muy versátiles en términos de producción. Los tipos de materiales que pueden ser producidos a través de los sistemas termoestables incluyen: moldes y objetos moldeados, resinas, adhesivos, recubrimientos, tintas, pinturas y materiales compuestos. Una gran variedad de monómeros son capaces de generar matrices poliméricas tridimensionales, responsables de la diversidad y el desarrollo de tecnologías específicas.[3]

1.1.2. Tipos de termoestables

Los termoestables más comunes empleados a nivel industrial son: [1]

- Urea-formaldehído: tableros de aglomerado, colas
- Resinas fenólicas: adhesivos y revestimientos, laminados
- Poliésteres insaturados: matrices para materiales compuestos reforzados con fibra de vidrio, laminados decorativos

- Poliuretanos: espumas, aislantes
- Epoxi: adhesivos, recubrimientos, pinturas
- Siliconas: adhesivos, juntas.

Entre los materiales termoestables con mayor demanda en el mercado mundial están las resinas epoxi, con aplicaciones que van desde recubrimientos,[4,5] adhesivos,[6] componentes eléctricos y electrónicos[7] y en la industria aeronáutica.[8] Su gran variedad de aplicaciones se debe al hecho de que estos termoestables pueden ser obtenidos variando no solo el tipo de resina y la naturaleza química del agente de curado, sino también a la posibilidad de adición de un gran número de agentes modificantes orgánicos e inorgánicos durante su preparación que les brindan grandes mejoras en sus propiedades finales.[6]

Las resinas epoxi son prepolímeros que se caracterizan por presentar al menos dos grupos epoxi capaces de reaccionar durante el proceso de polimerización (ver Figura 1.2). Estas resinas en combinación con diferentes agentes de curado permiten la fabricación de materiales termoestables con excelentes propiedades termomecánicas, químicas y térmicas.[9]

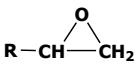

Figura 1.2. Estructura química del grupo epoxi

Entre las resinas epoxi con mayores aplicaciones industriales se encuentra la resina de diglicidiléter de bisfenol A, conocida con el acrónimo DGEBA. Esta resina se prepara mediante reacción de condensación entre la epiclorhidrina y el Bisfenol A en presencia de una base fuerte, tal y como muestra el siguiente esquema:

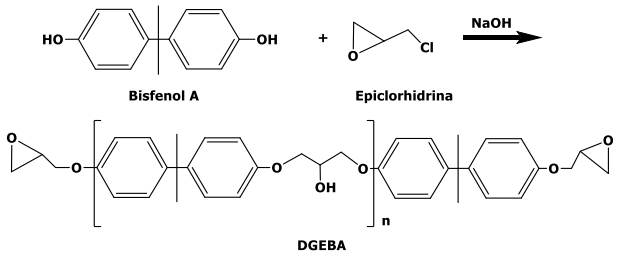

Figura 1.3. Preparación del DGEBA

La estructura química de las resinas epoxi juega un papel importante en sus propiedades y posibles aplicaciones. En el caso del DGEBA, los grupos epóxido e hidroxilo le proporcionan una excelente reactividad. Por su parte, los anillos aromáticos permiten que tenga una mayor resistencia térmica y química. Las secuencias alifáticas presentes en la estructura de la resina le confieren cierta flexibilidad. La Figura 1.4 representa la estructura química del DGEBA con sus características estructurales.

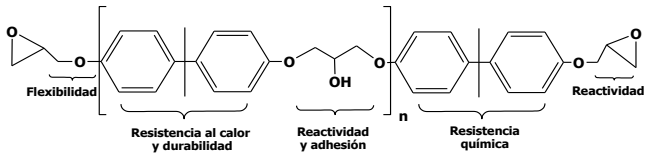

Figura 1.4. Estructura química y características del DGEBA

Aparte del DGEBA existen diferentes tipos de resinas con gran importancia a nivel comercial. Las más comunes son la de epoxi novolaca, las glicidil aminas (TGAP y TGMDA), resinas basadas en bisfenol F u otros bisfenoles y las resinas alifáticas y cicloalifáticas.[6] En la siguiente figura se muestran algunos ejemplos de resinas epoxi.

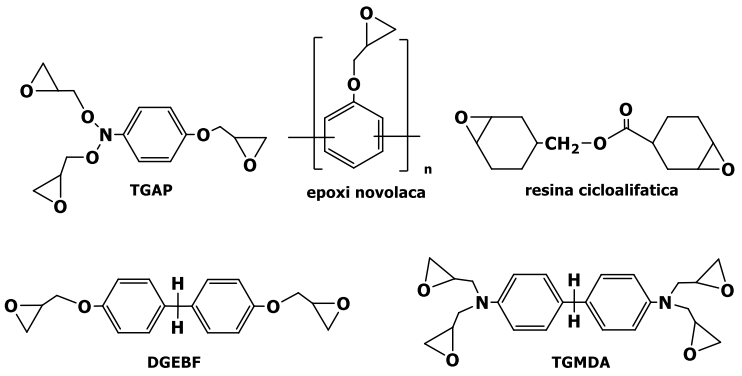

Figura 1.5. Estructura química de diferentes resinas epoxi

Las resinas epoxi deben su éxito comercial a la variedad de diferentes compuestos que sirven como endurecedores (agentes de curado) y que les proporcionan una alta versatilidad tanto en sus condiciones de aplicación como en sus propiedades, entre ellas: dureza, resistencia térmica, resistencia mecánica o adhesividad.[10] Dependiendo de la formulación (estructura y proporción de resina/agente de curado) el curado puede tener lugar a temperatura ambiente, con aplicación externa de calor o por irradiación con una fuente de energía diferente al calor como la radiación ultravioleta (UV) o el haz de electrones (EB). La elección del agente de curado depende del proceso y las propiedades deseadas, ya que determinan la cinética del curado, el tipo de enlace químico, la estructura y el grado de entrecruzamiento del material final.[6]

1.1.3. Preparación de materiales termoestables

Tal y como se ha expuesto, los materiales termoestables se preparan mediante la polimerización de monómeros multifuncionales en un proceso reactivo conocido como curado o entrecruzamiento. La funcionalidad de un monómero se define como el número de enlaces que puede formar en una reacción específica para dar una red polimérica. Así, la funcionalidad no depende tan solo de la estructura del monómero (ni de los grupos funcionales presentes) sino también de la reacción en la que participe.

Además de la química del proceso son muy importantes dos fenómenos físicos que tienen lugar durante el curado: gelificación y vitrificación, que afectan en gran medida al procesado y en determinadas circunstancias a las características del material final. La gelificación se produce como consecuencia del paso del estado líquido al estado gel que tienen lugar en el proceso de entrecruzamiento.[11,12,13] Macroscópicamente, la gelificación está asociada a un incremento drástico en la viscosidad y al hecho de que el material deja de ser procesable.[14] El punto de gel es un término empleado en el curado de los termoestables, y se define como el punto en el cual un líquido viscoso se convierte en un gel elástico, marcando el inicio de la formación de un retículo de peso molecular infinito.[15] El punto de gel es una de las características más importantes desde el punto de vista de procesabilidad de los termoestables. Por otra parte, la vitrificación ocurre cuando la temperatura de transición vítrea del termoestable en formación se hace igual a la temperatura de curado. Esto genera una disminución de la movilidad en las cadenas poliméricas, afectando de manera directa a la velocidad de la reacción y al grado de conversión alcanzado. Sin embargo, este fenómeno es reversible y puede ser revertido aumentando la temperatura por encima de la temperatura de transición vítrea, mediante el llamado proceso de desvitrificación.[15]

El proceso de curado de una resina epoxi puede darse por dos mecanismos de polimerización distintos: polimerización por etapas o polimerización en cadena.

Polimerización de crecimiento por etapas o policondensación: El mecanismo involucrado procede a través de una sucesión, paso a paso, de reacciones elementales entre grupos reactivos. Cada etapa independiente causa la desaparición de dos grupos reactivos y forma un nuevo enlace covalente entre un par de grupos funcionales. Para lograr un máximo grado de curado se requieren relaciones estequiométricas de agentes de curado como aminas, anhídridos, isocianatos o ácidos. Si bien las reacciones de policondensación producen a menudo pérdida de moléculas de bajo peso molecular, estas pérdidas deben ser evitadas en la formación de termoestables dado que llevarían a la formación de burbujas y defectos en el material. Por esta razón, las reacciones seleccionadas en el curado deben tener lugar sin eliminación de moléculas pequeñas. En el caso de los termoestables epoxídicos, el agente de curado por excelencia empleado son las aminas. La estructura de las aminas define el tipo de reacción polimerización, así las aminas primarias y secundarias conducen a polimerizaciones en etapas, mientras que las aminas terciarias no siguen este mecanismo y llevan a polimerizaciones en cadena, como se explicará posteriormente.

Las aminas alifáticas primarias y secundarias como dietilentriamina y trietilentetramina fueron los primeros agentes de curado empleados en resinas epoxi.[6]

Las aminas alifáticas primarias reaccionan rápidamente con los grupos epoxi a temperatura ambiente para formar estructuras entrecruzadas tridimensionales. A diferencia de éstas, las aminas aromáticas primarias pueden ser usadas para curar pero requieren temperaturas elevadas proporcionando estructuras con mayor rigidez, con

buena resistencia mecánica, estabilidad a temperatura elevada y resistencia química. Entre las más usadas se encuentran el 4,4´-diaminodifenilmetano, la 1,3-fenilendiamina o la 4,4´-diamino difenilsulfona.[6] La reactividad de la amina incrementa con su carácter nucleófilo: alifáticas > cicloalifáticas > aromáticas. Las aminas alifáticas son usadas en sistemas de curado a bajas temperaturas (adhesivos), mientras que las diaminas aromáticas son empleadas en la fabricación de materiales compuestos.[10]

En la polimerización por etapas los grupos epoxi sufren un ataque nucleófilo en el carbono menos sustituido formando un grupo alcóxido y una sal de amonio en carbonos adyacentes que por equilibrio ácido-base originan grupos β-aminoalcohol. En estas reacciones, los grupos hidroxilo catalizan la reacción por formación de un complejo trimolecular que facilita el ataque nucleófilo del grupo amino.[11] Debido a su mayor nucleofília, las aminas primarias reaccionan más rápidamente con los grupos epóxido que las secundarias y en consecuencia, en primer lugar se forman estructuras lineales. Éstas acabaran transformándose en estructuras reticuladas cuando reaccionen las aminas secundarias formadas con otros grupos epóxido en etapas posteriores. En la Figura 1.6 se muestran las reacciones que tienen lugar durante el curado de un epóxido con una amina primaria.

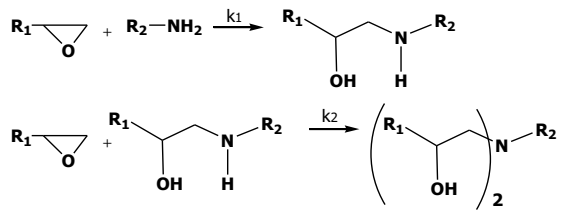

Figura 1.6. Reacciones elementales en el curado de un epóxido con una amina primaria

En reacciones epoxi-amina, el grupo epóxido actúa con una funcionalidad de 1, por lo que una resina como la DGEBA presenta una funcionalidad 2. Por su parte cada grupo amino primario participa en la reacción con una funcionalidad 2, por lo que una diamina como la 4,4'-diaminodifenilsulfona participa con una funcionalidad de 4. Con esta funcionalidad global de 2 más 4, se consiguen redes tridimensionales, que no se conseguirían con diaminas secundarias.

Polimerización por crecimiento de cadena (apertura del anillo): El mecanismo de este tipo de polimerización se caracteriza por presentar varios procesos reactivos distintos: iniciación, propagación, transferencia de cadena y terminación. En sistemas epoxídicos el ion activo puede ser generado por tratamiento térmico o por una fuente de irradiación en presencia del iniciador, que es un compuesto capaz de iniciar la polimerización y que a su vez puede tener un efecto catalítico. Durante la iniciación, que puede darse aniónica o catiónicamente, se forma un anión o un catión, llamado centro activo de la polimerización. Una vez generados los centros activos se producen cadenas

primarias por la adición consecutiva de monómeros a través de la etapa de propagación de la reacción.[16]

Las aminas terciarias como la 4-(N,N-dimetilamino) piridina (DMAP) o el 1-metilimidazol (1-MI)[17,18] son ampliamente usadas como iniciadores en polimerizaciones aniónicas de resinas epoxi debido a su alto carácter nucleófilo.[10] El mecanismo de polimerización en cadena que involucra aminas terciarias se representa en la Figura 1.7. En la etapa inicial la apertura del anillo epóxido por el ataque nucleófilo del iniciador forma un alcóxido. En pasos siguientes este alcóxido propaga la polimerización por apertura de otro epóxido, formando finalmente la red entrecruzada constituida por estructuras de poliéter.[19]

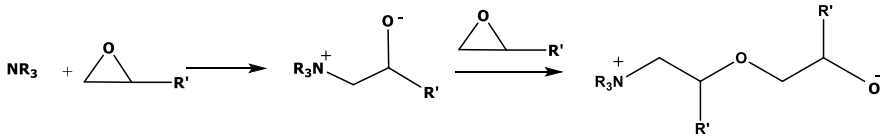

Figura 1.7. Polimerización de epóxidos iniciada por aminas terciarias

En este tipo de polimerizaciones cada grupo epóxido participa con una funcionalidad de 2, por lo que una resina como la DGEBA puede formar redes tridimensionales por este procedimiento por contar con una funcionalidad de 4. La presencia de grupos hidroxílicos, además de acelerar el curado, puede aumentar la funcionalidad del sistema debido a que éstos son activos tanto en homopolimerización aniónica[20] como en catiónica.[21]

1.1.4. Conceptos tecnológicos

En la obtención de materiales termoestables se parte de formulaciones con todos sus componentes: resina base y agente de curado, así como acelerantes, cargas, aditivos diluyentes, etc., añadidos con el fin de alcanzar mejoras en el procesado o en las propiedades finales. En general, la aditivación de las formulaciones pretende mejorar características como la estabilidad del sistema, la cinética de curado, la temperatura de transición vítrea (T_g), o bien otras propiedades como las mecánicas y la resistencia química o a las radiaciones solares.[22] Estas formulaciones pueden ser o no estables durante su almacenamiento. Si son estables durante un periodo largo, las resinas se califican como *one-pot* y se comercializan en un solo envase. En caso contrario, la formulación deberá hacerse por mezcla de los componentes antes de su aplicación y en general se conocen como sistemas bi-componente ya que se dispensan en dos envases separados. Desde este punto de vista, un aspecto importante es la posibilidad de controlar el tiempo que tarda en reaccionar la mezcla de monómero/agente de curado (*pot-life*) y que es el tiempo que tiene el operario para su aplicación una vez realizada la mezcla o activado el curado por acción externa. Dependiendo de la reactividad de la mezcla, el *pot-life* puede variar de pocos segundos hasta años.[23] El *pot-life* de la mezcla puede ser controlado empleando iniciadores latentes, que son estables en las condiciones de almacenamiento y que pueden ser activados a voluntad mediante estímulos externos

como son el calor o la luz ultravioleta.[24] La utilización de sistemas latentes permite elaborar sistemas epoxídicos *one-pot* con la ventaja de su fácil manipulación y aplicación y la alta reproducibilidad que se alcanza en las características finales del material termoestable.

1.1.5. Curado dual

El curado dual es una metodología que permite obtener materiales termoestables mediante la combinación de dos procesos de polimerización diferentes, pero compatibles, que pueden llevarse a cabo de forma secuencial o simultánea. Las reacciones de polimerización involucradas en cada etapa pueden ser activadas por iguales o diferentes estímulos como la temperatura o la luz UV. Este tipo de sistemas presenta una gran variedad de características atractivas desde el punto de vista tecnológico.[25,26]

El curado dual en dos etapas permite desarrollar materiales con características morfológicas particulares dependiendo de si los procesos de polimerización ocurren en forma simultánea o secuencial con gelificación o no de la etapa intermedia.[27,28,29] Sin embargo, el proceso secuencial presenta un mayor atractivo desde el punto de vista de aplicaciones en procesos *multi-stage*, en fabricación en discontinuo y en la preparación de materiales conformables al final de la primera etapa de curado.

Tal y como se ha dicho, el curado dual secuencial representa una ventajosa herramienta a nivel tecnológico, ya que puede ser empleado en muchos procesos de fabricación complejos que se realizan en diferentes etapas con tiempos de espera intermedios o bien en lugares distintos con transporte intermedio incluido. La conversión alcanzada y las propiedades al final de cada una de las dos etapas de curado pueden ser controladas fácilmente, mediante una cuidadosa selección de la formulación. Esto hace posible minimizar el riesgo de que ocurra un curado excesivo en la etapa intermedia y conseguir que el material sea estable e incluso procesable antes de que se active la segunda reacción de curado. En comparación con el enfoque de utilizar un pre-polímero en la formulación de partida, el procesado y la preparación de las formulaciones se pueden hacer de forma más sencilla y versátil con sistemas de curado dual, en los cuales el pre-polímero puede ser producido *in situ* durante la primera etapa de curado. En este caso la mezcla inicial contendrá monómeros de bajo peso molecular, en lugar de componentes poliméricos de mayor peso molecular y será por tanto más procesable, con más facilidad para rellenado de moldes o para ser aplicada en superficies. Por su parte, el material intermedio puede ser maleable y conformable a la vez que conserve sus características adhesivas, si son requeridas, y que no presente pegajosidad. Sin embargo, el concepto de curado dual va mucho más allá de estas aplicaciones y hace posible el desarrollo de materiales personalizados con una capacidad de procesamiento flexible que los hace muy útiles para una serie de aplicaciones avanzadas de alto valor añadido.[30]

El curado dual secuencial presenta los siguientes requerimientos:

- Los procesos de polimerización involucrados deben ser selectivos y compatibles. Este requerimiento es necesario para evitar inconvenientes como la inhibición del curado o efectos sobre la reactividad.
- Las reacciones en cada etapa deben ser activadas por diferentes estímulos ya sea por temperatura o empleando irradiación ultravioleta. Para este fin se pueden emplear catalizadores (iniciadores) que se activen con diferentes estímulos o en diferentes intervalos de temperatura o longitud de onda de la irradiación. La utilización de catalizadores latentes o fotolatentes permite además el diseño de formulaciones one-pot con una considerable estabilidad de almacenaje, tanto al inicio como después de la primera etapa de curado. El curado dual secuencial también puede llevarse a cabo empleando reacciones con velocidades lo suficientemente diferentes para que puedan ser controladas desde el punto de vista cinético en función del tiempo y la temperatura.
- Las propiedades intermedias y finales de los materiales han de poder ser controladas a voluntad, mediante una cuidadosa selección de monómeros, catalizadores, composición y sistema de activación.

La metodología de curado dual para la preparación de termoestables puede ser llevada a cabo empleando una gran variedad de reacciones de polimerización. Sin embargo, el uso de reacciones click para este fin resulta muy atractivo, debido a su ortogonalidad, selectividad y alta eficiencia.[31,32]

1.2. Química *click*

1.2.1. Aspectos generales

El concepto química *click* fue introducido por el profesor Sharpless y sus colaboradores en el año 2001[31] y define un tipo de química pensada para la fabricación de estructuras complejas a partir de la unión, vía enlaces C-heteroátomo (C-X-C), de una serie de moléculas más pequeñas mediante un número reducido de reacciones muy eficientes tanto en términos de conversión como de selectividad.[33] Las reacciones *click* transcurren en condiciones suaves y se pueden llevar a cabo de forma simple desde el punto de vista experimental. Son reacciones compatibles con una amplia variedad de grupos funcionales, insensibles al oxígeno o al agua, y altamente selectivas y regioespecíficas. La formación del producto de reacción tiene lugar de forma cuantitativa y su aislamiento es sencillo. La Figura 1.8 muestra una representación visual de la denominada química *click*.

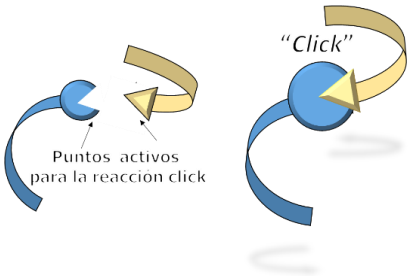

Figura 1.8. Representación conceptual de la química *click*

Hay un gran número de reacciones que se ajustan al criterio propuesto por Sharpless, las cuales se presentan a continuación:

- Cicloadiciones de especies insaturadas, incluidas las reacciones de cicloadición 1,3-dipolar y transformaciones Diels-Alder.[34,35]

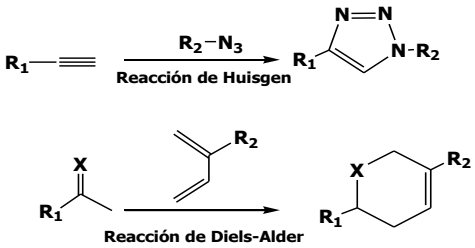

Figura 1.9. Ejemplos de cicloadiciones tipo *click*

- Apertura de anillos tensionados mediante sustitución nucleófila.[36]

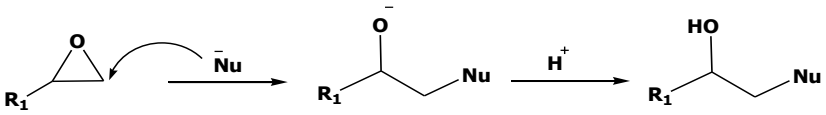

Figura 1.10. Esquema de apertura de anillo tipo *click*

- Adición a enlaces insaturados carbono-carbono, incluidas epoxidaciones, azidiración y dihidroxilación. También se clasifican en este apartado las reacciones nucleófilas de adición conjugada tipo Michael y las adiciones radicalarias de tioles a grupos vinílicos y acetilénicos.[37]

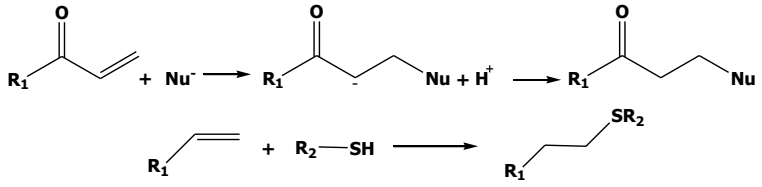

Figura 1.11. Ejemplos de adiciones tipo *click* a enlaces insaturados C-C

- Reacciones químicas del carbonilo del tipo "no-aldólicas", tales como formación de oximas, hidrazonas, etc. [38]

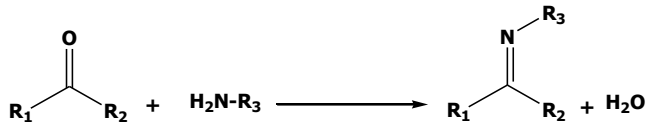

Figura 1.12. Ejemplo reacciones químicas no aldólicas tipo *click*

En los últimos años las reacciones *click* que involucran tioles han tenido un gran auge sobre todo en la preparación de nuevos materiales poliméricos. La reacción más empleada para este fin es la tiol-eno. Sin embargo, la reacción *click* tiol-epoxi aunque poco explorada es una herramienta potente, que puede ser aplicada en el curado de resinas epoxi.[37]

1.2.2. Reacciones tiol-*click*

Las reacciones tiol-*click* presentan ciertos beneficios en comparación con otras reacciones *click* debido a que los tioles, por su alta reactividad, son capaces de reaccionar con una gran variedad de sustratos, tanto mediante procesos radicalarios como procesos nucleófilos catalizados por bases en condiciones muy suaves.

Las reacciones que involucran tioles son altamente eficientes y pueden llevarse a cabo con una gran variedad de sustratos. Específicamente, vinilos ricos en electrones (via radicalaria), alquinos (radicalaria), dobles enlaces deficientes de electrones (adición nucleófila tipo Michael), isocianatos (adición nucleófila al carbonilo), epóxidos (apertura de anillo tipo SN_2) y compuestos halogenados (sustitución nucleofila tipo SN_2).[37]

Tal como se ha dicho, las reacciones tiol-*click* presentan muchas ventajas, entre ellas que son rápidas, se llevan a cabo en condiciones suaves y con altos porcentajes de conversión, son regioselectivas y generalmente conducen a un producto que requiere poca o ninguna purificación. Todas estas características permiten partir de una serie de tioles y diferentes sustratos crear/funcionalizar/modificar una excepcional variedad de moléculas y materiales con propiedades físicas, químicas y mecánicas para ajustarse a numerosos requerimientos.[39] Las reacciones tipo *click* que involucran tioles vienen recogidas en el esquema de la Figura 1.13.

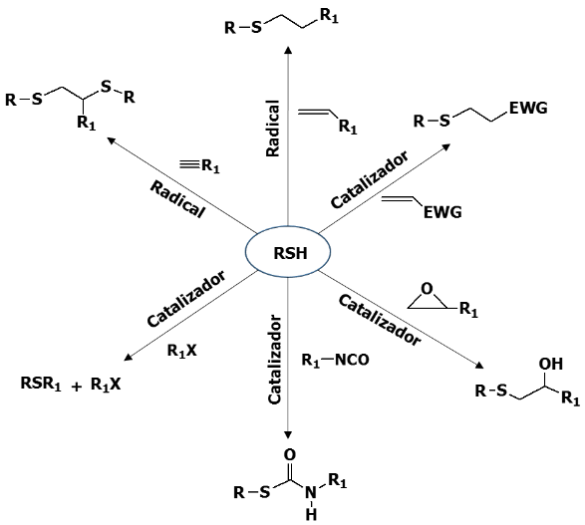

Figura 1.13. Diferentes tipos de reacciones tiol-*click*

1.2.3. Reacción tiol-eno

Las reacciones *click* tiol-eno evitan las limitaciones críticas de la fotopolimerización convencional, formando una red de polímero homogénea a través de una polimerización por pasos controlable al mismo tiempo que conjuntan la rápida producción y conveniencia del proceso de fotopolimerización. Es por ello que en los últimos años las reacciones tiol-eno han adquirido una importancia considerable en el campo tecnológico y científico en curado por irradiación UV.[40]

El mecanismo de la reacción tiol-eno consta de tres pasos y viene representado en la Figura 1.14. En la etapa inicial, el fotoiniciador es irradiado con luz ultravioleta a una frecuencia adecuada para generar el radical tiilo. El radical tiilo se adiciona de forma anti-Markovnikov al alqueno, generando un radical alquilo intermedio. Este radical puede reaccionar con otra molécula de tiol, formando un tioéter y otro radical tiilo, que puede continuar la reacción y así se va completando el ciclo radical hasta que no quede tiol libre. La reacción termina a través de la recombinación de radicales tiilo y alquilo con otros radicales o con ellos mismos. Sin embargo, este es un proceso no deseado, que puede limitar la aplicación de este tipo de reacción. De la misma forma, la posibilidad de que el carbono radical intermedio formado inicie una polimerización vinílica de la olefina presente es otra de las reacciones laterales que limitan la conversión en tioéter.[41] La formación del enlace carbono-azufre en la reacción tiol-eno sigue una regioselectividad anti-Markovnikov, la cual asegura la formación del radical alquilo más estable.[42,43] Si no ocurre homopolimerización del monómero vinílico ni acoplamiento entre radicales tiilo los grupos funcionales tiol y vinilo se consumen a la misma velocidad.[44]

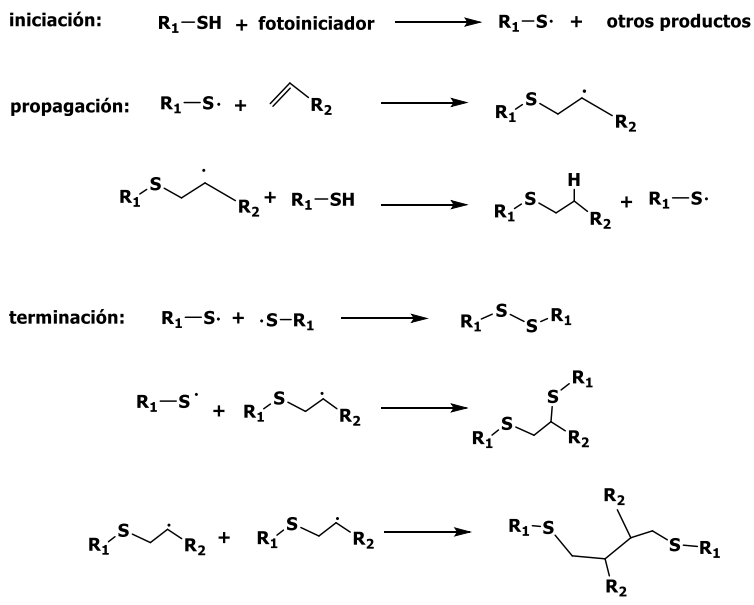

Figura 1.14. Mecanismo de la reacción tiol-eno

En las reacciones tiol-eno, el grado de adición del tiol a un doble enlace depende de las reactividades relativas del tiol y del compuesto vinílico. Las reactividades de estos grupos funcionales se ven influenciadas por la naturaleza de sus sustituyentes. El orden de reactividad de los compuestos vinílicos frente a la adición de tioles es el siguiente: éter vinílico >> éter alílico > alqueno > acrilato > diester >> estireno. La tendencia en la reactividad del grupo vinilo muestra que los compuestos ricos en electrones como éteres vinílicos y alquenos son mucho más reactivos que los compuestos pobres en electrónicamente como es el caso de los acrilatos. En el caso del estireno, es un compuesto poco adecuado para participar en una reacción tiol-eno, ya que tiene la habilidad de estabilizar sus radicales por efecto de resonancia.[45]

Los termoestables obtenidos a partir de reacciones tiol-eno exhiben una alta uniformidad en la densidad de entrecruzamiento. Estos materiales poseen además, como consecuencia de su mecanismo por etapas, propiedades termo-mecánicas homogéneas en todas las dimensiones espaciales, que asegura unas prestaciones mecánicas óptimas.[39] Sin embargo, suelen presentar valores de T_g bajos debido a la flexibilidad de los tioles comercialmente asequibles que se utilizan.[46]

1.2.4. Reacción tiol-epoxi

Las reacciones *click* con tioles que involucran apertura del anillo epóxido resultan atractivas industrialmente para la preparación de adhesivos, recubrimientos de alto rendimiento y materiales compuestos.[39]

El mecanismo de reacción tiol-epoxi en medio básico consiste en una sustitución nucleófila simple de apertura del anillo epoxi por el anión tiolato. El tiolato puede

formarse por equilibrio ácido-base entre el tiol y la amina, siempre que sea una amina muy básica.[47] Sin embargo, la baja basicidad de algunas aminas terciarias como el 1-MI, con un pKa del ácido conjugado de aprox. 7[48] y el pobre carácter ácido del tiol con un pKa de aprox. 9,[49] reduce la posibilidad de intercambio para formar el tiolato. Como alternativa se ha propuesto el mecanismo para la BDMA o para el 1-MI, que se representa en la Figura 1.15.[50,51] En este mecanismo la amina efectúa un ataque nucleófilo al metileno epoxídico, con asistencia de un proton hidroxílico que cataliza el proceso (a). Éste viene seguido por un proceso ácido-base en el que el alcóxido se protona mientras se forma el tiolato (b), que atacará nucleofílicamente al epóxido (proceso c). El tiolato se regenera mediante intercambio ácido-base con el alcóxido anteriormente formado (d), llevando al β-hidroxitioéter que es el producto de reacción esperado. Finalmente, las buenas características como grupo saliente de la amina (en el esquema 1-MI) permiten su regeneración, principalmente por sustitución nucleófila (proceso e). Como puede verse, el papel de la amina utilizada como base es puramente catalítico.

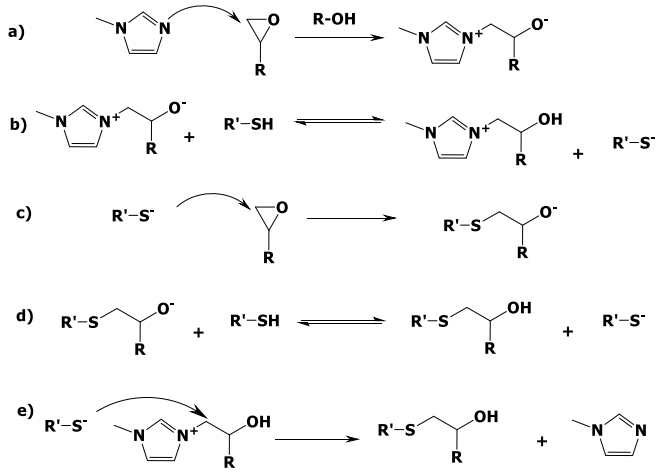

Figura 1.15. Mecanismo de la reacción tiol-epoxi

Se ha podido constatar, que cuando existe un exceso de epóxido respecto al tiol en la formulación y se calienta la mezcla a temperatura alta puede tener lugar la homopolimerización del epóxido.[51] Sin embargo, en sistemas estequiométricos tiol-epoxi esta homopolimerización no compite. Entre las ventajas de las formulaciones tiol-epoxi se encuentran su estabilidad térmica, baja toxicidad, alta adherencia y excepcional transparencia de los materiales resultantes.

Además de estas características especiales, los sistemas tiol-epoxi se pueden combinar con procesos tiol-eno, ambos con características *click*, para preparar sistemas de curado dual *one-pot*, que se activan por calor el primero y por irradiación UV el segundo y que pueden conducir a materiales con propiedades hechas a medida, dependiendo de la estructura de los monómeros y la estequiometría de la formulación.[52]

Aunque en general, el proceso tiol eno se activa primero a temperatura ambiente mediante irradiación y la segunda etapa tiol-epoxi después mediante calentamiento, ambas etapas de curado pueden llegar a invertirse con una selección adecuada de catalizadores y de las condiciones de trabajo.

1.2.5. Curado dual: "Tiol-*click*"

En la metodología de curado dual para la preparación de termoestables, las propiedades intermedias y finales del material dependen en gran medida de la estructura de la red al final de cada proceso de polimerización involucrado. Las propiedades de estas estructuras están controladas por la estructura y funcionalidad de los monómeros y por la proporción de los mismos en la formulación.[53]

Los procesos tiol-c*lick* mencionados en el apartado anterior llevan a polimerizaciones tipo policondensación. Por esta razón, la utilización de esta química es sistemas duales resulta muy atractiva, ya que los procesos implicados pueden ser analizados mediante metodologías y cálculos muy bien establecidos. Por ejemplo, parámetros estructurales relevantes tales como el peso molecular promedio en peso, la conversión en el punto de gel, la densidad de reticulación o la fracción de gel, que están estrechamente relacionados con las propiedades reológicas o termo-mecánicas de materiales parcialmente o totalmente curados pueden estimarse con una cierta facilidad.[54,55]

En estos sistemas duales además del monómero tiol, con la funcionalidad requerida, pueden participar uno o más monómeros diferentes (vinílicos, epoxídicos, etc.). En el caso de un único monómero substrato, éste debe tener los dos tipos de grupos funcionales requeridos para que se lleve a cabo la reacción en cada una de las etapas. Alternativamente, la formulación puede contener dos o más monómeros que presenten diferentes grupos funcionales, siendo posible que cada uno de ellos reaccione selectivamente en cada una de las etapas. La primera reacción *click* puede conducir o no a una estructura entrecruzada, dependiendo de la funcionalidad y la proporción de los diferentes monómeros o diferentes grupos funcionales en la formulación.

La preparación de sistemas de curado dual basados en reacciones tiol-eno/tiol-epoxi resulta un procedimiento muy ventajoso, ya que el uso de tioles multifuncionales permite conectar covalentemente ambas redes de tioéter.[56] Este procedimiento se esquematiza en la figura siguiente.

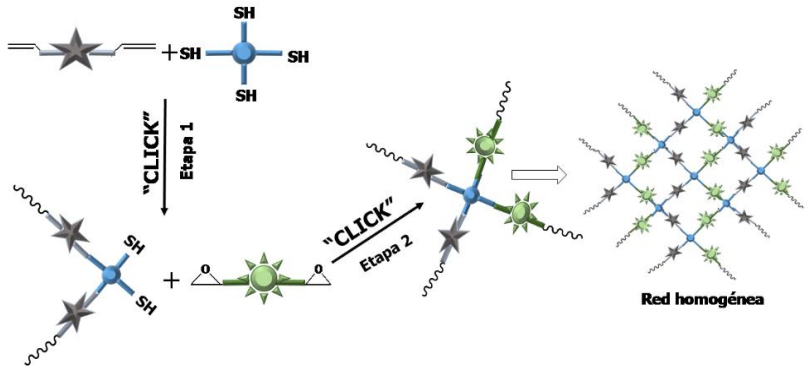

Figura 1.16. Esquema idealizado del curado dual mediante reacción tiol-eno/tiol-epoxi

En el curado dual tiol-eno/tiol-epoxi, la primera etapa está constituida por una reacción fotoquímica en la que el mecanismo de polimerización por etapas da como resultado un proceso de formación de red homogénea con gelificación a altos grados de conversión y contracción baja. Además, las fotopolimerizaciones tiol-eno no se inhiben en presencia del oxígeno, lo que constituye una gran ventaja en su aplicación tecnológica.[57] Por su parte, la reacción de los grupos epoxi con el exceso de grupos tioles en la segunda etapa permite obtener un material termoestable con excelentes propiedades térmicas y mecánicas y el hecho de que esta etapa sea térmica elimina la posible vitrificación del material.

Existe poca literatura sobre curados duales tiol-eno/tiol-epoxi. Saharil y colaboradores[56] emplearon sistemas tiol-eno/tiol-epoxi en aplicaciones para microfluídica. Demostraron la eficacia de la combinación de estas dos reacciones tiol-*click* en la obtención de materiales poliméricos con excelentes propiedades de adhesión a diferentes sustratos, empleando procedimientos relativamente sencillos. Sin embargo, los materiales obtenidos en la etapa intermedia eran poco estables a pesar de que la reacción tiol-epoxi se llevó a cabo lentamente a temperatura ambiente.

Este novedoso sistema de curado también ha sido estudiado como posible sustituto al empleo de resinas de dimetacrilato empleadas como restauradores dentales, concluyendo que el empleo de reacciones secuenciales tiol-eno/tiol-epoxi conduce a materiales con redes entrecruzadas altamente regulares, que además exhiben propiedades físicas y mecánicas óptimas. En este sistema dual se observó la homopolimerización parcial de algunos grupos epoxi.[46]

También se prepararon materiales termoestables a partir de mezclas no estequiométricas tiol-eno/tiol-epoxi, con las dos etapas fotoquímicamente iniciadas, empleando un fotoiniciador y una fotobase que son activados a diferentes longitudes de onda. Esta metodología permitió lograr un sistema de curado dual con una etapa intermedia estable durante sólo 24 h, aunque también se produjo un cierto grado de homopolimerización de grupos epóxido.[58]

1.3. Química sostenible

1.3.1. Aspectos generales

Uno de los responsables del deterioro medioambiental que sufrimos actualmente es la industria química, ya que libera grandes cantidades de residuos tóxicos.[59] Como medida para frenar este impacto negativo sobre el medioambiente surgen los conceptos de *ingeniería verde, química verde y química sostenible,* las cuales se basan en el desarrollo de nuevos procesos y tecnologías con el objetivo principal de controlar los niveles de toxicidad de los productos químicos empleados o generados como subproductos en las reacciones químicas manteniendo la calidad medioambiental.[60,61]

Como hemos señalado anteriormente, las reacciones *click* tienen lugar en condiciones suaves y por tanto, permiten llevar a cabo procesos de curado respetuosos con el medio ambiente. En este contexto, otro aspecto importante a considerar es la naturaleza de los productos de partida. La mayoría de los termoestables se fabrican a partir de compuestos provenientes del petróleo. Sin embargo, desde hace unos años ha surgido la necesidad de orientar la investigación a la búsqueda de nuevas estrategias con el objetivo de preparar resinas a partir de recursos renovables para preservar el medio ambiente de las agresiones provenientes de los procesos industriales y minimizar la dependencia del petróleo.[62]

1.3.2. Química e ingeniería verde

Los conceptos de química verde, ingeniería verde y sostenibilidad se han fusionado para ofrecer un conjunto de términos que a menudo se utilizan indistintamente para describir ideas similares.[63]

La química verde y la química sostenible son conceptos relativamente nuevos basados en el desarrollo de procesos y tecnologías que resultan en reacciones químicas más eficientes que generan muy poco residuo y menos emisiones medioambientales en comparación con las reacciones químicas tradicionales. La química verde abarca todos los aspectos y tipos de procesos químicos que reducen el impacto negativo en la salud humana y del medioambiente. Otro aspecto básico de estos dos conceptos es el empleo de materias primas y recursos energéticos renovables para los procesos sintéticos.

La química verde abarca casi todas las principales ramas de la química como síntesis orgánica o inorgánica, catálisis, ciencias de los materiales, polímeros, nanoquímica, química supramolecular y tratamiento de aguas residuales entre otros.[64]

Por su parte, la ingeniería verde es una disciplina que abarca todas las ramas de la ingeniería. En este contexto, la ingeniería química verde pretende diseñar procesos químicos minimizando el uso de solventes orgánicos, incorporando los principios de química verde o disminuyendo el consumo de energía.[63]

1.3.3. Principios básicos de la química verde

Los principios básicos de la química verde se centran en los criterios de diseño sostenible y han demostrado ser fuente de soluciones innovadoras para una amplia gama de problemas medioambientales. La química verde abarca esta capacidad de diseño e insiste en que si se usa sabiamente, se pueden lograr contribuciones significativas en sostenibilidad para el beneficio simultáneo del medio ambiente, la economía y la sociedad.[65]

El concepto de química verde fue desarrollado por Paul Anastas[66] y se basa en una serie de principios que describen cómo obtener un producto químico por un proceso más favorables medioambientalmente. Los 12 principios básicos de la química verde son:

- Prevención

  Es mejor prevenir los residuos que tratar o limpiar los residuos después de haber sido creados.

- Economía del átomo

  Los métodos sintéticos deben ser diseñados para maximizar la incorporación de todos los materiales utilizados durante el proceso en el producto final.

- Síntesis química menos peligrosa

  Siempre que sea posible, los métodos sintéticos deben diseñarse para utilizar y generar sustancias que tienen poca o ninguna toxicidad para la salud humana y el medio ambiente.

- Diseño de productos químicos más seguros

  Los productos químicos deben ser diseñados para efectuar la función deseada disminuyendo al máximo su toxicidad.

- Disolventes y auxiliares más seguros

  El uso de sustancias auxiliares (por ejemplo, disolventes, agentes de separación, etc.) debe disminurse o eliminarse. En casos necesarios, deben ser inocuos para el medio ambiente.

- Diseño para la eficiencia energética

  Los requerimientos energéticos de los procesos químicos deben clasificarse por su impacto ambiental y económico, minimizando su efecto sobre el medio ambiente y los costos de producción. Si es posible, los métodos sintéticos deben realizarse a temperatura ambiente y presión atmosférica.

- Uso de materias primas renovables

  Una materia prima debe ser renovable en lugar de no renovable, siempre que sea técnica y económicamente factible.

- Reducción de derivados

La derivatización innecesaria (uso de grupos de bloqueo, protección / desprotección, modificación temporal de procesos físicos / químicos) debe minimizarse o evitarse si es posible, ya que estos pasos requieren reactivos adicionales y pueden generar residuos.

- Catálisis

Los reactivos catalíticos deben ser lo mas selectivos posible y deben ser favorecidos frente al empleo de reactivos en cantidades estequiométricas.

- Diseño para la degradación

Los productos químicos deben diseñarse de manera que al final de su función se descompongan en productos de degradación inocuos y no persistentes en el medio ambiente.

- Análisis en tiempo real para la prevención de la contaminación

Las metodologías analíticas deben seguir desarrollándose para permitir la monitorización y control en tiempo real de la formación de sustancias peligrosas.

- Reducción del potencial de accidentes químicos

Las sustancias usadas en un proceso químico deben ser elegidas para minimizar el potencial de accidentes químicos, incluyendo liberaciones, explosiones e incendios.[65,67,68]

Los principios de la química verde han sido ampliamente aplicados a la preparación de termoestables eco-amigables, con el objetivo primordial de preservar el medioambiente y a la vez emplear diferentes recursos renovables para eliminar la dependencia existente con el petróleo.[69] En la Figura 1.17 se muestra a modo de resumen los criterios para que un proceso químico sea medio ambientalmente favorable, aplicables también a la preparación de termoestables.

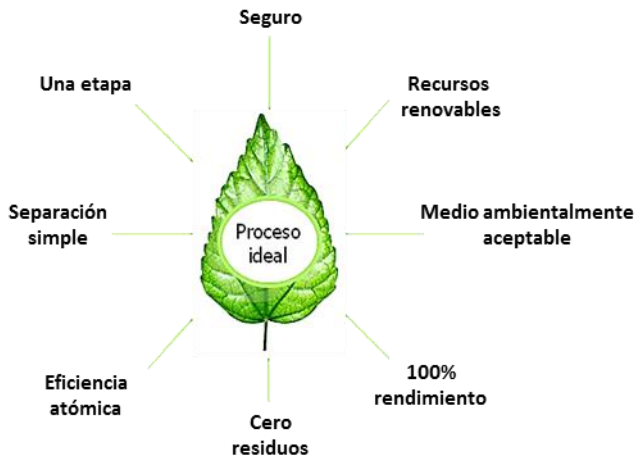

Figura 1.17. Criterio ideal de un proceso químico favorable medio ambientalmente

1.3.4. Materiales termoestables de fuentes renovables

Los termoestables con consumo a nivel industrial se preparan generalmente a partir de fuentes no renovables.[70,71] Sin embargo, la reducción del uso y dependencia de combustibles fósiles, no solo es necesario por razones asociadas al daño medio ambiental sino también es crucial económicamente.[72] Como alternativa a la utilización de productos derivados del petróleo, en la actualidad está ganando terreno la utilización de productos provenientes de fuentes renovables como materia prima.[73]

Existe una gran variedad de productos naturales que se emplean en aplicaciones industriales para sustituir parcialmente, y hasta cierto punto totalmente, los polímeros provenientes del petróleo. Los polímeros diseñados bajo esta estrategia pueden competir o incluso superar a los materiales existentes con altas cualidades de respeto al medio ambiente.[74, 75, 76, 77]

Recientemente se han enfocado muchas investigaciones a la obtención de materiales termoestables a partir de diferentes fuentes renovables.[78] Aouf y colaboradores[79] emplearon taninos como materia prima en la preparación de nuevas resinas epoxi, obteniendo materiales con buenas propiedades térmicas. Otros trabajos similares han confirmado que los taninos son una buena opción como sustitutos de las resinas epoxi convencionales.[80] Por su parte, Hu y colaboradores[81] emplearon derivados furánicos como sustitutos de las resinas termoestables derivadas del petróleo, demostrando que son un componente viable para la obtención de resinas epoxi renovables con altas prestaciones. Se han usado también derivados del aceite de soja para la preparación de polímeros entrecruzados, obteniendo materiales que posiblemente pueden ser usados en aplicaciones como en espumas, adhesivos, revestimientos y sellantes.[82] El ácido itacónico también resultó ser una excelente materia prima alternativa ideal para obtener materiales epoxídicos con propiedades adhesivas, térmicas y mecánicas iguales o mejores que las resinas comerciales.[83]

Sin embargo, muchos de estos materiales adolecen de pobres características termomecánicas, con valores bajos de T_g y de módulo de Young debido a su estructura flexible y bajos grados de entrecruzamiento. Por esta razón, es todavía necesario hallar nuevos productos procedentes de fuentes renovables, que con sus estructuras rígidas y alta funcionalidad permitan obtener materiales con mejores características para aplicación en tecnologías avanzadas y con requerimientos superiores.

1.3.5. Eugenol como materia prima renovable

El eugenol es altamente atractivo como materia prima para el desarrollo de nuevos materiales ya que además de su estructura, su mayor ventaja es su abundancia natural y su precio asequible. El eugenol es un compuesto fenólico que está presente en el aceite esencial del clavo de olor *[Eugenia caryophyllata (Myrtaceae) = Syzygium aromaticum]* hasta aproximadamente el 80% en peso. El aceite esencial de clavo de olor se obtiene generalmente por destilación con corriente de vapor o por extracción Soxhlet en etanol

a partir de hojas, brotes y tallos de los árboles de clavo.[84] El eugenol también se encuentra en la nuez moscada, canela y albahaca, entre otros, con lo cual su biodisponibilidad es muy alta.[85]

El eugenol tiene múltiples aplicaciones, entre ellas son de especial importancia las del campo de la odontología y de la medicina, gracias a sus excelentes propiedades terapéuticas.[86 ,87]

La estructura química del eugenol, (Figura 1.18), tan versátil por sus grupos funcionales, hace que este compuesto sea muy atractivo como materia prima en la preparación de nuevos materiales funcionales favorables al medio ambiente.[88,89] Sin embargo, se encuentran pocos trabajos que giren en torno a la utilización de este compuesto para obtener materiales termoestables.[73,90,91,92]

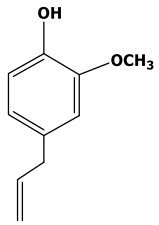

Figura 1.18. Estructura química del eugenol

Se ha descrito la obtención de un compuesto diepoxídico basado en el eugenol por epoxidación del doble enlace seguido por transformación del hidroxilo fenólico a un grupo glicidilo. Los resultados de este estudio indican que el eugenol constituye una buena materia prima y que las resinas derivadas de éste, una vez curadas, exhiben unas propiedades muy comparables a las de sus homólogas de origen petroquímico.[85]

En otro trabajo se describió la preparación de termoestables con altos contenido de derivados epoxi del eugenol con buenas propiedades mecánicas y capacidad de retardancia a la llama.[93]

El eugenol también ha sido empleado en la preparación de adhesivos fotocurables por reacciones tiol-eno, basados en los principios de la química sostenible[94] y como copolímeros con otros monómeros renovables en la preparación de materiales con buenas cualidades protectoras, tales como dureza, flexibilidad, adhesión, resistencia a los disolventes y absorción de agua.[95]

Una investigación reciente apunta a un derivado epoxi del eugenol, como un excelente agente diluyente en el curado de resinas comerciales, el cual contribuye a la disminución de la viscosidad del sistema y al mismo tiempo retarda el inicio de la formación de la red.[96]

Uno de los derivados del eugenol más interesanteses el bieugenol. Éste compuesto, que se muestra en la Figura 1.19, se sintetiza mediante acoplamiento oxidativo del

eugenol, por tratamiento con una mezcla acuosa de ferricianuro potásico en medio básico.[97] Sin embargo, también se encuentra presente en la naturaleza en compuestos naturales como magnolol y honokiol, que tienen importantes propiedades farmacológicas. Varios estudios han demostrado que este compuesto bifenólico presenta actividad antineoplásica, antimicrobiana, anti-inflamatoria, anti-artrítica y antiproliferativa.[98]

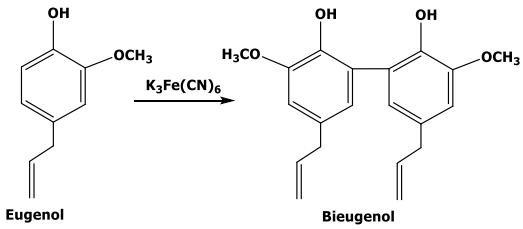

Figura 1.19. Síntesis del bieugenol

Al igual que el eugenol, este compuesto presenta una estructura química ideal como materia prima. Hasta el momento solo se han descrito dos estudios de su empleo como monómero para la preparación de termoestables, en los cuales se demuestra que este compuesto natural es una muy buena opción como sustitutivo de materiales derivados del petróleo.[99,100]

1.4. Objetivos

El objetivo final del trabajo es el desarrollo de nuevas metodologías de curado de monómeros multifuncionales, provenientes preferentemente de fuentes renovables, favorables al medio ambiente basados en los conceptos de química e ingeniería sostenible. Para avanzar hacia este objetivo final se han realizado una serie de estudios que han confluido en la aplicación de sistemas de curado dual basados en reacciones *click* tiol-eno/tiol-epoxi que han sido optimizadas para diferentes substratos comerciales. Estos sistemas desarrollados se han aplicado a la obtención de materiales termoestables basados en derivados del eugenol y otros compuestos procedentes de fuentes renovables.

La memoria se ha dividido en capítulos que, excluyendo la Introducción y las Técnicas y métodos, corresponden a objetivos concretos y que muestran los diferentes trabajos realizados y que han sido publicados o redactados en formato de artículos. Aunque cada uno de los capítulos tiene identidad en sí mismo, los resultados alcanzados se desarrollan o aplican en capítulos posteriores. Los capítulos tienen una organización común a todos ellos, que incluye el estudio del proceso de curado para los compuestos de partida seleccionados, por calorimetría diferencial de barrido, reología o espectroscopia infrarroja para seguir posteriormente con la caracterización de los materiales obtenidos mediante técnicas térmicas y mecánicas. En los capítulos en que los sistemas de curado desarrollados se aplican a compuestos procedentes de fuentes

renovables éstos incluyen un apartado de síntesis y de su correspondiente caracterización estructural.

Los objetivos concretos pueden resumirse en los siguientes puntos que corresponden a cada uno de los capítulos en el apartado de resultados en que se organiza la presente memoria:

- ✓ Estudio de nuevos catalizadores para alcanzar sistemas de curado latentes tiol-epoxi en base a resinas comerciales de diglicidiléter de bisfenol A.
- ✓ Aplicación de los sistemas latentes desarrollados a la obtención de termoestables tiol-epoxi con temperaturas de transición vítrea superiores.
- ✓ Obtención de materiales termoestables a partir de resinas epoxi cicloalifáticas comerciales con tioles de diferente estructura mediante curado latente tiol-epoxi.
- ✓ Desarrollo de un sistema controlado de curado dual tiol-eno/tiol-epoxi activado secuencialmente por irradiación con luz ultravioleta y posterior calentamiento y caracterización de los materiales intermedios y finales obtenidos.
- ✓ Aplicación del curado dual tiol-eno/tiol-epoxi desarrollado a derivados del eugenol y diferentes tioles de origen renovable. Comparación de estos materiales con los obtenidos por curado tiol-eno en una sola etapa.
- ✓ Obtención y caracterización de materiales termoestables tiol-epoxi a partir de un monómero triglicidílico derivado del eugenol con diferentes tioles de origen renovables.
- ✓ Obtención y caracterización de materiales termoestables tiol-eno y tiol-epoxi a partir de derivados del biseugenol empleando diferentes tioles de origen renovable.

1.5. Referencias

[1] H. Dodiuk, S. H. Goodman, *Handbook of thermoset plastics*, 3rd ed., Elsevier Inc, San Diego, USA, 2014.

[2] D. Lehmhus, M. Busse, A. Herrmann, K. Kayvantash, *Structural materials and processes in transportation*, Wiley –VCH, Weinheim, Germany, 2013.

[3] M. J. Forrest, *Analysis of thermoset materials, precursors and products*, Rapra Technology Ltd, Shropshire, 2003.

[4] R. S. Bauer, E. J. Marx, M. J. Watkins, *Paint and coating testing manual, ASTM publication,* Philadelphia, USA, 1995.

[5] A. Goldschmidt, H. Streitberger, *BASF Handbook on basics of coating technology*, BASF Coatings AG, Hannover, Germany, 2003.

[6] E. Petrie, *Epoxy adhesive formulations*, McGraw-Hill, New York, USA, 2006.

[7] J. Morris, *Electronics packaging forum: Vol 2*, Van Nostrand Reinhold, New York, USA, 1991.

[8] L. Guadagno, M. Raimondo, V. Vittoria, L. Vertuccio, C. Naddeo, S. Russo, B. De Vivo, P. Lamberti, G. Spinelli, V. Tucci, *RSC Advances*, 2014, 4, 15474–15488.

[9] B. Ellis, *Chemistry and technology of epoxy resins*, Blackie Academic & Professional, London, UK, 1993.

[10] C. May, G. Tanaka, *Epoxy Resins. Chemistry and technology*, Marcel Dekker Inc., New York, USA, 1988.

[11] S. L. Simon, J. K. Gillham, *Journal of Applied Polymer Science*, 1992, 46, 1245–1270.

[12] J. Lange, M. Johansson, C. T. Kelly, P. J. Halley, *Polymer*, 1999, 40, 5699–5707.

[13] H.H. Winter, *Polymer Engineering and Science*, 1987, 27, 1698-1702.

[14] R. Rothon, *Particulate-Filled Polymer Composites,* Rapra Technology Ltd., Shawbury, UK, 2003

[15] J.P. Pascault, H. Sautereau, J. Verdu, R.J.J. Williams, *Thermosetting Polymers* Marcel Dekker Inc, New York, USA, 2002.

[16] J. P. Pascault, R. J.J. Williams, *Epoxy polymers: New materials and innovations*, WILEY-VCH Verlag GmbH & Co. KGaA, Weinheim, Germany, 2010.

[17] F. Ricciardi, W. A. Romanchick and M. M. Joullié, *Journal of Polymer Science*: *Polymer Chemistry Edition*, 1983, 21, 1475-1490.

[18] I. E. Dell'Erba, R. J. J. Williams, *Polymer Engineering & Science*, 2006, 46, 351-359.

[19] B. A. Rozenberg, *Epoxy resins and composites II*, ed. K. Dušek, Springer, Berlin, Germany, 1986.

[20] X. Fernández-Francos, W.D. Cook, J.M. Salla, A. Serra, X. Ramis, *Polymer International* 2009, 58, 1401-1410.

[21] P. Kubisa, S. Penczek. *Progress in Polymer Science* 2000, 24, 1409-1437.

[22] H. Lee, K. Neville, *Handbook of epoxy resins*, McGraw-Hill Companies, New York, USA, 2008.

[23] C. Augustsson, *NM epoxy handbook*. 3rd ed. Nils Malmgren AB, Ytterby, Sweden, 2004.

[24] S. B Lee, T. Takata, T. Endo, *Macromolecules,* 1991; 24, 2689-2693.

[25] C. L. Sherman, R. C. Zeigler, N. E. Verghese, M. J. Marks, *Polymers*, 2008, 49, 1164-1172.

[26] X. Fernández-Francos, D. Santiago, F. Ferrando, X. Ramis, J. M. Salla, À. Serra, M. Sangermano, *Journal of Polymer Science Part B: Polymer Physics,* 2012, 50, 1489-1503.

[27] P. Penczek, P. Czub, J. Pielichowski, *Unsaturated polyester resins: Chemistry and technology. Crosslinking in materials science*, vol. 184, Springer-Verlag, Berlin, Germany, 2005.

[28] M. A. Tasdelen, M.U. Kahveci, Y. Yagci, *Progress in Polymer Science*, 2011, 36, 455-567.

[29] P. Vancaeter, E. J. Goethals, *Trends in Polymer Science*, 1995, 3, 227-233.

[30] X. Ramis, X. Fernández-Francos, S. De la Flor, F. Ferrando, A. Serra, *Click-Based Dual-Curing Thermosets, in Thermosets,* 2nd ed., Guo, Q. Ed.; Elsevier, Amsterdam, 2017, Chap. 9.

[31] H. C. Kolb, M. G. Finn, K. B. Sharpless, *Angewandte Chemie International*, 2001, 40, 2005-2021.

[32] W. H. Binder, R. Sachsenhofer, *Macromolecular Rapid Communications*, 2008, 29, 952-981.

[33] G. Lahann, *Click Chemistry for Biotechnology and Materials Science*. Wiley, Chichester, UK, 2009.

[34] G. Franc, A. K. Kakkar, *Chemistry -A European Journal*, 2009, 15, 5630-5639.

[35] B. Voit, *New Journal of Chemistry*, 2007, 31, 1139-1151.

[36] G. Kumaraswamy, K. Ankamma, A. Pitchaiah, *Journal of Organic Chemistry*, 2007, 72, 9822–9825.

[37] A. Lowe, C. Bowman, *Thiol-X chemistries in polymer and materials science*, RSC publishing, Cambridge, UK, 2013.

[38] K. L. Heredia, Z. P, Tolstyka, H. D. Maynard, *Macromolecules*, 2007, 40, 4772-4779.

[39] C. E. Hoyle, A. B. Lowe, C. N. Bowman, *Chemical Society Reviews*, 2010, 39, 1355–1387.

[40] C. E. Hoyle, T. Y. Lee, T. Roper, *Journal of Polymer Science Part A: Polymer Chemistry*, 2004, 42, 5301–5338.

[41] S. P. S. Koo, M. M. Stamenovic, R. A. Prasath, A. J. Inglis, F. E. Du Prez, C. Barner-Kowollik, W. Van Camp, T. Junkers, *Journal Polymer Science Part A: Polymer Chemistry*, 2010, 48, 1699–1713.

[42] S. Chandrasekaran, *Click reactions in organic synthesis*, Wiley-VCH Verlag GmbH & Co. KGaA, Weinheim, Germany, 2010.

[43] N. B. Cramer, T. Davies, A. K. O'Brien, C. N. Bowman, *Macromolecules*, 2003, 36, 4631–4636.

[44] C. R. Morgan, F. Magnotta, A. D. Ketley, *Journal of Polymer Science Part A: Polymer Chemistry*, 1977, 15, 627–645.

[45] B. H. Northrop, R. N. Coffey, *Journal of the American Chemical Society*, 2012, 134, 13804-1381.

[46] H. Lu, J. A. Carioscia, J. W. Stansbury, C. N. Bowman, *Dental Materials,* 2005, 21, 1129-1136.

[47] K. Jin, W. H. Heath, J. M. Torkelson, *Polymer*, 2015, 81, 70-78.

[48] M. Begtrup, P. Larsen, *Acta Chemica Scandinavica*, 1990, 44, 1050-1057.

[49] S. G. Tajc, B. S. Tolbert, R. Basavappa, B. L. Miller, *Journal of the American Chemical Society*, 2004, 126, 10508-10509.

[50] R. M. Loureiro, T. C. Amarelo, S. P. Abuin, E. R. Soulé, R. J. J. Williams, *Thermochimica Acta*, 2015, 616, 79-86.

[51] X. Fernández-Francos, A-O. Konuray, A. Belmonte, S. De la Flor, A. Serra, X. Ramis, *Polymer Chemistry,* 2016, 7, 2280-2290.

[52] J. A. Carioscia, J. W. Stansbury, C. N. Bowman, *Polymer*, 2007, 48, 1526–1532.

[53] K. Dušek, M. Dušková-Smrčková, *Progress in Polymer Science*, 2000, 25, 1215-1260.

[54] G. P. J. M. Tiemersma-Thoone, B. J. R. Scholtens, K. Dušek, M. Gordon, *Journal of Polymer Science: Part B: Polymer Physics*, 1991; 29, 463-482.

[55] R. J. J. Williams, C. C. Riccardi, K. Dušek, *Polymer Bulletin*, 1991; 25, 231-237.

[56] F, Saharil, F, Forsberg, Y. Liu, P. Bettotti, N. Kumar, F. N. Haraldsson. W. v. derWijngaart, K. B. Gylfason. *Journal of Micromechanics and Microengineering*, 2013; 23, 025021.

[57] C. N. Bowman, C. J. Kloxin. *AIChE Journal*, 2008, 54, 2775-2795.

[58] C. F. Carlborg, A. Vastesson, L. Yitong, W. van der Wijngaart, M. Johansson, T. Haraldsson, *Journal Polymer Science: Part A: Polymer Chemistry*, 2014, 52, 2604–2615.

[59] D. E. Newton, *Chemistry of the environment*, Facts on file, Inc, New York, USA, 2007.

[60] O. Ogunseitan. *Green health: An A-to-Z Guide,* SAGE publications Inc, California, USA, 2011.

[61] I. T. Horvath; P. T. Anastas, *Chemical Reviews*, 2007, 107, 2167-2168.

[62] Sanjay K. Sharma, Ackmez Mudhoo, *Green chemistry for environmental sustainability*, CRC press, Taylor & Francis group, New York, USA, 2011.

[63] M. A. A. Abraham, *Sustainability science and engineering: Defining principles,* Elsevier B.V, Amsterdam, Netherlands, 2006.

[64] M. Doble, K. Rollins, A. Kumar. *Green chemistry and engineering*, Elsevier Inc, San Diego, USA, 2007.

[65] P. T. Anastas, J. C. Warner, *Green chemistry:Theory and Practice*, Oxford University Press, New York, USA, 1998.

[66] P. T. Anastas, N. Eghbali, *Chemical Society Reviews.,* 2010, 39, 301-312.

[67] P. T. Anastas, M. M. Kirchhoff, *Accounts of Chemical Research*, 2002, 35, 686-694.

[68] A. Dicks, A. Hent, *Green chemistry metrics: A guide to determining and evaluating process greenness*, Springer, New York, USA, 2015.

[69] J. Salimon, N. Salih, E. Yousif, *Arabian Journal of Chemistry,* 2012, 5, 135–145.

[70] H. Janik, M. Sienkiewicz, J. Kucinska-Lipka, *Handbook of thermoset plastics*, Elsevier Inc, San Diego, USA, 2004.

[71] H. Panda, *Epoxy resins technology handbook* (Manufacturing process, synthesis, Epoxy adhesives and epoxy coatings), Asia pacific business press Inc., Delhi, India. 2016.

[72] P. Stansinoupolos, M. H Smith. *Whole system design: An integrated approach to sustainable engineering,* Vol. 10, Earthscan, London, UK, 2009.

[73] E. A. Baroncini, S. K. Yadav, G. R. Palmese, J. F. Stanzione, *Journal of Applied Polymer Science,* 2016, 133, 44103.

[74] J.-M. Raquez, M. Deléglise, M.-F. Lacrampe, P. Krawczak, *Progress in Polymer Science*, 2010, 35, 487-509.

[75] F. Fatemeh, Y. Zhongshun, A. Mark, X. Chunbao, *Thermochimica Acta*, 2015, 618, 48-55.

[76] M. Fache, B. Boutevin, S. Caillol, *ACS Sustainable Chemistry & Engineering*, 2016, 4, 35-46.

[77] M. Fache, B. Boutevin, S. Caillol, *European Polymer Journal*, 2015, 68, 488-502.

[78] H. Minghui, J. Shun, X. Ruixin, Y. Jianwen, Z. Zhaohua, C. Guangxue, *Progress in Organic Coatings*, 2014, 77, 868-871.

[79] C. Aouf, S. Benyahya, A. Esnouf, S. Caillol, B. Boutevin, H. Fulcrand, *European Polymer Journal*, 2014, 55, 186-198.

[80] S. Benyahya, C. Aouf, S. Caillol, B. Boutevin, J. P. Pascault, H. Fulcrand, *Industrial Crops and Products*, 2014, 53, 296-307.

[81] F. Hu, J. J. La Scala, J. M. Sadler, G. R. Palmese, *Macromolecules*, 2014, 47, 3332-3342.

[82] M. Ionescu, D. Radojčić, X. Wan, Z. S. Petrović, T. A. Upshaw, *European Polymer Journal*, 2015, 67, 439-448.

[83] S. Ma, X. Liu, Y. Jiang, Z. Tang, C. Zhang, J. Zhu, *Green Chemistry,* 2013, 15, 245-254.

[84] K. Chaieb, H. Hajlaoui, T. Zmantar, A. B. Kahla-Nakbi, M. Rouabhia, K. Mahdouani, A. Bakhrouf, *Phytotherapy Research*, 2007, 21, 501-506.

[85] T. S. Kaufman, *Journal of the Brazilian Chemical Society*, 2015, 26, 1055-1085.

[86] V. A. Parthasarathy, B. Chempakam, T. J Zachariah, *Chemistry of spices*, CAB International, London, UK, 2008.

[87] P. Prakash, N. Gupta, *Indian Journal of Physiology and Pharmacology*, 2005, 49, 125131.

[88] C. Cheng, X. Zhang, X. Chen, J. Li, Q. Huang, Z. Hu, Y. Tu, *Journal of Polymer Research*, 2016, 23, 110.

[89] T. Yoshimura, T. Shimasaki, N. Teramoto, M. Shibata. *European Polymer Journal*, 2015, 67, 397-408.

[90] J. Qin, H. Liu, P. Zhang, M. Wolcott, J. Zhang, *Polymer International* 2014, 63, 760-765.

[91] P. Thirukumaran, A. S. Parveen, M. Sarojadevi. *Polymer Composites* 2015, 36, 1973-1982.

[92] L. Rojo, B. Vazquez, J. Parra, A. López Bravo, S. Deb, J. San Roman, *Biomacromolecules* 2006, 7, 2751-2761.

[93] J. Wan, B. Gan, C. Li, J. Molina Aldagueria, E.N. Kalali, X. Wang, D. Wang, *Chemical Engineering Journal* 2016, 284, 1080-1093.

[94] B. R. Donovan, J. S. Cobb, E. F. T. Hoff, D. L. Patton, *RSC Advances*, 2014, 4, 61927-61935.

[95] J. Dai, Y. Jiang, X. Liu, J. Wang, J. Zhu, *RSC Advances*, 2016, 6, 17857-17866.

[96] A. Maioran, L. Yue, I. Manas-Zloczower, R. Gross, *Journal of Applied Polymer Science,* 2016, 133, 43635.

[97] A. de Farias Dias. *Phytochemistry,* 1988, 27, 3008-3009.

[98] L. C. Rodrigues, J. M. Barbosa-Filho, M. R. de Oliveira, P. Lima do Nascimento Néris, F. V. Pereira Borges, R. Mioso, *Chemistry & Biodiversity*, 2016, 13, 870-874.

[99] M. Shibata, N. Tetramoto, A. Imada, M. Neda, S. Sugimoto, *Reactive & Functional Polymers*, 2013, 73, 1086-1095.

[100] M. Neda, K. Okinaga, M. Shibata, *Materials Chemistry and Physics*, 2014, 148, 319-327.

UNIVERSITAT ROVIRA I VIRGILI
NUEVOS PROCESOS DE CURADO CLICK CON TIOLES Y SU APLICACIÓN A LA PREPARACIÓN DE MATERIALES BASADOS EN EUGENOL
Dailyn Guzmán Meneses

UNIVERSITAT ROVIRA I VIRGILI
NUEVOS PROCESOS DE CURADO CLICK CON TIOLES Y SU APLICACIÓN A LA PREPARACIÓN DE MATERIALES BASADOS EN EUGENOL
Dailyn Guzmán Meneses

CAPÍTULO 2

Técnicas de análisis

UNIVERSITAT ROVIRA I VIRGILI
NUEVOS PROCESOS DE CURADO CLICK CON TIOLES Y SU APLICACIÓN A LA PREPARACIÓN DE MATERIALES BASADOS EN EUGENOL
Dailyn Guzmán Meneses

2.1. Resonancia magnética nuclear (RMN)

La espectroscopia de resonancia magnética nuclear es una técnica analítica usada para determinar la estructura molecular de un compuesto químico, así como también para confirmar la pureza de la muestra.

La RMN está basada en el principio de que los núcleos estudiados tienen espines y que los núcleos activos de la estructura tienen un distinto entorno electrónico. Al aplicar un campo magnético externo, se produce una transferencia de energía entre el nivel más bajo y un nivel energético superior. Esta transferencia de energía ocurre a una longitud de onda que corresponde a la zona de las radiofrecuencias y cuando el espín retorna a su nivel inicial, se emite energía en la misma zona de radiofrecuencias. La señal emitida es medida y procesada para generar un espectro de RMN.[1]

Los espectros de RMN de ^{1}H y ^{13}C de los diferentes compuestos sintetizados fueron obtenidos empleando un espectrómetro Varian Mercury VX400 y un Varian NMR System 400 (ver Figura 2.1), con el fin de elucidar y confirmar sus estructuras químicas. En todos los casos se empleó $CDCl_3$ como disolvente. Las mediciones de RMN ^{1}H se realizaron a una frecuencia de 400 MHz, bajo las siguientes condiciones experimentales 1 s de tiempo de espera entre pulsos (D1) y 14 acumulaciones. Para el RMN ^{13}C la frecuencia de trabajo es de 100.6 MHz y se usaron un D1 de 0.5 s y 0.2 s de tiempo de adquisición. Para los dos núcleos se empleó el tetrametilsilano (TMS) como referencia.

Figura 2.1. Imágenes de los equipos de RMN usados para la determinación estructural

2.2. Infrarrojo con transformada de Fourier (FT-IR)

En la espectroscopia infrarroja, la radiación IR se hace incidir sobre una muestra, en este proceso algunas ondas son absorbidas y otros pasan a través de la muestra, obteniendo de esta manera un espectro de absorción y transmisión. La espectroscopia de infrarrojos ha sido una técnica muy importante para el análisis de materiales. Un espectro IR representa una huella dactilar de una muestra. El término transformada de Fourier se relaciona con el hecho de que se requiere un proceso matemático (transformada de Fourier) para convertir los datos originales en el espectro FT-IR.[2]

Dado que la absorbancia obtenida a partir de las señales del espectro FT-IR está relacionada con la concentración de diferentes grupos funcionales a través de la ley de Lambert-Beer, el proceso de curado puede ser seguido utilizando la expresión:

$$A = \varepsilon x\ CxL \qquad (2.1)$$

donde *A* es la absorbancia de una especie a una cierta frecuencia, ε es el coeficiente de absorbitividad, *C* es la concentración de la especie y *L* es la vía óptica.

La espectroscopia de IR es una herramienta útil para el seguimiento de ciertas reacciones mediante la monitorización de las señales correspondientes a los diferentes grupos reactivos involucrados. En este sentido, es posible seguir el entrecruzamiento de polímeros o monómeros, controlando las señales de los grupos que participan en la reacción antes y después del proceso de curado. Debido al hecho de que la absorbancia es proporcional a la vía óptica, *L*, es necesario normalizar la banda principal con respecto a una banda de referencia que permanece inalterada durante el proceso de curado. De este modo, la conversión *X*, determinada por las mediciones FT-IR puede escribirse como sigue:

$$X = 1 - \frac{\overline{A^t}}{\overline{A^o}} \qquad (2.2)$$

donde $\overline{A^t}$ es la absorbancia normalizada a un tiempo t y $\overline{A^o}$ es la absorbancia inicial correspondiente al máximo.

Se usaron dos dispositivos FT-IR diferentes. Para los procesos de curado térmico, las muestras curadas y no curadas se analizaron con un espectrómetro FTIR Jasco FTIR con un accesorio de reflexión total atenuado con control térmico y cristal de diamante (Golden Gate Heated Single Reflection Diamond ATR, Specac-Teknokroma). Los espectros se recogieron a diferentes temperaturas, resoluciones y rangos de longitud de onda descritos en detalle en los capítulos correspondientes.

En el caso de muestras curadas con UV, las formulaciones son expuestas simultáneamente al haz UV, que induce la polimerización, y al haz IR, que analiza in situ el desarrollo de la reacción. Para ello se utilizó un dispositivo FTIR Bruker Vertex 70 con un accesorio de reflexión total atenuado con control térmico (capaz de enfriarse con nitrógeno líquido) equipado con una lámpara de mercurio de presión media Hamamatsu Lightningcure LC5 con una guía óptica y una intensidad de luz en la superficie de la muestra de aproximadamente 5 $mW.cm^{-2}$. Ambos dispositivos se pueden observar en la Figura 2.2.

Figura 2.2. Equipos de FT-IR empleados en el seguimiento de las reacciones fotoquímicas (izquierda) y térmicas (derecha)

2.3. Calorimetría diferencial de barrido (DSC)

La calorimetría diferencial de barrido es la técnica más empleada en el estudio térmico de los polímeros, y se basa en la diferencia del flujo de calor entre una sustancia y una referencia en función de la temperatura, mientras que la muestra se somete a un programa de temperatura controlada. Entre las aplicaciones del DSC deben mencionarse la determinación fácil y rápida de la temperatura de transición vítrea, de las temperaturas de fusión y cristalización, calores de fusión y de reacción, determinación de pureza, así como la caracterización de termoestables y mediciones de temperaturas y entalpías de las transiciones de cristal líquido.[3]

Para realizar los diferentes estudios calorimétricos se emplearon los siguientes equipos: Mettler DSC821e equipado con un brazo robótico TSO801RO para realizar análisis de DSC desde temperatura ambiente hasta altas temperaturas y Mettler DSC822e con un sistema de enfriamiento por nitrógeno líquido para realizar mediciones a bajas temperaturas.

Ambos equipos fueron calibrados con un estándar de indio (calibración del flujo del calor) y un estándar de plomo-zinc-indio (calibración de la temperatura). Las muestras fueron preparadas en cápsulas de aluminio empleando de 5 a 10 mg. La Figura 2.3 muestra los calorímetros usados.

2.3.1 Estudio de la cinética de curado

La cinética de curado es una relación matemática entre tiempo, temperatura y conversión. En el estudio cinético por DSC, el calor liberado durante la reacción se asume que es proporcional al grado de conversión.[3] Adicionalmente, la velocidad de curado (*dx/dt*) es directamente proporcional al calor liberado (*dH/dt*). Cuando se completa la reacción, la integral relacionada con la señal obtenida produce el calor liberado total ΔH_{tot}. La velocidad de reacción y el grado de conversión se pueden calcular mediante la siguiente expresión:

$$\frac{dx}{dt} = \frac{dH/dt}{\Delta H\ total} = \frac{dh/dt}{\Delta h\ total} \qquad (2.3)$$

$$X = \frac{\Delta Ht}{\Delta H\ total} = \frac{\Delta ht}{\Delta h\ total} \qquad (2.4)$$

donde *dh/dt* y Δh_{tot} son la velocidad de liberación de calor y el calor total liberado normalizado con respecto al tamaño de la muestra, ΔH_t es el calor liberado hasta un tiempo *t*, y *Δht* es el calor liberado normalizado con respecto al tamaño de la muestra. Finalmente, *X* es el grado de curado, y también puede expresarse como α.

La cinética de un sistema puede estudiarse en condiciones isotérmicas o dinámicas. Los estudios dinámicos presentan más ventajas en comparación con los experimentos isotérmicos. Cuando se emplean condiciones isotérmicas, es posible tener pérdida de información al inicio del proceso de curado y, por otro lado, no siempre se completa el curado del material.[3]

La velocidad de reacción se expresa generalmente como *dx/dt=k f (x)* siendo k la constante cinética y *f (x)* una función dependiente de la conversión. La constante cinética, *k*, generalmente sigue la expresión de Arrhenius:

$$k = A\, e^{\frac{-E}{RT}} \qquad (2.5)$$

donde *A* es el factor pre exponencial, *E* la energía de activación, *R* la constante de los gases y *T* la temperatura absoluta.

En general, un proceso cinético está bien caracterizado si se conoce *E, A y f(x),* llamado triplete cinético. Aunque estrictamente hablando, esta metodología sólo debe ser válida para procesos de "un solo paso", también puede aplicarse en sistemas donde coexisten más de un proceso químico (o físico). Existen dos enfoques principales en el análisis cinético, los métodos isoconversionales y los métodos de ajuste del modelo. En la presente tesis sólo se ha utilizado el análisis cinético isoconversional.

La metodología isoconversional asume que la función de reacción *f(x)* es independiente de la velocidad de calentamiento β.[4] De este modo, la cinética de un proceso sólo depende del grado de conversión en un momento determinado. También requiere la realización de una serie de experimentos para determinar la energía de activación aparente. Estos experimentos pueden ser, por ejemplo, el curado dinámico a diferentes velocidades de calentamiento.

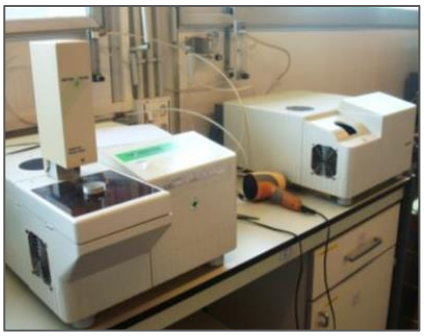

Figura 2.3. Imágenes de los equipos de DSC usados en el estudio del curado térmico

2.3.2 Temperatura de transición vítrea (Tg)

La temperatura de transición vítrea se define normalmente como la temperatura a la mitad de la diferencia de la capacidad calorífica (½ΔCp, véase la Figura 2.4). La Tg también puede tomarse como el punto de inflexión, que es ligeramente diferente y corresponde al pico en la derivada del flujo de calor o capacidad térmica en función de la temperatura.

Con el fin de determinar la Tg de los materiales preparados se realizaron experimentos de DSC en condiciones dinámicas a 20 °C/min.

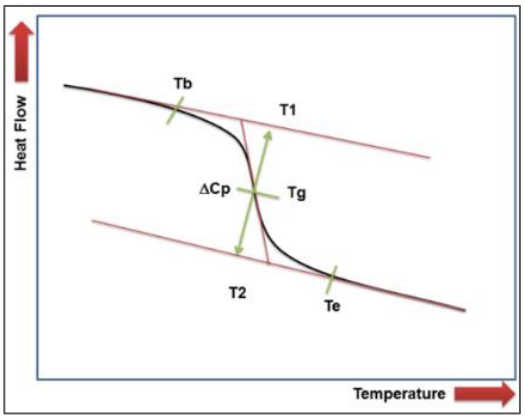

Figura 2.4. Determinación de la temperatura de transición vítrea en un experimento de calentamiento a partir de una curva DSC idealizada (endotérmica hacia abajo). Tb: inicio de la desviación de la curva DSC de la linealidad; T1: temperatura de inicio extrapolada de Tg; Tg: temperatura de transición vítrea; T2: temperatura final extrapolada de la transición vítrea; Te: temperatura final de Tg donde la dependencia de Cp pasa a ser lineal.

2.4. Fotocalorimetría (foto-DSC)

La fotocalorimetría de DSC permite medir cambios de entalpia en un material durante y después de la exposición a una luz ultravioleta, a ciertas longitudes de onda durante diferentes períodos de tiempo, bajo ciertas condiciones de temperatura.

Los experimentos fotocalorimétricos se realizaron en un Mettler DSC821e modificado para irradiar las muestras con un Hamamatsu LC5 UV con una lámpara Hg-Xe de doble haz que irradia simultáneamente tanto la muestra como la cápsula de referencia (Figura 2.5). El horno del calorímetro está cubierto con una tapa de plata con dos ventanas de cuarzo para colimar el haz de luz.

La conversión de curado se puede determinar directamente a partir de la curva foto-DSC utilizando la ecuación 2.6, o del calor restante liberado en un experimento de postcurado dinámico de la siguiente manera:

$$X = 1 - \frac{\Delta hres}{\Delta htotal} \qquad (2.6)$$

donde *Δhres* es el calor liberado en el barrido de post-curado y *Δhtotal* es un valor de referencia del calor liberado en un curado completo.

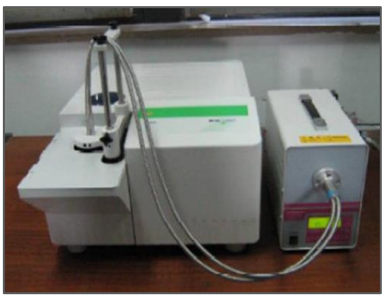

Figura 2.5. Foto-calorímetro utilizado para realizar experimentos con foto-DSC

2.5. Análisis térmico dinamomecánico (DMTA)

El análisis térmico dinamomecánico implica la imposición de una pequeña deformación cíclica en una muestra y la medición de la respuesta al esfuerzo, o, de manera equivalente, la imposición de una tensión cíclica en una muestra y la medición de la respuesta de deformación resultante. El DMTA se utiliza tanto para estudiar procesos de relajación de moléculas en polímeros como para determinar propiedades mecánicas o de flujo inherentes en función del tiempo y la temperatura.[5] En otras palabras, el DMTA estudia la naturaleza viscoelástica de un material aplicando una tensión oscilatoria con una frecuencia fija a la muestra y controlando su respuesta a diferentes temperaturas. Asimismo, se puede calcular el módulo complejo (E*) y el factor de pérdida (tan δ).

El módulo contiene contribuciones reales e imaginarias (E*= E'+ i E''). En cuanto a la parte real, E', es la medida de la respuesta elástica del material, mientras que la parte imaginaria, E'', es la respuesta viscosa. El máximo obtenido en la curva tan δ es, en la mayoría de los casos aceptado como la Tg de un material aunque cambia con la frecuencia utilizada en el experimento.

El módulo de Young también puede ser calculado por DMTA. Empleando la mordaza del tipo 3-point bending, es posible obtener el módulo de Young en una prueba de flexión no destructiva a temperatura ambiente. El módulo de elasticidad se calcula utilizando la pendiente de la curva de deformación de carga de acuerdo con la siguiente ecuación:

$$Ef = \frac{L^3 m}{4bd^3} \qquad (2.7)$$

donde *Ef* es el módulo de elasticidad de flexión (MPa); *L* es la longitud de la probeta de prueba (mm); m es el gradiente (es decir, la pendiente) de la porción de línea recta inicial de la curva de deflexión de carga (N/mm), b es el ancho (mm) y d el espesor de la probeta (mm). Para esta tesis se utilizó un TA Instruments DMA Q800 (Figura 2.6) empleando la mordaza 3-point bending sobre muestras prismáticas rectangulares previamente curadas en un molde bajo condiciones isotérmicas. Ésta técnica también fue empleada para determinar el grado de deformación de los materiales termoestables a través de ensayos de tracción usando la mordaza de tensión en probetas con forma de hueso.

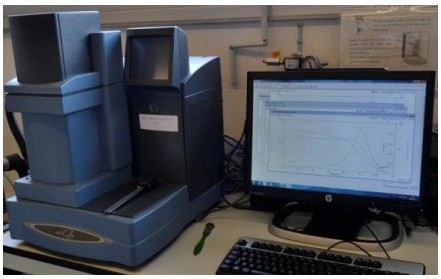

Figura 2.6. Equipo DMTA utilizado para estudiar las propiedades viscoelásticas de los termoestables preparados

2.6. Análisis termogravimétrico (TGA)

El análisis termogravimétrico es una técnica que se basa en las mediciones de masa en función de la temperatura o del tiempo, mientras que la muestra se somete a un programa de temperatura y atmósfera controlada.[6] El corazón del TGA es la termobalanza, que es capaz de medir la pérdida de masa de una muestra determinada, en función de la temperatura y el tiempo, mientras que un gas de purga que fluye a través de la balanza crea una atmósfera que puede ser inerte, oxidante o reductora. El contenido de humedad del gas de purga puede variar de seco a saturado.[7]

Para el análisis de la degradación térmica de las muestras curadas se utilizó una termobalanza Mettler TGA / SDTA 851e (Figura 2.7). En condiciones dinámicas se llevó a cabo la degradación de muestras a 10 °C/min de 30 a 600 °C bajo nitrógeno. A partir

del análisis termogravimétrico, se puede obtener la temperatura de degradación inicial (generalmente 5%), lo que indica el límite de estabilidad del material. Además, se puede obtener la temperatura de la velocidad máxima de pérdida de peso y el residuo a alta temperatura.

Figura 2.7. Termobalanza utilizada para la evaluación de la estabilidad térmica

2.7. Reología

La reología es la ciencia que estudia la deformación y el flujo de los materiales. Todos los materiales pueden fluir, aunque depende del tiempo de observación. En el caso de los polímeros, en tiempos de procesamiento muy cortos puede comportarse como un sólido, mientras que en largos tiempos de procesamiento el material puede comportarse como un fluido. Esta naturaleza dual (fluido-sólido) se conoce como comportamiento viscoelástico.[8]

La viscosidad es una de las propiedades de flujo más importantes que se miden por reometría, y se define como la resistencia que tiene un material determinado a fluir. Estrictamente hablando, es la resistencia a la cizalla y puede definirse como la relación entre el esfuerzo cortante impuesto y la velocidad de cizalla. De este modo, las mediciones reológicas se basan en el control de la tensión generada en la muestra como respuesta a la aplicación de una fuerza de cizalla oscilante.[8]

La viscosidad compleja (η*) se determina en experimentos multi-frecuencia a una cierta temperatura y amplitud. Esta amplitud debe estar comprendida dentro del intervalo de viscoelasticidad linea

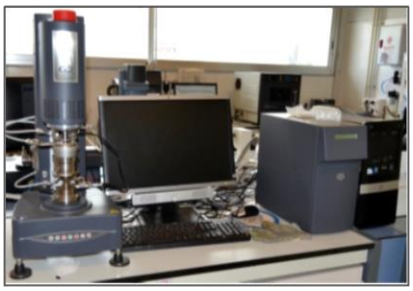

Figura 2.8. Reómetro ARG2 usado en la determinación de las viscosidades de las diferentes formulaciones

2.8. Microindentación

Un ensayo de microindentación es un ensayo no destructivo que determina la resistencia del material a la penetración.[9] Consiste en hacer penetrar en la muestra pulida un indentador de diamante bajo la acción de una carga estática durante un tiempo determinado (entre 10 y 15 s) y medir la superficie de la huella resultante tras retirar la carga. Es especialmente útil para muestras de pequeño espesor (recubrimientos) o bien de pequeñas dimensiones que requieren fuerzas de penetración inferiores a 9.8 N. En el caso específico de microdureza Vickers, el penetrador es piramidal de base cuadrada. Realizada la huella, la dureza del material se puede obtener midiendo la longitud de las dos diagonales (d1 y d2) y obteniendo la longitud media d. La dureza se obtiene a partir de la siguiente ecuación:

$$HV = \frac{1.8453 \cdot F}{d^2} \qquad (2.8)$$

donde *F* es la fuerza de penetración en kgf y *d* la media aritmética de la longitud de las dos diagonales medidas en mm.

Para evaluar la dureza de cada uno de los materiales trabajados se utilizó un Microdurómetro Wilson Wolpert 401 MVA con un indentador MicroVickers de peso variable entre 10 gf y 1000 gf y siguiendo el procedimiento estándar de ASTM E384-16. Para reducir al mínimo la incertidumbre en el resultado, se realizaron al menos 10 medidas con un nivel de confianza del 95%. La Figura 2.9 muestra la apariencia del microindentador utilizado.

Figura 2.9. Medidor de microdureza utilizado para la determinación de la dureza Vickers de los termoestables preparados

2. 9. Referencias

1 M. Balci, *Basic ^{1}H and ^{13}C-NMR Spectroscopy, Elsevier B. V*, Ankara, Turkey, 2005.
2 P. R. Griffiths, J. A. de Haseth, *Fourier Transform Infrared Spectrometry*, John Wiley & Sons, Hoboken, USA, 2006.
3 A. Turi, *Thermal Characterization of Polymeric Materials*, 2nd edition, Academic Press, San Diego, USA, 1997.

[4] S. Vyazovkin, C. A. Wight, *Thermochimica Acta*, 1999, 340-341, 53-68.
[5] R. P. Chartoff, J. D. Menczel, S. H. Dillman, *Thermal Analysis of Polymers*, John Wiley & Sons, Hoboken, USA, 2008, chapter 5.
[6] C. M. Earnest, *Compositional Analysis by Thermogravimetry*, ASTM, Philadelphia, USA, 1988.
[7] R. B. Prime, H. E. Bair, S. Vyazovkin, P. K. Gallagher, A. Riga, *Thermal Analysis of Polymers*, John Wiley & Sons, Hoboken, USA, 2008, chapter 3.
[8] A.Y. Malkin, A.I. Isayev, *Rheology: Concepts, Methods & Applications*, ChemTec, Toronto, USA, 2006.
[9] R. Brown, *Handbook of Polymer Testing-Short-Term Mechanical Tests*, Rapra Technology, Crewe, UK, 2002.

UNIVERSITAT ROVIRA I VIRGILI
NUEVOS PROCESOS DE CURADO CLICK CON TIOLES Y SU APLICACIÓN A LA PREPARACIÓN DE MATERIALES BASADOS EN EUGENOL
Dailyn Guzmán Meneses

UNIVERSITAT ROVIRA I VIRGILI
NUEVOS PROCESOS DE CURADO CLICK CON TIOLES Y SU APLICACIÓN A LA PREPARACIÓN DE MATERIALES BASADOS EN EUGENOL
Dailyn Guzmán Meneses

CAPÍTULO 3

European Polymer Journal, 2014, 59, 377–386

New catalysts for diglycidyl ether of bisphenol A curing based on thiol epoxy reaction

Dailyn Guzmán, Xavier Ramis, Xavier Fernández-Francos, Angels Serra

UNIVERSITAT ROVIRA I VIRGILI
NUEVOS PROCESOS DE CURADO CLICK CON TIOLES Y SU APLICACIÓN A LA PREPARACIÓN DE MATERIALES BASADOS EN EUGENOL
Dailyn Guzmán Meneses

New catalysts for diclycidyl ether of bisphenol A curing based on thiol-epoxy click reaction

Abstract

The thiol-epoxy click reaction has been employed in the curing of diglycidylether of bisphenol A (DGEBA) using latent amine precursors in ratios of 0.5 and 2 phr. The kinetics of the curing of mixtures of DGEBA/thiol/amine precursor was studied by calorimetry under isothermal and non-isothermal conditions. The latent characteristics of the formulations containing amine precursors were investigated by rheometry and calorimetry. The thermal stability of the thermosets and their thermomechanical characteristics were evaluated by thermogravimetry and dynamomechanical analysis. The new formulations were compared with those containing benzyl dimethyl amine or 1-methylimidazole as catalysts. The use of amine precursors in these systems extended the pot-life of the formulations and permitted a better control of the curing process.

Keywords: Thiol, epoxy resin, latency, pot-life, crosslinking.

Introduction

The so-called “click chemistry” incorporates a new generation of chemical reactions under the concept of ideal synthesis characterized by: efficiency, versatility, and selectivity.[1,2,3]Click reactions have been classified in the following categories:(a) cycloadditions of unsaturated compounds (e.g. Diels–Alder reaction); (b) nucleophilic attacks to strained heterocycles (epoxides, aziridines, etc.);(c) carbonyl chemistry of the non-aldol type (formation of ureas, thioureas, hydrazones, etc.) and d) additions to carbon-carbon multiple bonds (thiol-ene, Michael additions, etc.).[2,4,5]

Among click reactions, thiol-epoxy is very interesting because leads to the formation of hydroxyl and thioether groups in a single step, which can be further transformed to reach complex structures.[6] Thiols react with epoxides in a base catalyzed addition reaction through a nucleophilic attack to the less steric hindered carbon, as shown in the Scheme 1. The amine catalyst helps to transform the thiol to thiolate anion, which is the true nucleophile that opens the epoxy ring.[7] The alkoxide formed can regenerate the thiolate anion from the remaining thiol groups by a base-acid equilibrium and the reaction further proceeds until completion.[8,9]

Thiol-epoxy reactions have been applied to the preparation of polymers. Khan et al. reported the use of this reaction for the preparation of linear polymers with free hydroxyl groups, using 1,2-ethanedithiol and 1,4-butanediol diglycidyl ether.[10] The same group proposed the preparation of high molecular weight poly(β-hydroxythio-ether)s,[11] hydrogels[12] or even hyperbranched polymers by AB_2 methodology.[13] However, they used typical bases as LiOH or DBU or tetrabutylammonium fluoride to catalyze the thiol-epoxy

reaction and the polymerization occurs at room temperature or at temperatures not higher than 70 °C.

The crosslinking of pure epoxy resins to form a network is a very complex process, and it is impossible to give a definitive structure for the final product. The properties and performance of epoxy resins are dependent on the type of epoxy resin, the curing agent, and curing conditions. Although thiols have been scarcely studied as epoxy curing agents they seem interesting because of the type of networks formed.[14] Frey et al.[15] reported the ability of thioethers to complex metals and therefore thioether networks can be considered as ideal to prepare metal nanocomposites. Moreover, thiol-epoxy materials are already used in the adhesives industry.[1,16]

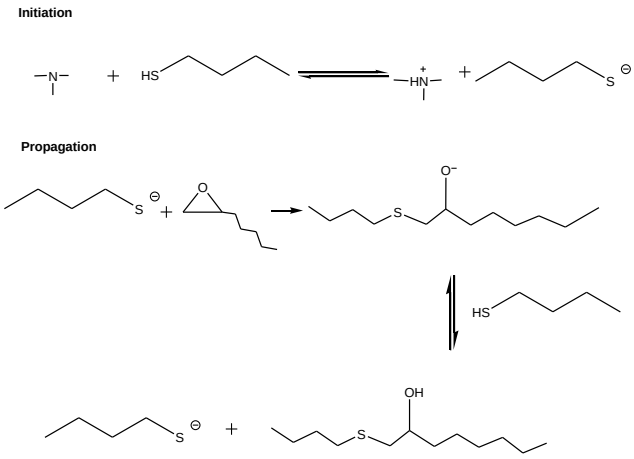

Scheme 1. Reaction mechanism of the thiol-epoxy catalyzed by amine

One of the major drawbacks of tertiary amine catalyzed thiol-epoxy formulations is their fast initial curing, leading to a short pot-life.[9] In this respect, latent amine precursors could be ideal to solve this limitation. Latent catalysts are those that show no activity under normal conditions but become active through external stimulation. These stimuli are usually heating and photoirradiation.[17] Thermal stimulation is easier from the technological point of view, because it allows a complete curing avoiding vitrification and can be used for the curing of thick samples or samples with complex shapes. Latent curing agents simplify the technological curing process because they allow the preparation of one-pot curing mixtures. Thermal latent curing agents can act mainly by two different mechanisms: the first one is based on their compatibility in epoxy resin because of their crystalline character or encapsulation of the active species.[18] The second mechanism is based on the use of a precursor compound, inactive at room temperature, but which under triggering by heat it transforms into an active curing agent.[19] Since amines are needed in the catalysis of thiol-epoxy reactions, latent systems able to release amines can be of interest to increase pot-life of these curing systems. Alternatively, Sangermano et

al.[20] proposed the use of photo-activated amine precursors in the preparation of thiol-cycloaliphatic epoxy/sol-gel hybrid materials.

The motivation for studying the thermal curing of thiol–epoxy formulations is the thermal stability, low toxicity, high adhesion and exceptional transparency and appearance of the resulting materials. In addition to these special characteristics, thiol-epoxy systems can be combined with thiol-ene processes, both with click characteristics, to prepare one-pot dual curing systems with photo- and thermal curing conditions that should lead to versatile materials, based on the structure and stoichiometry.[21,22] However, the thermal thiol-epoxy reaction catalyzed by tertiary amines takes place so fast that there is no possibility of producing B-stageable materials by sequential thiol-ene followed by thiol-epoxy reaction. A true B-stageable character requires that the material is stable after the first stage and therefore a latent catalyst is required in the second stage of the curing process.

In this work, a 3-functional thiol was used to cure diglycidyl ether of bisphenol A resin (DGEBA) with different amines and amine precursors as accelerators of this process. The kinetics of the process was studied by calorimetry and the latent character was tested by the evolution of viscosities by rheometry. The materials obtained were characterized by thermogravimetry and thermomechanical studies. The new proposed formulations were compared with benzyl dimethyl amine or 1-methylimidazole catalyzed DGEBA/thiol formulations to investigate the advantages of the amine precursors, especially with regards to pot-life, latency and curing kinetics.

Experimental part

Materials

Diglycidylether of bisphenol A (DGEBA, GY240, Huntsman, epoxy equivalent 182 g/eq) was dried at 80 °C under vacuum for 6h. The amine precursors were Technicure®LC-80 (is an encapsulated imidazole) and Technicure®PDU-250 (N,N-dimethyl phenyl urea) both from AC Catalysts. Benzyl dimethylamine (BDMA, Huntsman), 1-methylimidazole (1-MI) and trimethylol propane tris (3-mercaptopropionate) were supplied by Sigma Aldrich. All these products were used as received.

Preparation of the curing mixtures

The mixtures were prepared by mixing stoichiometric proportions (1:1) of epoxide and thiol (3 mol of DGEBA by 2 mol of trithiol). In catalyzed formulations, 0.5 and 2 phr (parts of catalyst for hundred parts of epoxy resin) was added after homogenization of DGEBA/trithiol mixture with a spatula and then magnetic stirring.

Characterization techniques

A differential scanning calorimeter (DSC) Mettler DSC-821e calibrated using an indium standard (heat flow calibration) and an indium-lead-zinc standard (temperature

calibration) was used to determine the kinetics of the curing process. Samples of ca. 10 mg were analyzed under isothermal and non-isothermal conditions under a constant N_2 atmosphere with a gas flow of 100mL/min. The dynamic studies were performed in the temperatures range of 30-300 °C, with a heating rate of 2,5,10 and 20 °C min^{-1}, whereas the isothermal experiments were carried out at temperatures of80 and 120 °C.

The glass transition temperatures (T_{gs}) of the cured samples were determined in a dynamic scan at 10 °C/min starting at -100 °C in a Mettler DSC-822e device.

The degree of conversion by DSC is calculated as follows:

$$\alpha = \frac{\Delta h_T}{\Delta h_{dyn}} \qquad (1)$$

where Δh_T is the heat released up to a temperature *T* or up to a time *t*, obtained by integration of the calorimetric signal up to this temperature or time, and Δh_{dyn} is the total reaction heat associated with the complete conversion of all reactive groups.

The curing kinetics of non-isothermal DSC curing experiments was analyzed by means of isoconversional integral and Coats-Redfern procedures applied to non-isothermal DSC data.[23,24,25]

The isoconversional activation energy at different degrees of conversion *x* was determined from multiple heating rate experiments using the Kissinger-Akahira-Sunose method:

$$\ln\left(\frac{\beta}{T^2}\right) = \ln\left(\frac{A \cdot R}{g(x) \cdot E}\right) - \frac{E}{R \cdot T} \qquad (2)$$

Where β is the heating rate, *A* is the pre-exponential factor, *E* is the activation energy and *g(x)* is an integral function corresponding to the kinetic model. The representation of $ln(\beta/T^2)$ in front of $-1/RT$ for the experimental results should produce a straight line, in which the slope of the line is related to *E*, the activation energy of the process, and the ordinate in the origin is related to the pre-exponential factor, *A*, and to the kinetic model, represented by the function *g(x)*.

The kinetic model was determined by using the Coats-Redfern equation:

$$\ln\left(\frac{g(x)}{T^2}\right) = \ln\left(\frac{A \cdot R}{\beta \cdot E}\right) - \frac{E}{R \cdot T} \qquad (3)$$

For a given kinetic model, linear representative of $ln(g(x)/T^2)$ *vs* T^{-1} makes it possible to determine *E* and *A*. We selected the kinetic model that had the best linear correlation in equation (3) and that had an *E* value similar to the obtained by KAS procedure

determined without knowing the kinetic model. Details of the kinetic methodology are given in previous studies.[20,21]

The time needed to reach a given conversion in an isothermal experiment can be determined from the results of the isoconversional analysis of non-isothermal experiments using the following expression:

$$\ln t = \ln\left(\frac{g(x)}{A}\right) + \frac{E}{R \cdot T} \qquad (4)$$

The thermal stability of cured samples was studied by thermogravimetric analysis (TGA), using a Mettler TGA/SDTA 851e thermobalance. All experiments were performed under inert atmosphere (N_2 at 100 mL/min), pieces of the cured samples with an approximate mass of 8 mg were degraded between 30 and 600 °C at a heating rate of 10 K/min.

Dynamic mechanical thermal analyses (DMTA) were carried out with a TA Instruments DMA Q800 analyzer. The samples were cured isothermally in a mould at 120°C for different times between 30 and 60 min, depending on the type of amine catalysts used. Prismatic rectangular samples (15 × 7.3 × 1.4 mm^3) were analyzed by 3-point bending at a heating rate of 2 °C/min from -50 to 120 °C, using a frequency of 1 Hz and an oscillation amplitude of 20 µm.

The latency tests were performed for mixtures stored in an oven at controlled temperature of 35 °C and the viscosities were measured at different storage times. Viscosity measurements were performed in a TA Instruments ARG2 rheometer equipped with disposable parallel plates. A sample gap between 0.4 and 0.6 mm was exactly set with an accuracy of 0.001 mm. A shear rate of 100 s^{-1} was applied at 35 °C after 5 minutes of temperature stabilization. A maximum of 2 minutes was needed to measure a steady value of viscosity. The values were corrected for non-uniform stresses in the parallel plates.

The isothermal degree of conversion *(x)* reached at a selected time was determined from stored samples that were subsequently heated up at 10 °C/min to determine the residual heat Δh_{res}, using the following expression:

$$x = 1 - \frac{\Delta h_{res}}{\Delta h_{total}} \qquad (5)$$

Results and discussion

Study of the curing process

In order to check whether the advantages of the new amine precursors selected in the present work could be advantageous, we studied the thiol-epoxy curing reaction by calorimetry in isothermal and dynamic conditions. Figure 1 shows the DSC thermograms of the dynamic curing studies at 10 °C/min for mixtures with 0.5 phr of two typical amines (BDMA and 1-MI) and two amine precursors (LC-80 and PDU-250). As can be observed, in case of the mixtures containing amines as BDMA and 1-MI the reaction occurs at low temperatures, as expected from the literature reports.[9] In contrast, in mixtures containing the amine precursors LC-80 and PDU-250, higher curing temperatures were needed. In order to understand this behaviour, certain insight into the nature of LC-80 and PDU-250 is needed.

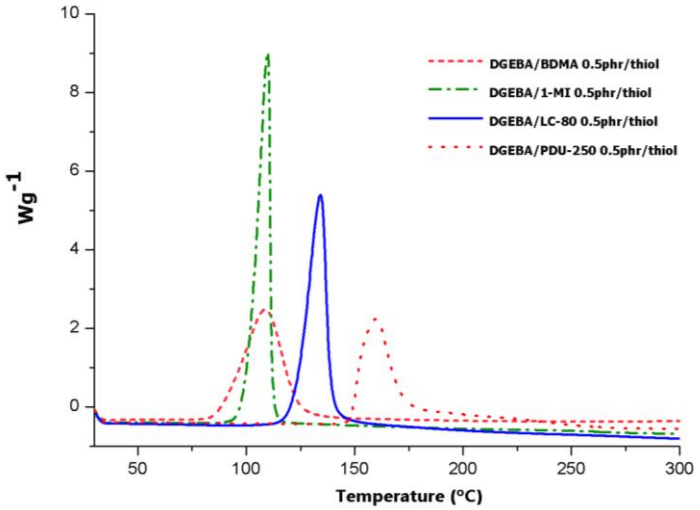

Figure 1. DSC thermograms corresponding to the dynamic curing at 10 °C/min of the mixtures epoxy resin-thiol with a proportion of 0.5 phr of the different amines and amine precursors

LC-80 is an encapsulated imidazole designed for one pot epoxy systems where a long pot life and a fast cure are required. LC-80 can be used as a curing agent or as an accelerator for dicyandiamide, anhydrides, etc., decreasing the cure temperature, while maintaining a long pot-life.[26] It has a melting point at about 65 °C and after melting the encapsulated imidazole is released and the mixture begins to cure at about 110 °C.

PDU-250, N,N-dimethyl phenyl urea, is used as an accelerator for dicyandiamide (DICY) to produce self-stable one-pot systems, combining excellent latency at ambient temperature and rapid cure. It is reported in its data sheet that at room temperature shelf life of resins compounded PDU-250 are stable for well over 4 months.[26] It has a melting point at 129-134 °C and after melting, the urea decompose, releasing N,N-dimethylamine,

which leads to curing at about 140 °C and phenyl isocyanate, as represented in Scheme 2.

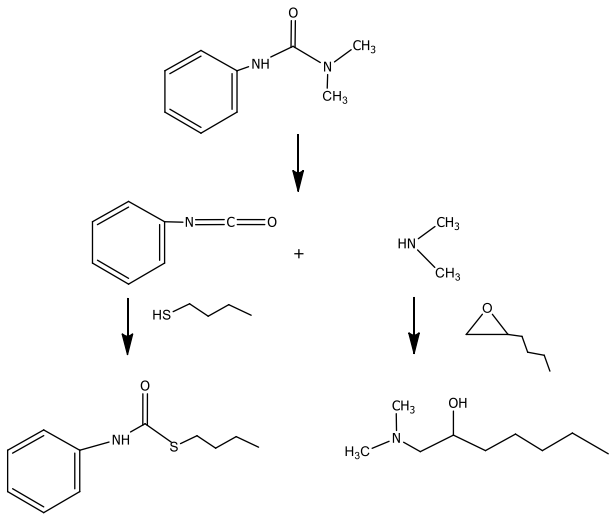

Scheme 2. Proposed mechanism to explain the decrease in the crosslinking density in PDU-250 catalyzed formulations

Therefore, it follows that unless a sufficiently high temperature is reached, release or activation of the amine catalyst does not take place in the case of LC-80 and PDU-250 and curing is prevented from taking place. It seems that the use of amine precursors such as LC-80 and PDU-250 may permit to have better control of the initiation of the thiol-epoxy click reaction. As represented in Scheme 1, amines catalyze the thiol-epoxy reaction by increasing the nucleophilicity of thiols, converting them to thiolates.

The effect of increasing the proportion of amine precursor was also tested. Figure 2 represents the DSC curves of mixtures containing 0.5 and 2 phr of the amine precursors. As we can see, the higher the proportion of amine precursor the lower the curing temperature is. Moreover, a different shape of the curve was observed for PDU-250 catalyzed formulations. A higher proportion of this compound not only reduces the curing temperature but also increases the curing rate. Moreover, when 0.5 phr of PDU-250 is used a shoulder in the calorimetric curve can be appreciated, which is eliminated when 2 phr were used. This can be rationalized in terms of a slow curing rate or incomplete curing in the presence of a too low amount of PDU-250, leading to thermal homopolymerization when the temperature was sufficiently high. From these results the need of 2 phr of PDU-250 to cure the thiol-epoxy mixture was put into evidence. temperatures. Thus, with the exception of PDU-250 0.5 phr the curing curves are sharp and begin at a defined temperature and once initiated the curing is fast. This is another indication of latent character of these systems, which opens the possibility of the preparation of one-pot formulations.

The latent character was studied by rheometric tests and DSC, and will be discussed afterwards. The effect of the proportion of precursor on the curing temperature is more noticeable in case of LC-80. From these studies it is obvious that the selection of the proportion and type of amine precursor allows the selection of the adequate curing temperature.

Table 1 shows the values of enthalpy released and the temperatures of the maximum of the calorimetric peak for the curing of all the mixtures with different amines and precursors in different proportions studied in the present work.

The values of the enthalpy released are similar for all the formulations indicating that the degree of curing achieved is also similar. Moreover, the enthalpy released by epoxy equivalent was 120-128 kJ/eq, which indicates complete curing taking into account that, for the curing epoxy-amine formulations, the reaction heat is of ca. 100-110 kJ/eq.[27,28]

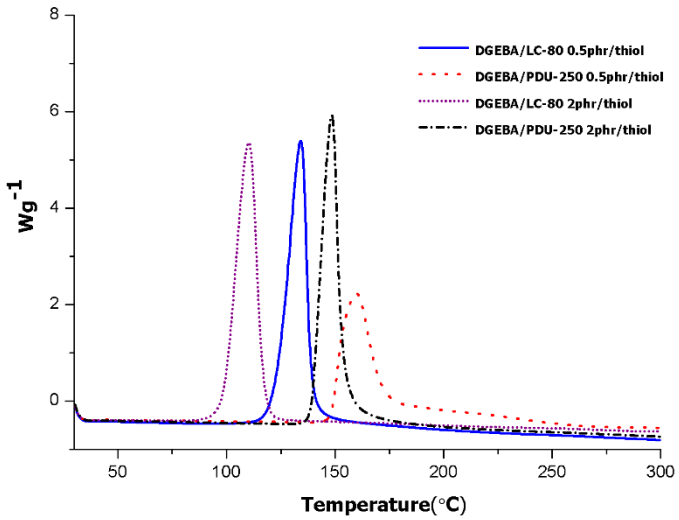

Figure 2. DSC thermograms corresponding to the dynamic curing at 10 °C/min of the mixtures epoxy resin-thiol with a different proportion of the amine precursors

Table 1. Calorimetric data and kinetic parameters obtained for the thiol-epoxy formulations containing different catalysts and proportions

Type of Catalyst	Prop. (phr)	Δh^a (J/g)	Δh (kJ/eq)	T_{max} (°C)	E^a (kJ/mol)	ln A ^{b} (min^{-1})	$k_{80°C}$ (min^{-1})	$k_{120°C}$ (min^{-1})
LC-80	0.5	394	125	134	75.2	29.97	0.0094	0.3203
LC-80	2	393	126	110	84.3	34.97	0.0599	2.799
1-MI	0.5	405	128	110	61.7	29.61	0.0728	1.9322
PDU-250	0.5	380	120	160	-		-	-
PDU-250	2	386	124	148	57.3	15.71	0.0124	0.0959
BDMA	0.5	389	123	108	32.2	13.35	0.1547	0.7277

a. Curing enthalpy measured in a DSC scan at 10 °C/min
b. ln A has been calculated using the kinetic model A_3 with $g(\alpha)=[-\ln(1-\alpha)]^{1/3}$

The evolution of the activation energy with the degree of conversion was calculated by the isoconversional method and the values obtained are represented in Figure 3. As we can see, there are no big variations in the activation energy along the curing process with the only exception of the sample prepared with 0.5 phr of PDU-250, in which the activation energy decreases continuously. Although it is generally not advised to derive mechanistic interpretations from the changes in integral isoconversional energy,[29] this different evolution can be attributed to the coexistence of the thiol-epoxy polycondensation and thermal homopolymerization curing mechanisms, as discussed above for this formulation. In the other cases, the rather constant activation energy makes it possible to derive an easy interpretation on the basis of the energy barrier, related to the temperature needed to react. Thus, the higher the activation energies the higher the temperature at which the reaction occurs. Moreover, the greater value of activation energy leads to a significantly stronger temperature dependence which is related to latent characteristics. In the upper limit, LC-80 leads to the highest energy values (between 85-75 kJ/mol) while BDMA leads to the lowest values, around 35 kJ/mol. From this point of view, LC-80 is the best candidate to reach a higher latency, whereas BDMA should have a low latent character as it is reported in the literature.[9]

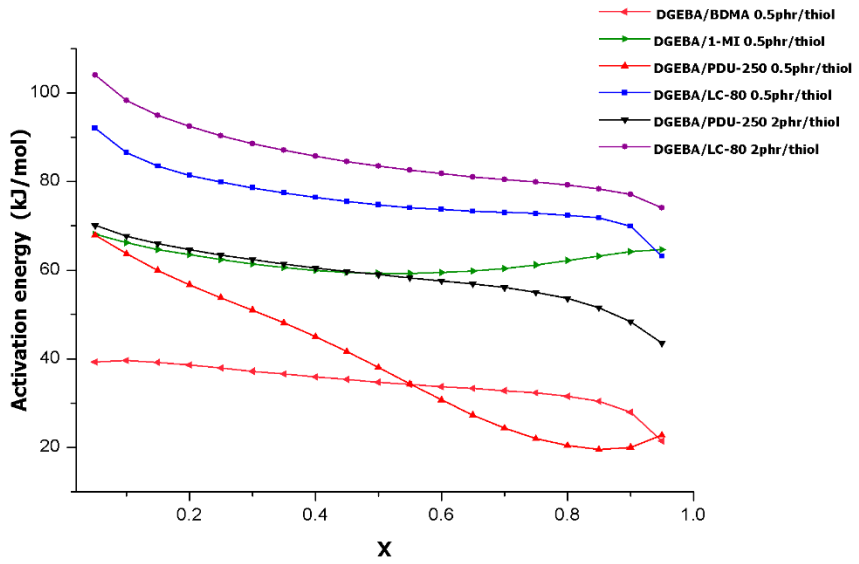

Figure 3. Activation energy *vs* degree of conversion of the epoxy resin-thiol mixtures using different amine precursors

We determined the kinetic model that best fits the experimental results according to the procedures described in the experimental part and references therein, which in these formulations was the Avrami-Erofeev model A_3. From the activation energy and the kinetic model and using the Kissinger-Akahira-Sunose equation, we could obtain the pre-exponential factor for a conversion of 0.5, which are collected in Table 1. The kinetic constants were obtained by the Arrhenius equation at the temperature of the isothermal

curing and also reported in the table. It can be seen that, at lower curing temperatures, BDMA leads to the fastest curing but, upon increasing the temperature, the curing is faster with other catalysts such as 1-MI. Due to the fact that the activation energy was not constant during curing it was not possible to find an accurate kinetic model describing the process for the formulation containing 0.5 phr of PDU-250 and therefore the kinetic data were not calculated.

The technological curing of epoxy resins is usually done in isothermal conditions. Therefore, it is interesting to study these systems by isothermal calorimetric experiments.

Figure 4 represents the curing curves obtained at 120 °C for the formulations catalyzed by the less active amine precursors.

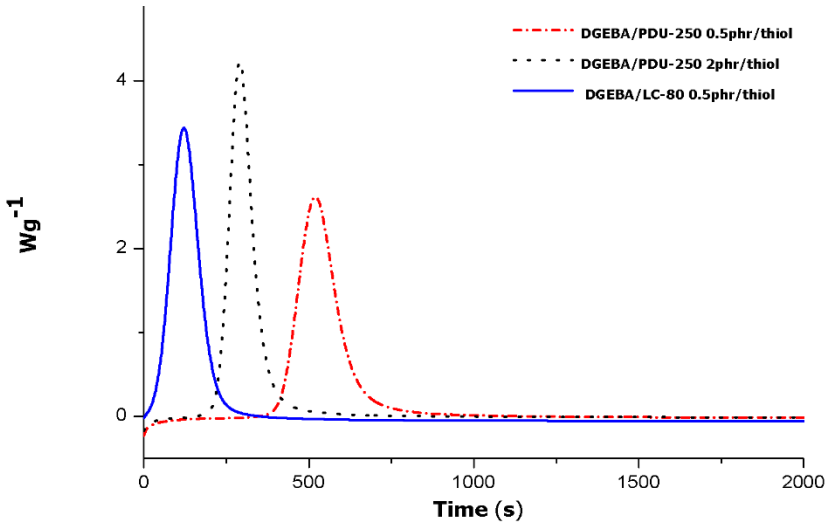

Figure 4. DSC thermograms corresponding to the isothermal curing at 120 °C of the epoxy-thiol mixtures with different catalysts and proportions

As it is observed in the isothermal curves, the activation of the different formulations needs different time to occur and it is inversely proportional to the amount of catalyst in the formulation. The times needed to reach a complete curing are also quite different, between 400 and 1000 s. The increase of the proportion of PDU-250 in the formulation from 0.5 to 2 phr, not only reduces the time of activation and curing but it leads to a sharper exotherm that indicates a quicker curing at this temperature and to the elimination of the above mentioned thermal homopolymerization. The most reactive precursor is LC-80. In fact, the increase in the proportion of LC-80 in the formulation leads to a so quick curing that is difficult to monitor it at 120 °C, since it begins instantaneously on introducing the sample in the DSC oven, making difficult the observation of the exotherm. Therefore, the most active formulations were studied isothermally at 80 °C. The curves obtained are represented in Figure 5.

On comparing the curves in Figures 4 and 5 broader peaks are observed in the latter, because the slow curing rate at this temperature. The most active curing system is the one catalyzed by BDMA, which reaches completion in about 500 s at 80 °C. The other two systems initiated by 0.5 phr of 1-MI or 2 phr of LC-80 needs a longer curing time to be completed. Although the curing of mixtures with 1-MI stars later it finishes at the same time that LC-80 2 phr formulation.

The isothermal curves collected in Figures 4 and 5 reflect the order in the kinetic constant values in Table 1. From the constant rate values and experimental data we can state that the most reactive system at 120 °C is the one catalyzed by 2 phr of LC-80 and at 80 °C is the one catalyzed by 0.5 phr of BDMA. It can be seen that the less active system is the one containing 0.5 phr of PDU-250, which reaches completion in longer curing times at higher temperature, in agreement with the results of the dynamic curing experiments. Keeping in mind that it is important to have a good latent character but fast curing upon increasing the temperature, it can be concluded that 0.5 phr of PDU-250 are not sufficient and that higher catalyst content is required.

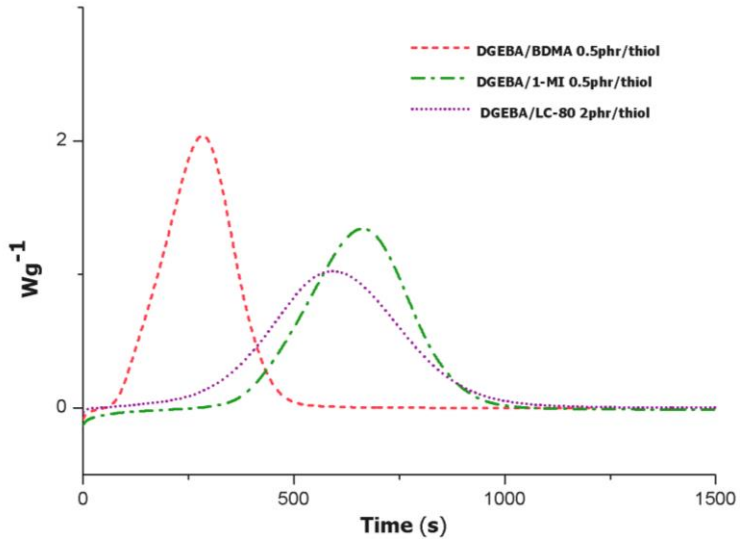

Figure 5. DSC isothermal curves registered at 80 °C of the mixtures epoxy-thiol with different catalysts

Latency tests

The determination of the latent character of the amine precursors used on the thiol-epoxy mixtures was studied by rheometry, by measuring the viscosities after several times of storage. All mixtures were stored at 35 °C in an oven and the viscosity determined each two or three days. The results obtained are shown in Figure 6. The enthalpy released after the periods of storage was also measured to determine the degree of curing achieved. The values are collected in Table 2.

In the plot we can see that the viscosity of the mixture with BDMA was significantly higher than the others, indicating that it had already reacted to a significant extent in the few minutes elapsed from sample preparation to viscosity measurement. The enthalpy released also changed dramatically after few minutes (data not reported). This indicates that the pot-life is quite short, as previously described for such curing systems.[9] In the case of 1-MI formulation the reaction does not take place as quickly as with BDMA, but after 2 days of storage the sample was already gelled and vitrified and it was not possible to measure any remaining enthalpy nor viscosity. These tests confirm that both amines do not have latent character, which prevents the preparation of one-pot formulations. Formulations containing PDU-250and LC-80 as amine precursors present viscosity values practically constant during several days. The mixture with 2phr of PDU-250 was cured after 4 days of storage. However, in formulations with a lower proportion of PDU-250, the viscosity after 10 days of storage increased up to 1753 Pa.s, but there was still some remaining enthalpy (45 J/g). In the case of the mixture containing 2 phr of LC-80a small increase in viscosity on increasing storage time was observed and between the days 12 and 13 the complete curing was reached, since no remaining enthalpy could be measured on the 14th day. If the proportion of LC-80 is reduced to 0.5 phr the viscosity and the remaining curing heat is practically invariable after 18 days of storage in the oven, but in the 21st day a significant increase in viscosity up to 10.4 Pa.s could be measured, but a significant remaining enthalpy still exists. Overall, the reaction extent of the formulation containing 0.5 phr of LC-80 after 3 weeks of storage at 35 °C was of only 0.12. This implies a higher latency character for the amine precursor LC-80, which presents a high pot-life at this temperature.

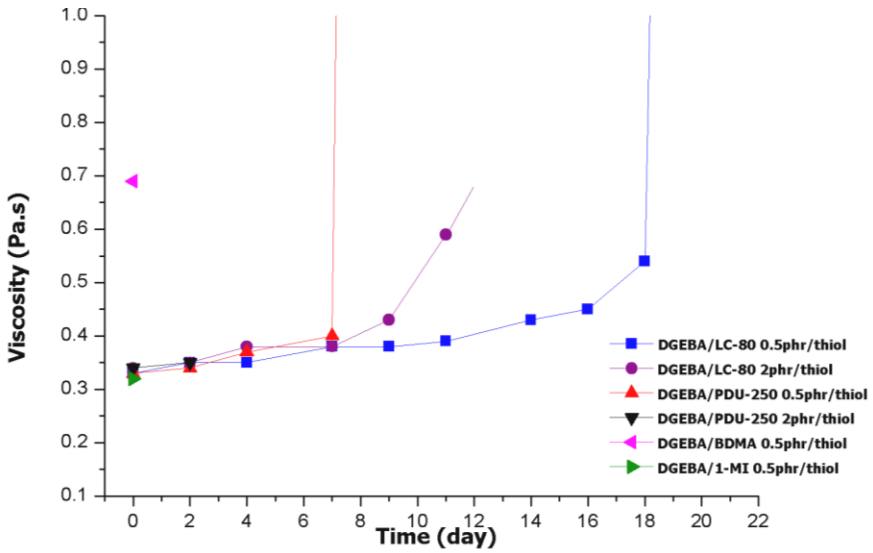

Figure 6. Plot of viscosities of the different formulations against storage time

In principle, according to the information given in their data sheet, it was expected that the precursors LC-80 and PDU-250 presented similar latency of more than two months, but they did not, especially PDU-250. In fact, the pot-life was much shorter than expected. It should be commented that the latency reported by the delivering companies was determined at room temperature, supposed to be 25 °C, lower than the used in our studies. However, some other effects on the latency of these precursors could arise from the different chemical environment in the formulation. In the case of LC-80, this can be caused by a specific interaction of the thiol with the encapsulating polymer or to an easier solubilization, leading to an early release of the imidazole. In the case of PDU-250, one can hypothesize that the presence of thiol groups can catalyze the urea decomposition leading to an early release of the free amine.

Table 2. Residual heat (in J/g) after several days of storage at 35 °C for the different formulations studied. Calculated conversion is shown in parentheses

Days	LC-80 0.5phr	LC-80 2phr	PDU-250 0.5phr	PDU-250 2phr	BDMA 0.5phr	1MI 0.5phr
0	406 (0)	404 (0)	387 (0)	391 (0)	a	373 (0)
2	403 (0)	403 (0)	380 (0)	393 (0)	-----	-----
4	405 (0)	394 (0)	357 (0.06)	-----	-----	-----
7	402 (0)	394 (0)	354 (0.07)	-----	-----	-----
9	402 (0)	399 (0)	108 (0.71)	-----	-----	-----
11	389 (0.02)	377 (0.04)	45 (0.88)	-----	-----	-----
14	389 (0.02)	-----	-----	-----	-----	-----
16	369 (0.06)	-----	-----	-----	-----	-----
18	359 (0.09)					
21	356 (0.1)					

a. The enthalpy released changes dramatically depending on the time used to be measured

After latency tests and kinetic studies it seems that the use of LC-80 is the most advisable for the preparation of thiol-epoxy formulations, since the mixture can be stored during several days and once started the curing is fast, depending on the proportion of LC-80 added to the formulation. It should also be noted that the calorimetric analysis is not sufficient to determine the latency of an initiator. Although PDU-250 starts to react at higher temperature than the LC-80 in the calorimeter, its latency is much lower. The latency of the initiator is mainly controlled by the rate of formation of the active species at a given temperature and is highly dependent on the specific interactions between the catalyst and the other species present in the formulation.

Characterization of the materials

The materials obtained from the different formulations were studied by TGA, DSC and DMTA for the determination of the thermal and thermomechanical properties.

The thermal stability of the thermosets was determined by thermogravimetry under inert atmosphere and some of the curves obtained are shown in Figure 7. The main parameters are collected in Table 3. In general, the curves reveal the excellent thermal stability of these materials, with a generally single degradation process. There are no much noticeable differences among the thermal stability of these materials, which are stable up to temperatures of 340 °C (less than 5 % weight loss). Neither the proportion of amine precursor gives significant differences. The only difference is the broad shoulder that appears at temperature above 400 °C for the LC-80 and BDMA formulation.

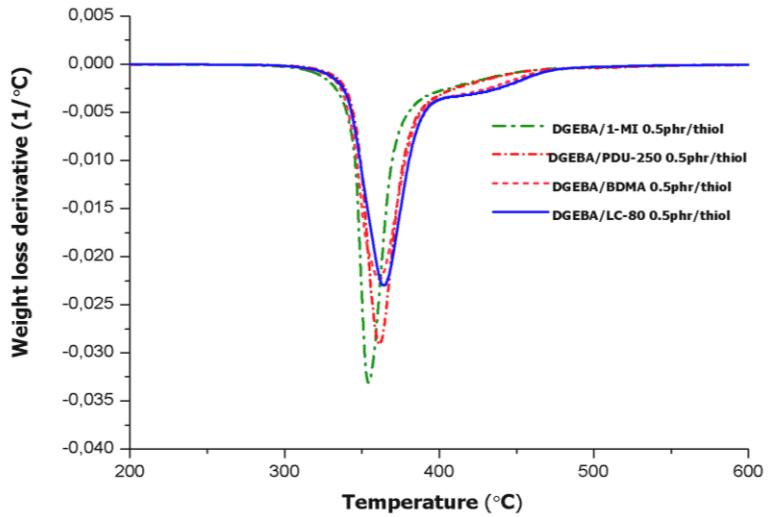

Figure 7. DTG curves under N_2 at 10 K/min of the materials obtained with a proportion of 0.5 phr of the different catalysts

Table 3. Thermal and dynamic mechanical data of the materials obtained from thiol-epoxy formulations with different catalysts and proportions

Type of catalyst	Proportion (phr)	$T_{5\%}$ (°C)	T_{max} (°C)	Char yield (%)	Tg^a (°C)	$T_{tan\delta}{}^b$ (°C)	E (MPa)	E_r (MPa)	FWHM[c] (°C)
LC-80	0.5	344	369	4	37	43	2281	9.11	12
LC-80	2	344	370	4	37	44	2429	10.78	10
1MI	0.5	345	362	7	32	45	2314	10.08	9
PDU-250	0.5	346	367	7	37	44	2024	7.71	8
PDU-250	2	338	365	6	30	45	2039	5.61	12
BDMA	0.5	342	362	4	32	44	2383	9.63	10

a. Tgs determined by calorimetric analysis
b. Temperature of maximum of tan δ determined by DMTA

c. FWHM stands by full width at half maximum

The dependence of the viscoelastic properties with the temperature was studied by DMA. Figure 8 and Figure 9 plot the storage modulus and the loss factor, respectively, for all the materials prepared. The main data obtained from these studies are summarized in Table 3. Although the DMA experiments were registered from -100 °C to 120 °C no relaxations under room temperature were observed and the plots in the figures were cut to be clearer.

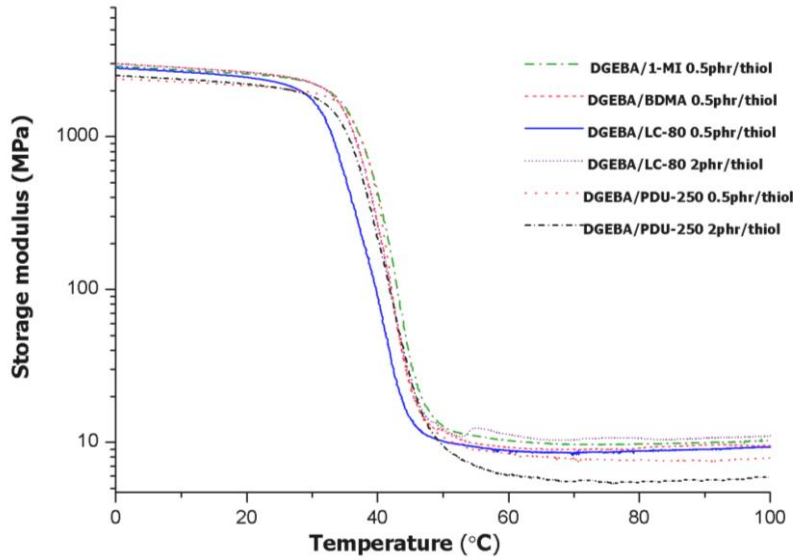

Figure 8. Plot of storage modulus against temperature for the different materials prepared

Figure 8 shows that the storage modulus in the glassy state remains quite stable before the occurrence of the α-relaxation, related to the Tg, leading to a drop in modulus of about 2-3 orders of magnitude reaching an almost constant value in the rubbery state. Crosslinking has a dramatic effect on the dynamic mechanical properties in the transition and in the plateau. According to the theory of rubber elasticity, the rubbery modulus is inversely proportional to the molecular weight between crosslinks.[30] Thus, from the values of the storage modulus in the rubbery region (E_r) collected in the table, a lower crosslinking density or higher molecular weight between crosslinks are evidenced for the materials obtained by catalyzing with PDU-250. The higher the proportion of PDU-250 the lower the rubbery modulus is. However, there are no much differences among the other materials. Also, storage modulus in the glassy state is lower for the materials obtained using PDU-250.

The explanation to the lower crosslinking density of the materials obtained by using PDU-250 can be found in the reaction of the decomposition products of urea in PDU-250 with the components of the formulation. Scheme 2 represents some possible reactions that can occur during curing. Isocyanate groups can react with thiols whereas secondary

amine can react with epoxides, both processes leading to a reduction of the crosslinking points.

The plot of loss factor against temperature in Figure 9 shows the α-relaxation, characterized by a narrow peak, which is strongly related to the Tg. The peak temperatures shown in Table 3 are similar to each other regardless of the catalyst used, indicating that very similar materials are obtained in any case, and compare well with the values of the calorimetric Tg measured by DSC and shown in the same table. It should be remarked that the values of Tgs are very low due to the flexible character of the thiol structure and the low crosslinking density of the materials. It is expected that higher functionalities of thiol monomer or a more rigid structure may help to reach higher Tg values.

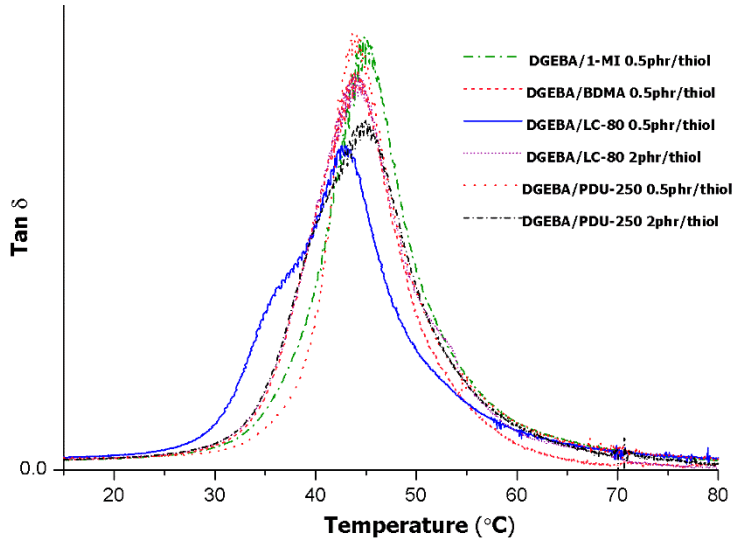

Figure 9. Plot of tan δ against temperature of the different materials prepared

The area of the peak is related to the damping characteristics, but no differences in the areas could be measured for these materials. The material with 0.5 phr of LC-80 presents a shoulder in the tan δ curve at lower temperature (see Figure 9). Broadening of the tan δ curve is commonly assumed to be due to a distribution in the molecular weight between crosslinks or some other kind of heterogeneity in the network structure.[30] A representative parameter of the network homogeneity is the value of FWHM, or width of the curve at half height of the peak. According to the data shown in Table 3, the materials with 0.5 phr of LC-80 and 2 phr of PDU-250 seem to be somewhat less homogeneous but the differences are nevertheless small.

Conclusions

Amine precursors, LC-80 and PDU-250, were studied as catalyst of thiol-epoxy formulations and were compared with amines such as BDMA and 1-MI. From preliminary

kinetic analysis, it was shown that LC-80 and PDU-250 had a potential as latent catalysts for the thiol-epoxy reaction, producing a higher activation temperature than BDMA and 1-MI and promoting fast cure at high temperatures, especially LC-80.

The latency tests showed that BDMA and 1-MI promoted fast curing at room temperature, leading to complete cure in less than 1 and 2 days, respectively. The use of PDU-250 led only to a discrete latent character, while 0.5 phr of LC-80 led to the greatest storage stability, reaching only a degree of cure of ca 0.12 after 21 days of storage and a modest increase in viscosity. This, coupled with the extremely fast cure at 120 °C, makes LC-80 a promising latent catalyst to be used in one-pot thiol-epoxy formulations or dual-curable B-stageable formulations combining thiol-ene and thiol-epoxy chemistry.

The materials obtained were thermally stable until 350 °C and had a simple degradation profile. They were transparent and colourless and quite flexible, with Tgs near room temperature. In order to increase the thermomechanical properties of the cured materials, monomers with a higher functionality or rigidity should be used.

Acknowledgments

The authors would like to thank MINECO (MAT2011-27039-C03-01, MAT2011-27039-C03-02) and Generalitat de Catalunya (2014-SGR-67) for giving financial support. X.F. acknowledges the contract JCI-2010-06187.

References

[1] C. E. Hoyle, A. B. Lowe, C. N. Bowman, *Chemical Society Reviews*, 2010, 39, 1355–1387.

[2] J. E. Moses, A. D. Moorhouse, *Chemical Society Reviews*, 2007, 36, 1249–1262.

[3] W. H. Binder, R. Sachsenhofer, *Macromolecular Rapid Communications*, 2007, 28, 15–54.

[4] M. Uygun, M. Atilla Tasdelen, Y. Yagci, *Macromolecular Chemistry and Physics,* 2010, 211, 103–110.

[5] H. C. Kolb, M. G. Finn, K. B. Sharpless, *Angewandte Chemie International Edition*, 2001, 40, 2004-2021.

[6] S. De, A. Khan, *Chemical Communications,* 2012, 48, 3130–3132.

[7] Tanaka Y, Bauer R.S. *Epoxy Resins Chemistry and Technology. Curing Reactions*. Marcel Dekker. In: May, CA, editor; 2nd ed, New York, USA, 1988.

[8] T. Ware, D. Simon, K. Hearon, T. H. Kang, D. J. Maitland, W. Voit, *Macromolecular Bioscience*, 2013, 13, 1640–1647.

[9] E. M Petrie. *Epoxy adhesive formulations. Epoxy curing agents and catalysts*. McGraw-Hill Companies, USA, 2006.

[10] A. Brändle, A. Khan, *Polymer Chemistry*, 2012, 3, 3224-3227.

[11] S. Binder, I. Gadwal, A. Bielmann, A. Khan, *Journal of Polymer Science Part A: Polymer Chemistry,* 2014, 52, 2040–2046.

[12] N. Cengiz, J. Rao, A. Sanyal, A. Khan, *Chemical Communications*, 2013, 49, 11191-11193.

[13] I. Gadwal, S. Binder, M. Stuparu, A. Khan, *Macromolecules,* DOI:10.1021/ma500920z.

[14] R. L. Mays, P. Pourhossein, D. Savithri, J. Genzer, R. C. Chiechi, M. D. Dickey, *Journal of Materials Chemistry C*, 2013, 1, 121–130.

[15] S. Skaria, R. Thomann, C. J. Gomez-Garcia, L. Vanmaele, J. Loccufier, H. Frey, S. Eddine Stiriba, *Journal of Polymer Science Part A: Polymer Chemistry,* 2014, 52, 1369–1375.

[16] W. R. Ashcroft, C*hemistry and Technology of Epoxy Resins. Curing Agents for Epoxy Resins,* Blackie Academic & Professional; Glasgow, U.K. 1993.

[17] T. Endo, F. Sanda*, Macromolecular Symposia*, 1996, 107, 237-242.

[18] A. M. Tomuta, X. Ramis, F. Ferrando, A. Serra, *Progress in Organic Coatings*, 2011, 74, 59-66.

[19] C. H. Zhao, S. J. Wan, L. Wang, X. D. Liu, T. Endo, *Journal of Polymer Science Part A: Polymer Chemistry,* 2014, 52, 375–382.

[20] M. Sangermano, A. Vitale, K. Dietliker, *Polymer,* 2014, 55, 1628-1635.

[21] F. Saharil, F. Forsberg, Y. Liu, P. Bettotti, N. Kumar, F. Niklaus, T. Haraldsson, W. van der Wijngaart, Kristinn B. Gylfason, *Journal of Micromechanics and Microengineering*, 2013, 23, 025021.

[22] J. A. Carioscia, J. W. Stansbury, C. N. Bowman, Polymer, 2007, 48, 1526–1532.

[23] S. González, X. Fernández-Francos, J. M. Salla, A. Serra, A. Mantecón, X. Ramis, *Journal of Applied Polymer Science*, 2007, 104, 3407-3416.

[24] X. Ramis, J. M. Salla, C. Mas, A. Mantecón, A. Serra, *Journal of Applied Polymer Science,* 2004, 92, 381-393.

[25] A.W. Coats, J.P. Redfern, Nature, 1964, 201, 68-69.

[26] A&C Catalysts, Inc. Accessed in June 17th 2014. *http://www.accatalysts.com/prodCuring.html*.

[27] K.J. Ivin, In: Brandrup J, Immergut EH, editors, *Polymer Handbook*, Wiley, New York, USA, 1975.

[28] B. A. Rozenberg, *Advances in Polymer Science*, 1986, 75,113-165.

[29] Sergei Vyazovkin, *Journal of Computational Chemistry*, 2001, 22, 78-183.

[30] L. E. Nielsen, R. F. Landel, *Mechanical Properties of Polymers and Composites*, Marcel Dekker, Inc., 2nd ed Edition, New York, USA, 1994.

UNIVERSITAT ROVIRA I VIRGILI
NUEVOS PROCESOS DE CURADO CLICK CON TIOLES Y SU APLICACIÓN A LA PREPARACIÓN DE MATERIALES BASADOS EN EUGENOL
Dailyn Guzmán Meneses

UNIVERSITAT ROVIRA I VIRGILI
NUEVOS PROCESOS DE CURADO CLICK CON TIOLES Y SU APLICACIÓN A LA PREPARACIÓN DE MATERIALES BASADOS EN EUGENOL
Dailyn Guzmán Meneses

CAPÍTULO 4

Polymers, 2015, 7, 680-694

Enhancement in the Glass Transition Temperature in Latent Thiol-Epoxy Click Cured Thermosets

Dailyn Guzmán, Xavier Ramis, Xavier Fernández-Francos, Angels Serra

UNIVERSITAT ROVIRA I VIRGILI
NUEVOS PROCESOS DE CURADO CLICK CON TIOLES Y SU APLICACIÓN A LA PREPARACIÓN DE MATERIALES BASADOS EN EUGENOL
Dailyn Guzmán Meneses

Enhancement in the glass transition temperature in latent thiol-epoxy click cured thermosets

Abstract

Tri and tetrafunctional thiol were used as curing agent for diglycidyl ether of bisphenol A (DGEBA) catalyzed by a commercially available amine precursor, LC-80. Triglycidyl isocianurate (TGIC) was added in different proportions to the mixture to increase rigidity and glass transition temperature (Tg). The cooperative effect of increasing functionality of thiol and the presence of TGIC in the formulation leads to an increased Tg without affecting thermal stability. The kinetics of the curing of mixtures was studied by calorimetry under isothermal and non-isothermal conditions. The latent characteristics of the formulations containing amine precursors were investigated by rheometry and calorimetry. The increase in the functionality of the thiol produces a slight decrease in the storage lifetime of the mixture. The materials obtained with tetrathiol as curing agent showed the highest values of Young's modulus and Tg.

Keywords: thermosets; thiol; epoxy resin; triglycidyl isocyanurate; click reaction; latency.

Introduction

In recent years, an increasing interest in the preparation of thermosets by click methodologies has appeared. [1,2,3]This is because of the characteristics of click reactions: environmentally-friendly conditions, efficiency, orthogonality and quantitativity. These characteristics have allowed for the discovery of innovative solutions in the field of coatings technology.[4,5] Among click reactions, thiol-epoxy systems have broad applications[6,7,8,9,10,11] but they present an important drawback which is the low reactivity of the formulation that requires the addition of a catalyst. However, the disadvantage of a too short pot-life appears on catalysing with amines.[12]

In a previous paper, we reported new latent thiol-epoxy curing systems by using amine precursors, like an encapsulated imidazole or a urea, which at a defined temperature release the corresponding amines.[13] The released amine catalyses the thiol-epoxy reaction by acting as a base and increasing the nucleophilicity of thiol groups by forming thiolates.[12] Depending on the type of amine precursor and its proportion, the curing temperature or the formulation stability can be selected.

One of the most important characteristics in thermosets is the glass transition temperature (Tg). The values of Tg are directly related to the behaviour of the materials and therefore to their final application and characteristics such as modulus, hardness, fragility, etc.[14,15] One of the most extensively used epoxy resin is diglycidyl ether of bisphenol A (DGEBA) but when reacting with stoichiometric amounts of thiols as curing

agents, the values of Tg are rather low due to the flexibility of the aliphatic thiol structure and the low crosslinking density.[13]

The main strategy to improve Tg value is to increase the functionality or the rigidity of the components of the curing system or reduce the molar mass maintaining its functionality. In our case, the trifunctional thiol structure, previously studied, can be substituted by a commercially available tetrafunctional thiol, pentaerythritol tetrakis (3-mercaptopropionate) (PETMP), with a higher functionality and a slightly lower molar mass per thiol group. However, no rigid thiols are commercially available, to the best of our knowledge. DGEBA resin has only a functionality of two in the thiol-epoxy curing and can be substituted by triglycidyl isocyanurate (TGIC), with a functionality of three, a low molar mass per reactive group and high rigidity. These features should contribute, in principle, to increase the Tg of the modified materials.

In this paper, we have studied the influence of a partial substitution of DGEBA by TGIC and/or the use of PETMP as the thiol curing agent in the characteristics of the materials and in their curing process and latency. The structures of the products used are depicted in Scheme 1. As the catalyst, the encapsulated imidazole LC-80 was used in a proportion of 0.5 phr in reference to the epoxy resin, according to our previous results.[13] The kinetics of the curing was followed by differential calorimetry and the thermal stability and thermomechanical characteristics of the materials were evaluated and related to the theoretical network parameters calculated. These new formulations were compared with the system previously reported.[13]

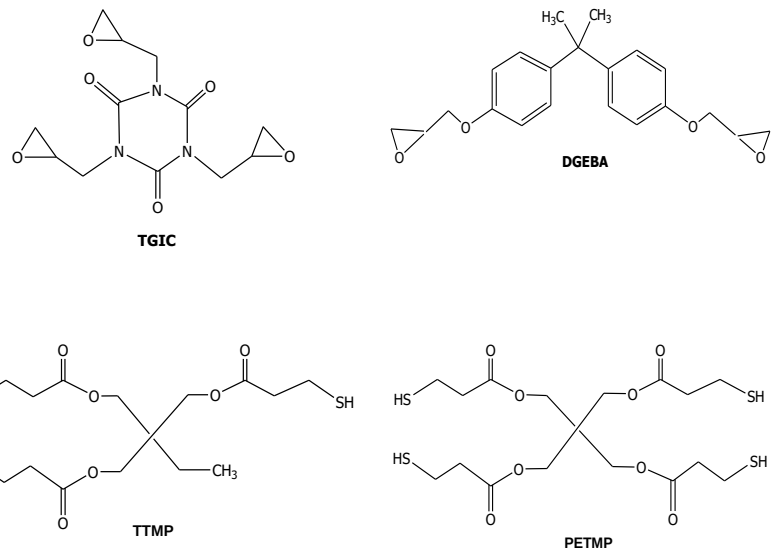

Scheme 1. Chemical structures of the compounds us

Experimental part

Materials

Diglycidylether of bisphenol A (DGEBA, Araldite GY240, HuntsMaterials, Everberg, Belgium, epoxy equivalent 182 g/eq) was dried at 80 °C under vacuum for 6 h. The latent amine precursor which is an encapsulated imidazole was Technicure® LC-80 (LC-80). Trimethylolpropane tris (3-mercaptopropionate) (TTMP), pentaerythritol tetrakis (3-mercaptopropionate) (PETMP) and tris(2,3-epoxypropyl) isocyanurate (TGIC) from Sigma Aldrich (St. Louis, MO, USA) were used as received.

Preparation of the curing mixtures

The mixtures were prepared by mixing stoichiometric proportions (1:1) of epoxide and thiol. In case of mixtures with DGEBA and TGIC, the selected proportions of resin were homogenized by heating at 150 °C under magnetic stirring. The epoxy mixture was allowed to cool down and the thiol was added. After homogenization of DGEBA/TGIC/thiol mixtures, 0.5 phr of LC-80 (parts of catalyst per 100 parts of epoxy resin) were added and dissolved by stirring at room temperature. Neat samples were prepared by mixing the formulation under stirring at ambient temperature.

Characterization techniques

The kinetic experiments were performed by differential scanning calorimetric (DSC) in a Mettler (Greifensee, Switzerland) DSC-821e apparatus. For dynamic and isothermal studies, a flow of N_2 at 100 mL/min was used and the weight of the samples for the analysis was 10 mg. The calorimeter was calibrated using an indium standard (heat flow calibration) and an indium-lead-zinc standard (temperature calibration). The dynamic studies were performed in the temperatures range of 30–300 °C, with a heating rate of 2, 5, 10 and 20 K/min, whereas for the isothermal experiments, a temperature of 100 °C was used.

The glass transition temperatures (Tgs) of the cured samples were determined after two consecutive heating dynamic scans at 10 °C/min starting at −50 °C in a Mettler DSC-822e device to delete the thermal history. The Tg value was taken as the middle point in the heat capacity step of the glass transition.

The latency tests were performed for the mixture stored in an oven at controlled temperature of 35 °C and the viscosity was measured at different storage times. Viscosity measurements were performed in a TA Instruments (New Castle, DE, USA) ARG2 rheometer equipped with disposable parallel plates. A sample gap of 0.4 mm was exactly set with an accuracy of 0.001 mm. A shear rate of 100 s^{-1} was applied at 35 °C after 5 min of temperature stabilization. A maximum of 2 min was needed to measure a steady value of viscosity. The values were corrected for non-uniform stresses in the parallel plates.

The isothermal degree of conversion in percentage *(x)* reached at a selected time was determined from stored samples that were subsequently heated up at 10 K/min to determine the residual heat Δhres, using the following expression:

$$x = \left(1 - \frac{\Delta h_{res}}{\Delta h_{total}}\right) \times 100 \qquad (1)$$

The thermal stability of cured samples was studied by thermogravimetric analysis (TGA), using a Mettler TGA/SDTA 851e thermobalance. All experiments were performed under inert atmosphere (N_2 at 100 mL/min). Pieces of the cured samples with an approximate mass of 8 mg were degraded between 30 and 600 °C at a heating rate of 10 K/min.

Dynamic mechanical thermal analyses (DMTA) were carried out with a TA Instruments DMA Q800 analyzer. The samples were cured isothermally in a mould at 120 °C for 1 h with a postcuring at 150 °C for 1 h. Three point bending clamp was used on prismatic rectangular samples (10 × 7.5 × 1.6 mm^3).

The apparatus operated dynamically at 2 K/min from 30 to 120 °C at a frequency of 1 Hz with and oscillation amplitude of 10 µm. Young´s modulus was determined by the stress/strain test, under the same clamp and geometry testing conditions, at 30 °C using a force ramp of 1 $N \cdot min^{-1}$ and upper force limit 18 N. In all cases, samples were previously heated to delete thermal history.

Results and Discussion

Study of the curing process

To prepare homogenous thermosets with the expected degree of curing from stoichiometric formulations, a good compatibility among reactants is always needed. Thus, the compatibility of resins and curing agents is the key point in the selection of the components in the curing mixture.

The substitution of DGEBA by the trifunctional TGIC to prepare thiol epoxy thermosets with high Tg presents the challenge of low compatibility between both components, which have a very low miscibility. Indeed, the resins needed to be heated to 150 °C, significantly above the melting temperature of TGIC, to allow preparation of homogeneous mixtures. According to that, TGIC/DGEBA mixtures in different proportions (0%, 10%, 20%, 30% and 40% w/w of TGIC in reference to the epoxy resin) were prepared. It should be said that he maximum proportion of the trifunctional resin allowing homogeneous mixture was 40%.

The substitution of trifunctional by tetrafunctional thiol was only studied for the neat DGEBA formulation and the formulation containing a 30% of TGIC (in reference to the resin), because 40% of TGIC led to in homogeneities in the cured sample.

Table collects the composition of all the formulations studied which also contains a 0.5 phr of LC-80 as the amine precursor. This table also contains the enthalpies per gram and epoxy equivalent evolved during curin

Table 1. Notation, composition and calorimetric data for the mixtures studied

Notation	TGIC (mmol/g)	TTMP (mmol/g)	PETMP (mmol/g)	DGEBA (mmol/g)	ΔH[a] (J/g)	ΔH[b] (kJ/eq)	Tpeak[c] (°C)
Neat (TTMP)	0	1.05	0	1.59	394	125	137
10%TGIC/TTMP	0.19	1.10	0	1.38	415	125	136
20%TGIC/TTMP	0.36	1.15	0	1.18	427	124	134
30%TGIC/TTMP	0.53	1.20	0	1.00	432	124	131
40%TGIC/TTMP	0.68	1.24	0	0.83	452	123	129
Neat (PETMP)	0	0	0.82	1.64	415	127	123
30%TGIC/PETMP	0.55	0	0.93	1.04	470	126	122

a. Enthalpy evolved by gram of curing mixture
b. Enthalpy released by epoxy equivalent
c. Temperature of the maximum of the curing exotherm

As we can see, there are some variations in the enthalpy released by gram but values for epoxy equivalent are similar among the different formulations, indicating that the degree of curing is similar. The values obtained for the enthalpy range between 123 and 127 kJ/eq, which indicates that the complete curing of epoxides has been achieved.[16]

To know the kinetic influence of adding TGIC to the curing mixture of the epoxy/thiol formulations, dynamic scanning calorimetry in dynamic and isothermal modes was performed.

Figure 1 shows the DSC thermograms of the dynamic curing studies at 10 °C/min for mixtures DGEBA/TTMP with different proportions of TGIC. As can be observed, the curing of the different formulations starts at temperatures higher than 110 °C. It should be taken into account that LC-80 has a melting onset temperature of 60°C determined by DSC, although it is described as a melting point at about 100 °C in its data sheet.[17] After melting, the encapsulated imidazole is released, but the activation of the reaction is not immediate, leading to the initiation of the curing at about 110 °C. On increasing the proportion of TGIC in the formulation, the curing exotherm is shifted to lower temperatures and increases the curing rate. The increase in reaction rate seems to be connected with the increase in the amount of reactive epoxy and thiol groups in the mixture, as deduced from the data shown in Table 1, but it might be that TGIC is more active than DGEBA in the reaction with thiolates, allowing it to cure in a shorter time. The trend observed in the dynamic curing experiments was confirmed by isothermal curing at 100 °C, as shown in Figure 2.

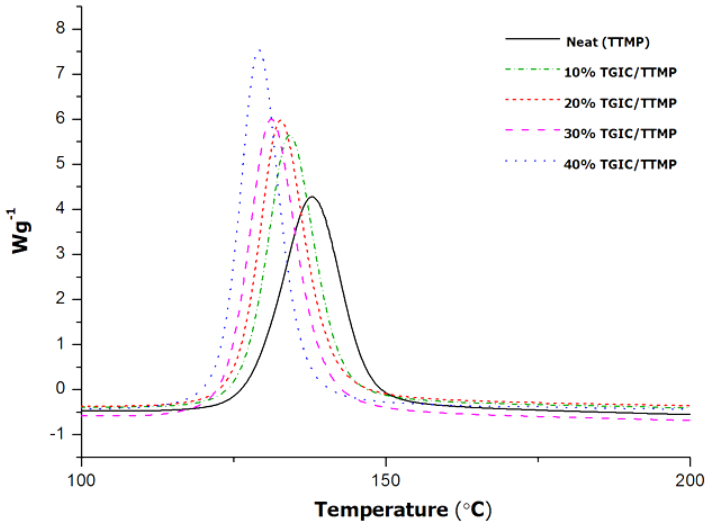

Figure 1. DSC thermograms corresponding to the dynamic curing at 10 °C/min of mixtures with TTMP and different proportions of TGIC catalyzed by 0.5 phr of LC-80

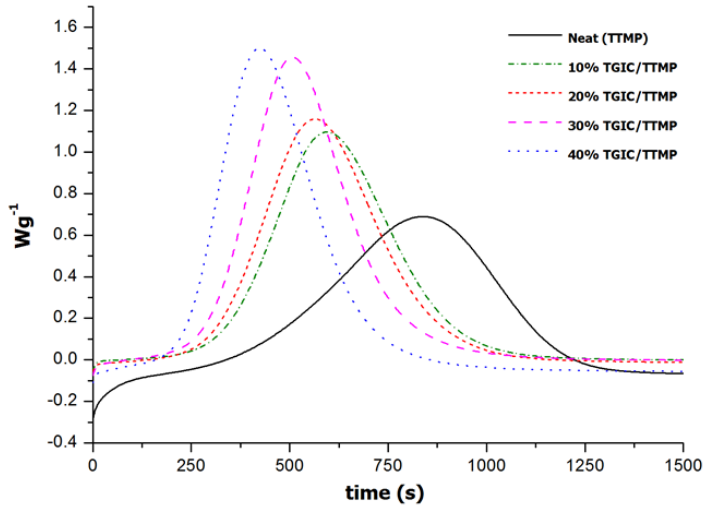

Figure 2. DSC thermograms of the isothermal curing at 100 °C of the mixtures with TTMP and different proportions of TGIC catalyzed by 0.5 phr of LC-80

As we can see, on increasing the proportion of TGIC, the curing time is notably reduced at 100 °C, but a first induction time, related to the slow release of the catalyst from its encapsulation and activation of the curing process, is observed for all

formulations. The most notable difference among the curves is the longer time needed to complete the cure for the neat formulation, which takes more than 20 min.

As we commented above, the increase in Tg could be accomplished on increasing the functionality of thiol. There are not many commercially available thiols but we can increase the functionality from 3 to 4 by taking PETMP instead of TTMP, both of which are commercially available. In the case of tetrathiol, we have only studied the neat formulation with DGEBA and the formulation containing 30% TGIC. Figure 3 shows the calorimetric dynamic curves of these formulations.

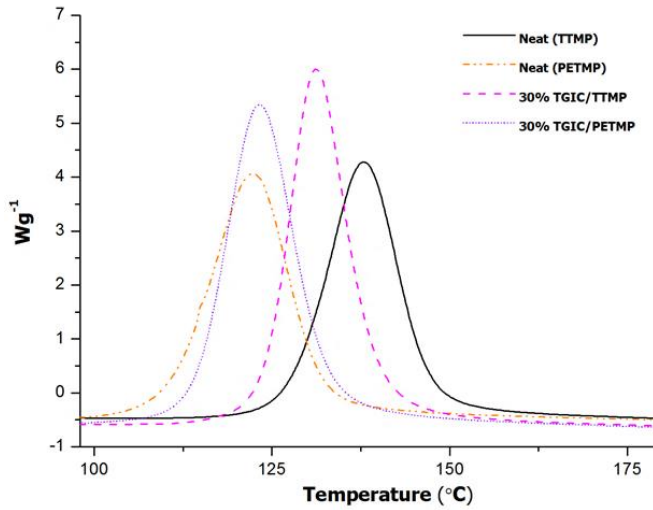

Figure 3. DSC thermograms corresponding to the dynamic curing at 10 °C/min of the mixtures epoxy resin-thiol tri- and tetrafunctional thiol catalyzed for 0.5 phr of LC-80.

The curing of the neat formulation with PETMP takes place at a much lower temperature indicating a higher reactivity of the curing system, due to a lower stability of the amine precursor LC-80 in the formulation. Since it is an encapsulated imidazole, little changes in the polarity or in the concentration of reactive groups in the mixture can lead to an easier release of the encapsulated imidazole, which acts as a base favoring the attack of the thiol groups to the epoxides.

In mixtures with PETMP, the addition of TGIC does not change significantly within curing temperature range. In contrast, with TTMP, the addition of TGIC to PETMP slightly increases the temperature range of the curing. This seems to support the effect of the chemical environment in the stability of the encapsulated LC-80, but the effect is quite complex. The thiol groups in both TTMP and PETMP have similar stereoelectronic effects and therefore the different reactivity cannot be attributed to the sole structure of the curing agents, but to other factors. In a previous paper, we observed that on increasing the proportion of LC-80, the curing took place at a much lower temperature, even lower than 100 °C or in a shorter amount of time, and in latency tests performed at 35 °C we could observe that with 2 phr of LC-80, the curing was complete in 14 days.[13]

This means that the capsules can be opened in thiol media even without reaching the melting temperature of the capsule.

The acceleration caused by the presence of PETMP was confirmed by an isothermal study of these formulations. In Figure 4, we can see that at 100 °C the induction time in PETMP formulations is dramatically shortened and the formulations begin to cure just when the samples were introduced in the furnace. Thus, the higher reactivity of the formulations with the tetrathiol as the curing agent can be confirmed.

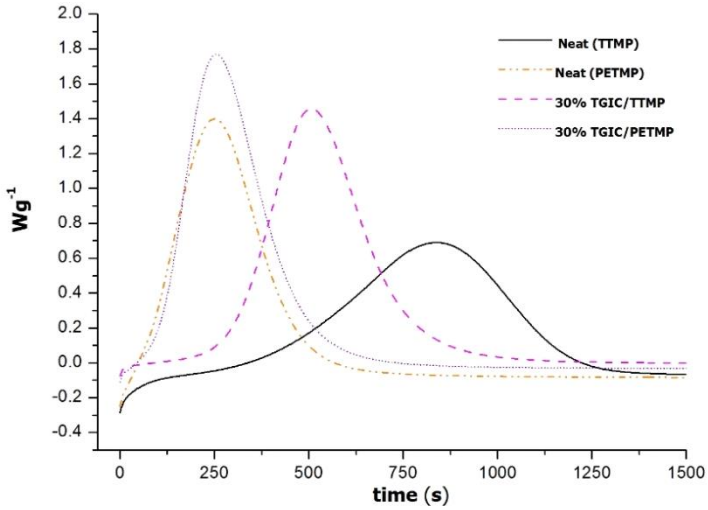

Figure 4. DSC thermograms of the isothermal curing at 100 °C of neat and TGIC mixtures with tri- and tetrathiol as curing agent.

study of the latency

In a previous work, [13] the latent character of the DGEBA/TTMP catalysed by 0.5 phr of LC-80 was studied and a period of save storage of 21 days at 35 °C could be determined. In the present study, DSC analysis showed that PETMP formulations were more active than TTMP formulations, and therefore the latency of PETMP formulations was in doubt. Latency has been determined by rheometry, measuring the viscosities after several times of storage at 35 °C. The evolution of the viscosity for the DGEBA formulations with both thiols is represented in Figure 5.

As we can see, the viscosity of the formulation with PETMP is somewhat higher than the one with TTMP. The viscosities are quite stable up to 19 days for TTMP formulations and 13 days for PETMP. The viscosity began to increase steadily and PETMP mixtures became hard after 19 days and TTMP mixtures after 23 days. After the different periods of storage, the enthalpy released in a DSC scan was also measured to determine the degree of curing achieved, also represented in Figure 5. TTMP reached 12% conversion after 21 days of storage, while PETMP reached the same conversion after 16 days of storage. According to the figure, the increase in viscosity about 1–2

orders of magnitude is more noticeable than the evolution of the conversion degree during storage, and therefore should be taken as reference for the evaluation of latency.

The reported latency data agree with the higher reactivity of PETMP shown before.

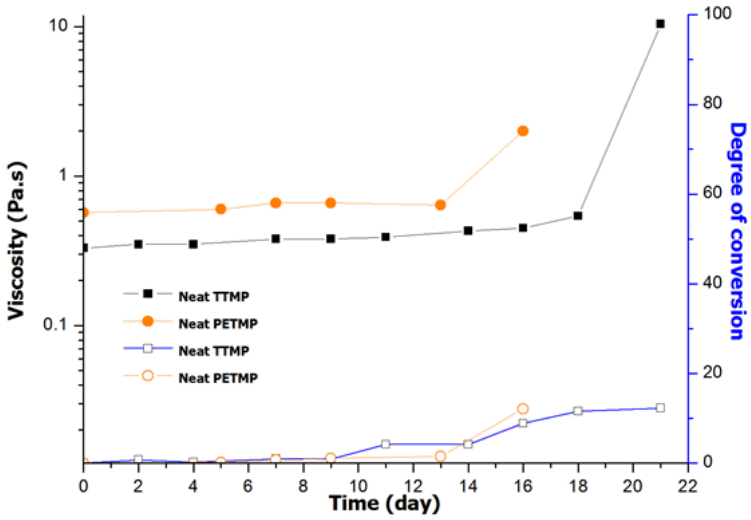

Figure 5. Plot of viscosities and degree of curing achieved of the different DGEBA formulations with tri- and tetrathiol against storage time. Filled symbols represent the viscosity and open symbols represent the degree of conversion

The difference between TTMP and PETMP formulations can be related to the difference in the polarity of the mixture, higher in the case of PETMP because of the higher proportion of S–H polar groups. The higher polarity should affect the stability of the capsule of LC-80, leading to an earlier release of the reactive imidazole. We demonstrated in a previous work that imidazole begins to react at low temperature in a short time.[13] However, in the present case, the latency period is enough for technological applications, because of the long pot-life achieved even at 35 °C. Lower temperatures can help to keep prepared formulations for a much longer time, but these formulations are not stable enough to prepare one-component epoxy formulations.

Thermal characterization of the materials

The materials obtained from the different formulations were studied by TGA, DMTA and DSC. The thermal stability of the materials was determined by thermogravimetry under inert atmosphere and the derivative of the thermograms of some formulations is represented in Figure 6. In Table 2, the most characteristic thermal data are given.

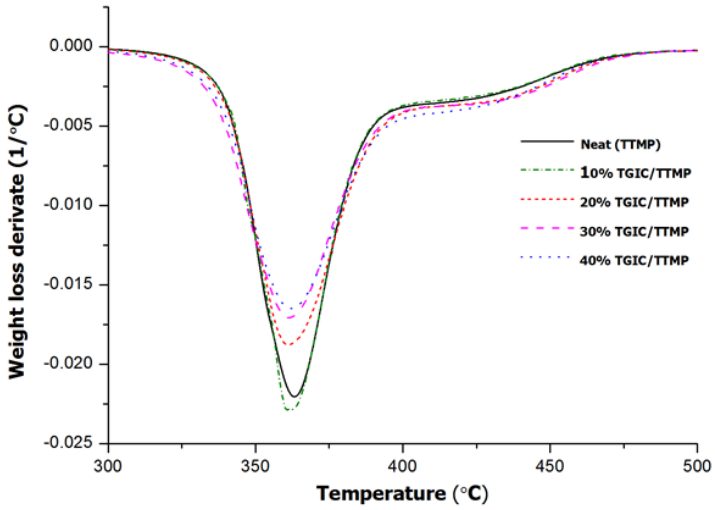

Figure 6. Derivative of the thermogravimetric curves registered under N_2 at 10 K/min of thermosets obtained from TTMP/TGIC/DGEBA mixtures

Table 2. Thermal data of the thermosets prepared

Notation	$T_{5\%}$[a] (°C)	$T_{50\%}$[b] (°C)	T_{max}[c] (°C)	T_g[d] (°C)	$T_{tan\delta}$[d] (°C)	E_r[f] (MPa)	FWHM[g] (°C)	Ar $_{tan\delta}$[h] (°C)	E^i (MPa)
Neat (TTMP)	342	370	363	35	51	7.89	10.0	16.0	391.4
10%TGIC/TTMP	342	370	361	37	55	7.92	10.6	16.3	551.7
20%TGIC/TTMP	341	373	361	40	59	9.04	11.1	15.6	678.2
30%TGIC/TTMP	335	369	361	44	62	10.82	10.9	15.7	736.1
40%TGIC/TTMP	336	374	362	44	63	9.99	12.2	16.0	720.8
Neat (PETMP)	341	371	361	55	68	9.77	8.5	12.8	1069
30%TGIC/PETMP	341	376	360	63	83	19.30	9.9	12.0	1250

a. Temperature of the weight loss of 5% in N_2 atmosphere
b. Temperature of the weight loss of 50% in N_2 atmosphere
c. Temperature of the maximum rate of degradation in N_2 atmosphere
d. Glass transition temperature determined by calorimetric analysis from −50 to 100 °C
e. Temperature of maximum of tan δ determined by DMTA
f. Storage modulus in the rubbery state determined at tanδ + 50 °C
g. Full width at half maximum of tanδ peak
h. Area of tanδ peak.
i. Young's modulus at 30 °C

In Figure 6, we can see that the derivative curves show a main degradation process at about 360 °C, without much difference in the maximum of the peak for all the materials, as is detailed in Table 2.

In addition to the main degradation peak, there is a shoulder at higher temperatures. In general, the presence of TGIC gradually decreases the decomposition rate because the higher crosslinking density provided by the isocyanurate rings reduces

the likelihood of producing volatile fragments during the thermal decomposition process. There is an only slight decrease in the initial degradation temperature (taken as $T_{5\%}$) on adding TGIC to the reactive mixture, because the thermal stability of the bonds is not changed. Thus, the addition of TGIC to DGEBA/TTMP systems provides no clear advantages in terms of thermal stability of the thermosets.

When TTMP was replaced by PETMP in the thermosets, a similar behavior was observed with a main degradation process in the same range (see Figure 7).

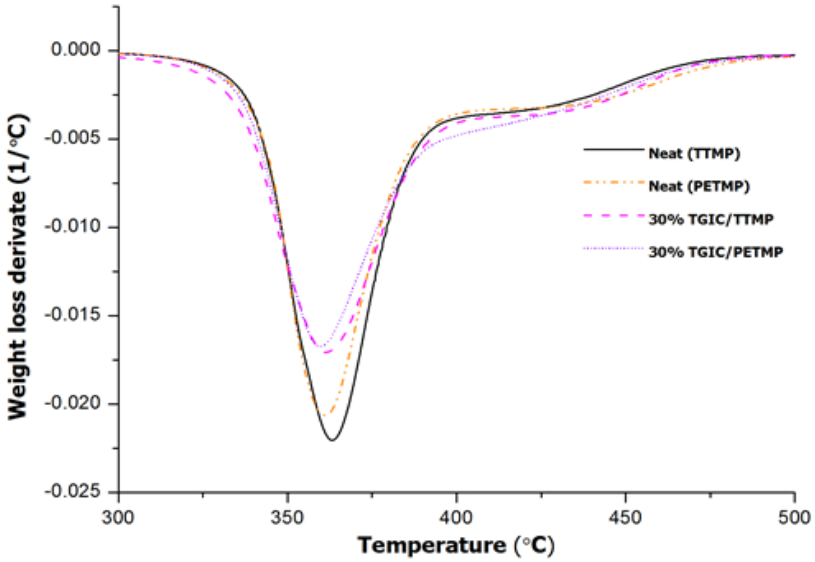

Figure 7. DTG curves registered under N_2 at 10 K/min of thermosets obtained by using TTMP and PETMP as curing materials

Tgs were determined by DSC from the samples prepared for DMTA measurements. As we can see in Table 2, on increasing the proportion of TGIC in the formulation or increasing the functionality of the thiol, this value also increases, reaching a Tg of 63 °C for the 30%TGIC/PETMP material. The values in the table demonstrate that the change from TTMP to PETMP, which increases the thiol crosslinker functionality, produces a significant enhancement in Tg. The use of TGIC introduces an increasing amount of rigid isocyanurate rings acting as crosslinks in the cured material. The increase in crosslinking density should contribute to increase the rigidity of the network structure and, consequently, the Tg. However, the inherent rigidity of the material may decrease, because the overall concentration of aromatic rings from DGEBA and the isocyanurate rings from TGIC decrease upon addition of TGIC. Both factors—crosslinking density and network rigidity—act in opposite directions but the overall effect should depend on their relative strength. Indeed, Table 2 and Figure 8 show that at low proportions of TGIC the Tg increases gradually but, above 30%, the effect is not clear.

The viscoelastic properties of the cured materials were analysed by DMTA. Figure 8 represents the curves corresponding to the variation of loss tangent against temperature for the materials obtained with TTMP and different proportions of TGIC. The maximum of tanδ is the temperature of α relaxation of the network and is related to the Tg of the material. In the figure, we can observe that as the TGIC proportion increases, the tanδ peak is shifted to higher temperatures. In Table 2, we can see that the temperature of the maximum of the peak goes from 51 to 63 °C for the maximum percentage of TGIC in the formulation. Similarly to the evolution of Tg determined by DSC, above 30% of TGIC there is not a clear increase in the tan δ peak temperature. On increasing the proportion of TGIC, there is a general increase in the storage modulus in the rubbery state up to the material 30%TGIC/TTMP, but further increase in the proportion of TGIC led to a decrease in this value.

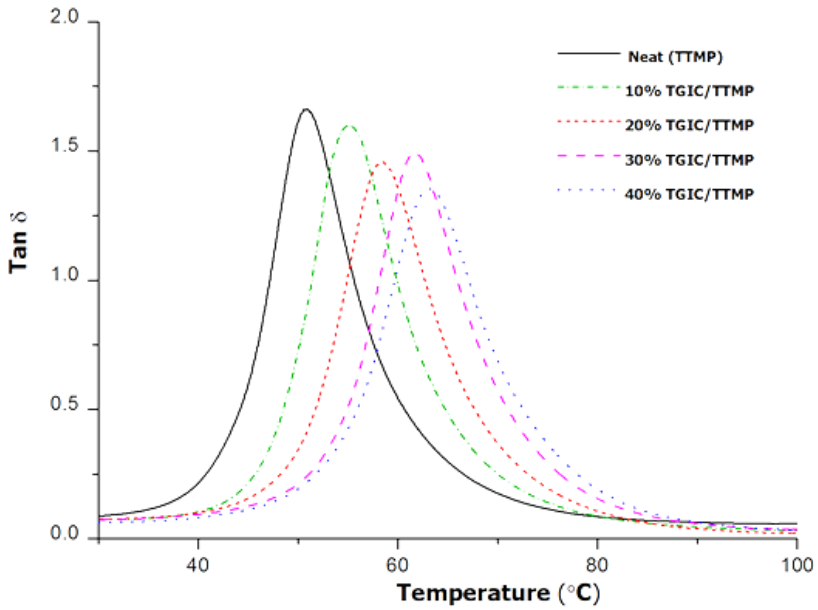

Figure 8. Plots of tanδ against temperature for the thermosets obtained for TTMP with different proportions of TGIC

According to the rubber elasticity theory, the relaxed modulus should be proportional to the crosslinking density or, more specifically, to the density of network strands. The theoretical crosslinking density of the formulations was calculated taking into account the contribution of the thiol curing agents and TGIC, and the theoretical network strand density was calculated taking into account that TTMP and TGIC which lead to tri-functional crosslinks, but PETMP leads to tetra-functional crosslinks and every strand is shared by two crosslinks. The results of these calculations are shown in Table 3.

Table 3. Crosslinking density of the different cured materials calculated according to the formulation composition

Notation	Crosslinking Density (eq/kg)				Network Strands (eq/kg)		
	TTMP	PETMP	TGIC	Total	DGEBA	TGIC	Total
Neat (TTMP)	1.06	-	-	1.06	1.59	-	1.59
10%TGIC/TTMP	1.11	-	0.19	1.30	1.38	0.59	1.95
20%TGIC/TTMP	1.16	-	0.36	1.52	1.19	1.09	2.28
30%TGIC/TTMP	1.20	-	0.53	1.73	1.01	1.58	2.59
40%TGIC/TTMP	1.24	-	0.68	1.92	0.84	2.05	2.88
Neat (PETMP)	-	0.82	-	0.82	1.64	-	1.64
30%TGIC/PETMP	-	0.93	0.55	1.48	1.05	1.65	2.69

In accordance with the values shown in the table, the addition of TGIC to the formulation results in an increase in the number of TTMP crosslinks. However, the modulus increase reported in Table 2 is not strictly proportional to the increase network strand density, especially above 30% of TGIC. While this may be due, in part, to the uncertainties associated with the measurement of oscillatory mechanical properties in the relaxed state using the DMTA apparatus, because of their very small stiffness, these results are in agreement with the observed trends in Tg. One can therefore use the same argumentation here to justify these results. It must be taken into account that the mechanical response of crosslinked polymers is highly complex and departures from the ideal elastomeric behaviour can be expected.[18,19] As an example, Xie and Rousseau[20] showed that it was possible to increase the number of crosslinks by replacing DGEBA with a shorter and flexible diepoxide, but leading to an actual decrease of the Tg and of the relaxed modulus due to the enhanced mobility of the network structure. In the present case, it is verified that the constraining effect of the increased crosslinking density and the presence of rigid isocyanurate crosslinks dominate, at least in the formulations with a low amount of TGIC but, upon increasing the TGIC content, furthermore, the resulting effect could be a balance between different factors. However, there is still the possibility that the curing has not been completed by topological reasons in formulations with 40% TGIC, which helps to explain the low modulus in the rubbery region and the lack of increase in Tg value.

The width of the tan δ peak can be related to the degree of inhomogeneity of the distribution of the comonomers and crosslinking points in the network structure. On increasing the proportion of TGIC in the formulation, this parameter is not increased significantly, indicating a random and regular distribution of crosslinks and network strands in the network structure, up to 40% of TGIC content, because of the similar reactivity of the epoxy groups of both DGEBA and TGIC. The area of the peak accounts for the damping characteristics of the network structure, but there is no significant variation in this characteristic on adding TGIC to the formulation.

Figure 9 plots the variation in tanδ curves on changing the curing agent, from TTMP to PETMP for neat and TGIC containing materials. As we can see, there is a remarkable shift of the curves when increasing the functionality of the curing agent, as expected, and a temperature of the maximum of the peak at 83 °C has been reached in the sample with a 30% of TGIC. Thus, the cooperative effect of increasing the functionality of the thiol and increasing the proportion of TGIC in the formulation leads to an increase of 32 °C in the Tg of the material. Although Table 3 shows that the total number of crosslinks decreases when PETMP is used instead of TTMP, it should be taken into account that they are tetrafunctional so that the total number of network strands is similar. This should constrain the network mobility, resulting in an increase in Tg, and of the relaxed modulus as well, given the similar amount of network strands. This is indeed what takes place and, overall, there is an additive effect on this parameter by increasing the functionality of the curing agent and the functionality of the epoxy resin. The lower values of FWHM indicate higher network homogeneity, while the lower area reflects the immobilization caused by the presence of tetrafunctional cross-links coming from PETMP in comparison with the trifunctional ones coming from TTMP.

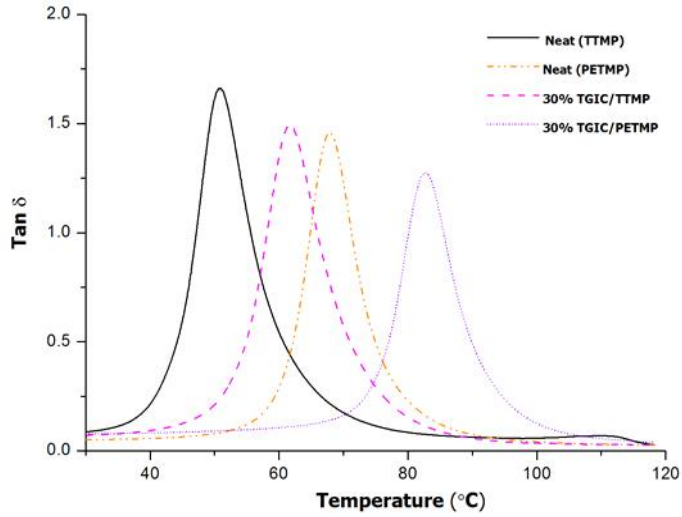

Figure 9. Plots of tanδ against temperature for the thermosets obtained by using TTMP and PETMP as curing agent

Young's modulus was measured by three-point bending in the DMTA device. On increasing the proportion of TGIC in the formulation, the material becomes more rigid at room temperature up to the material containing a 30% of TGIC. The modulus is higher for PETMP materials. Thus, the functionality of the crosslinking agent affects more notably this parameter.

The materials obtained were colorless and transparent but the high transparency of DGEBA/TTMP and DGEBA/PETMP formulations were slightly decreased on adding TGIC at the naked eye.

Conclusions

Different thiol/epoxy formulations were studied by using 0.5 phr of LC-80 as latent amine precursor. The kinetic study by DSC shows that on increasing the proportion of TGIC in the formulation, the curing is accelerated at low temperature. The acceleration was also observed when the functionality of the thiol was increased.

The formulations prepared from PETMP showed a shorter storage time than the formulations prepared with TTMP. However, a period of stability of 13 days at 35 °C can be assured.

The thermosets prepared presented good thermal stability without large differences when changing the composition.

The Tg of the materials prepared increased with the proportion of the triglycidyl isocyanurate in the formulation or by the substitution of TTMP by PETMP. A maximum increase of about 30 °C in this parameter was achieved when PETMP and a 30% of TGIC were in the formulation.

The partial substitution of DGEBA by TGIC did not increase the inhomogeneity of the network structure by the random copolymerization of both epoxy resins.

Young modulus of the thermosets prepared was increased on increasing the proportion of TGIC in the formulations. The increase in modulus was higher on PETMP formulations.

The materials obtained were colourless and highly transparent, but the transparency slightly decreased when adding TGIC to the formulations.

Acknowledgments

The authors would like to thank Ministerio de Economia y Competitividad (MAT2011-27039-C03-01 and C03-02) and Generalitat de Catalunya (2014-SGR-67) for giving financial support.

References

[1] K. Sunitha, K. S. Santhosh Kumar, D. Mathew, C. P. Reghunadhan Nair, *Materials Letters,* 2013, 99, 101–104.
[2] Y. Jian, Y. He, Y. Sun, H. Yang, W. Yang, J. Nie, *Journal of Materials Chemistry C*, 2013, 1, 4481–4489.
[3] M. Flores, A.M. Tomuta, X. Fernández-Francos, X. Ramis, M. Sangermano, A. Serra, *Polymer*, 2013, 54, 5473–5481.
[4] J. A. Carioscia; J.W. Stansbury, C.N. Bowman, *Polymer*, 2007, 48, 1526–1532.

[5] D. P. Nair, N. B. Cramer, J. C. Gaipa, M. K. McBride, E. M. Matherly, R. R. McLeod, R. Shandas, C. N. Bowman, *Advanced Functional Materials*, 2012, 22, 1502–1510.
[6] S. De, A. Khan, *Chemical Communications*, 2012, 48, 3130–3132.
[7] N. Cengiz, J. Rao, A. Sanyal, A. Khan, *Chemical Communications*, 2013, 49, 11191–11193.
[8] I. Gadwal, J. Rao, J. Baettig, Khan, A, *Macromolecules*, 2014, 47, 35–40.
[9] I. Gadwal, S. Binder, M.C. Stuparu, A. Khan, *Macromolecules,* 2014, 47, 5070–5080.
[10] S. Binder, I. Gadwal, A. Bielmann, A. Khan, *Journal of Polymer Science Part A*, 2014, 52, 2040–2050.
[11] I. Gadwal, M.C Stuparu, A. Khan, *Polymer Chemistry*, 2015, 6, 1393–1404.
[12] E. M Petrie, *Epoxy adhesive formulations. Epoxy curing agents and catalysts*, McGraw-Hill Companies, USA, 2006.
[13] D. Guzmán, X. Ramis, X. Fernández-Francos, A. Serra, *Polymer Journal*, 2014, 59, 377–386.
[14] May, C.A. *Introduction to epoxy resins. In Epoxy Resins: Chemistry and Technology*, 2nd ed.; May, C.A., Ed.; Marcel Dekker: New York, USA, 1988.
[15] J. P. Pascault, R. J. J. Williams, *General concepts about epoxy polymers. In Epoxy Polymers: New Materials and Innovations*; Wiley VCH: Weinheim, Germany, 2010.
[16] W.K. Busfield, *Polymer Handbook*, 3rd ed.; Wiley, New York, USA, 1989.
[17] *A&C Catalysts Inc. Technicure® Curing Agents.* Available online: http://www.accatalysts.com/ prodCuring.html (accessed on 13 January 2015).
[18] J. M. Charlesworth, *Polymer Engineering & Science*, 1988, 28, 230–236.
[19] J.M. Charlesworth, *Journal of Macromolecular Science, Part B*, 1987, 26, 105–133.
[20] T. Xie, I.A. Rousseau, *Polymer,* 2009, 50, 1852–1856.

UNIVERSITAT ROVIRA I VIRGILI
NUEVOS PROCESOS DE CURADO CLICK CON TIOLES Y SU APLICACIÓN A LA PREPARACIÓN DE MATERIALES BASADOS EN EUGENOL
Dailyn Guzmán Meneses

UNIVERSITAT ROVIRA I VIRGILI
NUEVOS PROCESOS DE CURADO CLICK CON TIOLES Y SU APLICACIÓN A LA PREPARACIÓN DE MATERIALES BASADOS EN EUGENOL
Dailyn Guzmán Meneses

CAPÍTULO 5

RSC Advances, 2015, 5, 101623–101633

Preparation of click thiol-ene/thiol-epoxy thermosets by controlled photo/thermal dual curing sequence

Dailyn Guzmán, Xavier Ramis, Xavier Fernández-Francos, Angels Serra

UNIVERSITAT ROVIRA I VIRGILI
NUEVOS PROCESOS DE CURADO CLICK CON TIOLES Y SU APLICACIÓN A LA PREPARACIÓN DE MATERIALES BASADOS EN EUGENOL
Dailyn Guzmán Meneses

Preparation of click thiol-ene/thiol-epoxy thermosets by controlled photo/thermal dual curing sequence

Abstract

A new sequential two steps photo and thermal process for the preparation of click thiol-ene/thiol-epoxy thermosets is described. Commercially available diglycidyl ether of bisphenol A (DGEBA), triallylisocyanurate (TAIC) and pentaerythritol tetrakis (3-mercaptopropionate) (PETMP) were combined to produce tailored materials with a 75, 50 and 25% of thiol-ene/thiol-epoxy networks. A photoinitiator was used to trigger the radical thiol-ene polymerization and a latent amine precursor was used to start the base-catalyzed thiol-epoxy click reaction. Neat thiol-ene and thiol-epoxy materials were prepared and taken as the references. The use of a latent amine precursor in adequate proportion and under suitable reaction conditions allowed us to reach a dual system with two well-defined steps, stable intermediate materials and well-controlled structure after the first curing stage and at the end of the curing process. This process overcomes some limitations observed in analogous curing systems reported previously such as the absence of latency for the second curing stage leading to unstable materials in the intermediate stage. Both chemical reactions were studied by FTIR and calorimetry. The latency of the different formulations was studied by DSC and rheometry. The materials prepared were characterized by thermal mechanical analysis and thermogravimetry.

Keywords: Dual curing; thiol; epoxy; thermosets; click reaction.

Introduction

Dual curing combines two different and compatible polymerization reactions, which take place separately in a well-controlled way. This process is used to obtain stable materials after the first stage that maintain the ability, upon application of a second stimulus, to further react and achieve the final properties desired.[1,2] Dual processes usually combine two different curing methodologies, being usually photocuring followed by thermal curing.[3,4] The interest in such complex curing procedures is because of the processing advantages, such as: a) application one day and bonding of the parts at later date; b) application at one location and shipping them to a 2nd location for assembly; c) avoiding manufacturing bottlenecks; d) flip chip processes-flip chip and wafer passivation enabling 3D stacking, e) gasket and perimeter sealing of glasses in LCDs displays and f) automated in line processes assembly.

Click reactions have been extensively employed in material science because they are considered easy and fast methods of obtaining new substances, generally without the need of solvents.[5,6,7] The orthogonality of click reactions, their simplicity, efficiency and environmentally-friendly conditions make them highly advisable for combination in two curing step procedures. This orthogonality allows these reactions to be combined in a convenient way so as to reach technological applicability.[8] Thiol-click reactions are

suitable candidates since thiols are able to react under mild conditions by forming radical or anionic species selecting the appropriate conditions and catalysts,[9] making it possible to prepare thermosets in a controlled manner.

Thiol-ene and thiol-epoxy reactions are one of the most used in the last years to prepare new polymeric structures, linear, branched or crosslinked.[10,11,12] Radical thiol-ene polymerization is a step-wise process consisting in the alternation between thiol radical propagation through the -ene functional group and the chain transfer reaction, which involves the abstraction of hydrogen radical from the thiol by the carbon radical. This mechanism is depicted in Scheme 1. Studies of these reactions reveal that the thiol-ene can proceed without photoinitiator,[13] but their use assures a complete reaction, especially in thick specimens. One of the most commonly used photoinitiators is 2,2-dimethoxy-2-phenylacetophenone (DMPA).[14] One advantage of these reactions is that they are not inhibited by oxygen. During propagation carbon radical is capable of generating peroxides, but this reaction is slow and does not contribute much to the global process.[15] Although the thiol-ene reaction is a valuable strategy for the production of crosslinked polymers, it usually leads to low Tg materials.

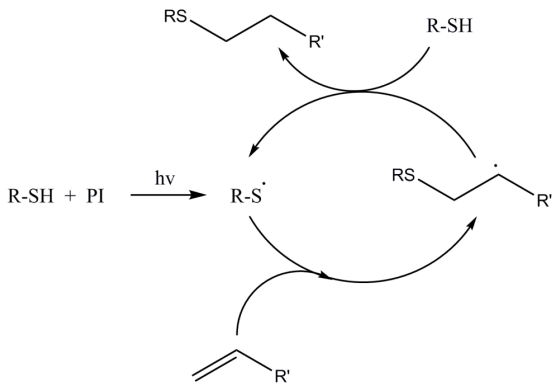

Scheme 1. Proposed mechanism of thiol-ene reaction

In the present work the thiol-ene is combined with a thiol-epoxy click reaction[16] that can be carried out under moderate temperature conditions to overcome vitrification during curing.[17] This reaction usually requires tertiary amines for activation. The reaction mechanism is step-wise and consists, essentially, in a nucleophilic attack to the oxirane group by the thiol. However, the thiol group can be transformed into a more nucleophilic thiolate anion, by the presence of amines acting as a base. The true mechanism of formation of the propagating species is complex and may involve either proton exchange between the thiol and the amine or nucleophilic attack of the amine to the epoxy, depending on the basicity and nucleophilicity of the tertiary amine, or the presence of proton donors acting as co-catalysts.[18] The formed nucleophilic thiolate anion attacks the oxirane ring, forming an alkoxide ion, according to the mechanism

presented below. Proton transfer takes place between the protonated amine or a thiol leading eventually to the formation of another thiolate anion. [19,20,21] The mechanism is depicted in Scheme 2.

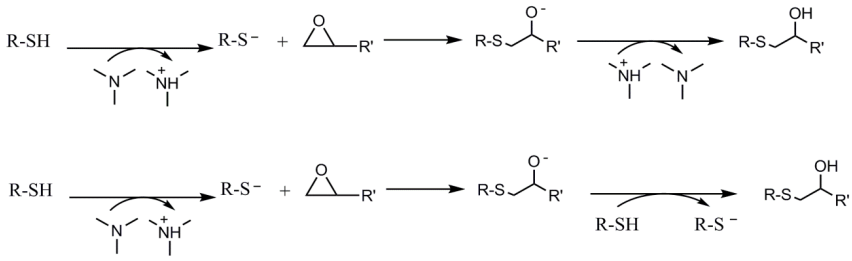

Scheme 2. Proposed mechanism of thiol-epoxy reaction

One of the problems that arise when using this methodology is that the use of tertiary amines leads to a too short pot life.[12] In a previous work we proposed the use of latent catalysts that are activated only by thermal stimuli,[22] with the purpose of preparing stable one-pot curing mixtures and facilitating their application in a more comfortable way. Compounds able to release amines such as encapsulated imidazoles or ureas can be of interest not only to increase pot-life of thiol-epoxy formulations but also to permit controlled activation of the thiol-epoxy reaction in a dual-curing process.

The strategy of combining these two thiol-click reactions has been studied previously by different research groups. An advantage coming from this combination is that the thiol component can participate in both processes and therefore the networks arising form tiol-ene and thiol-epoxy reactions are covalently interconnected. Another advantage comes from the fact that both thiol-ene and thiol-epoxy reactions are step-wise so that relevant network build-up parameters during both curing stages such as gel point conversion, gel fraction or crosslinking density can be easily calculated using well-established methods,[23,24] thus making it possible to tailor the curing process and the material properties in the intermediate stage and at the end of it in order to fit different processes and material requisites in a flexible way.

Cariosca et al.[25] studied thiol-ene/thiol-epoxy hybrid systems for dental applications. They used a tertiary amine as the catalyst and they reported homopolymerization of epoxide side-reaction to occur, because of the low activity of thiols after the first curing stage. Carlborg et al.[26] prepared thermosets from non-stoichiometric thiol-ene/thiol-epoxy mixtures using a two-stage UV curing with a photoinitiator and a photobase that were activated at different wavelengths. This methodology allowed achieving a dual curing system with an intermediate stage stable for only 24 h and they also reported that epoxy homopolymerization took place. However, it has been shown that the epoxy-thiol reaction takes place preferently while there is still remaining thiol, so that homopolymerization is not observed in epoxy-thiol systems.[18] Saharil et al.[27] used non-stoichiometric two-stage thiol-ene/thiol-epoxy

systems for the manufacture of microfluidic chips. In the first step the photocuring was carried out, whereas the second stage was done at 70 °C. This paper reported that the intermediate material was stable for 1-2 days, but the thiol-epoxy reaction occurred slowly at room temperature.

In the present work, a new dual curing system combining sequential thiol-ene/thiol-epoxy reactions, overcoming the above stability limitations and without the occurrence of undesired side-reactions, is described. The first stage is a radical thiol-ene reaction initiated by 2,2-dimethoxy-2-phenylacetophenone (DMPA) and the second one is a base-catalyzed thiol-epoxy reaction initiated by a latent catalyst (an encapsulated imidazole, LC-80 or a urea, PDU-250) that release the amine at a given temperature leading to the formation of the thiolate active species. What is sought by this methodology is to define a dual-curing system with a controlled curing sequence, with no overlapping between both curing reactions, and with sufficient stability in the intermediate stage, so that the second curing process is only activated at the time deemed appropriate. There is an important advantage coming from the fact that the first process is activated by UV-light and the second one is thermal and latent. This would make it possible, for instance to apply the material to a substrate and irradiate to promote the first reaction, then join two parts that adhere by contact with the partially cured material so that the final reaction and permanent bonding is triggered by temperature only when it is considered safe, something not possible if the second reaction is activated by UV light as well, or else is not stable enough. The proportions of -ene and epoxy compound in the formulation have been varied so as to control the extent of each process and consequently the characteristics of the intermediate and final materials. Both curing stages have been studied by DSC and FTIR. The latency and stability at the intermediate stage, as well as that of the unreacted formulation, have been evaluated. The thermal and mechanical properties of the intermediate and final materials have also been characterized.

Experimental part

Materials

Diglycidylether of bisphenol A (DGEBA, GY240, Huntsman, epoxy equivalent 182 g/eq) was dried at 80 °C under vacuum for 6h. The latent amine precursors were PDU-250 (N,N-dimethyl phenyl urea) and an encapsulated imidazole (Technicure® LC-80) both from AC Catalysts. Pentaerythritol tetrakis (3-mercaptopropionate) (PETMP), 1,3,5-triallyl-1,3,5-triazine-2,4,6(1H,3H,5H)-trione (TAIC) and 2,2-dimethoxy-2-phenyl-acetophenone (DMPA) from Sigma Aldrich were used as received. The structures of the compounds used are shown in Scheme 3.

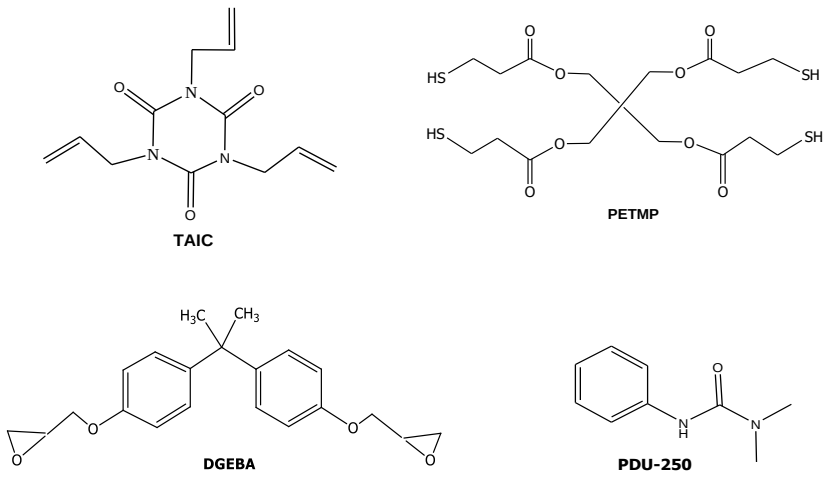

Scheme 3. Chemical structures of the starting compounds

Preparation of the curing mixtures

For the preparation of the curing mixtures it was initially necessary to prepare two different stoichiometric mixtures: TAIC-PETMP (thiol-ene) and DGEBA-PETMP (thiol-epoxy) both without any catalyst. Different proportions of these mixtures were mixed just before needed with a spatula to prepare homogeneous formulations (named as 75A%-25E%, 50A%-50E% and 25A%-75E%), being A the thiol-ene mixture and E the thiol-epoxy. To these formulations 0.1 phr of DMPA (parts per hundred of total mixture) as photoinitiator was added and different proportions of PDU-250 or 1 phr of LC80 as latent amine catalyst. For comparison purposes, neat thiol-ene and thiol-epoxy formulations were prepared with the corresponding catalysts.

The different formulations have been chosen so that they have significant differences between them at the intermediate stage, in terms of network structure and properties. The critical gelation ratio r_c for a step-wise reaction is given by the following expression:

$$r_c = \frac{1}{(f-1)\ (g-1)} \qquad (1)$$

where *f* and *g* are the functionalities of the different monomers. Taking into account that the first reaction taking place is the thiol-ene reaction, with f=4 (tetrathiol component) and g=3 (allyl component), the critical gelation ratio r_c would be equal to 0.167. Taking the allyl as the limiting component, this means that all the studied formulations, with a 25, 50, 75% of allyl component would be gelled after the first curing stage and have dimensional and mechanical stability to some extent. The differences

between them would be the increasing crosslinking density and decreasing soluble fraction and therefore increasing Tg with increasing allyl content. This could also have an effect on other interesting properties such as adhesion in the intermediate stage.

Characterization techniques

Samples of the different compositions were photocured at 35 °C, in a Mettler DSC-821e calorimeter appropriately modified with a Hamamatsu Lightning cure LC5 (Hg–Xe lamp) with two beams, one for the sample side and the other for the reference side. 5 mg samples were cured in open aluminium pans in nitrogen atmosphere. Two scans were performed on each sample, the second one needed to subtract the thermal effect of the radiation. The method consisted of 1 min without irradiation for temperature stabilization, followed by 1 min irradiation and finally 0.50 min without irradiation. The light intensity used was 21 mW/cm^2 (total light intensity measured with a pan filled with carbon black).

Larger rectangular specimens (40 mm x 10 mm x 1.5 mm) were prepared using a suitable mould. The samples were irradiated in an ultraviolet oven Dymax ECE 2000 UV-curing flood system (UV-intensity of 105 mW/cm^2, 365 nm) for a period of 30 s on each face, waiting for 5 min in between to control the temperature of the sample.

The curing kinetics of the following thermal thiol-epoxy reaction was analyzed by differential scanning calorimetry (DSC) in a Mettler DSC-821e apparatus calibrated using an indium standard (heat flow calibration) and an indium-lead-zinc standard (temperature calibration). Samples of ca. 10 mg weight were analyzed under N_2 atmosphere (100 mL/min flow rate). Dynamic curing was studied at a heating rate of 10 °C/min from 30 to 300 °C, and isothermal experiments were carried out at 120 °C.

The glass transition temperatures (Tgs) of the samples after irradiation were determined by a dynamic DSC scan at 20 °C/min from -50 °C to 50 °C. The Tgs of the final thermosets were determined after two consecutive heating dynamic scans at 20 °C/min starting at -50 °C in a Mettler DSC-822e device to delete the thermal history. The Tg value was taken as the middle point in the heat capacity step of the glass transition.

The unreacted mixtures were stored in an oven at controlled temperature of 35 °C for latency tests. The viscosity of the mixtures was measured at different storage times in a TA Instruments ARG2 rheometer equipped with disposable parallel plates. A sample gap of 0.4 mm was exactly set with an accuracy of 0.001 mm. A shear rate of 100 s^{-1} was applied at 35 °C after 5 min of temperature stabilization. A maximum of 2 min was needed to measure a steady value of viscosity. The values were corrected for non-uniform stresses in the parallel plates. The remaining enthalpy after storage was evaluated by DSC and compared with the enthalpy of a fresh prepared sample to determine the degree of curing occurred during storage.

A Bruker Vertex 70 FTIR spectrometer equipped with an attenuated total reflection accessory (ATR) (Golden Gate, Specac Ltd. Teknokroma) which is temperature controlled (heated single-reflection diamond ATR crystal) equipped with a liquid nitrogen-cooled mercury-cadmium-telluride (MCT) detector was used to register the FTIR spectra of uncured samples, after 1 min of UV irradiation and on fully cured samples. The spectra were registered in the wave number range between 4000 and 600 cm^{-1} with a resolution of 4 cm^{-1} and averaged over 100 scans. UV-curing was performed using a Hamamatsu Lightning cure LC5 (Hg-Xe lamp) with one beam conveniently adapted to the ATR accessory. A wire-wound rod was used to set a sample thickness of 50 μm. OPUS software was used for the analysis of the spectra. The spectra were corrected for the dependence of the penetration depth on the wavelength and normalized with respect to the absorbance of C=C and C=O peaks between 1900 and 1560 cm^{-1} (neglecting the contribution of the overlapping tiny signal associated with the allyl group). The normalized thiol band at 2570 cm^{-1} was integrated and the thiol conversions after the photocuring and after thermal curing were determined as:

$$X_{UV} = 1 - \frac{A'_{UV}}{A'_0} \qquad (2)$$

$$X_{final} = 1 - \frac{A'_{final}}{A'_0} \qquad (3)$$

where A'_{UV}, A'_{final} and A'_0 are the normalized area of thiol band after photocuring and thermal curing and at the beginning of the curing, respectively.

The thermal stability of cured samples was determined by thermogravimetric analysis (TGA), using a Mettler-Toledo TGA/DSC 1 stare system. All experiments were performed under inert atmosphere (N_2 at 50 mL/min). Pieces of the cured samples with an approximate mass of 10 mg were degraded between 30 and 600 °C at a heating rate of 10 K/min.

Dynamic mechanical thermal analyses (DMTA) were carried out with a TA Instruments DMA Q800 analyzer. The samples were photocured as described before and then isothermally cured in a mould at 120 °C for 1h with a postcuring at 150 °C for 1 h. Three point bending clamp was used on the prismatic rectangular samples (10 × 7.4 × 1.6 mm^3) that were analyzed first of all at 5 °C/min to delete the thermal history and then at 2 °C/min from 30 to 120 °C at a frequency of 1 Hz with and oscillation amplitude of 10 μm. Young modulus was determined by the stress/strain test, under the same clamp and geometry testing conditions, at 30 °C using a force ramp of 1 N min^{-1} and upper force limit of 18 N.

Results and discussion

Calorimetric study of the curing process

An important issue concerning dual-curing processes with a photo-activated first stage and a thermally activated second stage is that the photocuring conditions and the combination of catalysts needs to be optimized in order to prevent the occurrence of any thermal reaction (in this case thiol-epoxy or epoxy homopolymerization) during the first photocuring step. While this may not be of importance when small samples are studied under well-controlled temperature conditions in a DSC, photocuring of thicker samples such as those prepared for further thermal and mechanical analysis needs to be carried out carefully, that is, using the minimum possible amount of photoinitiator and adjusting the exposure time and intensity so as to avoid an excessive temperature increase (due to the exothermicity of the thiol-ene reaction and the thermal effect of the UV light) leading to premature activation of the latent catalysts used for the second stage. Therefore, the suitable proportion of DMPA as photoinitiator was determined. The photocalorimetric study of formulations containing 0.1 or 1 phr of DMPA in different thiol-ene/thiol-epoxy formulations produced no relevant difference, possibly due to the opposing effects of increased photoinitiator in reaction rate and penetration depth. Thus, and in order to prevent undesired excessive exothermicity effects, the amount of DMPA was fixed at 0.1 phr for all the studied formulations.

After that, the optimization of the catalyst in the thermal step was carried out using two formulations containing 50% of allyl (TAIC) and 50% of epoxy (DGEBA) compounds (from now 50%A-50%E) with stoichiometric amounts of tetrathiol (PETMP) and 1 phr of different base precursor (LC-80 or PDU-250).

To test whether the thermal thiol-epoxy reaction started during photocuring we determined the remaining heat of the formulation 50%A-50%E after irradiation in the UV chamber, and compared it with that of non-irradiated formulation. The dynamic DSC thermograms of the irradiated and non-irradiated samples are represented in Figure 1.

In agreement with a previous study,[17] some relevant differences were observed depending on the type of latent catalyst used. From the analysis of the non-irradiated samples, it is seen that LC-80 is clearly more active because of the lower curing temperature in comparison with PDU-250. However, this is also a disadvantage since the exotherm of the irradiated sample with LC-80 is entirely different from that of the initial mixture. This puts in evidence that the latent catalyst is unintentionally activated during the photoirradiation stage, leading to an overlapping of both processes. Possibly there is a too high temperature increase during the photocuring due to the exothermicity of the reaction or the thermal effect of the UV light leading to partial melting of the encapsulating polymer and early release of the imidazole catalyst. A temperature of 78 °C could be measured by pirometry in thiol-ene processes initiated by DMPA[28] which indicates that the thiol-ene process is quite exothermic. In the case of the

formulation with PDU-250, reaction enthalpy remains almost unchanged on comparing the exotherms before and after being exposed to photoirradiation, which indicates that the catalyst is not released due to its higher activation temperature, so that the epoxy-thiol reaction is not initiated during the first photocuring stage. Thus, PDU-250 has been selected as latent curing agent to further studies. It was not observed a significant influence of the catalyst on the Tg of the cured material, in both cases producing a value around 60 °C.

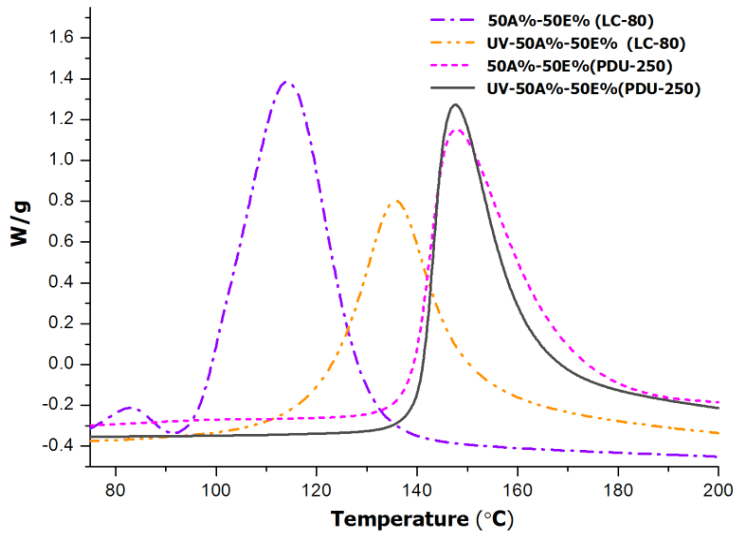

Figure 1. DSC thermograms corresponding to the 50%A-50%E before and after UV-irradiation for formulations containing 1 phr of PDU-250 or LC-80

Another point to be optimized is the curing rate of the second thermal process. Although initially 1 phr of PDU-250 catalyst in reference to the global mixture was used, it was put in evidence that the quantity of PDU-250 required was different depending on the formulation. In a previous paper, we found an optimum value of 2 phr (in reference to the amount of DGEBA) for a DGEBA-thiol mixture in order to reduce curing time and temperature,[17] although it was observed that a smaller amount such as 0.5 phr would also lead to complete curing but in a longer curing process. In the dual-curable formulations, the presence of a primary network originated after the photocuring stage and the dilution of the remaining epoxy and thiol groups depending on the formulation composition requires to find out the adequate proportion of amine precursor to be added to the formulation to promote complete and quick curing but, at the same time, ensuring enough stability in the intermediate stage. Different tests were done changing the proportion of PDU-250 in reference to the global mixture in non-irradiated samples. The most suitable proportions are the ones detailed in Table 1. The ratio PDU-250/DGEBA in the 75A%/25E% sample is quite high but lower proportions of catalyst led to a lower reaction heat than expected and the curing began at such high temperature

that epoxides might homopolymerize. The sample 50A%/50E% was the one that cured completely in the adequate range of temperatures with less catalyst.

In order to further understand the evolution of both processes and the possible overlapping among them, we first determined the reaction enthalpy of the mixtures without photoirradiation by DSC in order to evaluate the heat evolved in the thermal process without any influence of the photopolymerization stage. Figure 2 shows the thermograms of curing of the initial non-irradiated mixtures with the compositions detailed in Table 1.

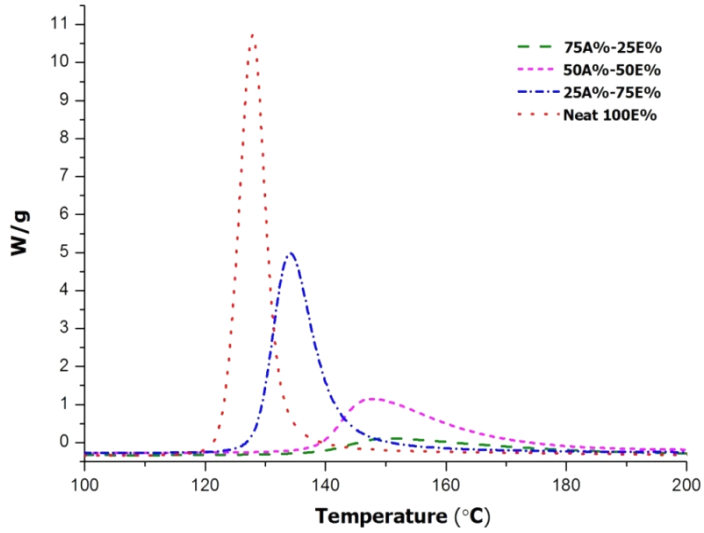

Figure 2. Dynamic DSC thermograms at 10 °C/min of non-irradiated thiol-ene/thiol-epoxy mixtures with different proportions of epoxy and allyl compounds

In the curves we can see how the curing reaction is accelerated on increasing the thiol-epoxy proportion within the system. The composition of the formulation also influences the onset temperature of the reaction. It is important to note that although the formulation 75%A-25E% contains a higher proportion of PDU-250, the curing starts at higher temperature, above 140 °C because of the significant dilution of epoxy groups in the mixture, resulting in lower initiation and propagation rates. In Table 1 the enthalpies determined are collected in the first column. Although the enthalpy per gram changes in the different formulations, the value by epoxy equivalent ranges between 105-126 kJ/eq, since the only process is the thiol-epoxy reaction. In a previous study we determined a reaction enthalpy between 120-128 kJ/eq in pure thiol-epoxy formulations.[17] From the values of the table it seems that the increase of the proportion of TAIC in the formulation apparently reduces the conversion of epoxide, although there might also be some error associated with the measurement of the reaction heat in a smaller exotherm (i.e. baseline determination).

Table 1. Calorimetric data for the reaction of the mixtures studied

		Initial mixture		1st stage			2nd stage		
Sample	**PDU-250[a] (phr)**	**ΔH[b] (J/g)**	**ΔH[c] (kJ/eq)**	**ΔH[d] (J/g)**	**ΔH[e] (kJ/eq)**	**Tg[f] (°C)**	**ΔH[g] (J/g)**	**ΔH[h] (kJ/eq)**	**Tg[i] (°C)**
Neat 100A%	-	---	---	243	50	65	---	-	65
75A%/25E%	2.5	86.2	105.0	229	64	24	94.0	114.5	63
50A%/50E%	1	182.2	112.1	165	68	0	185.6	114.2	61
25A%/75E%	2	302.9	126.0	83	70	-19	301.0	125.2	60
Neat 100E%	2	409.7	124.8	---	---	---	406.5	123.8	57

a. Parts of PDU-250 per hundred parts of the global mixture
b. Enthalpy evolved by gram of curing of the initial mixture (without photocuring)
c. Enthalpy by equivalent epoxy of curing of the initial mixture (without photocuring)
d. Enthalpy evolved by gram of sample in an isothermal photocuring scan at 35 °C
e. Enthalpy by equivalent of allyl group in an isothermal photocuring scan at 35 °C
f. Glass transition temperature of the material after completion of the thiol-ene reaction
g. Enthalpy evolved by gram of sample in dynamic thermal curing process after photoirradiation
h. Enthalpy evolved by epoxy equivalent in dynamic thermal curing process after photoirradiation
i. Glass transition temperature of the material after photo and thermal curing

The first stage of the dual curing, corresponding to the thiol-ene reaction, was studied by photocalorimetry. In the exotherms in Figure 3 we can appreciate that on increasing the content of allyl compound in the formulation the photocuring occurs faster. However, the reaction rate of the mixture with 100% thiol-ene (Neat 100A%) and the area below the exotherm (i.e. the reaction heat) is comparable to that of the 75A%-25E% formulation. In terms of reaction heat per amount of reacted allyl group, the reaction heat might be even lower taking into account the higher concentration of reactive allyl groups. The reason for this unexpected effect is unclear but the lower reaction heat may be caused by vitrification of the material at room temperature, as will be discussed below.

Table 1 shows the values of the heat released during the photocuring reaction measured by photocalorimetry at a controlled temperature of 35 °C. Upon decreasing the proportion of the allyl component in the formulation, the heat released during photocuring decreases but, in terms of the heat released by allyl equivalent they are similar, regardless of the proportion of the thiol-ene reaction, between 64-70 kJ/eq. The only exception is the lower value obtained for the neat 100A%, because of the before mentioned vitrification of the sample. The Tg values of the material at the intermediate stage were measured by DSC for the materials previously photocured in a curing chamber. In the case of the Neat 100A% formulation, it was determined after a second DSC run because of the release of some remaining heat during the first DSC scan (devitrification process). Indeed, Table 1 shows that the Tg of the completely cured neat allyl formulation is 65 °C while, in contrast, all the other formulations have a Tg in the intermediate stage below photocuring temperature, decreasing with increasing proportion of the epoxy component, because of the lower crosslinking density and the

presence of significant soluble fraction containing unreacted DGEBA and thiol monomers with a plasticizing effect.

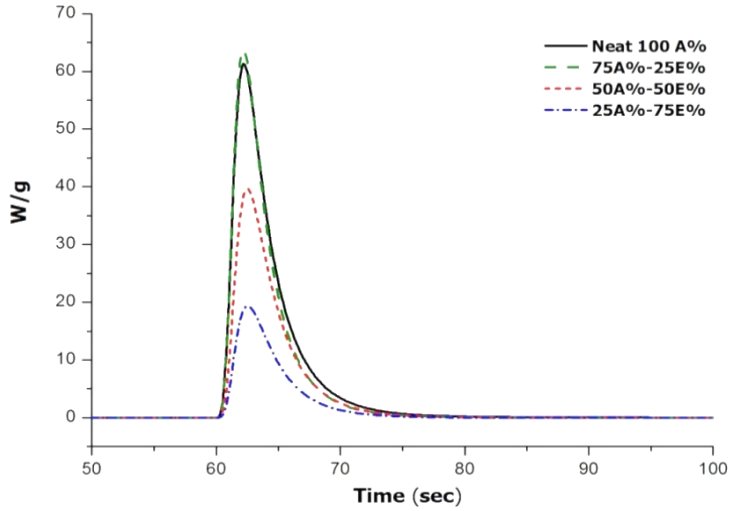

Figure 3. DSC thermograms corresponding to the photocuring stage at 35 °C of the mixtures thiol-ene/thiol-epoxy with different proportions

After studying both processes separately, the sequential dual-curing process was studied in order to confirm that no overlapping between both processes occurred. In Table 1 the values of the heat evolved in the thermal process in previously irradiated samples are detailed in the 2nd stage column. No relevant differences could be observed between the measured heat and that corresponding to non-irradiated samples, indicating that epoxy-thiol reaction did not take place and therefore there is no overlapping between both stages. This confirms the dual character of the curing obtained by using a latent amine precursor.

Study of the reactive processes by FTIR

Although the results of DSC analysis indicated that the dual curing process could take place in a controlled and sequential way, with no overlapping between processes, it did not provide evidence that other side reactions such as the epoxy homopolymerization did not occur. Cariosca et al.[25] determined that homopolymerization could take place to a measurable extent by monitoring the thiol band by FTIR. In the present study, we have followed a similar approach and we have irradiated the samples directly on the ATR/FTIR device with a UV lamp and then we performed the analysis of fully cured samples. The study was conducted qualitatively and quantitatively. Qualitative results are shown in the spectra of Figures 4 and 5 for two different formulations, 75A%-25E% and Neat 100A% respectively.

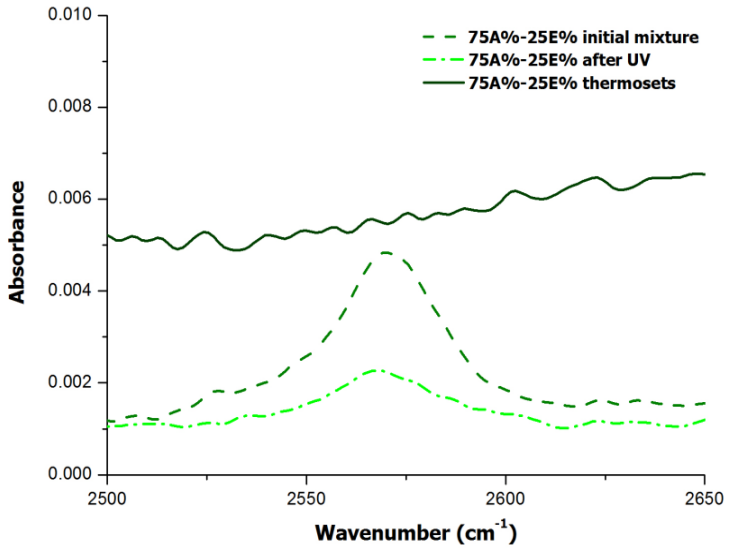

Figure 4. FTIR region corresponding to S-H st. for the formulation with 75 % of thiol-ene of the initial mixture, after irradiation and after complete curing

In the case of the formulation 75A%-25E%, Figure 4 shows that the band about 2570 cm^{-1} assigned to SH stretching decreases after UV irradiation and finally disappears when the material is thermally cured. This result is in line with the expected reaction mechanism for both stages, first the thiol-ene reaction and second the thiol-epoxy reaction. Given that no unreacted thiol group was detected, and the fact that the amount of thiol is stoichiometric with respect to allyl and epoxy groups, the occurrence of epoxy homopolymerization can be ruled out. In contrast, in the spectrum of the photocured neat thiol-ene formulation (Figure 5) the absorption of S-H st does not disappear completely, which indicates that the process has not been fully reacted due to the vitrification, as discussed above and in agreement with the lower heat released per allyl group (see Table 1).

Table 2 shows the results of the quantitative analysis. All calculations were done using equations 2 and 3 detailed in the experimental part. In the case of the neat 100% thiol-ene sample, the thiol conversion after the photocuring process is about 0.71, because of vitrification. This is in excellent agreement with the measured heat of 50 kJ/mol, in comparison with the 64-70 kJ/mol for complete reaction of allyl groups in the other formulations. After heating, this material devitrifies so that the thiol-ene reaction can resume and proceed up to almost complete conversion, reaching a final value of 0.93. Some topological restrictions may be operative, leading to incomplete cure, but it must be acknowledged there may be some experimental error in its determination because the thiol peak is very small. For the formulations with different contributions of thiol-ene and thiol-epoxy reaction, the thiol conversion after the photocuring process is

in good agreement with the expected reaction of thiol groups in the first curing stage by thiol-ene reaction, taking into account the composition and experimental error in the integration of such small peaks. At the end of the curing process, after heating the samples to promote epoxy-thiol reaction, no thiol was detected. Therefore it can be assumed that the system reacted quantitatively to full conversion of thiol, allyl and epoxy groups so that no homopolymerization could be detected. This is in contrast with previous works reporting a certain amount of epoxy homopolymerization that the authors attributed to the reduced mobility of the thiol groups in the intermediate material.[25] It was attempted to obtain further ascertainment of the above hypothesis on the curing mechanism by analysing the epoxy signal at 915 cm^{-1}, but the overlapping of other signals appearing during curing at the region around 900 cm^{-1} made it difficult to compare the epoxy and thiol conversions in the second curing stage in quantitative terms, to verify there is a one to one reaction. However, it has been recently shown that epoxy homopolymerization should not take place while there is remaining thiol, because the presence of remaining thiol groups promotes fast formation of thiolate anion to the detriment of epoxy homopolymerization.[18] Therefore it is quite safe to assume that epoxy homopolymerization does not take place in stoichiometric formulations such as the ones studied in this work.

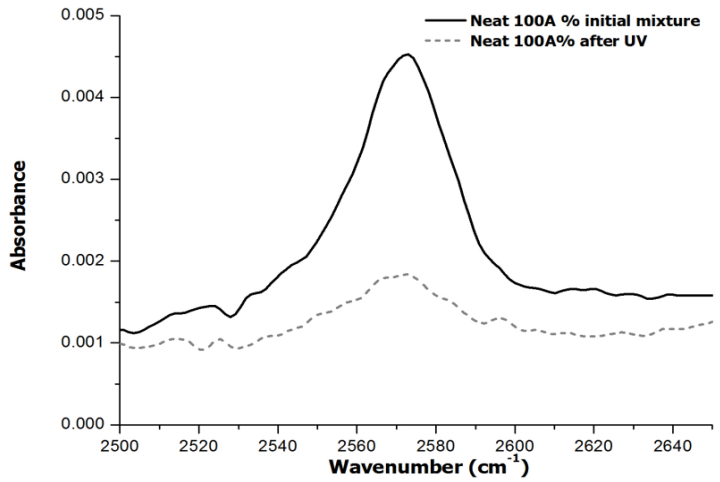

Figure 5. FTIR region corresponding to S-H st. for the formulation with 100 % of thiol-ene of the initial mixture and after irradiation

Table 2. Quantitative analysis of the SH absorption band of the initial mixtures and materials after each curing stage

Sample	A'_0	A'_{UV}	A'_{final}	X_{UV}	X_{final}
Neat 100A%	0.101	0.029	0.007	0.71	0.93
75A%/25E%	0.137	0.040	0	0.71	1
50A%/50E%	0.159	0.081	0	0.49	1
25A%/75E%	0.244	0.181	0	0.26	1

Storage stability of the formulations without irradiation

Curing formulations that show no activity under normal conditions but show activity by external stimulation can be considered latent.[29] Latency is an important concept in terms of storage stability and the possibility of preparing one-pot formulations. The latency of pure thiol-epoxy formulations with different proportions of amine precursors was previously studied in our research team and the period of save storage determined, but the addition of thiol-ene and DMPA could affect the results.[17,22] The latency studies were done by calorimetry (determining the residual heat) and by rheometry (measuring the viscosity changes). The data obtained are collected in Table 3.

Table 3. Viscosity and residual heat values of the initial mixtures and after one day of storage at 35 °C for the different formulations studied

Sample	η^a (Pa.s)	η^b (Pa.s)	ΔH^c (J/g)	ΔH^d (J/eq)
Neat 100A%	1.7	7.6	---	---
75A%/25E%	0.5	e	82	83
50A%/50E%	0.5	e	193	194
25A%/75E%	0.5	13	320	323
Neat 100E%	0.5	0.6	408	410

a. Viscosity of the initial mixture
b. Viscosity of the initial mixture after one day of storage
c. Remaining heat of the initial mixture determined by DSC in a dynamic scan
d. Remaining heat after one day of storage determined by DSC in a dynamic scan
e. The viscosity could not be measured because of gelation

In the table it is shown that the viscosity increases with only one day of storage, making it impossible its measurement in formulations with high thiol-allyl proportion. However, it remains practically unchanged in the case of neat epoxy-thiol formulation. After two days of storage the viscosity of any sample with allyl compound could not be measured. If we look to the difference in heat evolved after one day of storage, corresponding to the epoxy-thiol reaction, there is no difference for all the formulations prepared, giving very similar values to those shown in Table 1. This clearly indicates that whereas the second stage may keep its latent characteristics during this period the first photochemical stage has a low latency and that the reaction starts even without the application of any light source. This study indicates that it is not possible to prepare one pot-formulations with this curing system, but they could be stored for several days at room temperature without adding the catalysts, since uncatalyzed formulations keep good processability. It should be commented that PDU-250 is advantageous in comparison with other amine catalysts, such as those used by other authors in similar curing systems.[25]

Stability of the materials after the photoirradiation stage

To test the stability of the intermediate materials with the storage time, it was necessary to track the remaining heat by DSC after irradiation, since rheological measurements were not possible due to thiol-ene crosslinking after the first stage. To do this, we proceeded to irradiate all the mixtures in the UV chamber. The resulting samples were stored at room temperature and then the remaining enthalpy was periodically measured. In this way, the advancement of the epoxy-thiol process could be evaluated. It should be pointed out, for comparison purposes, that mixtures of DGEBA/thiol containing 2 phr of PDU-250 (in reference to DGEBA) showed a latency of only 2 days at 35 °C.[22] The results obtained for the present formulations are represented in Figure 6.

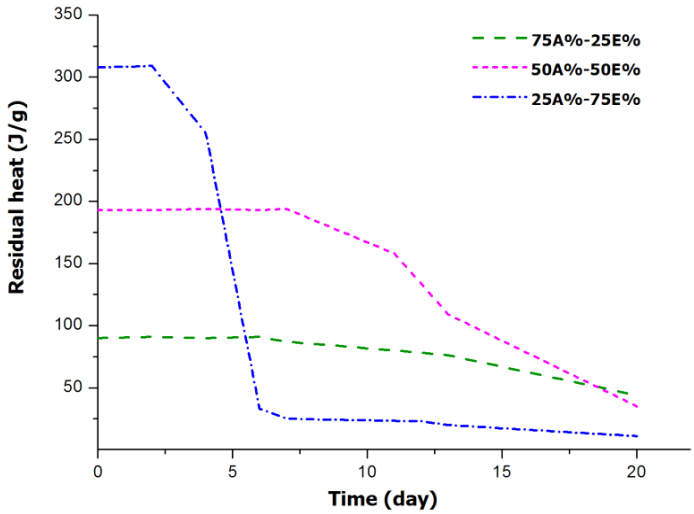

Figure 6. Plot of remaining enthalpy of curing against storage time for the materials obtained from different formulations

The plot shows the influence of the proportion of thiol-ene system in the stability of the intermediate material. For the 25A%-75E% formulation, with lower amount of thiol-ene, there is a significant decrease in remaining heat after the second day of storage because of the activation of the thiol-epoxy reaction. After six days of storage the process stops (reaching a conversion of 89%), possibly due to the vitrification. The other two formulations behave in a different manner, showing a longer stability. The sample 50A%-50%E is completely stable up one week and then the reaction begins and reaches a conversion of 18% after 11 days. After three weeks, the epoxy conversion is 81%. The formulation 75A%-25%E with less epoxy-thiol proportion shows a higher stability. After one week of storage, a conversion of 11% could be measured. Epoxy-thiol reaction proceeds further but at a slow rate, so that after three weeks the epoxy conversion is only 51%. In general, the lower the proportion of epoxide in the formulation, the longer the storage time of the intermediate material. This reflects the

effect of the primary thiol-ene network formed in the photoirradiation stage in the immobilization of the thiol-epoxy reactive groups. According to these results, the dual system proposed could be of interest for assembling devices, for flip chip processes, for perimeter sealing and especially for automated in line assemblies, but it shall not apply to uses that require a long transport or long time between both curing stages. However, the curing system proposed keeps the characteristics of the intermediate material much longer than those previously described.[25, 26]

Characterization of the materials

The materials obtained after dual curing were transparent but coloured because of the thermal treatment (Figure 7).

Figure 7. Photographs of the materials obtained

There are few differences in the transparency due to the good compatibility between thiol-ene and thiol-epoxy structures by the covalent bonding between them in the network.

The thermosets obtained from the different formulations were studied by TGA to evaluate their thermal stability. The materials were photocured and then thermally cured at 120 °C for 1h with a post-curing at 150 °C for 1h. Figure 8 shows the derivative curves registered in inert atmosphere. Other relevant degradation parameters, the onset temperature of degradation ($T_{5\%}$, temperature at which a mass loss of 5 % is observed) and degradation peak temperature, are presented in Table 4.

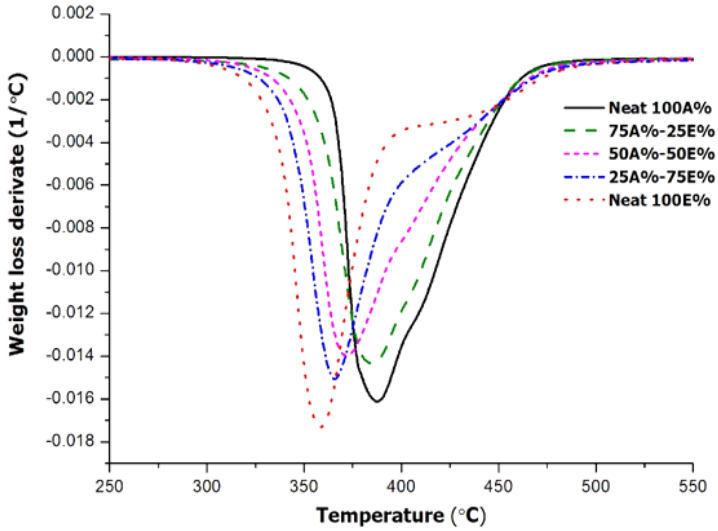

Figure 8. DTG curves under N_2 at 10 K/min of the materials obtained

The curves show unimodal/bimodal shapes, with an overlapping between two processes, indicating a complex degradation profile. Unlike other epoxy systems combining two curing processes, such as epoxy-amine/epoxy homopolymerization[30] or dual-curing combining aza-Michael and radical homopolymerization of acrylates,[31] it is not possible to assign these processes to the individual contribution of each one of the networks being formed in the dual-curing process. This may be explained by the fact that the thiol is present in both networks so that the thermal stability of the materials are intermediate between both. In fact, as a general trend, it can be observed that the whole degradation peak is shifted at lower temperatures with increasing proportion of epoxide in the formulation. The shoulder at higher temperatures remains in the same position and decreases in intensity with increasing epoxy content, but is present already in the neat thiol-epoxy formulation. The global stability trend is also observed in Table 4. The thermal stability of all materials is remarkable in any case ($T_{5\%}$ above 330 °C) but both the T5% and the peak degradation temperature decrease with increasing epoxy in the formulation. It should be considered the different structure of the monomers that leads to a higher crosslinking density for thiol-ene network due the compact structure of TAIC.

The thermomechanical characteristics of the materials were tested by DMTA. Figure 9 shows the tan δ curves for the thermosets and the relevant parameters are collected in Table 4.

As we can see, the curves are unimodal and quite narrow indicating the homogeneity of the samples. The maximum of tan δ is shifted to higher temperatures on increasing the proportion of allyl compound in the formulation as the result of the higher functionality and stiffness of its structure in comparison with DGEBA. The values

obtained follow the same trend as those obtained by DSC, which are collected in Table 1. Similarly, in a previous work, we were able to increase the Tgs of thiol-epoxy thermosets by substituting bisphenol A epoxide by triglycidyl isocyanurate due the stiffness and higher functionality of this compound.[17]

Table 4. Thermal data of the cured materials obtained from different formulations

Notation	$T_{5\%}$[a] (°C)	T_{max}[b] (°C)	$T_{tan\delta}$[c] (°C)	E_r[d] (MPa)	E[e] (MPa)
Neat 100A%	372	388	74	30.0	1177.0
75A%/25E%	350	386	73	24.8	1122.0
50A%/50E%	348	373	72	22.3	1029.0
25A%/75E%	338	367	68	15.1	933.6
Neat 100E%	330	359	62	11.4	920.9

a. Temperature of 5% of weight loss in N_2 atmosphere
b. Temperature of the maximum rate of degradation in N_2 atmosphere
c. Temperature of maximum of tan δ determined by DMTA
d. Storage modulus in the rubbery state determined at tan δ + 50 °C
e. Young´s modulus at 30 °C

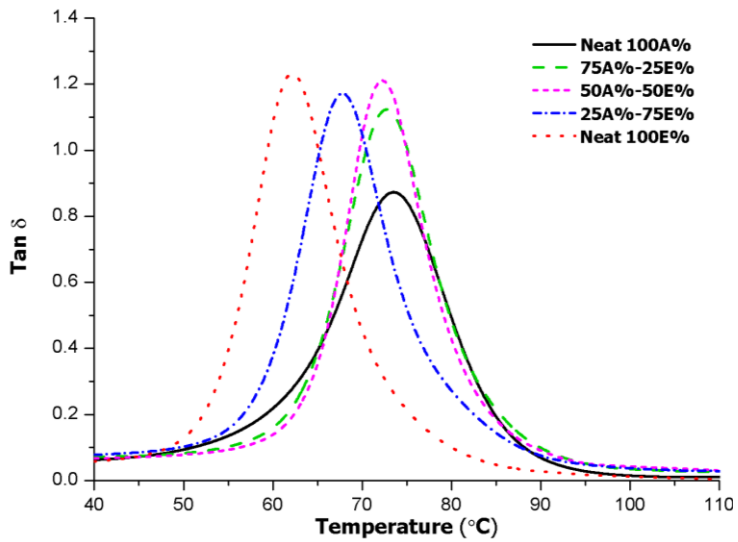

Figure 9. Plot of tan δ against temperature of the different materials prepared

The Young modulus of the material at 30 °C shows an increase in stiffness on increasing the proportion of allyl compound in the formulation. This could be expected taking into account the increase in Tg with the increase in the more rigid allyl component, so that the measurement of the Young modulus is less affected by the slow relaxation of the network, given the proximity of the measurement temperature and the Tg of all the materials. There is also a noticeable increase in the moduli in the rubbery state on increasing the proportion of allyl that could be expected taking into

account the increase in crosslinking density given the higher functionality obtained when the allyl component is used instead of DGEBA.

As it has been demonstrated in this study, the structure and proportion of comonomers can be varied to tailor the characteristics of the dual-cured materials in both the intermediate stage and at the end of the curing process, although the flexible structure of the commercially available thiol compounds is the main limitation of these processes to reach materials with a higher Tg and mechanical characteristics.

Conclusions

A new dual curing procedure based in the combination of UV-induced thiol-ene and thermal thiol-epoxy click reactions has been stablished by the use of a latent amine precursor that can catalyze the thermal process. The application of this procedure makes it possible to obtain tailored intermediate and final materials by just changing the formulation composition, and to store them for a certain period of time in the intermediate state before the final application and completion of the curing process.

From the DSC analysis of different TAIC/DGEBA formulations with the stoichiometric amount of tetrathiol using LC-80 or PDU-250 as latent catalysts it was possible to determine that PDU-250 was a more suitable catalyst to suppress the overlapping between photo and thermal processes as it was more resistant to the possible temperature overshot occurring during the first photocuring stage. The amount of PDU-250 was adjusted to reach complete curing in all formulations. FTIR confirmed that homopolymerization of epoxides did not occur.

The materials in the intermediate stage, after photoirradiation, showed higher storage stability on increasing the proportion of allyl compound in the formulation. The new dual curing system could be applied to assemble devices, in flip chip processes, in perimeter sealing and especially in automated in line assemblies.

The increasing presence of the allyl compound in the formulation increased the Tg in the intermediate stage due to the higher extent of cure and also that of the final material due to the increase in crosslinking density and the lower mobility of the resulting network.

Thermosetting materials exhibited good transparency and thermal stability, with an increase in the initial degradation temperature with the amount of TAIC in the formulation. The moduli of these materials were also affected by the ratio of this compound in agreement with its more rigid structure and the increase in Tg.

Acknowledgments

The authors would like to thank MINECO (MAT2014-53706-C03-01, MAT2014-53706-C03-02) and Generalitat de Catalunya (2014-SGR-67) for the financial support.

References

[1] D. P. Nair, N. B. Cramer, J. C. Gaipa, M. K. McBride, E. M. Matherly, R. R. McLeod, R. Shandas, C. N. Bowman, *Advanced Functional Materials*, 2012, 22, 1502–1510.

[2] C-H. Park, S-W. Lee, J-W. Park, H-J. Kim, *Reactive and Functional Polymers*, 2013, 73, 641–646.

[3] R. Acosta Ortiz, A. E. Garcia Valdez, L. Berlanga Duarte, R. Guerrero Santos, L. R. Ovando Flores, M. D. Soucek, *Macromolecular Chemistry and Physics*, 2008, 209, 2157-2168.

[4] D. Foix, X. Ramis, A. Serra, M. Sangermano, *Polymer*, 2011, 52, 3269-3276.

[5] C. E. Hoyle, C. N. Bowman, *Angewandte Chemie*, 2010, 49, 1540-1573.

[6] M. J. Kade, D. J. Burke, C. J. Hawker, *Angewandte Chemie*, 2010, 48.

[7] A. B. Lowe, *Polymer Chemistry*, 2010, 1, 17–36.

[8] U. Tunca, *Journal of Polymer Science Part A: Polymer Chemistry*, 2014, 52, 3147–3165.

[9] Y. Jian, Y. He, Y. Sun, H. Yang, W. Yang, J. Nie, *Journal of Materials Chemistry C*, 2013, 1, 4481–4489.

[10] V. S. Khire, T. Y. Lee, C. N. Bowman, *Macromolecules*, 2008, 41, 7440-7447.

[11] B-S. Chiou, R. J. English, S. A. Khan, *Macromolecules*, 1996, 29, 5368-5374.

[12] Y-H. Li, D. Wang, J. M. Buriak, *Langmuir*, 2010, 26, 1232-1238.

[13] N. B. Cramer, J. P. Scott, C. N. Bowman, *Macromolecules*, 2002, 35, 5361-5365.

[14] M. Uygun, M. A. Tasdelen, Y. Yagci, *Macromolecular Chemistry and Physics*, 2010, 211, 103–110.

[15] M. Kharasch, W. Nudemberg, G. Mantell, *Journal of Organical Chemistry*, 1951, 16, 524-532.

[16] A. Brandle, A. Khan, *Polymer Chemistry*, 2012, 3, 3224-3227.

[17] D. Guzmán, X. Ramis, X. Fernández-Francos, A. Serra, *Polymers*, 2015, 7, 680-694.

[18] R. Meizoso Loureiro; T. Carballeira Amarelo; S. Paz Abuin, E. R. Soulé, R. J .J. Williams, *Thermochimica Acta*, 2015, 616, 79-86.

[19] Y. Tanaka and R.S. Bauer, *Curing Reactions*, Marcel Dekker In: C.A. May, Ed. New York, 2nd ed, 1988, chapter 3, pp. 310-312.

[20] T. Ware, D. Simon, K. Hearon, T. H. Kang, D. J. Maitland, W. Voit, *Macromolecular Bioscience,* 2013, 13, 1640–1647.

[21] E. M. Petrie, *Epoxy adhesive formulations*, McGraw-Hill Companies Inc, USA, 2006.

[22] D. Guzmán, X. Ramis, X. Fernández-Francos, A. Serra, *Polymer Journal*, 2014, 59, 377–386.

[23] J. P. Pascault, H. Sautereau, J. Verdu, J. J. Williams, *Thermosetting Polymers*. Marcel Dekker, New York, USA, 2002.

[24] D. R. Miller, E. M. Valles, C. W. Macosko, *Polymer Engineering & Science*, 1979, 19, 272-283.

[25] J. A. Carioscia, J. W. Stansbury, C. N. Bowman, *Polymer*, 2007, 48, 1526–1532.

[26] C. F. Carlborg, A. Vastesson, Liu Yitong, W. van der Wijngaart, M. Johansso, T. Haraldsson, *Journal Polymer Science, Part A: Polymer Chemistry*, 2014, 52, 2604-2615.

[27] F. Saharil, F. Forsberg, Y. Liu, P. Bettotti, N. Kumar, F. Niklaus, T. Haraldsson, W. van derWijngaart, K. B. Gylfason, *Journal of Micromechanics and Microengineering*, 2013, 23, 025021.

[28] M. Sangermano, M Cerrone, G. Colucci, I. Roppolo, R. Acosta Ortiz, *Polymer International*, 2010, 59, 1046-1051.

[29] T. Endo, F. Sanda, *Macromolecular Symposia*, 1996, 107, 237-242.

[30] X. Fernández-Francos, D. Santiago, F. Ferrando, X. Ramis, J. M. Salla, À. Serra, M. Sangermano. *Journal of Polymer Science Part B: Polymer Physics*, 2012, 50, 1489-1503.

[31] G. Gonzalez, X. Fernández-Francos, A. Serra, M. Sangermano, X. Ramis, *Polymer. Chemistry,* 2015, 6, 6987-6997.

UNIVERSITAT ROVIRA I VIRGILI
NUEVOS PROCESOS DE CURADO CLICK CON TIOLES Y SU APLICACIÓN A LA PREPARACIÓN DE MATERIALES BASADOS EN EUGENOL
Dailyn Guzmán Meneses

UNIVERSITAT ROVIRA I VIRGILI
NUEVOS PROCESOS DE CURADO CLICK CON TIOLES Y SU APLICACIÓN A LA PREPARACIÓN DE MATERIALES BASADOS EN EUGENOL
Dailyn Guzmán Meneses

CAPÍTULO 6

Polymer International, 2017

Novel thermal curing of cycloaliphatic resins by thiol-epoxy click process with several multifunctional thiols

Dailyn Guzmán, Blai Mateu, Xavier Fernández-Francos, Xavier Ramis, Angels Serra

UNIVERSITAT ROVIRA I VIRGILI
NUEVOS PROCESOS DE CURADO CLICK CON TIOLES Y SU APLICACIÓN A LA PREPARACIÓN DE MATERIALES BASADOS EN EUGENOL
Dailyn Guzmán Meneses

Novel thermal curing ofcycloaliphatic resins by thiol-epoxy clickprocesswithseveral multifunctional thiols

Abstract

Novelthermosetswere prepared by the base-catalyzed reaction between a cycloaliphatic resin (ECC) and different thiol crosslinkers. 4-(N,N-dimethyl-aminopyridine) (DMAP) was used asbase catalyst for the thiol-epoxy reaction. A commercial tetrathiol (PETMP) and three different thiols synthesized by us, 6SH-SQ, 3SH-EU and 3SH-ISO, were tested.6SH-SQ and 3SH-EU were prepared from vinyl or allyl compounds from renewable resources such as squalene and eugenol,respectively. The thiol 3SH-ISO was prepared starting from commercially available triallyl isocyanurate. The kinetic study of the mixtures was performed by DSC. Stoichiometric ECC/thiol/DMAP formulations were cured at 120°C for 1h, at 150°C for 1h and post cured for 30 min at 200°C. The materials were characterized by FTIR, TGA and DMTA. The results revealed that the materials obtained fromthe synthesizedthiols had higher thermal stability and glass transition temperatures than those obtained fromthe commercial PETMP. In addition, all the materials obtained exhibited very good transparency. This study proves the ability of multifunctional thiols to crosslink cycloaliphatic epoxy resins, leading to more flexible materials than those obtained by cationic homopolymerization of ECC or base-catalyzed ECC-anhydride copolymerization.

Keywords: Cycloaliphaticepoxides, thiol-epoxy, click, thermosets,eugenol, squalene.

Introduction

There is no doubt that click reactions are highly interesting tools in the organic chemistrysynthetic world. The philosophy of the click chemistry is based on generating new substances starting from small units, by highly controlled reactions, clean and energy saving processes without the formation of by-products or organic volatiles, emulating nature.[1,2,3] The thiol-epoxy reaction is a good example among the great variety of click reactions.[4] Its mechanism is based on the nucleophilic attack to the less substituted carbon on the epoxy ring by a thiolate anion.[5,6]

In recent years,thiol-epoxy reaction has been applied in the curing of epoxy resins, specifically for diglycidyl ether of bisphenol A (DGEBA),obtaining materials with good thermal properties and high transparency.[7]Although DGEBAresins arethe most widely used for various applications, cycloaliphatic epoxy resins present some advantages that make them more adequate in the field of the electrical and electronic industry. Among their most notable features, excellent weathering, inherently low viscosity, low dielectric loss and high electrical resistivity are of utmost importance for the fabrication of electronic devices. Because of their high resistance to yellowing by ultra-violet light absorption, they are also useful in applications like light emitting diodes. Wang's group synthesized and characterized a great variety of cycloaliphatic epoxy resins with

different structure adequate for several special applications,[8,9] among them for optical materials,[10]electronics[11]or fire retardancy,[12] but nowadays the most widely used in industrial applications is 3,4-epoxycyclohexyl-3',4'-epoxycyclohexanecarboxylate (ECC).

Cycloaliphatic epoxy resins aremore reactive than DGEBA in front of cationic curing agents and therefore these resins are usually homopolymerized via cationic ring-opening in thermal or photoinitiated conditions.[13,14]Cycloaliphatic epoxy resins are not reactive bynucleophilic attack of amines because of the high topological hindrance of the epoxy in the cycloaliphatic ring. However, they can be cured by anhydrides through ring-opening copolymerization mechanism.[15,16]Homopolymerized and anhydride-cured cycloaliphatic epoxy resins are usually brittle materials because of the compactand rigid nature of the network structure and the inherent rigidity of the network chains. Therefore, it is quite interesting to modify the network by curing with other stoichiometric hardeners or copolymerization with flexible comonomers, leading to a more open and flexible network structures and with higher versatility in mechanical and thermomechanical behavior.[17]

The use of thiols as crosslinking agents in thiol-ene, thiol-epoxy or thiol-acrylate materials[18,19] is a good strategy to obtain materials with a flexible network structure and lower crosslinking density than homopolymerized thermosets, with a subsequent increase in toughness or impact resistance. By selecting the structure and functionality of the thiol, Tg and modulusof the cured materials can be adequately tailored.[20]The curing of ECC by thiol-epoxy click reaction has been little explored, being the only report in the literature the investigation of Sangermano et al.[21]They prepared hybrid nanocomposites using a combination of thiol-epoxy and sol-gel processes. As starting formulations, they used different mixtures of commercial trithiol and a photolatent tertiary amine, ECC, tetraethoxysilane (TEOS) and 3-mercaptopropyl trimethoxysilane (MPTS). They obtained organic/inorganic hybrid materials with a potential interest in optical applications. However, such systems are only adequate for thin layers, because of the limitations of photoirradiation technologies.

Thiols from renewable sources are very attractive because they are a good alternative to prepare thermosets from non-petroleum basedderivatives. Among natural products, terpenes show a high functionality in a quite compact structure and therefore they are good candidates for thermosetting materials. Acosta Ortizet al.[22]reported the preparation of a hexathiol derivative of squalene prepared through a thiol-ene reaction preceded by hydrolysis. It has, in principle, a flexible aliphatic structure but, given its high functionality and the low molecular weight of each reactive unit, once the material is crosslinked, the presence of internal branching points and the short distance between crosslinking points would lead to rigid materials with a high Tg. Following the same synthetic procedure, two new trithiols with rigid core were also synthesized. One of them, is derived from eugenol, which is also a natural product, and the other is derived from commercially available triallylisocyanurate (see Scheme 1).

In this paper we describe the curing of a cycloaliphatic epoxy resin(ECC) with the threethiols synthesized and we also include the widely used and commercially available tetrafunctional thiolPETMP, with a highly flexible structure. The kinetics of the curing process has been analyzed by calorimetry. The crosslinked materials obtained were characterized by thermogravimetry and thermomechanicalanalysis.

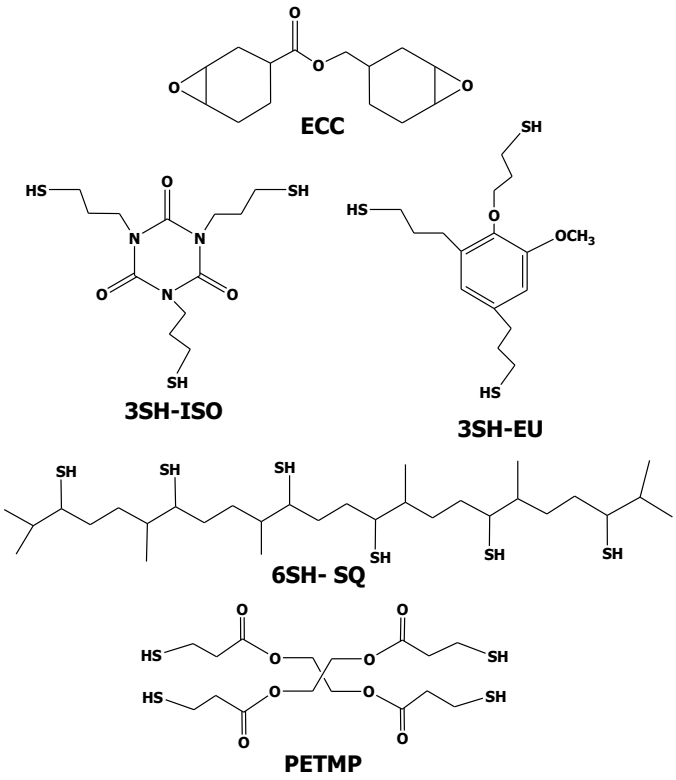

Scheme 1. Chemical structures of the epoxy resin and the thiols studied

Experimental part

Materials

3,4-Epoxycyclohexyl-3',4'-epoxycyclohexanecarboxylate (ECC), eugenol (EU), squalene (SQ), triallyl isocyanurate (TAIC), pentaerytritol tetrakis (3-mercaptopropionate) (PETMP), thioacetic acid (TAA), allyl bromide, 2,2-dimethoxy-2-phenylacetophenone (DMPA), 4-(N,N-dimethylamino)pyridine (DMAP), 1-methylimidazole (1-MI) and 2-methylimidazole (2-MI) were purchased from Sigma-Aldrich and were used without further purification.The latent amine precursor was LC-80 (encapsulated imidazole) and was received from AC Catalysts. Inorganic salts and bases were purchased from Scharlab. Methanol from Carlo Erba has been used as received. N,N-dimethylformamide (DMF) from VWRwas dried by standard procedures.

Preparation of starting products

- *Synthesis of thiol from squalene (6SH-SQ)*

The product was obtained following a two-step procedure previously reported.[22]

Photochemical thiol-ene reaction (6STA-SQ)

A mixture of 5 g (12.2 mmol) of SQ,11.1 g (146 mmol) of TAA and 0.062 g (0.24 mmol) of DMPA were photoirradiated with a UV lamp at 356nm for 30 min. The product was dissolved in $CHCl_3$ and extracted with a 10% NaOH solution and then washed with water and dried over anhydrous $MgSO_4$. The solvent was removed on a rotary evaporator. A clear viscous liquid was obtained with87%yield.^{1}H NMR ($CDCl_3$, δ in ppm),3.3 broad (CH-S, 6H), 2.3 s (CH_3-CO-, 18H), 1.1-2.0broad (-CH_2- and –CH-, 26H) and0.8-0.9 broad (CH3-, 24H). FT-IR (ATR): 2960, 2925, 1680, 1450, 1380, 1365, 1110, 1140, 950, 752 and 620 cm^{-1}.

Hydrolysis of 6STA-SQ (6SH-SQ)

9 g(10.4 mmol) of the 6STA-SQ were put in a round-bottomed flask with 60 mL of methanol and 1.8 g (45 mmol) of pulverized NaOH and vigorously stirred for 5.5h at reflux temperature and inert atmosphere. The solution was allowed to cool and the solvent was removed. The product obtained was dissolved in water and acidified with 0.1 M HCl solution and then extracted with $CHCl_3$. The organic phase was washed with distilled water and dried over anhydrous $MgSO_4$. After solvent evaporation the purification of 6SH-SQ was carried out by silica gel column chromatography using hexane/ethyl acetate 8/2 mixture as eluent. The purified product was a pale yellow viscous liquid with a 71% yield.^{1}H NMR ($CDCl_3$, δ in ppm), 2.60 broad (-CH-S-, 6H), 1.10-1.95 unresolved broad signals (-CH_2-,-CH- and -SH, 32H) and0.8-1.05broad (CH_3-, 24H). FT-IR (ATR): 2955, 2923, 2570, 1450, 1378, 1350 and 752 cm^{-1}. Spectra are fully coincident to those reported in the literature.[22]

- *Synthesis of thiol from triallyl isocyanurate (3SH-ISO)*

Photochemical thiol-ene reaction (3STA-ISO)

A mixture of 6 g (24.1 mmol) of triallyl isocyanurate (TAIC) and 21.98g (288.7 mmol) of TAA were photoirradiated with a UV lamp at 356 nm for 1h adding0.1286 g (0.5 mmol) of DMPA as photoinitiator. The product was dissolved in $CHCl_3$ and extracted with a saturated NaOH solution and then washed with water and dried over anhydrous $MgSO_4$. The solvent was removed on a rotary evaporator and the product obtained was a white solid with 96 % yield. (m.p. 77 °C). ^{1}H NMR ($CDCl_3$,δ in ppm):3.90 t (-CH_2-N-, 6H), 2.87 t(-CH_2-S-, 6H), 2.30 s(CH_3-CO-, 9H) and1.90 q (-CH_2-CH_2-CH_2-, 6H). ^{13}C NMR ($CDCl_3$, δ in ppm):200 (CO-S), 149 (-N-CO-N-), 42 (-N-CH_2-), 30 (CH_3CO-S-),27 (-CH_2-S-) and 25 (-CH_2-CH_2-CH_2-). FT-IR (ATR):2800, 2780, 1660, 1458, 1424, 1140, 960, 810, 776 and 620 cm^{-1}.

Hydrolysis of 3STA-ISO (3SH-ISO)

11.92g (25 mmol) ofSTA-ISO was put into a round bottomed flask equipped with a magnetic stirrer with120 mL of methanol and 2.15 g (53.8 mmol) of pulverized NaOH. The solutionwas maintained for 5.5h at reflux temperature under inert atmosphere and then allowed to cool down and the solvent was removed. The solid obtained was dissolved in water and acidified with 0.1 M HCl solution. Then, it was extracted with $CHCl_3$and the organic phase was washed with distilled water several times and dried over anhydrous $MgSO_4$. The thiol 3SH-ISO obtained after the solvent evaporation was a colourless viscous liquid, 95% yield. ^{1}H NMR ($CDCl_3$, δ in ppm):4.05 t (-CH_2-N-, 6H), 2.60 (-CH_2-S, 6H), 1.95 q (-CH_2-CH_2-CH_2-, 6H) and1.60 t (-SH, 3H). ^{13}C NMR ($CDCl_3$, δ in ppm):149.5 (-N-CO-N), 42.0 (CH_2-N), 32.5 (CH_2-SH) and21 (-CH_2-CH_2-CH_2-).FT-IR (ATR):2800, 2778, 2570, 1675, 1456, 1420 and 772 cm^{-1}.

- *Synthesis of thiol from eugenol (3SH-EU)*

The trithiol of eugenol was prepared from eugenol by a five-step synthetic procedure.

Preparation of triallyl eugenol (3A-EU)

Triallyl eugenol was prepared following a previously reported procedure.[23]

Synthesis of 1-allyl-4-allyloxy-3-methoxybenzene (2A-EU)

16.4 g of eugenol (100 mmol) and 4.40 g of pulverized NaOH (110 mmol) were dissolved in 120 mL of dry DMF in a 500 mLthree necked round bottomedflask under inert atmosphere. The mixture was stirred for 10 min and then allyl bromide (13.30 g, 110 mmol) was added dropwise over 1 h at 40°C, once the addition was finished the solution was maintained at 40°C for 3 h and then half an hour at 70°C.The solvent was eliminated in the rotavap and the oil was dissolved in $CHCl_3$ and filtered to eliminate the precipitate of inorganic salts. The organic phase was washed twice with distilled water, dried over anhydrous $MgSO_4$and the solvent eliminated to obtain 96% yield of 2A-EU as a yellowish oil.^{1}H NMR ($CDCl_3$, δ in ppm):6.7 d(Ar, 1H), 6.6m (Ar, 2H), 6.1 m(-CH=,1H), 5.9 m(-CH=,1H), 5.3 dd (CH_2=, 1H), 5.2 dd (CH_2=, 1H), 5.0 m (CH_2=, 2H), 4.50d (-CH_2-O-, 2H), 3.8s (CH_3-O-, 3H) and 3.3 d(-CH_2-Ar, 2H).^{13}C NMR ($CDCl_3$, δ in ppm):149.2 (Ar), 146.2 (Ar), 137.8 (-CH=CH_2),133.7 (-CH=CH_2),133.0 (Ar), 120.2 (Ar), 118.0 (=CH_2), 115.8 (=CH_2), 113.5 (Ar), 112.0 (Ar), 70.0 (-CH_2-O), 56.0 (CH_3-O-) and 40.0 (-CH_2-). FT-IR (ATR):3070, 3015, 2970, 2830, 1680, 1630,1592, 1505, 1460, 1423, 1250, 1225, 1145, 1023, 997, 910, 850, 803 and 749 cm^{-1}.

Pyrolysis of 1-allyl-4-allyloxy-3-methoxybenzene (r2A-EU)

In a glass tube provided with a gas outlet 19.48 g (95.5 mmol) of 2A-EUwere stirred at 200 °C for 3 h to obtain a 98% yield of a yellowish oil.^{1}H NMR ($CDCl_3$, δ in ppm):6.59s (Ar, 2H), 5.91 m (-CH=, 2H), 5.6s (-OH, 1H), 5.1m (CH_2=, 4H), 3.9s (CH_3-O-, 3H), 3.4 dd (-CH_2-Ar, 2H) and 3.3 dd (-CH_2-Ar, 2H). ^{13}C NMR ($CDCl_3$, δ in ppm):146.4 (Ar), 141.6 (Ar),

138.0 (-CH=CH_2)136.8 (-CH=CH_2, 131.1 (Ar), 125.5 (Ar), 122.0 (Ar), 115.5 (=CH_2), 115.4 (=CH_2), 108.9 (Ar), 56.0 (CH_3-O-), 40.0 (-CH_2-) and 34.0 (-CH_2-). FT-IR (ATR) 3540, 3075, 3012, 2970, 2900, 2845, 1630, 1605, 1442, 1498, 1293, 1227, 1205, 1146, 1070, 993, 910, 848 and 750 cm^{-1}.

Synthesis of 1,3-diallyl-4-allyloxy-5-methoxybenzene (3A-EU)

19.14 g of the previously obtainedr2A-EU (94 mmol), 4.13 g (103 mmol)of pulverized NaOH and 120 mL of DMF were placed in a three necked round bottomed flask under inert atmosphere. The mixture was stirred for 10 min and then allyl bromide (12.49 g, 105 mmol) was added dropwise over 1 h at 40°C.Once theaddition was completed the mixture was kept at 40°C for 3 h and then half an hour at 70°C. The reaction product was treated with distilled water to dissolve the NaBr formed and extracted with chloroform. The organic phase was washed twice with distilled water, dried with anhydrous $MgSO_4$and concentrated on a rotary evaporator to obtain 97% yield of 3A-EU as a yellowish oil.^{1}H NMR ($CDCl_3$, δ in ppm):6.7 s (Ar, 2H), 6.05 m (-CH=, 1H), 5.90 m (-CH=, 2H), 5.34 dd (CH_2=, 1H), 5.19 dd(CH_2=, 1H), 5.15-5.0m (CH_2=, 4H), 4.46 d (-CH_2-O-, 2H), 3.87 s (CH_3-O-, 3H), 3.38d (-CH_2-Ar, 2H), 3.31d (-CH_2-Ar, 2H). ^{13}C NMR ($CDCl_3$, δ in ppm):152.6 (Ar), 144.1 (Ar), 137.5 (-CH=CH_2), 137.3 (-CH=CH_2), 135.7 (Ar), 134.5 (Ar), 133.7 (-CH=CH_2), 121.7 (Ar), 117.0 (=CH_2), 115.8 (=CH_2), 115.5 (=CH_2), 110.5 (Ar), 73.7 (-CH_2-O-), 55.7 (CH_3-O-), 40.1 (-CH_2-) and 34.3 (-CH_2-). FT-IR (ATR) 3072, 3018, 2901, 2825, 1637, 1583, 1510, 1451, 1418, 1256, 1230, 1141, 1026, 986, 907, 804 and752 cm^{-1}.

Photochemical thiol-ene reaction (3STA-EU)

A mixture of 5 g (20.5 mmol) of triallyl eugenol derivative (3A-EU), 22.2 g (291.6 mmol) of TAA and 0.1290 g (0.50 mmol) of DMPA were photoirradiated with a UV lamp at 356 nm for 1h. The product obtained was dissolved in $CHCl_3$ and extracted with a saturated NaOH solution and then washed with water and dried over anhydrous $MgSO_4$. The solvent was removed on a rotary evaporator. The product obtained was a viscous liquid with 96% yield.^{1}H NMR ($CDCl_3$, δ in ppm): 6.52s and 6.50 s (Ar, 2H), 3.91t (-CH_2-O-, 2H), 3.80 s (CH_3-O-, 3H), 3.10 (-CH_2-S-, 2H), 2.85 m (-CH_2-Ar, 4H), 2.56 m (-CH_2-S-, 4H), 2.31s (CH_3-CO-S-, 9H), 1.99 m (-CH_2-CH_2-CH_2-O-, 2H), 1.8m (-CH_2-CH_2-CH_2-Ar, 4H). ^{13}C NMR ($CDCl_3$, δ in ppm): 195.7,195.6and195.5 (3C, -CO-S-), 152.3 (Ar), 143.9 (Ar), 136.6 (Ar), 134.5 (Ar), 121.4 (Ar), 110.3 (Ar), 70.0 (-O-CH_2-), 55.5 (CH_3-O-), 34.5 and 31.0(-CH_2-Ar) and 30.5, 30.3 and 30.2 (3C, CH_3CO-S-), 29.1, 28.7and 28.4 (3C, CH_2-S-), and 25.8 (3C, CH_2-CH_2-CH_2-).FT-IR (ATR): 2930, 2825, 1680, 1587, 1505, 1460, 1424, 1355, 1260, 1232, 1135, 1010, 950, 800 and 607 cm^{-1}.

Hydrolysis of 3STA-EU(3SH-EU)

9.31 g (19.7 mmol) of 3STA-EU were added to 100 mL of methanol in a flask equipped with magnetic stirrer.1.70 g (42.5 mmol) of pulverized NaOH were added and the mixture heated at reflux temperature under inert atmosphere for 5.5 h. The solution was allowed to cool down and the solvent was removed. The product obtained was

dissolved in water and acidified with 0.1 M HCl solution and then extracted with $CHCl_3$. The organic phase was washed with distilled water and then dried over anhydrous $MgSO_4$. The product obtained was a pale-yellow viscous liquid.84% yield.^{1}H NMR ($CDCl_3$, δ in ppm): 6.56 s (Ar, 2H), 3.98t (-CH_2-O-, 2H), 3.82s (CH_3-O-, 3H), 2.77 q (-CH_2-S-, 2H), 2.61m (-CH_2-S-, 4H), 2.51 q (-CH_2-Ar, 4H), 2.1m (-CH_2-CH_2-CH_2-O-, 2H), 1.85 m (-CH_2-CH_2-CH_2-Ar, 4H), 1.5 t (-SH, 1H), 1.35t (-SH, 1H) and 1.33 t (-SH, 1H). ^{13}C NMR ($CDCl_3$, δ in ppm): 152.2 (Ar), 143.9 (Ar), 136.7 (Ar), 134.6 (Ar), 121.5 (Ar), 110.2 (Ar), 70.3 (-O-CH_2-), 55.5(CH_3-O-), 35.3 (–CH_2-Ar), 34.6, 34.3 and 34.0 (3C, -CH_2-SH), 28.5 (-CH_2-Ar), 24.1, 23.8 and 21.2 (3C, CH_2-CH_2-CH_2-). FT-IR (ATR), 2930, 2825, 2580, 1587, 1503, 1460, 1430, 1260, 1230, 1150, 1090, 1010, 950 and 830 cm^{-1}.

Preparation of the curing mixtures

The mixtures were prepared by mixing stoichiometric amounts ofepoxide/SH groups (1:1) of ECC with thedifferent thiols. It should be taken into account that the functionality of ECC is two and the functionality of the thiols are 6 for SQ-6H, 4 for PETMP, and 3 for both 3SH-ISO and 3SH-EU in this reactive process. In catalyzed formulations, 2phr of basic catalyst (parts of catalyst for hundred parts of epoxy resin) was added after homogenization of ECC/thiol mixture with a spatula. Formulations were prepared using four different catalysts in order to test their reactivity and choose the most suitable one for thethermal curing process.

Characterization techniques

^{1}H NMR and ^{13}C NMR spectra were registered in a Varian Gemini 400 spectrometer. $CDCl_3$ was used as the solvent. For internal calibration the solvent signal corresponding to $CDCl_3$ was used:δ (^{1}H) = 7.26 ppm, δ (^{13}C) = 77.16 ppm.

A Jasco FTIR spectrometer equipment (resolution of 4 cm^{-1}) with an attenuated-total-reflectance accessory with a diamond crystal (Golden Gate heated single-reflection diamond ATR, Specac-Teknokroma). All the measurements were performed at room temperature. IR was used to follow the formation of thiol band at 2570 cm^{-1} and the evolution of the curing process of the different formulations. In this case, the spectra were collect before and after thermal process.

ADSC instrument (Mettler DSC-821e) differential scanning calorimeter (DSC) Mettler DSC-821e calibrated using an indium standard (heat flow calibration) and an indium-lead-zinc standard (temperature calibration) was used to determine the evolution and kinetics of the curing process. Samples of ca. 10 mg were analyzed under non-isothermal conditions under a constant N_2 atmosphere with a gas flow of 100mL/min. The non-isothermal studies were performed in the temperature range of 30 to 240°C, with a heating rate of 2, 5, 10 and 15°C min^{-1}.

Values of Tg of the final thermosets were determined after two consecutive heating dynamic scans at 20°C/min starting at -20°C in a Mettler DSC-822e device to

delete the thermal history. The Tg value was taken as the middle point in the heat capacity step of the glass transition.

The degree of conversion by DSC was calculated as follows:

$$\alpha = \frac{\Delta h_T}{\Delta h_{dyn}} \qquad (1)$$

where Δh_T is the heat released up to a temperature *T* or up to a time t, obtained by integration of the calorimetric signal up to this temperature or time, and Δh_{dyn} is the total reaction heat associated with the complete conversion of all reactive groups.

The linear integral isoconversional, model-free method of Kissinger-Akahira-Sunose (KAS) was used for the determination of the activation energy based on the non-isothermal curing curves[24]

$$\ln\left(\frac{\beta}{T^2}\right) = \ln\left(\frac{A \cdot R}{g(x) \cdot E}\right) - \frac{E}{R \cdot T} \qquad (2)$$

Where β is the heating rate, *T* the temperature, *E* the activation energy, *A* the pre-exponential factor, R the gas constant, and *g(x)* the integral conversion function. For each conversion degree, the representation of $ln(\beta/T^2)$ versus $1/T$ produces a straight line and makes it possible to determine E and *ln[AR/g(x)E]* from the slope and the intercept without knowing the kinetic model.

Assuming that the approximation given by Eqn (2)is valid, we can determine the kinetic model that best describes the curing process by rearranging Eqn (2)as

$$\ln\left(\frac{g(x)}{T^2}\right) = \ln\left(\frac{A \cdot R}{\beta \cdot E}\right) - \frac{E}{R \cdot T} \qquad (3)$$

which is the basis for the composite integral method for the determination of the kinetic model.[25]The plot of ln $(g(\alpha)\cdot\beta/T^2)$ against $-1/R\cdot T$ for all the heating rates should yield a perfectly straight line, with a slope E equivalent to the isoconversional activation energy if the kinetic model *g(x)* is right. Given that the curing of epoxy-thiol reactions can be satisfactory modelled using autocatalytic kinetic models,[6,26]we have fitted the experimental data to autocatalytic kinetic models with $n+m=2$, where n and m are the non-catalytic and catalytic orders of reaction respectively. Details of the model fitting methodology used can be found elsewhere.[27]

The thermal stability of cured samples was evaluated by thermogravimetric analysis (TGA), using a Mettler TGA/SDTA 851e thermobalance. All experiments were performed under inert atmosphere (N_2 at 100 mL/min). Pieces of the cured samples

with an approximate mass of 8 mg were degraded between 30 and 600 °C at a heating rate of 10 K/min.

Dynamic mechanical thermal analyses (DMTA) were carried out with a TA Instruments DMA Q800 analyzer. The samples were prepared as described before. Three point bending clamp was used on the prismatic rectangular samples (15 × 7.9 × 1.5 mm^3). The curing schedule applied to cure the samples was 1 h at 120°C, 1 h at 150 °C and a final post curing at 200°C for 30 min. The sample was first heated at 5 K/min from 30 to 180°C to erase the thermal history and then analyzed at 3 K/min from 30 to 180°C at a frequency of 1 Hz with and oscillation amplitude of 10 µm. Young modulus was determined by a stress/strain test, under the same clamp and geometry testing conditions, at 30°C using a force ramp of 3N min^{-1} and upper force limit 18 N.

Results and discussion

Synthesis of thiolsfrom vinylic compounds

The synthesis of the various thiols was carried out following a two-step procedure from the vinyl compounds as reported for squalene derivatives.[22] The first synthetic step consists in a photochemical thiol-ene click reaction of thioacetic acid to the multifunctional-ene compound in the presence of a radical photoinitiator. The thiol-ene reaction is not inhibited by oxygen, which constitutes a great advantage in technological applications. The radical formed by the photo-cleavage of the photoinitiator abstracts a hydrogen atom from thioacetic acid, generating a thiyl radical that is added toa reactive double bond of the vinyl compound creating a carbon radical. The carbon radical abstracts a hydrogen from a thiol group, generating a new thiyl radical.5This alternating mechanism, cycling between thiyl addition to the double bond and chain-transfer leading to a new thiyl radical, results in the consumption of thiol and -ene groups at the same rate. If stoichiometric thiol-ene mixtures are used, complete reaction of thiol and -ene groups is achieved.The second step in the thiol synthesis is the hydrolysis reaction of the corresponding thioacetate by treatment with a methanolic solution of NaOH at reflux temperature, followed by acidification with diluted HCl. This synthetic procedure,previously described for the preparation of the thiol derived from squalene (6SH-SQ),[22] has been successfully applied in the present study for the synthesis of 3SH-EU and 3SH-ISO from the corresponding triallyl derivatives, being the yields notably high. The two-step synthetic process is represented for the eugenol derivative in Scheme 2.

Structural characterization of the thiols synthesized and their synthetic intermediates

The FTIR characterization of the products prepared renders as the most typical absorptions a strong band at 1700 cm^{-1} of carbonyl stretching in the intermediate thioacetates and a weak band at 2560 cm^{-1}, assigned to the SH absorption in all the thiols prepared. The structure of the products prepared was confirmed by ^1H NMR spectroscopy.

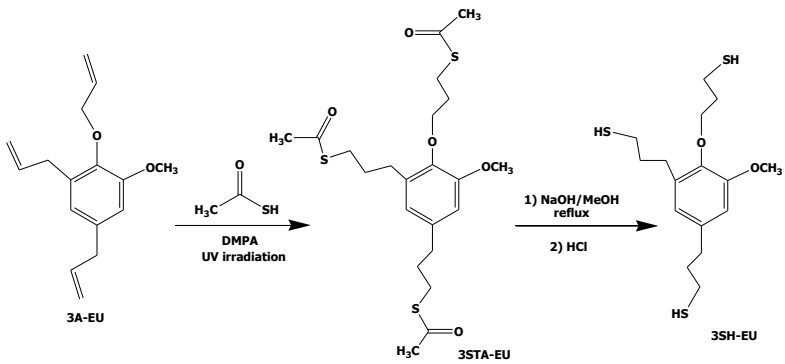

Scheme 2. Two-step synthetic procedure for the transformation of triallyl eugenol (3A-EU) to the trithiol of eugenol (3SH-EU)

The ^{1}H NMR spectra of squalene derivatives were compared to those previously published, showing a complete agreement.[22]The complex structure of this compound that includes a great number of stereoisomers make the structural characterization by this technique difficult but the appearance of acetate peaks in the intermediate materials and the complete elimination by saponification are valuable indicators to confirm that the synthetic process has occurred as expected.

The trithiol derived from triallyl isocyanurate (3SH-ISO) has not been reported in the literature up to now. The structure of this compound and of the intermediate thioacetate was determined by their ^{1}H NMR spectra, which are shown in Figure 1.The spectra present few signals according to the third order symmetry axis.

In the spectrum of 3STA-ISO the most characteristic signal is the peak at 2.31 ppm corresponding to the methyl protons of the thioacetate group that appears as a singlet, which has disappeared completely in the spectrum of the 3SH-ISO. It is worth to note that signals corresponding to vinyl protons cannot be observed in the spectrum of 3STA-ISO, which confirms that the photoinduced thioacetic addition to triallyl isocyanurate was complete. Signals a and b at about 3.95 and 1.9 ppm, practically remain unchanged in both spectra. However, the signal corresponding to the methylene protons c, which appears as a triplet at 2.87 ppm in the acetate shifts to 2.55 ppm after hydrolysis and shows a more splitted peak because of the coupling with the proton of the thiol that appears as a triplet at 1.55 ppm in the thiol spectrum. ^{13} C NMR spectrum of 3SH-ISO is included as Figure A in the supporting information.

Figure 2 shows the spectra of the eugenol derivatives. As in the previous case, the thiol-ene process is complete since no vinylic protons appear in the 3STA-EU spectrum. As before, the formation of the thiol was confirmed by the disappearance of the peak at 2.34 ppm, corresponding to the methyl protons from the thioacetate groups. However, the eugenol derivative has no symmetry and therefore more signals appear, making the assignment more difficult.

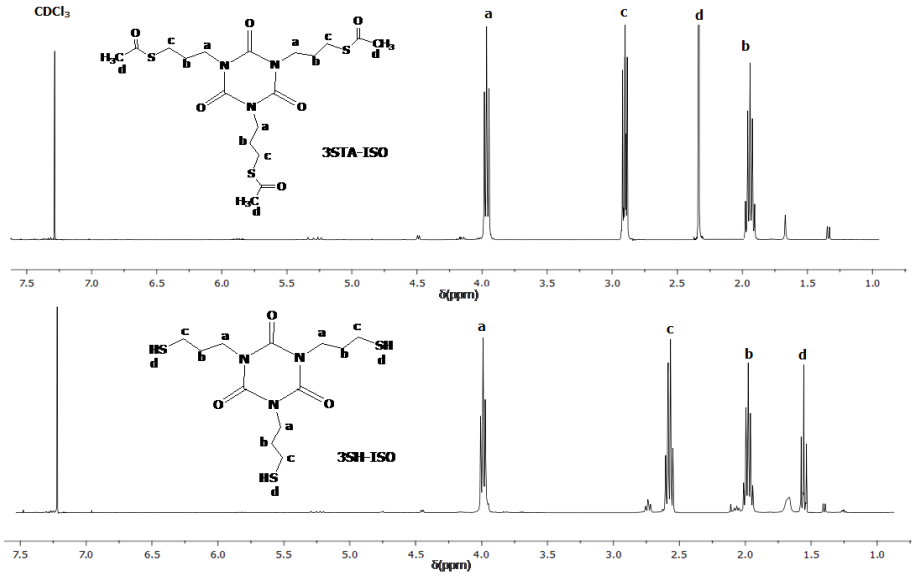

Figure 1. ^{1}H NMR spectrum of the trithioacetate (3STA-ISO) and trithiol (3SH-ISO) derived from triallyl isocyanurate registered in $CDCl_3$

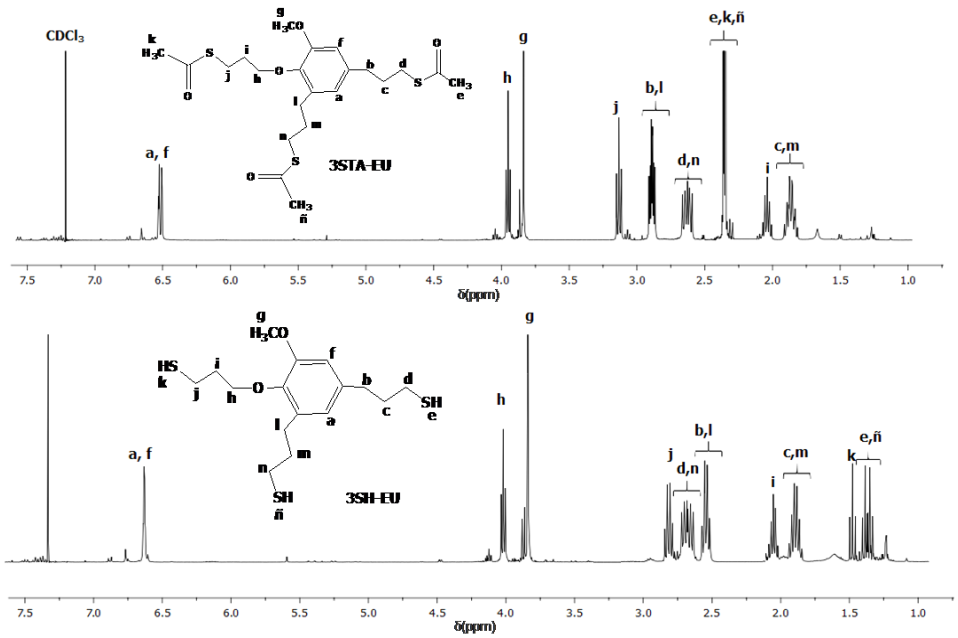

Figure 2.^{1}H NMR spectrum of the trithioacetate (3STA-EU) and trithiol (3SH-EU) derived from eugenol registered in $CDCl_3$

In a similar way to what happens in the TAIC derivatives, the presence of thiol leads to a higher splitting of the methylene protons attached to this group. The three signals due to the thiol protons appear as triplets below 1.5 ppm, two of them partially overlapped by the similarity of the electronic surroundings.

^{13}C-NMR spectrum was also registered and it is included as Figure B in the supporting information.

Study of the curing process

The reaction of thiolates with epoxides follows a nucleophylic SN_2 mechanism with a well-defined stereochemical control. Thiols require an amine as basic catalyst to increase the nucleophilic character of thiols by the formation of thiolates.[6,7,20] However, the use of bases like trimethylamine in thiol-DGEBA reactions leads to a too short pot-life that makes difficult the application.[28] For that reason the use of latent basic catalyst is recommended.[7]

With the aim of selecting the best basic catalyst to perform the thermal curing of ECC, different amineslike 1-MI, 2MI, DMAP and LC-80 were tested. All of them are tertiary amines, being LC-80 an encapsulated imidazole. The DSC thermograms corresponding to thermal curing of ECC/PETMPstoichiometric formulations with 2 phr of each catalyst are shown inFigure 3.

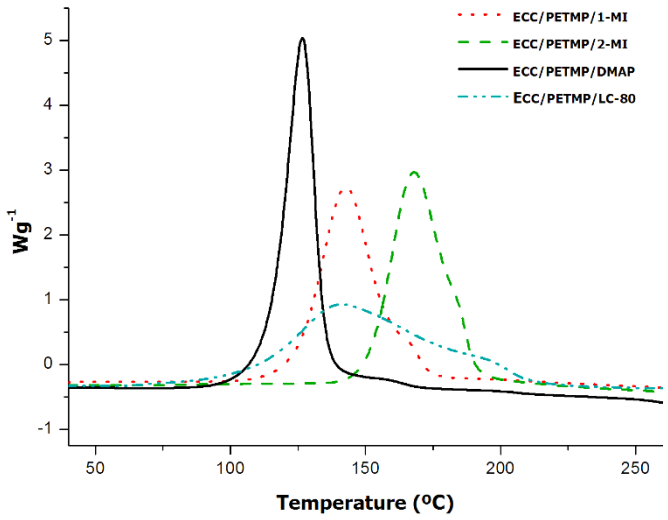

Figure 3. DSC thermograms corresponding to the dynamic curing at 10°C/min of the mixtures cycloaliphatic resin/PETMP with a proportion of 2 phr of the different catalysts

It can be observed in the figure that the formulation catalyzed by LC-80 begins to cure at relatively lower temperature and finishes at about 200°C showing a low curing rate and a broad curing temperature range. On the other hand,the curing with DMAP starts around 100°C, with a very fast curingreaction that finishes at about 140 °C in a

narrow temperature range. 1-MI shows an intermediate activity and 2-MI is the one that is activated at a highest temperature.

In previous studies on the curing of DGEBA resins with thiols we used 2 phr of LC-80 as the catalyst and its latent character was demonstrated.[7] However, according to our experience, different catalysts can be used and the most adequate depends on the composition of the formulation.[29] We also reported[7,30] that the curing of mixtures of DGEBA and PETMP or TTMP (trimethylolpropane tris-(3-mercaptopropionate)) with smaller amounts of catalysts such as 1-MI and LC-80 took place at lower temperatures. It is well-known that primary amines are not able to cure cycloaliphatic epoxy resins,[31] so it could be expected that the curing of ECC with thiol crosslinkers would be more difficult but, as seen in Figure 3, it takes place within an acceptable temperature range.Given that the curing with DMAP is activated within the same temperature range as the curing with latent catalyst LC-80, and that the curing takes place within a narrower temperature range, it is suggested that DMAP is the most suitable catalyst for this systems.

The effect of the different catalyst was also analyzed for the different formulations prepared from the synthesized thiol crosslinkers. Figure 4 shows, as an example, that the activity of the different catalysts in formulations using 6SH-SQ as thiol crosslinking agent follows the same trend as with PETMP. In the case of 3SH-ISO and 3SH-EU (see Figures C and D in the supporting information), similar results were obtained and DMAP was the most active catalyst, with an activation temperature close to that of LC-80. Therefore, DMAP was selected as the most suitable catalyst and used for further studies in this work.

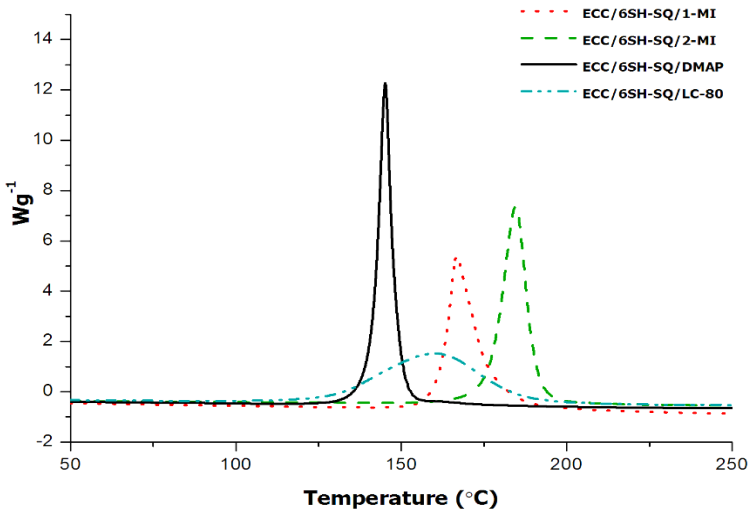

Figure 4. DSC thermograms corresponding to the dynamic curing at 10°C/min of ECC/6SH-SQ stoichiometric mixtures with 2 phr of the different catalysts

Figure 5 collects the calorimetric curves for the curing of ECC with the four thiols selected using 2 phr of DMAP as the catalyst. It is known[32]that the structure and the chemical environment of the thiol group has a very strong influence on its pKa and the nucleophilicity of the thiolate anion. Thus, it could be expected that 6SH-SQ was less reactive than PETMP due to the lower nucleophilicity of the thiolate anion. It can be seen that the less reactive thiol crosslinker, with a highest activation temperature, is the one derived from triallylisocyanurate.

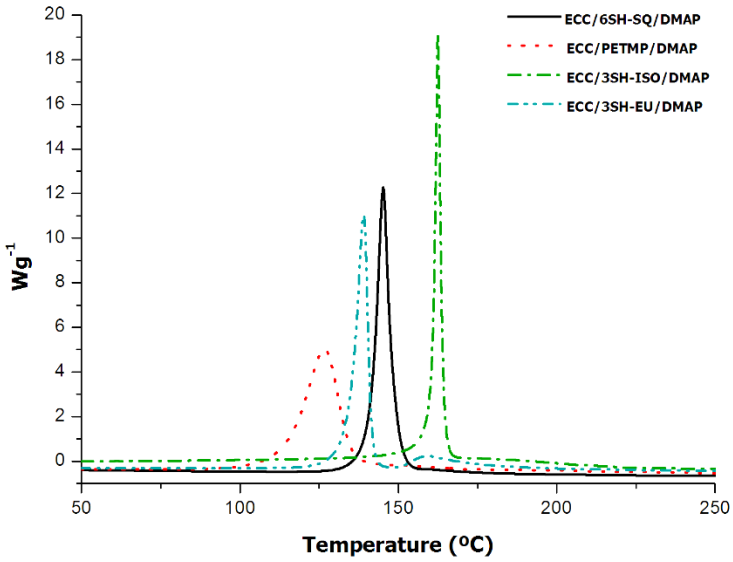

Figure5. DSC thermograms corresponding to the dynamic curing at 10°C/min of the mixtures cycloaliphatic resin with different thiols using a proportion of DMAP as catalyst

Table 1shows the values of enthalpy released and the temperatures of the maximum of the calorimetric peaks for the curing of the mixtures with different thiols and DMAP as the catalyst. As we can see, the heat released by epoxy equivalent is higher than 100 kJ/eq in all the mixtures with the thiols synthesized and a little a higher for the commercial PETMP. In DGEBA/PETMP formulations catalyzed by LC-80 enthalpies of 127 kJ/eq were measured during curing.The curing of ECC with PETMP releases a comparable amount of heat, but the other thiol crosslinkers lead to lower enthalpy released per epoxy equivalent. On one hand, there are experimental uncertainties associated with the baseline determination and integration of the curing peaks, especially those extending to higher temperatures, where side degradation reactions might also occur. On the other hand, it may be hypothesized that PETMP leads to somewhat higher conversion than the other thiols, due to its more flexible structure. For instance, one could expect some topological hindrance leading to incomplete cure in 6SH-SQ, because of its small molecular size and high functionality. It might be argued likewise in the case of 3SH-ISO and 3SH-EU, with a rigid core structure and flexible but short arms.

Table 1. Calorimetric data and kinetic parameters obtained for the curing of formulations with different thiols containing 2 phr of DMAP

Formulation	Δh^a (J/g)	Δh^a (kJ/eq)	T_{max} (°C)	Ea^b (kJ/mol)	ln A^b (min^{-1})	$k_{130°C}{}^c$ (min^{-1})	$(d\alpha/dt)_{0.5}{}^d$ (min^{-1})
ECC/6SH-SQ	473.1	108.1	145	65.8	20.3	1.98	0.50
ECC/ PETMP	511.8	131.0	127	61.0	19.1	2.45	0.61
ECC/3SH-ISO	435.9	107.0	163	65.9	20.0	1.39	0.35
ECC/3SH-EU	430.2	107.7	134	68.6	21.2	2.15	0.54

a. Curing enthalpy measured in a DSC scan at 10°C/min
b. Kinetic parameters obtained by model-fitting using an autocatalytic model with n+m=2
c. Values of rate constant at 130°C using the Arrhenius equation and the parameters E and ln A
d. Values of reaction rate at 130°C obtained using the equation rate $d\alpha/dt=k\cdot f(\alpha)=k\cdot(1-\alpha)^{n-\alpha m}$ at 50% conversion

However, FTIR-ATR analysis of the cured samples showed that the curing was quantitative. Figure 6 shows, as an example, the most significant regions of the spectra before and after curing of the formulation cured with 3SH-ISO. The initial spectrum shows the typical absorptions of S-H st. at 2570 cm^{-1} and the band at 795 cm^{-1} corresponding to the cycloaliphatic epoxy ring. Both absorptions have disappeared completely in the spectrum of the cured material, confirming that the curing was complete. In addition, a new broad absorption at 3500 cm^{-1} appears because of the formation of the β-hydroxy thioether group in the network structure.

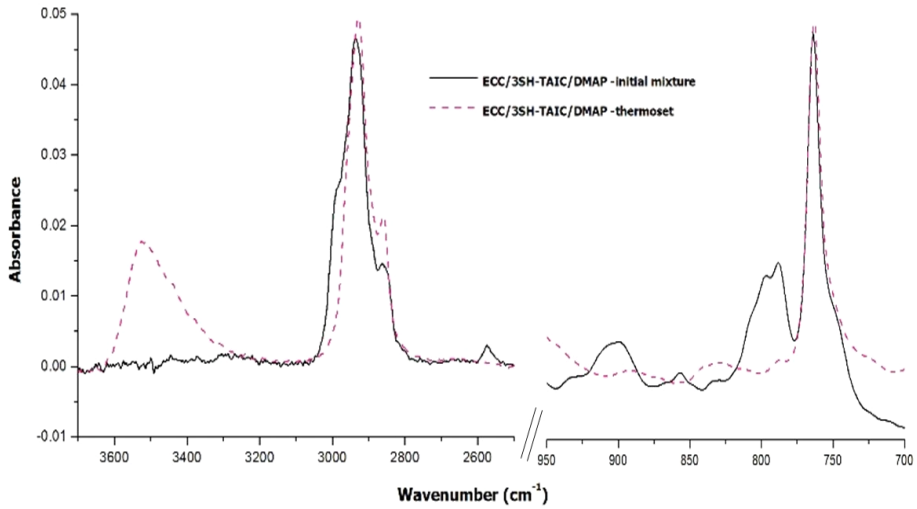

Figure 6. FTIR spectra of a mixture ECC/3SH-ISO catalyzed by 2 phr of DMAP before and after curing

The kinetics of the curing of the different formulations wasstudied by DSC. From calorimetric curves performed at different heating rates and applying the isoconversional methodology we could determine the activation energy of these curing processes. Figure 7 shows the evolution of activation energy during the curing process. No great differences among them are observed and the values are more or less constant

during all the curing process indicating that the reaction mechanism is the same during the whole curingand no epoxy homopolymerization occurs, as expected for stoichiometric thiol-epoxy formulations.[30,33] The apparent activation energy during curing of thiol-epoxy formulations depends largely on the type and proportion of catalyst[7] and in consequence on the underlying curing mechanism.[26,30,33]Therefore, comparison with other systems is difficult, but the values are in general agreement with previous reports.[7,30]

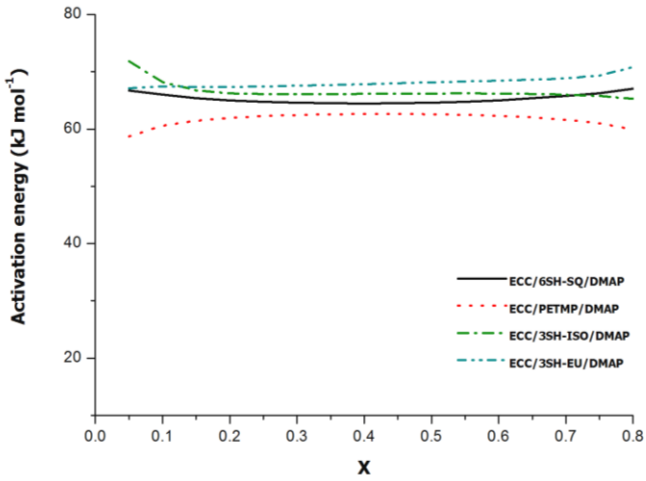

Figure 7. Activation energy vs degree of conversion of the cycloaliphatic resin with different thiols using a proportion of DMAP as catalyst

Given that the isoconversional activation energy is constant, it is possible to model the curing kinetics using a kinetic model with a single rate constant. Given that the curing kinetics of thiol-epoxy formulations with tertiary amines has an autocatalytic behaviour[26,30,33] we selected an autocatalytic kinetic model type *n+m=2*to fit our experimental results. The kinetic valuesof the curing of the formulations with different thiolsare collected in Table 1. The kinetic constant and reaction rate at 130°C of the curing process was significantly affected by the reactivity of the thiol employed. The results obtained show that PETMP was the most reactive, followed by 3SH-EU and 6SH-SQ. The less reactivethiol was 3SH-ISO which needed higher temperature to be initiated.These results agree with the trend in reactivity shown in Figure 5.

Characterization of the thermosets

The thermosets obtained by curing the four formulations with the different thiols were thermally characterized by DSC, TGA and DMTA. The formulations were cured with the following schedule:1 h at 120°C, 1 h at 150°C and a post-curing of half hour at 200 °C. The materials obtained were transparent as previously reported in thiol-epoxy

materials[7] and the colour depended on the thiol used in the curing. Figure 8shows the corresponding photographs.

Figure8. Photographs of the thermosets obtained from different ECC/thiol formulations catalyzed by 2 phr of DMAP: A) 6SH-SQ; B) PETMP; C) 3SH-ISO and D) 3SH-EU

Table 2 collects the main data obtained from the thermal characterization. The Tg determined by DSC is correlated with the structural characteristics of the thiol. PETMP, with a functionality of 4 but quite a flexible structure, leads to a Tg of 53°C. In spite of the different epoxy used, this value compares well with that obtained for DGEBA-PETMP materials.[20] Trifunctional thiol crosslinkers with a rigid core, 3SH-ISO and 3SH-EU, lead to materials with comparable Tgs of 69 and 70°C, which are significantly higher than those that can be obtained using a flexible trifunctional crosslinker such as TTMP.[7] The squalene derivative,6SH-SQ, with an aliphatic structure but higher functionality, leads to the material with the highest Tg, of 116°C. This can be explained by the densely crosslinked structure, with internal branching points in the thiol crosslinker structure and very short distance between crosslinks.

Table 2. Thermal and dynamic mechanical data of the materials obtained from obtained from cycloaliphatic resin with different thiols using a proportion of DMAP as catalyst

Formulation	T_g[a] (°C)	$T_{5\%}$[b] (°C)	T_{max}[c] (°C)	$T_{tan\delta}$[d] (°C)	E[e] (MPa)	E_r[f] (MPa)
ECC/6SH-SQ	116	322	341	135	2231	15.8
ECC/PETMP	53	268	336	80	2048	8.0
ECC/3SH-ISO	70	327	377	91	2070	7.6
ECC/3SH-EU	69	294	367	88	2043	6.8

a. Glass transition temperature determined by DSC at 10°C/min from -20 to 250 °C
b. Temperature of 5% of weight loss in N_2 atmosphere
c. Temperature of the maximum rate of degradation in N_2 atmosphere
d. Temperature of maximum of tan δ determined by DMTA
e. Young´s modulus at 30 °C
f. Storage modulus in the rubbery state at T =T tan δ + 50 °C

Figure 9plots the loss factor tan δagainst temperature for the four thermosets prepared, determined by DMTA. The tan δ peak temperature shows the same trend as the Tgs measured by DSC (see Table 2), but the values are higher due to the effect of the frequency on the αrelaxation. The tan δ curves show a narrow unimodal shape, indicating that the materials are homogeneous. The curve corresponding to the thiol 6SH-SQ is the one with the highest tan δpeak temperature and the lowest intensity. This is in agreement with a densely crosslinked network structure, having internal branching points within the structure of the thiol crosslinker with very short arm distance.In contrast, the lowest tan δpeak temperature is obtained with PETMP, given its more

flexible structure in spite of its higher functionality, in comparison with 3SH-ISO and 3SH-EU.The differences between the materials obtained with 3SH-ISO and 3SH-EU are not relevant, because of their similar structure.

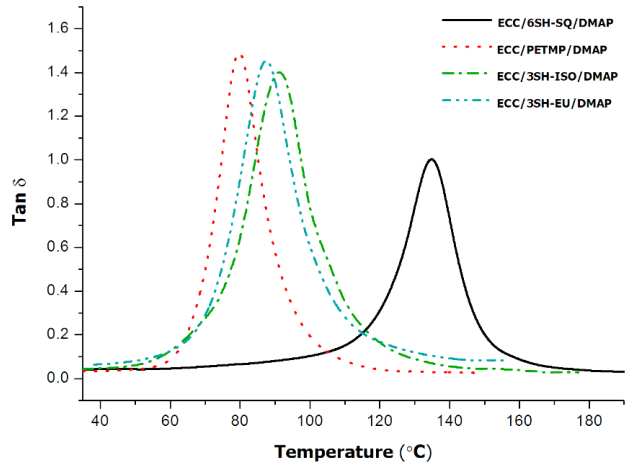

Figure9. Plot of tan δ against temperature for the different materials prepared

Theevolution of storage moduli measured with DMTA is shown in Figure 10. The drop in storage modulus during the mechanical relaxation of the network structure follows the same trend as the calorimetric Tgs and tan δ peak temperature, as expected (see Table 2). The material obtained with 6SH-SQ has the highest value of storage modulus in the rubbery state, owing to the higher functionality of the crosslinking agent and the more densely crosslinked network structure.[34]Accordingly,PETMP leads to a somewhat higher relaxed modulus than 3SH-ISO and 3SH-EU because of its higher functionality.

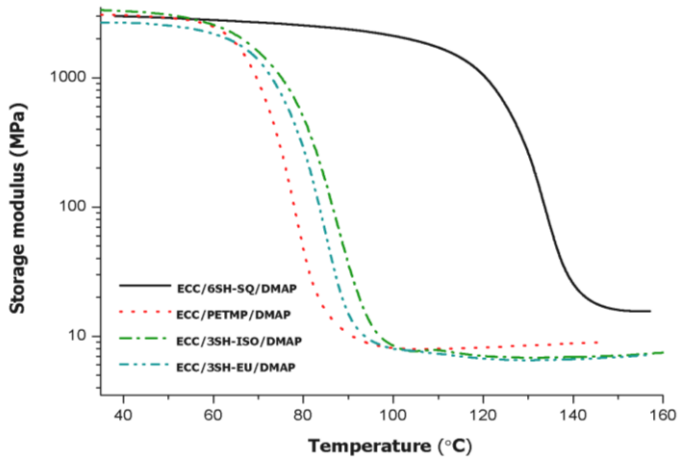

Figure 10. Plot of storage modulus against temperature for the different materials prepared

The thermal stability of the thermosets was studied by TGA under inert atmosphere. Figure 11 shows the derivative of the degradation curves. As we can see, the degradation of the material with PETMP starts earlier and shows two clear steps, while the other ones degrade in a single step. The presence of ester groups in PETMP, which are absent in the other thiol crosslinkers, may explain the lower degradation temperature and the multi-step degradation process. The most relevant degradation parameters are summarized also in Table 2. The material showing the lowest initial degradation was the thermoset obtained from PETMP because of the existence of a higher proportion of ester groups in the network structure that can degrade much more easily. The highest thermal stability was obtained with 3SH-ISO, because of the presence of the isocyanurate moiety.

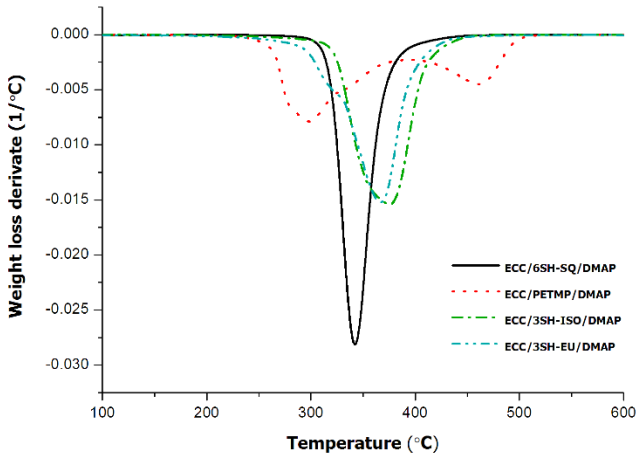

Figure 11. DTG curves under N_2 at 10 K/min of the thermosets obtained from ECC and the different thiols and 2 phr of DMAP as catalyst

To summarize, it has been seen that the structure of the thiol crosslinking agent has a very strong influence on the thermomechanical properties of the thermosets prepared from cycloaliphatic epoxy resins, making it possible meet a wide range of application requirements. In particular, the network structure of thiol-crosslinked ECC thermosets is less densely crosslinked than other ECC thermosets based on epoxy homopolymerization or epoxy-anhydride copolymerization, making it possible to adapt them to less-demanding situations from the thermal and mechanical point of view. The greater flexibility of these networks should lead to an improvement in the impact resistance in comparison to homopolymerized cycloaliphatic epoxy thermosets.

Conclusions

Multifunctional thiols can be easily prepared from vinyl monomers by photochemical thiol-ene reaction with thioacetic acid followed by saponification of the acetyl thioesters formed. By this synthetic way, new trithiols derived from eugenol and triallyl isocyanurate and the hexathiol from squalene were obtained with good yields.

Thermosets based on cycloaliphatic epoxy resin ECC crosslinked with a commercially available thiol crosslinker PETMP and the other synthesized thiols (6SH-SQ, 3SH-ISO, 3SH-EU) have been prepared using 4-(N,N-dimethylamino)pyridine as catalyst. The reactivity order in the curing process of the thiols tested followed the trend: PETMP>3SH-EU>6SH-SQ>3SH-ISO. Complete reaction of thiol and epoxy groups was confirmed by FTIR spectroscopy.

The obtained materials have lower Tg and storage moduli in the rubbery state than homopolymerized cycloaliphatic epoxy thermosets, derived from ECC, because of their lower crosslinking density and higher flexibility of the network structure, making it possible to adapt ECC thermosets to less demanding applications from the thermal point of view. The structure of the thiol crosslinker had a strong influence on the thermal-mechanical properties of the resulting materials. The squalene derivative 6SH-SQ led to the highest Tg, and moduli in the rubbery state due to its higher functionality and the presence of internal branching points and short arm distances. However, the trithiols derived from eugenol and triallyl isocyanurate present Tgs and moduli similar to PETMP derived materials in spite of their different functionality and structure. The synthesized thiol crosslinkers led to more stable thermosets than that obtained with PETMP, because of the presence of thermally labile ester groups in the latter.

Acknowledgments

The authors would like to thank MINECO (MAT2014-53706-C03-01, MAT2014-53706-C03-02) and Generalitat de Catalunya (2014-SGR-67 and SerraHúnter programme) for the financial support.

References

[1] H.C. Kolb, M. G Finn, K.B Sharpless, *Angewandte Chemie International Edition*, 2001, 40, 2004-2021.

[2] J. Lahann, Ed,*Click Chemistry for Biotechnology and Materials Science*. Wiley & Sons, Chichester, UK, 2009.

[3] J.E Moses, A.D.Moorhouse, *Chemical Society Review,* 2007, 36, 1249–1262.

[4] A. Brändle, A. Khan, *Polymer Chemistry,* 2012, 3, 3224-3227.

[5] A.B. Lowe, C.N.Bowman, Eds,*Thiol-X Chemistries in Polymer and Materials Science*, RSC Publishing, Cambridge, UK, 2013.

[6] R. Meizoso Loureiro, T. Carballeira Amarelo, S. Paz Abuin, E. R. Soulé, R.J.J. Williams, *Thermochimica Acta,* 2015, 616, 79-86.

[7] D. Guzmán, X. Ramis, X.Fernández-Francos, A. Serra,*European Polymer Journal,* 2014, 59, 377–386.

[8] M. Xie, Z. Wang, *Macromolecular Rapid Communications*, 2001, 22, 620-623.

[9] M. Xie, Z. Wang, Y. Zhao,*Journal Polymer Science Part A: Polymer Chemistry,*2001, 39, 2799-2804.

[10] W. Liu, Z. Wang, *Polymer International,*2013, 62, 515-522.

[11] Z, Wang, M. Xie, Y. Zhao, Y. Yu, S. Fang,*Polymer,* 2003, 44, 923-929.

[12] W. Liu, Z. Wang, L. Xiong, L. Zhao,*Polymer,* 2010, 51, 4776-4783.

[13] C. E. Corcicone, A. Greco, A. Maffezzoli, *Journal of Applied Polymer Science,* 2004, 92, 3484-3491.

[14] C. Mas, A. Serra, A. Mantecón, J. M. Salla, X. Ramis, *Macromolecular Chemistry and Physics,* 2001, 202, 2554-2564.

[15] M. J. Yoo, S. H. Kim, S. D. Park, W. S. Lee, J-W. Sun, J-H. Choi, S, Nahm, *European Polymer Journal,* 2010, 46, 1158-1162.

[16] A. Belmonte, F. Däbritz, X. Ramis, A. Serra, B. Voit, X. Fernández-Francos, *Journal of Polymer Science Part B: Polymer Physics,*2014, 52, 1227-1242.

[17] X. Fernández-Francos, J.M. Salla, A. Serra, A. Mantecón, X. Ramis, *Journal Polymer Science Part A: Polymer Chemistry,* 2005, 43, 3421-3432.

[18] J. A. Carioscia, J. W. Stansbury, C. N. Bowman, *Polymer,* 2007, 48, 1526-1532.

[19] D. P. Nair, N. B. Cramer, J. C. Gaipa, M. K. McBride, E. M. Matherly, R. R. McLeod, R. Shandas, C. N. Bowman, *Advanced Functional Materials,* 2012, 22, 1502-1510.

[20] D. Guzmán, X. Ramis, X. Fernández-Francos, A. Serra, *Polymer*, 2015, 7,680-694.

[21] M. Sangermano, A. Vitale, K. Dietliker, *Polymer,* 2014, 55, 1628-1635.

[22] R. Acosta Ortiz, E. A. Obregón Blandón, R. Guerrero Santos, *Green Sustainable Chemistry*, 2012, 2, 62-70.

[23] T. Yoshimura, T. Shimasaki, N. Teramoto, M .Shibata, *European Polymer Journal,* 2015, 67, 397–408.

[24] S. Vyazovkin, A. K. Burnham, J. M. Criado, L. A. Pérez-Maqueda, C. Popesco, N. Sbirrazzuoli*, Thermochimica Acta*, 2011, 520, 1-19.

[25] S. J García, X. Ramis, A. Serra, J. Suay, *Journal of Thermal Analysis and Calorimetry,* 2007,89, 233-244.

[26] K. Jin, W. H. Heath, J. M. Torkelson, *Polymer,* 2015, 81, 70-78.

[27] M. Flores, X. Fernández-Francos, X. Ramis, A. Serra, *Thermochimica Acta,* 2012, 544, 17-26.

[28] E. M. Petrie, *Epoxy adhesive formulations. Epoxy curing agents and catalysts*, McGraw-Hill Companies, USA, 2006.

[29] D. Guzmán, X. Ramis, X. Fernández-Francos, A. Serra, *RSC Advances,* 2015, 5, 101623-101633.

[30] X. Fernández-Francos, A-O Konuray, A. Belmonte, S. De la Flor, A.Serra, X. Ramis,*PolymerChemistry,* 2016*,* 7, 2280-2290.

[31] May CA, ed*. Epoxy Resins, Chemistry and Technology*, 2nd ed, Marcel Dekker, Inc. New York, USA, 1988.

[32] C. E. Hoyle, A. B. Lowe, C. N. Bowman, *Chemical Society Reviews,* 2010, 39, 1355-1387.

[33] R. M. Loureiro, T. C. Amarelo, S. P. Abuin, E. R.Soulé, R. J. J. Williams*, Thermochimica Acta,*2015, 616, 79-86.

[34] A. J.Lesser, E. Crawford, *Journal of Applied Polymer Science,* 1997, 66, 387-395.

Supporting information

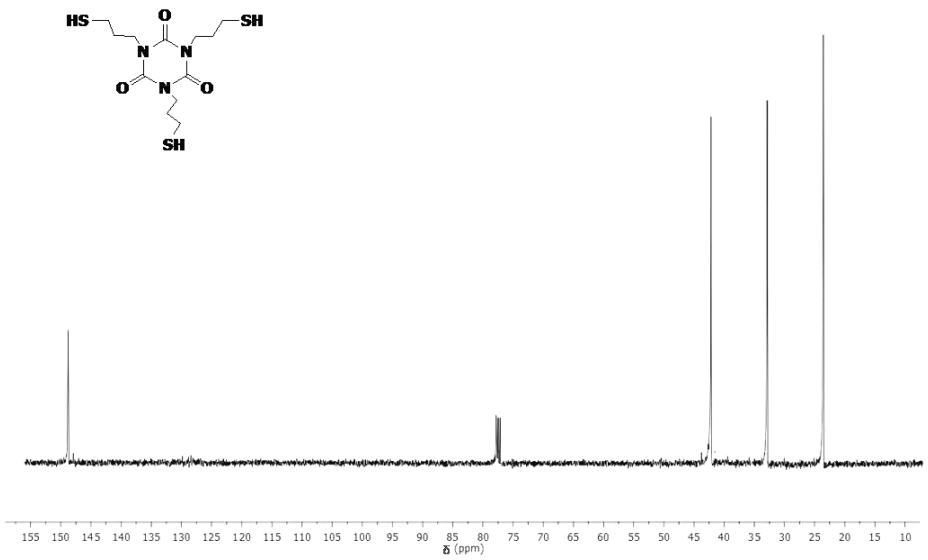

Figure A. ^{13}C NMR spectrum of the trithiol (3SH-ISO) derived from triallyl isocyanurate registered in $CDCl_3$

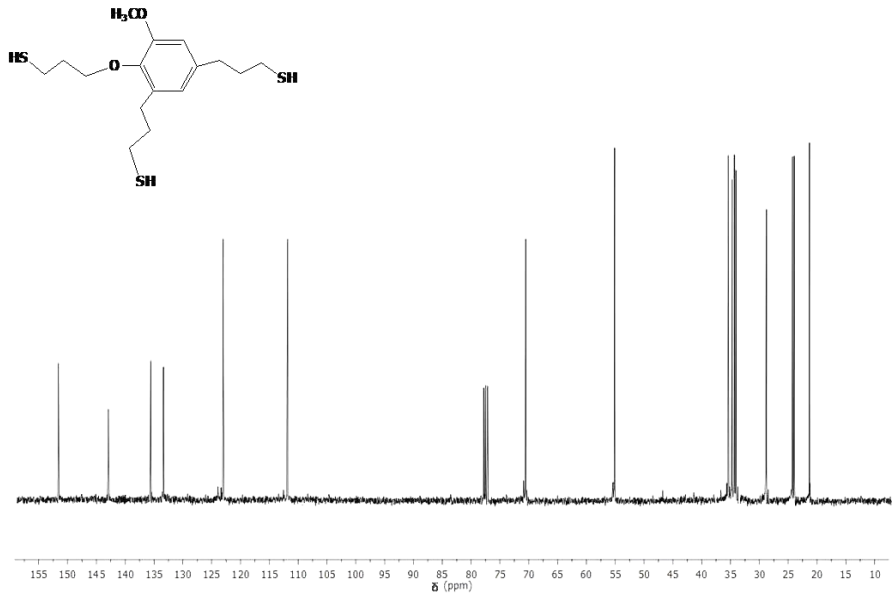

Figure B. ^{13}C NMR spectrum of the trithiol (3SH-EU) derived from eugenol registered in $CDCl_3$

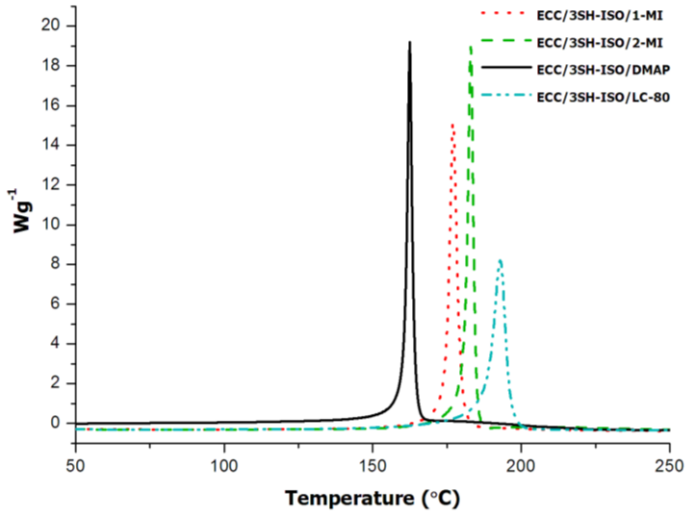

Figure C. DSC thermograms corresponding to the dynamic curing at 10°C/min of ECC/3SH-ISO stoichiometric mixtures with 2 phr of the different catalysts

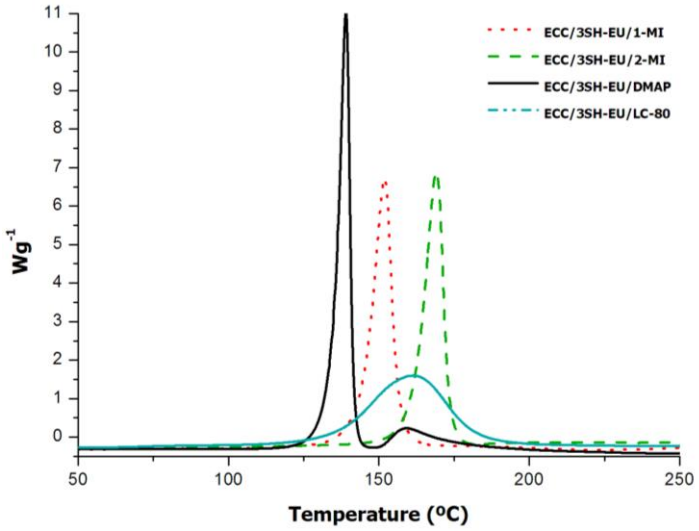

Figure D. DSC thermograms corresponding to the dynamic curing at 10°C/min of ECC/3SH-EU stoichiometric mixtures with 2 phr of the different catalysts

UNIVERSITAT ROVIRA I VIRGILI
NUEVOS PROCESOS DE CURADO CLICK CON TIOLES Y SU APLICACIÓN A LA PREPARACIÓN DE MATERIALES BASADOS EN EUGENOL
Dailyn Guzmán Meneses

UNIVERSITAT ROVIRA I VIRGILI
NUEVOS PROCESOS DE CURADO CLICK CON TIOLES Y SU APLICACIÓN A LA PREPARACIÓN DE MATERIALES BASADOS EN EUGENOL
Dailyn Guzmán Meneses

UNIVERSITAT ROVIRA I VIRGILI
NUEVOS PROCESOS DE CURADO CLICK CON TIOLES Y SU APLICACIÓN A LA PREPARACIÓN DE MATERIALES BASADOS EN EUGENOL
Dailyn Guzmán Meneses

CAPÍTULO 7

European Polymer Journal, 2017, 93, 530–544

New bio-based materials obtained by thiol-ene/thiol-epoxy dual curing click procedures from eugenol

Dailyn Guzmán, Xavier Ramis, Xavier Fernández-Francos, Silvia De la Flor, Angels Serra

UNIVERSITAT ROVIRA I VIRGILI
NUEVOS PROCESOS DE CURADO CLICK CON TIOLES Y SU APLICACIÓN A LA PREPARACIÓN DE MATERIALES BASADOS EN EUGENOL
Dailyn Guzmán Meneses

New bio-based materials obtained by thiol-ene/thiol-epoxy dual curing procedures from eugenol derivatives

Abstract

Novel bio-based and dual-curable thermosets were prepared from eugenol derivatives. The curing sequence combined two click reactions, a photoinduced radical thiol-ene reaction followed by a thermally activated thiol-epoxy reaction. Eugenol was transformed into a triallyl (3A-EU) and a diallyl glycidyl derivative (2AG-EU) with high yields, and they were used as starting monomers in order to study the thiol-ene reaction and the dual-curing process, respectively. Three different thiol crosslinkers were tested, one commercially available tetrathiol derived from pentaerithrytol (PETMP) and two other that were also synthesized: a trithiol derived from eugenol (3SH-EU) and a hexathiol derived from squalene (6SH-SQ).

FTIR and DSC were used to monitor both curing stages and analyze the obtained materials. The results evidenced the occurrence of side reactions that led to incomplete thiol-ene reaction. The dual-curable materials showed higher Tgs than the materials obtained by a simple thiol-ene process and presented higher mechanical and thermomechanical performance.

Keywords: Green chemistry, bio-based, eugenol, dual curing, click reaction, thermosets.

Introduction

Green chemistry is synonymous of health and environmental sustainability. Green chemistry explores new ways of preparing chemical substances or materials in more environment-friendly conditions from renewable resources. This concept includes the reduction or elimination of dangerous substances in the design, manufacture, and use of chemical products.[1,2,3] This is the reason behind the increasing demand for novel synthetic polymers made from components derived from renewable sources that has appeared in the recent years.[4,5] The use of natural components allows to reduce the dependence on fossil resources and implies a positive economic impact.[6,7,8,9,10]

There are several biomass resources that have been proposed to prepare new biobased materials as rosin,[11,12,13] fatty acids,[14] gallic acid,[15] tannins,[16,17] itaconic acid,[18] lignin,[19] vanillin,[20] cardanol,[21] succinic acid[10] and furan derivatives.[22,23] Eugenol (4-allyl-2-methoxyphenol), obtained from the essential oil of clove tree, is highly attractive as feedstock for development of new materials, since it is a phenolic compound that can be further modified to reach the convenient functionality and a rigid structure.[24,25] This aromatic compound is used in the pharmaceutical industry and therapeutic medicine because it has properties of reduction on blood sugar, triglyceride and cholesterol levels.[26] In addition, it can act as antioxidant agent preventing typical processes of oxidation of lipids in the first stages of inflammatory processes working as captor agent

of free radicals.[27] According to that, eugenol derivatives can be a good alternative to get monomeric compounds without toxicological issues.

Recently, many researchers opted for the use of eugenol to prepare new biobased materials. Donovan et al.[28] prepared adhesives by thiol-ene reactions from an eugenol derivative as vinylic compound and pentaerithritol triallylether and PETMP as thiols. Increasing the concentration of eugenol derivative in the thiol-ene network resulted in improved adhesion on a variety of substrates, including glass, aluminium, steel and marble. In another study, Yoshimura et al.[29] prepared new materials by thiol-ene reactions from a triallyl derivative of eugenol. This compound was prepared by allylation of eugenol, followed by a Claisen reaction, and further allylation of the phenol formed. Three different thiols were used to crosslink but the materials obtained did not reach Tg values higher than 10 °C and therefore their applicability was quite limited.

Green engineering is another concept strongly related to green chemistry. It focuses on the optimization of processes and systems to maximize mass, energy, space, and time efficiency. Renewable rather than depleting material and energy inputs are other concepts included in the green engineering principles.[30]

Dual curing procedures have been proposed for clean and efficient processing, which facilitates manufacturing and assembling, reducing the waste production. Dual curing methodologies consist in a first stage of curing leading to a stable intermediate material, which upon application of a second stimulus, undergoes further reaction and crosslinking to achieve the ultimate properties.

In a previous study, we developed a completely sequential dual curing procedure based in a first photochemically induced thiol-ene reaction followed by a thermal thiol-epoxy reaction, using commercially available diglycidylether of bisphenol A (DGEBA), triallylisocyanurate (TAIC) and pentaerythritol tetrakis(3-mercaptopropionate) (PETMP).[31] This procedure allowed us to obtain materials with tailored intermediate and final properties by just changing the formulation composition, and to store them for a certain time in the intermediate state before the final application and completion of the curing process. Due to the toxicological issues of DGEBA and TAIC, the substitution of these monomers by other bio-based derived from a renewable feedstock such as eugenol could contribute to obtain safer thermosetting materials from more sustainable procedures.

Considering both green chemistry and engineering concepts, in the present study the preparation of new sustainable materials from eugenol by thiol-ene or the combination of thiol-ene and thiol-epoxy click reactions will be tackled. The strategy of using dual curing by combination of thiol-ene and thiol-epoxy is aimed at increasing the Tg of the final materials, whereas at the same time improvements in the processability could be reached. As starting monomers we have prepared different compounds derived from eugenol with a functionality of three, being the functional groups allyl or epoxide.

As thiol monomers we selected three different compounds derived from renewable resources: commercially available PETMP, derived from pentaerythritol that can be obtained from biosynthetic procedures [32] and two thiols synthesized from squalene [33] and eugenol, by a clean methodology consisting in the thiol-ene addition of thioacetic acid and further saponification. From the combination of the different monomers shown in Scheme 1, we have prepared new bio-based materials with different characteristics that have been evaluated.

As far as we know, the work reported in the present paper is the first one addressing the preparation of renewable thermosets from bio-based compounds using an efficient environmentally friendly dual click curing methodology.

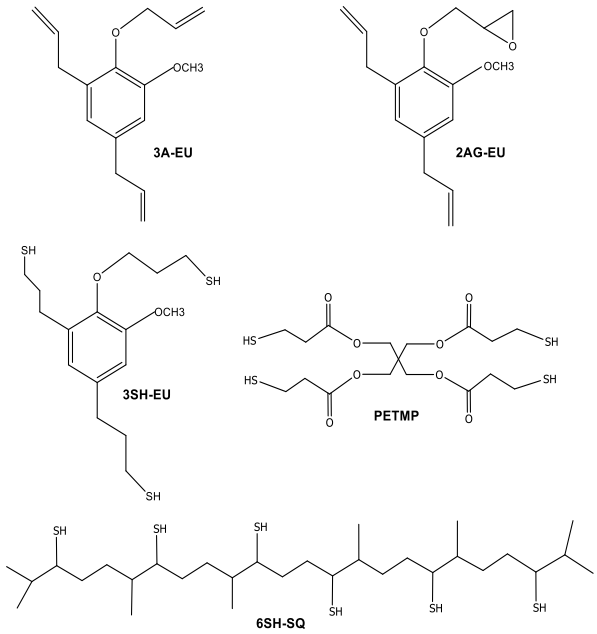

Scheme 1. Chemical structures of the allyl and epoxy eugenol derivatives and the thiols selected as monomers

Experimental part

Materials

Eugenol (EU), allyl bromide, thioacetic acid (TAA), 2,2-dimethoxy-2-phenylacetophenone (DMPA), pentaerythritol tetrakis (3-mercaptopropionate) (PETMP), squalene (SQ), 1-methylimidazole (1-MI), Irgacure 184 (1-hydroxycyclohexyl phenyl ketone), benzyl triethylammonium chloride (TEBAC) and epichlorohydrin (EPC) were purchased from Sigma-Aldrich and were used without further purification. Irgacure 819 (phenylbis (2,4,6-trimethylbenzoyl)phosphine oxide) was supplied by BASF. Inorganic

salts and bases were purchased from Scharlab. Methanol (Carlo Erba) has been used as received. N,N-dimethylformamide (DMF) from VWR was dried by standard procedures.

Preparation of starting products

- *Synthesis of the triallyl compound from eugenol (3A-EU)*

Triallyl eugenol was prepared following a previously reported procedure.[29] The synthesis includes the allylation of eugenol in basic medium to obtain O-allyl eugenol (2A-EU) and then a Claisen rearrangement on heating to obtain 6-allyleugenol (r2A-UE). This product was allylated and the triallyl eugenol (3A-EU) was obtained (see supporting information).^{1}H NMR ($CDCl_3$, δ in ppm): 6.7 s (Ar, 2H), 6.05 m (-CH=,1H), 5.90 m (-CH=, 2H), 5.34 dd (CH_2=, 1H), 5.19 dd (CH_2=, 1H), 5.15-5.0 m (CH_2=, 4H), 4.46 d (-CH_2-O-, 2H), 3.87 s (CH_3-O-, 3H), 3.38 d (-CH_2-Ar, 2H), 3.31 d (-CH_2-Ar, 2H) (see Figure A in supporting information).^{13}C NMR ($CDCl_3$, δ in ppm): 152.6, 144.1, 137.5, 137.3, 135.7, 134.5, 133.7, 121.7, 117.0, 115.8, 115.5, 110.5, 73.7, 55.7, 40.1 and 34.3. FT-IR (ATR): 3072, 3018, 2901, 2825, 1637, 1583, 1510, 1451, 1418, 1256, 1230, 1141, 1026, 986, 907, 804 and 752 cm^{-1}.

- *Synthesis of diallylglycidyl derivative of eugenol (2AG-EU)*

10.49 g (51.4 mmol) of r2A-EU, 30.76 g (332.4 mmol) of epichlorohydrin and 0.84 g (3 mmol) of benzyltriethylammonium chloride (TEBAC) were stirred in a 250 mL flask at 100 °C for one hour. The mixture was cooled down to 30 °C and then 30 mL of an aqueous solution of 20% NaOH and 0.84 gr of TEBAC were added and maintained under stirring for 90 min. Once finished 20 mL of ethyl acetate was added to the mixture for dilution. The phases were separated and the organic layer was washed twice with water and dried with magnesium sulphate. The solvent and excess epichlorohydrin were eliminated in a rotary evaporator at 60 °C. The product obtained, with 97% yield, was purified by silica-gel chromatography using hexane/ethyl acetate 7/3. The product is a pale yellow liquid. ^{1}H NMR ($CDCl_3$, δ in ppm): 6.6 s (Ar, 2H), 5.95 m (-CH=, 2H), 5.06 m (CH_2=, 4H), 4.15 dd (-CH_2-O-, 1H), 3.93 dd (-CH_2-O-, 1H), 3.83 s (CH_3-O-, 3H), 3.42 d (-CH_2-Ar, 1H), 3.33 m (CH epoxy ring, 1H), 3.28 d (-CH_2-Ar, 1H), 2.85 dd and 2.68 dd (CH_2 epoxy ring, 2H). ^{13}C NMR ($CDCl_3$, δ in ppm): 152.2, 143.8, 137.3, 137.2, 135.8, 133.5, 121.8, 115.7, 115.4, 110.6, 73.6, 55.5, 50.5, 44.4, 39.9 and 34.0. FT-IR (ATR): 3072, 3050, 3018, 2901, 2825, 1583, 1451, 1418, 1256, 1230, 1141, 1110, 1026, 986, 915, 907, 804 and 752 cm^{-1}.

- Synthesis of the trithiol derivative of eugenol (3SH-EU)

Photochemical thiol-ene reaction (3STA-EU)

A mixture of 5 g (20.5 mmol) of triallyl eugenol derivative (3A-EU), 22.2 g (291.6 mmol) of TAA and 0.1290 g (0.50 mmol) of DMPA were photoirradiated with a UV lamp at 356 nm for 1 h. The product obtained was dissolved in $CHCl_3$ and extracted with a saturated NaOH solution and then washed with water and dried over anhydrous $MgSO_4$. The solvent was removed on a rotary evaporator. The product obtained was a viscous

liquid with 96% yield. 1H NMR ($CDCl_3$, δ in ppm): 6.52 s and 6.50 s (Ar, 2H), 3.91 t (-CH_2-O-, 2H), 3.80 s (CH_3-O-, 3H), 3.10 (-CH_2-S-, 2H), 2.85 m (-CH_2-Ar, 4H), 2.56 m (-CH_2-S-, 4H), 2.31 s (CH_3-CO-S-, 9H), 1.99 m (-CH_2-CH_2-CH_2-O-, 2H), 1.8 m (-CH_2-CH_2-CH_2-Ar, 4H). ^{13}C NMR ($CDCl_3$, δ in ppm): 195.7, 195.6, 195.5, 152.3, 143.9, 136.6, 134.5, 121.4, 110.3, 70.0, 55.5, 34.5, 31.0, 30.5, 30.3, 30.2, 29.1, 28.7, 28.4 and 25.8. FT-IR (ATR): 2930, 2825, 1680, 1587, 1505, 1460, 1424, 1355, 1260, 1232, 1135, 1010, 950, 800 and 607 cm^{-1}.

Hydrolysis of 3STA-EU (3SH-EU)

9.31 g (19.7 mmol) of 3STA-EU were added to 100 mL of methanol in a flask equipped with magnetic stirrer. 1.70 g (42.5 mmol) of pulverized NaOH were added and the mixture was heated to reflux temperature under inert atmosphere for 5.5 h. The solution was allowed to cool down and the solvent was removed. The product obtained was dissolved in water and acidified with 0.1 M HCl solution and then extracted with $CHCl_3$. The organic phase was washed with distilled water and then dried over anhydrous $MgSO_4$. The product obtained was a pale-yellow viscous liquid. 84% yield. ^{1}H NMR ($CDCl_3$, δ in ppm): 6.56 s (Ar, 2H), 3.98 t (-CH_2-O-, 2H), 3.82 s (CH_3-O, 3H), 2.77 q (-CH_2-S-, 2H), 2.61 m (-CH_2-S-, 4H), 2.51 q (-CH_2-Ar, 4H), 2.1 m (-CH_2-CH_2-CH_2-O-, 2H), 1.85 m (-CH_2-CH_2-CH_2-Ar, 4H), 1.5 t (-SH, 1H), 1.35 t (-SH, 1H) and 1.33 t (-SH, 1H). (Figure B in supporting information). ^{13}C NMR ($CDCl_3$, δ in ppm): 152.2, 143.9, 136.7, 134.6, 121.5, 110.2, 70.3, 55.5, 35.3, 34.6, 34.3, 34.0, 28.5, 24.1, 23.8 and 21.2. FT-IR (ATR): 2930, 2825, 2580, 1587, 1503, 1460, 1430, 1260, 1230, 1150, 1090, 1010, 950 and 830 cm^{-1}.

- Synthesis of the hexathiol derived from squalene (6SH-SQ)

The product was obtained following a two-step procedure previously reported,[33] which includes a thiol-ene photochemical reaction of squalene with thioacetic acid followed by a saponification of the thioester groups (see supporting information).

Preparation of the curing mixtures

Two different types of formulations were prepared. Thiol-ene formulations named as 3A-EU/thiol and dual formulations named as 2AG-EU/thiol. The mixtures were prepared by mixing with a spatula stoichiometric amounts of allyl/SH and allyl-epoxy/SH groups until reaching homogenous mixtures.

Four different thiol-ene formulations were prepared from 3A-EU as allyl monomer and three different thiols: PETMP, 3SH-EU, 6SH-SQ and PETMP/3SH-EU in equimolecular proportion. The photochemical reaction was catalyzed by adding a 0.2 or 4% of a mixture of Irgacure 184 and Irgacure 819 in weight ratio 3:1 in some drops of acetone to obtain a homogenous mixture. Then, acetone was eliminated in a vacuum oven for 30 minutes.

Four different dual formulations were prepared similarly from 2AG-EU with three thiols: PETMP, 3SH-EU, 6SH-SQ and an equimolecular thiol mixture PETMP/3SH-EU. The formulations contained a 0.2 or 4% of a mixture of Irgacure 184 and Irgacure 819 in weight

ratio 3:1 to activate thiol-ene reaction and 1 phr (part per hundred of total mixture) of 1-MI as a basic catalyst for the activation of thiol-epoxy thermal process.

Characterization techniques

^{1}H and ^{13}C NMR spectra were registered in a Varian Gemini 400 spectrometer. $CDCl_3$ was used as the solvent. For internal calibration the solvent signal corresponding to $CDCl_3$ was used: δ (^{1}H) = 7.26 ppm, δ (^{13}C) = 77.16 ppm.

Samples of the different compositions were photocured at 35 °C, in a Mettler DSC-821e calorimeter appropriately modified with a Hamamatsu Lightning cure LC5 (Hg–Xe lamp) with two beams, one for the sample side and the other for the reference side. 5 mg samples were cured in open aluminium pans in nitrogen atmosphere. Two scans were performed on each sample, the second one needed to subtract the thermal effect of the radiation. The method consisted of 1 min without irradiation for temperature stabilization, followed by 12 min irradiation and finally 0.50 min without irradiation. The light intensity used was 35.6 mW/cm^2, measured at 365 nm using a radiometer.

Studies of the thermal reaction were performed by differential scanning calorimetry (DSC) in a Mettler DSC-821e apparatus. For dynamic studies a flow of N_2 at 100 mL/min was used and the weight of the samples for the analysis was 10 mg. The calorimeter was calibrated using an indium standard (heat flow calibration) and an indium-lead-zinc standard (temperature calibration). The studies were performed in the temperature range of 30-250 °C, with a heating rate of 10 K/min.

The glass transition temperatures (Tgs) of the samples after irradiation were determined in dynamic scans at 20 °C/min from -100 °C to 100 °C. The Tgs of the final thermosets were determined after two consecutive dynamic scans at 20 °C/min starting at -100 °C in a Mettler DSC-822e device to delete the thermal history. The Tg value was taken as the middle point in the heat capacity step of the glass transition.

A Bruker Vertex 70 FTIR spectrometer equipped with an attenuated total reflection accessory (ATR) (Golden Gate, Specac Ltd. Teknokroma) which is temperature controlled (heated single-reflection diamond ATR crystal) equipped with a liquid nitrogen-cooled mercury-cadmium-telluride (MCT) detector was used to register the FTIR spectra of the mixtures during UV irradiation and fully cured samples. The spectra were registered in the wave number range between 4000 and 600 cm^{-1} with a resolution of 4 cm^{-1} and averaged over 20 scans. UV-curing was performed using a Hamamatsu Lightning cure LC5 (Hg-Xe lamp) with one beam conveniently adapted to the ATR accessory. A wire-wound rod was used to set a sample thickness of 50 μm. OPUS software was used for the analysis of the spectra. The spectra were corrected for the dependence of the penetration depth on the wavelength and normalized with respect to the absorbance of C=C aromatic peaks at 1587 cm^{-1} (neglecting the contribution of the overlapping tiny signal associated with the allyl group). The normalized thiol band at 2576 cm^{-1} and the allyl band at 1639 cm^{-1}

were integrated and the thiol and allyl conversions after the photocuring (X_{uv}) and after thermal curing (X_{final}) were

$$X_{UV} = 1 - \frac{A'_{UV}}{A'_0} \quad (1)$$

$$X_{final} = 1 - \frac{A'_{final}}{A'_0} \quad (2)$$

Where A'_{UV}, A'_{final} and A'_0 are the normalized area of thiol or allyl bands after photocuring and thermal curing and at the beginning of the curing, respectively.

The thermal stability of the cured samples was studied by thermogravimetric analysis (TGA), using a Mettler TGA/SDTA 851e thermobalance. All the experiments were performed under inert atmosphere (N_2 at 100 mL/min). Pieces of the cured samples with an approximate mass of 8 mg were degraded between 30 and 600 °C at a heating rate of 10 K/min.

Dynamic mechanical thermal analyses (DMTA) were carried out with a TA Instruments DMA Q800 analyser. Cured rectangular samples (40 mm x 7.7 mm x 1.6 mm) from the different formulations based on 3A-EU were obtained in silicon moulds irradiated in an ultraviolet chamber (320-390 nm), DymaxECE 2000 UV model systems. The samples were irradiated with an intensity of 105 mW/cm^2 for a period of 60 seconds each face 14 times, waiting 60 s minimum between irradiations, to control the temperature of the sample. The dual cured samples with the selected formulations based on 2AG-EU were photocured as described before and then isothermally cured without mould at 120 °C for 1 h with a post curing at 150 °C for 30 min. Three point bending clamp was used on the prismatic rectangular samples. The apparatus operated dynamically at 5 K/min from 30 to 150 °C to delete the thermal history and then dynamically at 3 K/min from -20 to 120°C at a frequency of 1 Hz with and oscillation amplitude of 10 µm. Young's modulus was determined under flexural conditions at 30 °C, with the same clamp and geometry samples, applying a force ramp at constant load rate of 3 N/min, from 0.001 N to 18 N. Three samples of each material were analyzed and the results were averaged. Stress strain at break tests were performed with the film-tension clamp in force controlled mode. Dogbone samples were used at a force rate of 1 N/min and the averaged values of at least three different samples were reported.

Microindentation hardness was measured with a Wilson Wolpert 401 MAV device following the ASTM E384-16 standard procedure. For each material 10 determinations were made with a confidence level of 95%. The Vickers hardness number *(HV)* was calculated from the following equation:

$$HV = \frac{1.8544 \cdot F}{d^2} \qquad (3)$$

Where, *F* is the load applied to the indenter in kg f and *d* is the arithmetic mean of the length of the two diagonals of the surface area of the indentation measured after load removal in mm.

Results and discussion

Synthesis and characterization of monomers

The synthetic procedure applied to the preparation of eugenol derivatives used as monomers in the present study is depicted in Scheme 2.

This synthetic procedure is based on the preparation of the diallyl derivative (r2A-EU), previously reported by Yoshimura et al.[29] They described that the allylation of the phenol group of eugenol followed by a Claisen rearrangement allows the preparation of the diallyl compound r2A-EU, from which the triallyl (3A-EU) or the glycidyl derivative (2AG-EU) can be, alternatively obtained. This glycidylic compound has not been previously described but the synthesis is quite conventional and based in the reaction of phenols with epichlorohydrin in excess in the presence of a quaternary ammonium salt. The triallyl derivative was converted into the trithiol (3SH-EU) following the synthetic procedure consisting in a photochemical thiol-ene addition of thioacetic acid and further saponification with a base, as previously reported.[34]

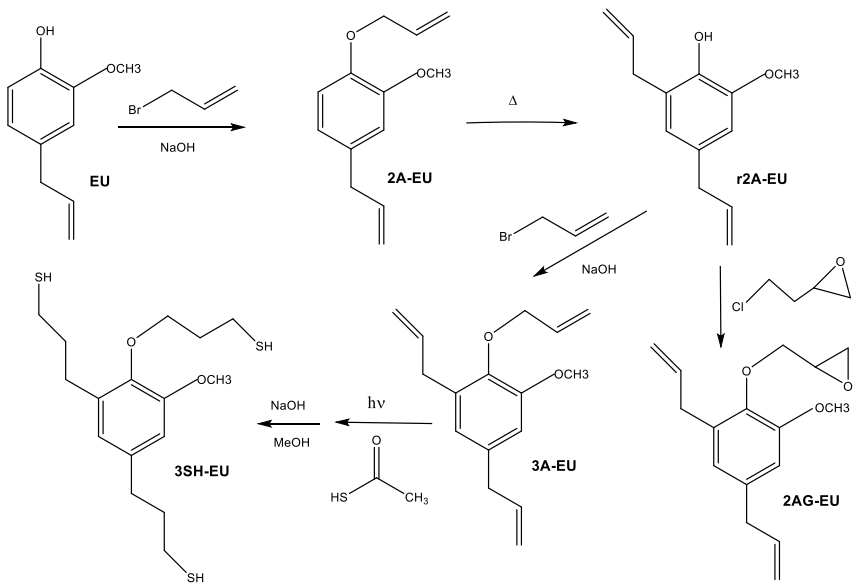

Scheme 2. Synthetic procedure used in the preparation of the triallyl derivative (3A-EU), the glycidyl derivative (2AG-EU) and the trithiol (3SH-EU) from eugenol

The synthesized compounds did not required further purification with the exception of 2AG-EU, which was purified by column chromatography. The characterization of the previously reported compounds was performed by ^{1}H and ^{13}C NMR spectroscopy and they perfectly agree with those previously published and confirmed their high purity (see spectra in supporting information).

Figure 1 and 2 show the ^{1}H and ^{13}C NMR spectra of 2AG-EU with the corresponding assignments. As we can see, and in spite of the complexity due to the lack of symmetry, the ^{1}H NMR spectrum of 2AG-EU shows the typical pattern expected for both allyl groups, partially overlapped among them, and the five signals expected for the five unequivalent protons of glycidyl group. Aromatic protons and methoxy group appear as singlets. The ^{13}C NMR spectrum of this compound also shows its high purity and confirms the expected structure of the compound. The assignments have been performed on the basis of similar compounds previously reported.[24,29]

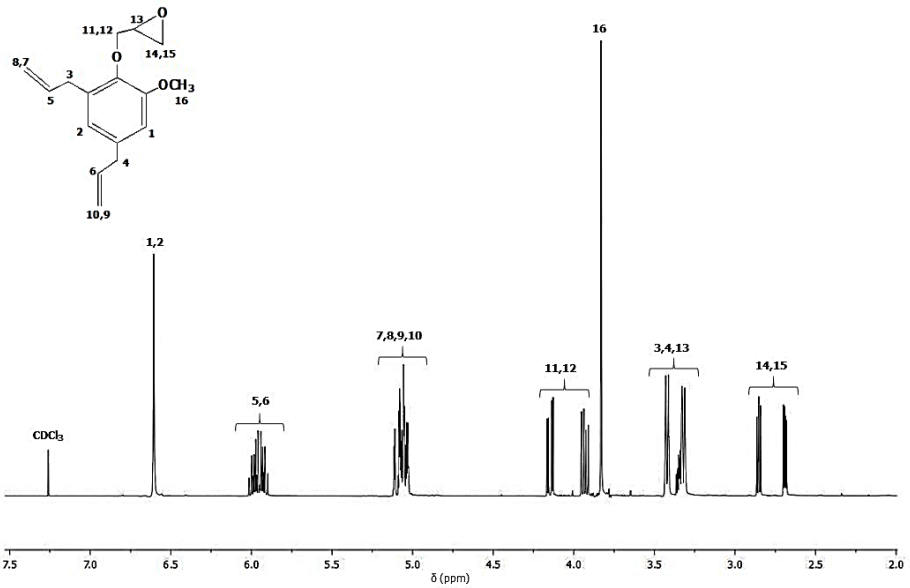

Figure 1. ^{1}H NMR spectrum of the 2AG-EU in $CDCl_3$

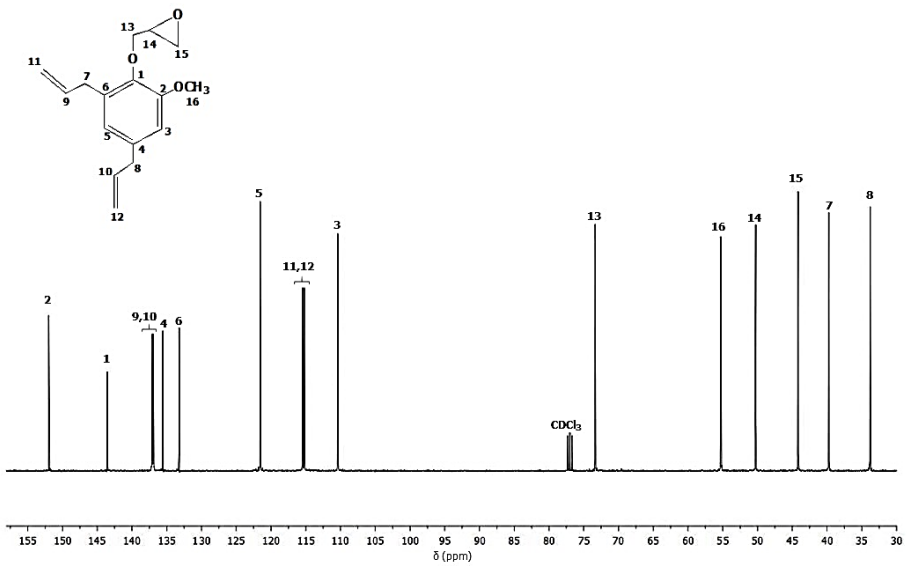

Figure 2. ^{13}C NMR spectrum of the 2AG-EU in $CDCl_3$

In the FTIR spectra the most typical signals could be observed, as for 2A-EU and r2A-Eu, the vinyl stretching signals at 1637 and 1630 cm^{-1} respectively and the absorptions at 1637 cm^{-1} for vinyl and 907 cm^{-1} for epoxy groups for the compound 2AG-EU. The spectrum of the thiol 3SH-EU shows a weak band at 2570 cm^{-1} corresponding to the S-H stretching.

In addition to eugenol derivatives, a biobased thiol derived from squalene (6SH-SQ) was synthesized following a reported procedure.[33] Its characterization was done by ^{1}H NMR and FTIR spectroscopy, which were coincident with the reported data. The structure of 6SH-SQ, although aliphatic and therefore quite flexible, allowed to reach high Tgs in thiol-epoxy formulations because of the six thiol reactive groups per molecule, as it was proved in the curing of cycloaliphatic resins.[34] According to that, it has been selected in the present study to help to increase the Tgs of the thermosets prepared.

Preparation and characterization of materials based on 3A-EU by thiol-ene reaction

First of all, we studied the preparation of thermosets by thiol-ene reaction triggered by photoirradiation and in the presence of a radical photoinitiator. This was already done by Yoshimura et al.[29] using 3A-EU, but using in our case, different thiols as comonomers. First, we tried DMPA as radical initiator, since it catalysed thiol-ene reactions even in low proportion (0.1 phr).[31] However, in the case of eugenol derivatives this reaction did not occur even when proportions of 3 phr of DMPA were added to the formulation. Thus, we tried with a 0.2% wt% of a mixture of Irgacure 184/Irgacure 819 in 3:1 weight ratio as used by Yoshimura.[29]

Photocalorimetric studies were done to see the evolution of the curing process. Figure 3 shows the exothermic curing curves for the various formulations studied.

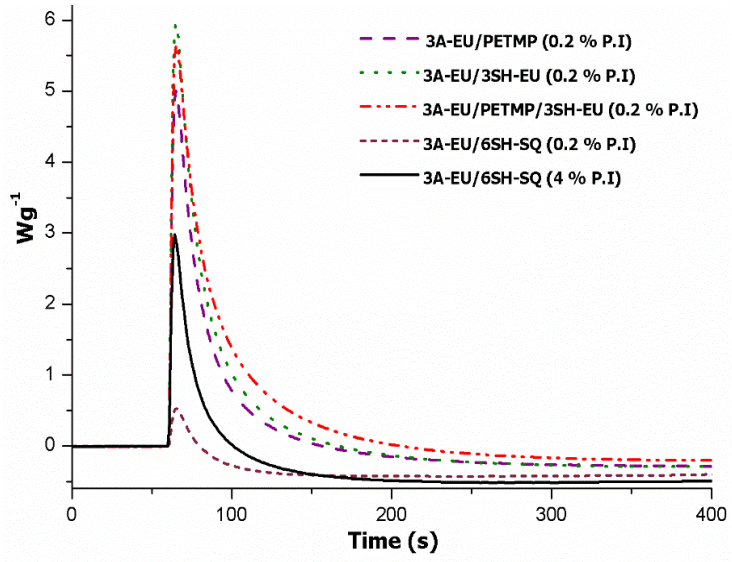

Figure 3. DSC thermograms corresponding to the photocuring at 30 °C of the mixtures of 3A-EU with different thiols

As we can see in the photocalorimetric curves, the reaction seems to proceed quite well for all the mixtures with the exception of the formulation prepared from 6SH-SQ. However, on increasing the proportion of photoinitiator in this formulation up to 4%wt the heat evolved increased, but it does not reach the maximum observed in the other formulations. This seems to indicate a lower reactivity of this thiol that can be explained by its structure with a high functionality and thiols attached to methine carbons.

In the mixture of PETMP/3SH-EU as thiol, the system appears to be more reactive than formulations with each one of the thiols (PETMP or 3SH-EU) separately. The shape of these curves made the evaluation of heat quite unreliable but values around 50 kJ/thiol eq could be calculated. In a previous study we could determine similar enthalpies for thiol-ene process.[31]

Although calorimetric studies give valuable insight to the curing process, the evolution of the reactions contributing to the curing must be evaluated from the point of view of the chemical transformations. Thus, the evolution of the most significant bands of the monomers was followed by FTIR spectroscopy during irradiation of a film of the sample on the ATR. Thiol groups evolution was monitored by the band at 2576 cm^{-1} corresponding to S-H st and the reduction of allyl groups by the band at 1639 cm^{-1} attributable to C=C st. As reference band we selected the absorption at 1587 cm^{-1} of the aromatic ring. Table 1 shows the final conversion of allyl and thiol groups reached in the cured material.

Table 1. Conversions of the reactive species after thiol-ene process calculated by FTIR/ATR

Sample	Photoinitiator (wt%)	Allyl conversion (%)	Thiol conversion (%)
3A-EU/3SH-EU	0.2	71	100
3A-EU/PETMP	0.2	60	67
3A-EU/PETMP/3SH-EU	0.2	65	87
3A-EU/6SH-SQ	4	54	55

It should be commented that if the reaction was complete and occurred by an only thiol-ene process, the conversion of allyl and thiol groups should approach both to 100%. However, the values in Table 1 evidence the lower reactivity of 6SH-SQ, with parallel conversions of thiol and allyl eugenol during the photoirradiation, but reaching only partial conversion, even when a high amount of photoinitiator was added to the formulation. The mixture 3A-EU/PETMP does not react completely either, but the conversion of thiol and allyl moieties are quite similar. In contrast, the use of 3SH-EU as thiol crosslinker leads to a surprising difference in conversions of thiol and allyl moieties. In the case of the 3A-EU/3SH-EU mixture, the thiol disappears completely but allyl is converted in only 71%. A similar behaviour is observed in the case of the 3A-EU/PETMP/3SH-EU mixture, although the difference between thiol and allyl conversion is not as high and there are still thiol groups remaining. Several authors reported on the limitations of thiol-ene processes due to the possibility of thiol-thiol coupling and carbon-carbon radical coupling.[35] The thiol-thiol coupling should be the responsible of the thiol exhaustion when 3SH-EU is selected. The run out of thiol leads to the prompt termination in the crosslinking process. Yoshimura et al.[29] also reported there was a different evolution of allyl and thiol groups, leading to remaining unreacted allyl, when 3A-EU was cured with thiols of different structure, and they attributed the difference to thiol-thiol coupling reactions. It seems that the structure of eugenol monomers could also make difficult the quantitative thiol-ene reaction. Given that thiol-ene reactions involve the formation of radical intermediates, it can be hypothesized that these unexpected results can be related to the possible formation and stabilization of radical species in the methylene carbon of the allyl group directly attached to the aromatic ring by resonance as represented in Scheme 3. The formation of such species would contribute to the slow and incomplete thiol-ene reaction, leading to the presence of unreacted allyl or -ene groups.

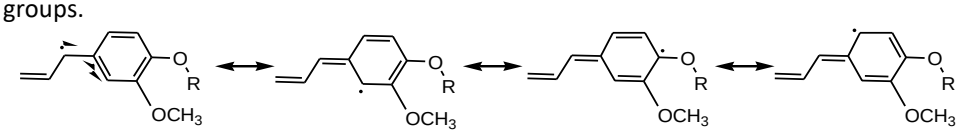

Scheme 3. Stabilization of eugenol radical species by resonance

Different samples were obtained from the various formulations by irradiation in a UV chamber during the adequate time to reach the ultimate properties. However, the amount of photoinitiator was raised to 4%wt in all the formulations to get the maximum curing degree, because of the size of the samples made difficult reaching the complete

and homogenous curing and lower amounts of initiator led to sticky samples. The results of the thermal analysis of the cured samples are collected in Table 2.

Table 2. Thermal data of the materials obtained by thiol-ene reaction

Sample	$T_{5\%}$[a] (°C)	T_{max}[b] (°C)	Res.[c] (%)	T_g[d] (°C)	$T_{tan\delta}$[e] (°C)	E_r[f] (MPa)	E[g] (MPa)
3A-EU/3SH-EU	249	386	16	1	14	2.7	6.7
3A-EU/PETMP	237	369	16	9	18	6.7	23.9
3A-EU/PETMP/3SH-EU	241	373	16	8	16	3.7	18.2
3A-EU/6SH-SQ	252	356	3	14	30	2.2	20.6

a. Temperature of 5% of weight loss in N_2 atmosphere.
b. Temperature of the maximum rate of degradation in N_2 atmosphere
c. Residue after thermal degradation in N_2 atmosphere
d. Glass transition temperature determined by DSC
e. Temperature of maximum of tan δ determined by DMTA
f. Storage modulus in the rubbery state determined at tan δ + 50°C
g. Young´s modulus at 30 °C under flexural conditions

As we can see, the results from TGA analysis do not show large differences between the different materials but the presence of ester groups in the PETMP structure slightly decreases the temperature of initial degradation.

By DSC and DMTA the Tg of these materials was determined. The maximum value reached was 14 °C (by DSC) or 30 °C (by DMTA) for the material obtained from the squalene thiol derivative, because of its high functionality, although the reaction was not complete. The Tgs of the other materials were lower than the one obtained from 6SH-SQ material. Yoshimura et al.[29] reached a maximum Tg value of 9.1 °C for the material obtained from PETMP as the thiol which is coincident with the value reached by us. The moduli measured reflect not only the degree of curing achieved but also the structure of the thiol used and therefore the rationalization of the values measured is not an easy task. The Young's moduli were measured at 30 °C and the low values agree with their rubbery state, according to the low Tgs of these materials. Moreover, from the values of the table we can conclude that the use of 3SH-EU is highly detrimental for the quality of the thiol-ene cured formulations and only improves when a mixture of 3SH-EU and PETMP was used as crosslinker agent.

The results obtained lead to the conclusion that the applicability of the materials derived from 3A-EU by thiol-ene curing is quite limited because of their low thermomechanical characteristics. The structure and functionality of the thiol crosslinker usually have a significant influence on the thermal-mechanical properties of the materials, but the tailoring of the properties of these materials is negatively affected by the incomplete reaction and the occurrence of undesired side-reactions that occurs in a greater extent in eugenol monomers, according to the results reported by Yoshimura.[29]

Preparation and characterization of the materials derived from 2AG-EU by thiol-ene/thiol-epoxy dual curing process

To improve the performance of eugenol-derived materials we proposed the combination of thiol-ene with thiol-epoxy reactions, following a dual curing procedure. Once studied the thiol-ene stage and characterized the materials obtained from 3A-EU, the study of this dual curing process was attempted starting from 2AG-EU formulations with 3SH-EU, PETMP, 6SH-EU and the mixture of PETMP and 3SH-EU. In addition to the photoinitiator, a base must be included in the formulation to catalyse the thermal thiol-epoxy reaction. In the present study 1-MI was selected as the base.[36]

Sequential thiol-ene/thiol-epoxy dual curing systems were developed in our group for formulations of DGEBA/TAIC/PETMP.[31] Thiol epoxy reaction requires an amine to convert the thiol groups into thiolates, which are more nucleophilic and able to attack epoxy rings, forming networks through thioether bonds. The use of latent amine precursors allowed the second step to be triggered at will. This fact opens the possibility of irradiating the initial formulation to complete the thiol-ene reaction obtaining an intermediate material able to be stored, manipulated or transformed safely. On heating this material at the required temperature the second reaction can be activated and the material can be further crosslink until it achieves the ultimate network structure and properties. However, dual systems are in general quite complex and the structure of the monomers has an enormous influence in the reactivity and can lead to a partial overlapping between processes or even limit the conversion in one of the steps. Therefore, it is necessary to adjust the curing conditions for each reactive system.[37]

The implementation of a new dual curing process requires a previous study to find out the right proportion of initiator or catalyst, the reaction times required and the best reaction conditions to get the maximum degree of curing in each stage. After that, it is important to determine if both processes overlap in the conditions selected.

Figure 4 shows the calorimetric curves of the thermal stage in irradiated and non-irradiated samples.

In clean sequential dual curing processes irradiation should not affect the second thermal process. As we can see in the figure, in the present case the initial irradiation step has a notable influence on the second thermal stage, both in the shape of the curve and especially in the heat evolved, reported in Table 3 for all the formulations studied. In that table, the enthalpies released during the first photochemical step and during the second thermal thiol-epoxy stage are given separately. In addition, the enthalpies released by thermal curing of non-irradiated mixtures (initial mixture) are also given. The values of enthalpy are expressed by gram and by reactive equivalent (allyl groups in the photochemical step and epoxides in the thermal). The Tgs of the materials in the intermediate stage and after curing completion are also detailed.

The difference between the reaction enthalpy in the epoxy-thiol thermal reaction in previously irradiated and virgin formulations gives information about the overlapping among photochemical and thermal processes. In the case of completely controlled sequential curing, both enthalpies must be similar.[31] However, from the values of the table we can see that the heat released in the second curing stage, after irradiation, is lower in all the formulations than that of the non-irradiated mixtures. This result can be related to the occurrence of two different undesired processes during photoirradiation: a) thiol-epoxy reaction can start because of the increased temperature caused by the thiol-ene process and b) the remaining amount of thiol groups can be lower than expected due to thiol-thiol coupling, as previously detected in the curing of 3A-EU formulations. The difference between enthalpies in irradiated and non-irradiated samples is minimal for 2AG-EU/PETMP formulations (89% of conversion in epoxide during the second step) and maximal for 3SH-EU formulations (29 and 58% of conversion in epoxide during the thermal step for 3SH-EU and PETMP/3SH-EU, respectively). In the case of 6SH-SQ mixture, a 64% of the epoxide conversion occurs during the thermal process.

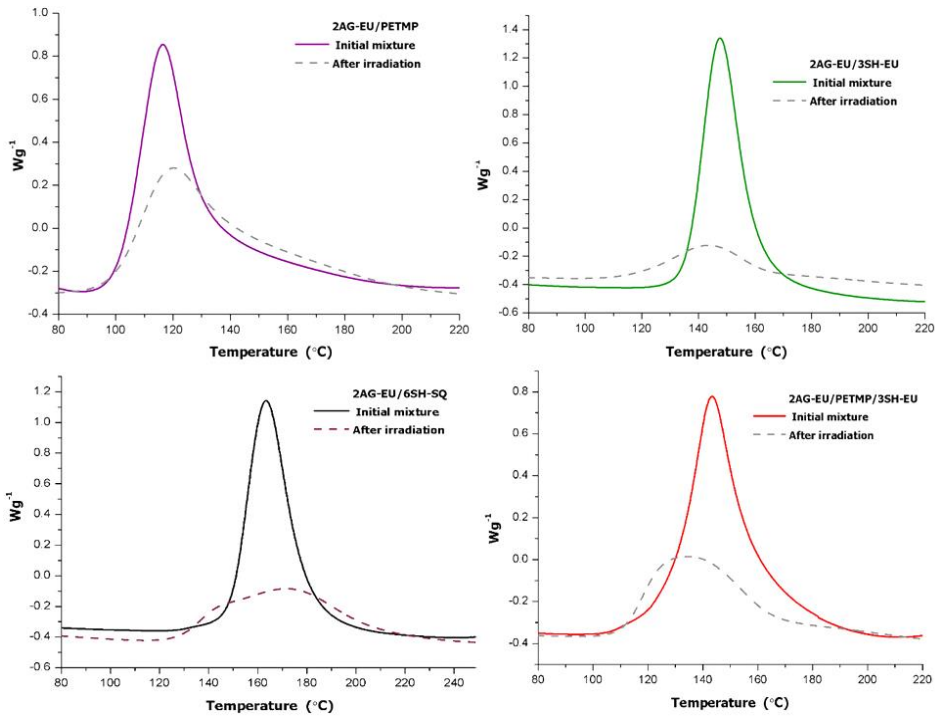

Figure 4. Calorimetric curves of irradiated and non-irradiated 2AG-EU formulations with the thiols tested

Table 3. Reaction enthalpies and Tgs of the different formulations determined by DSC

Sample	Initial mixture		1st stage			2nd stage		
	Δh[a] (J/g)	Δh[b] (kJ/eq)	Δh[c] (J/g)	Δh[d] (kJ/eq)	Tg[e] (°C)	Δh[f] (J/g)	Δh[g] (kJ/eq)	Tg[h] (°C)
2AG-EU/3SH-EU	197.1	121.9	154.0	30.0	-	57.3	35.4	-
2AG-EU/PETMP	192.4	124.1	138.0	28.2	-12	171.0	110.8	36
2AG-EU/PETMP/3SH-EU	184.8	117.4	183.9	36.9	-6	106.9	68.0	28
2AG-EU/6SH-SQ	203.6	123.2	86.5	24.8	1	129.0	78.6	57

a. Enthalpy released per gram on heating the initial mixture
b. Enthalpy released per epoxy equivalent on heating the initial mixture
c. Enthalpy released per gram during the irradiation of the mixture
d. Enthalpy released per allyl equivalent during the irradiation of the mixture
e. Glass transition temperature of the intermediate material
f. Enthalpy released per gram of previously irradiated samples during the thermal step
g. Enthalpy released per epoxy equivalent of previously irradiated samples during the thermal step
h. Glass transition temperature of the final cured material

To investigate the evolution of the different reactive groups during the photochemical stage, FTIR spectra were taken during irradiation. Table 4 shows the conversion of allyl and thiol groups and the values of the theoretical conversion of thiol have been added to the table, since thiol groups also participates in the thermal thiol-epoxy process and therefore should be in excess in reference to the ally groups. The measured conversion in allyl groups has been included in these calculations for every mixture. The evaluation of epoxide, although very interesting to determine the real conversion of epoxy groups in this step, was not possible because the overlapping of the 907 cm^{-1} band of the oxirane ring with other absorptions in this zone.

Table 4. Conversion of allyl and thiol groups in the photochemical stage of the dual curing of 2AG-EU formulations calculated by FTIR spectroscopy

Sample	Allyl conversion (%)	Thiol conversion (%)	Theoretical thiol conversion (%)
2AG-EU/3SH-EU	99	100	66
2AG-EU/PETMP	76	53	51
2AG-EU/PETMP/3SH-EU	99	76	66
2AG-EU/6SH-SQ	93	64	62

As we can see in the table, allyl groups disappear completely during photoirradiation when 3SH-EU is in the formulation, but in both cases, thiol reacts much more than the theoretically calculated, confirming that undesired thiol-thiol coupling takes place. This reaction leads to the exhaustion of thiol in the 2AG-EU/3SH-EU mixture, which implies that the second thermal thiol-epoxy process will not occur. However, some enthalpy is released in this process (see Table 3) which can be related to the homopolymerization of epoxide by the 1-MI acting as a thermal anionic initiator.[36]

The conversion of allyl groups in the 2AG-EU/PETMP formulation is quite low, but the conversion of thiol barely exceed the theoretical one and confirms that PETMP has not the tendency to thiol-thiol coupling as observed previously by us.[31] In addition, the enthalpy released in the thermal step is quite high (see Table 3) and only slightly lower

that the obtained from the non-irradiated samples. Thus, the curing of this mixture is the more controlled and could be considered as a sequential dual curing, although some allyl groups might not react completely because of the special features of the eugenol structure.

Finally, 6SH-SQ seems to have the best structure to reach a practically quantitative conversion in thiol-ene process when the proportion of thiol is higher than the stoichiometric, because of the thiol excess required to react with epoxide in the second step. It must be remembered that the 3A-EU/6SH-SQ formulation reached an only 54-55% of conversion in stoichiometric thiol-ene formulations previously studied. However, the enthalpy released in the thermal stage by epoxy equivalent is lower than expected (78.6 kJ/ee that corresponds to a 64% of epoxy reaction). Both results suggest the existence of topological restrictions in 6SH-SQ due to the high functionality of its structure that prevents completion of the reaction.

As expected, the Tgs of the intermediate materials are low (see Table 3), but the highest value corresponds to the material cured with the squalene derivative, because of its high functionality. On comparing the Tgs of the cured materials derived from 2AG-EU with the corresponding materials prepared from 3A-EU we can see a notable increase by the occurrence of the second thermal process that leads to a tighter network structure. In case of 6SH-SQ cured materials an increase in more than 50 °C are achieved by the contribution of the epoxy thermal step that leads to a final Tg of 57 °C that impart rigid characteristics to this material at room temperature. The Tgs of the materials prepared in the present study were higher than others reported in the literature for eugenol derivatives.[28, 29]

The materials prepared were characterized by TGA and DMTA and the main data obtained are collected in Table 5. The material prepared from 2AG-EU/3SH-EU formulation has not been included in this characterization because of the non-comparable structure of the network, coming from different unexpected reactions taken place.

Table 5. Thermal data of the materials obtained after dual curing process from 2AG-EU

Sample	$T_{5\%}$[a] (°C)	T_{max}[b] (°C)	Residue[c] (%)	$T_{tan\delta}$[d] (°C)	E_r[e] (MPa)	E[f] (MPa)
2AG-EU/PETMP	329	364	19	52	10.1	184.7
2AG-EU/PETMP/3SH-EU	317	372	17	41	3.7	44.2
2AG-EU/6SH-SQ	298	366	4	76	10.2	935.7

a. Temperature of 5% of weight loss in N_2 atmosphere
b. Temperature of the maximum rate of degradation in N_2 atmosphere
c. Residue after thermal degradation in N_2 atmosphere
d. Temperature of maximum of tan δ determined by DMTA
e. Storage modulus in the rubbery state determined at tan δ + 50 °C
f. Young's modulus at 30 ° C under flexural conditions

The dual cured materials show higher temperature of initial degradation, but similar temperature of the maximum rate of weight loss and char yield in comparison with the materials obtained by thiol-ene photochemical curing from 3A-EU (see Table 2). This is related to the more densely crosslinked structure of the dual thermosets and the absence of uncrosslinked fraction, leading to a delay in the apparent start of the degradation process.

Figure 5 shows the storage modulus and tan δ variations against temperature for the materials prepared obtained by the DMTA technique. The plots of tan δ are unimodal according to the homogeneity of these materials because of the participation of thiol structures in both reactive processes that hinders phase separation of the two types of network structures. The tan δ maximum shifts to higher temperature for the squalene-derived material because of the tight network formed. Similarly, the decrease in storage modulus associated with the network relaxation takes place at higher temperature than the other materials. The values of relaxed modulus are similar for the materials obtained from 6SH-SQ and PETMP, in spite of having very different structures. This may be caused by the different final conversion of the cured materials and the coexistence of side-reactions producing a network structure different from the one expected. It is noticeable the low thermomechanical characteristics of the material containing 3SH-EU structures.

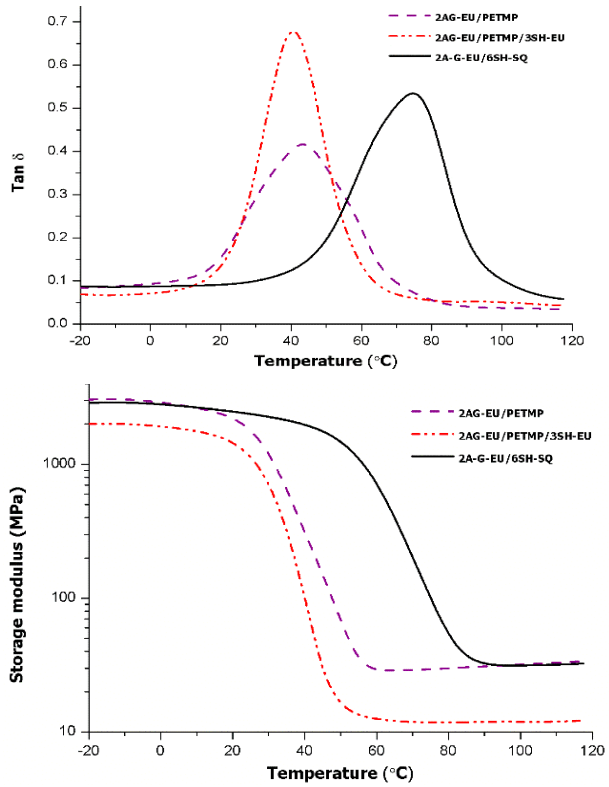

Figure 5. Plots of tan δ and storage modulus against temperature for the various materials prepared

Young's moduli, determined at 30 °C (see Table 5), show notable differences on comparing the three materials, being the more rigid the thermoset obtained from 6SH-SQ.

The comparison of the thermomechanical data of the materials obtained from 2A-EU and 3A-EU (Tables 5 and 2, respectively) allows to see the valuable contribution of the thiol-epoxy reaction in the enhancement of the characteristics of the cured materials. Although from the point of view of the structure, thiol-ene and thiol-epoxy processes should lead to similar thermomechanical properties, the undesired side-reactions of thiol-ene process and incomplete conversion in these eugenol monomers justify the observed differences.

Dogbone samples of dual cured materials were prepared to perform stress-strain at break tests in DMTA at 30 °C. Table 6 shows the values obtained, together with the values of microindentation hardness measured from the prismatic samples prepared for DMTA studies.

From the mechanical point of view, it can be confirmed that the material derived from 6SH-SQ shows the highest stress at break, stiffness and microindentation hardness because of the multifunctionality and smaller size of the structure between thiol groups, leading to stiffer materials and a higher crosslinking density. The worst mechanical performance in the same terms (stress at break, stiffness and microindentation hardness) was obtained for the material prepared from the PETMP/3SH-EU formulation, which also presents higher ductility because of the smaller difference between Tg and measurement temperature (room temperature).

Table 6. Mechanical data of the materials obtained by dual curing by stress-strain at break and microindentation hardness testing. Coefficients of variation less than 8% for stress, strain and tensile modulus, and less than 5% for microindentation hardness

Sample	Strain at break (%)	Stress at break (MPa)	Tensile elastic modulus [a] (MPa)	Microindentation hardness [b] (HV)
2AG-EU/PETMP	20.5	11.7	315.9	7.6
2AG-EU /PETMP/3SH-EU	27.5	13.8	152.2	2.0
2AG-EU /6SH-SQ	3.7	39.1	1814.9	11.0

a. The tensile elastic modulus was determined as the slope of the curve at the initial and proportional part of the curve
b. Indentation test load of 10 g for 2AG-EU /PETMP/3SH-EU and 50 g for the others

Conclusions

The monomer 2AG-EU, derived from eugenol, has been synthesized by a three-step procedure that includes a first allylation of eugenol, a Claisen rearrangement a glycidation of the phenol obtained with epichlorohydrin in basic medium. The other eugenol derivatives, 3A-EU, with three allyl groups in the structure, and 3SH-EU, with three thiol groups were successfully prepared according to previous descriptions.

The photoinduced thiol-ene polymerization of 3A-EU with three different thiols was studied by photocalorimetry and FTIR spectroscopy. The curing was incomplete in all cases by the low reactivity of thiol and eugenol allyl derivatives, and in some cases, undesired side-reactions took place, leading to materials with low Tg and poor thermomechanical performance.

The curing of the allyl-glycidyl eugenol derivative, 2AG-EU, with different thiols by means of a combination of photoinduced thiol-ene and thermally-activated thiol-epoxy polymerization reactions was studied. Calorimetric and spectroscopic measurements showed, however, that the dual-curing procedure applied in this work did not have a clean sequential character, since the first thiol-ene process did not reach completion and photochemical and thermal process partially overlapped. This was rationalized in terms of the structure of the eugenol derivatives, which had a negative effect on the photochemical thiol-ene processes.

The dual-cured materials obtained from the eugenol derivative 2AG-EU had enhanced thermal and mechanical properties in comparison with those obtained from 3A-EU. A Tg of 57 °C (by DSC) and 76 °C (by DMTA) could be obtained for the material obtained from the combination of 2AG-EU with a hexathiol derived from squalene (6SH-SQ). This material also had higher stiffness, microindentation hardness and tensile strength values. In contrast, dual-cured materials obtained from the combination of 2AG-EU with the trithiol derived from eugenol, 3SH-EU, had a very low thermal and mechanical performance.

The contribution of thermal thiol-epoxy reactions to thiol-ene cured eugenol materials improves thermal and thermomechanical characteristics of the thermosets in comparison to purely photocrosslinked materials.

Acknowledgments

The authors would like to thank MINECO (MAT2014-53706-C03-01, MAT2014-53706-C03-02) and Generalitat de Catalunya (2014-SGR-67) for the financial support. Xavier F-F. Also acknowledges the Serra-Húnter programme (Generalitat de Catalunya).

References

[1] P.T. Anastas, J.C. Warner, *Green Chemistry: Theory and Practice*, Oxford University Press, New York, USA, 1998.

[2] M. Lancaster. *Green Chemistry: An Introductory Text*. RSC Publishing, 2nd edition, London, UK, 2010.

[3] S.K. Sharma, A. Mudhoo, *Green Chemistry for Environmental Sustainability,* CRC Press, Florida, USA, 2011.

[4] L. Montero de Espinosa, M.A.R. Meier. *European Polymer Journal*, 2011, 47, 837–852.

[5] S. Ma, T. Li, X. Liu, J. Zhu, *Polymer International*. 2016, 65, 164–173.

[6] C. Aouf, C. Le Guernevé, S. Caillol, H. Fulcrand, *Tetrahedron*, 2013, 69, 1345-1353.

[7] H. Nouailhas, C. Aouf, C. Le Guernevé, S. Caillol, B. Boutevin, H. Fulcrand. *Journal Polymer Science, Part A Polymer Chemistry*, 2011, 49, 2261–2270.

[8] F.I. Altuna. L.H. Espósito, R.A. Ruseckaite, P.M. Stefani. *Journal of Applied Polymer Science*, 2011, 120, 789–798.

[9] J. Zhu, K. Chandrashekhara, V. Flanigan, S. Kapila, *Journal of Applied Polymer Science*, 2004, 91, 3513–3518.

[10] B. Inna, K. Bretz, S. Kabasci, R. Kopitzky, *Chemical Engineering and Technology*, 2008, 31, 647–654.

[11] L. Deng, M. Shen, J. Yu, K. Wu, C. Ha, *Industrial and Engineering Chemistry Research*, 2012, 51, 8178-8184.

[12] K. Huang, J. Zhang, M. Li, J. Xia, Y. Zhou, *Industrial Crops and Products*, 2013, 49, 497-506.

[13] X. Liu, J. Zhang, *Polymer International*, 2010, 59, 607-609.

[14] K. Huang, P. Zhang, J. Zhang, S. Li, M. Li, J. Xia, Y. Zhou, *Green Chemistry*, 2013, 15, 2466-2475.

[15] C. Aouf, H. Nouailhas, M. Fache, S. Caillol, B. Boutevin, H. Fulcrand, *Polymer Journal*, 2013, 49, 1185-1195.

[16] C. Aouf, S. Benyahya, A. Esnouf, S. Caillol, B. Boutevin, H. Fulcrand, *European Polymer Journal*, 2014, 55, 186-198.

[17] S. Benyahya, C. Aouf, S. Caillol, B. Boutevin, J. P. Pascault, H. Fulcrand, *Industrial Crops and Products*, 2014, 53, 296-307.

[18] S. Ma, X. Liu, Y. Jiang, Z. Tang, C. Zhang, J. Zhu, *Green Chemistry*, 2013, 15, 245–254.

[19] F. Ferdosian, Z. Yuan, M. Anderson, C. Xu, *Thermochimica Acta*, 2015, 618, 48–55.

[20] M. Fache, A. Viola, R. Auvergne, B. Boutevin, S. Caillol, *European Polymer Journal*, 2015, 68, 526–535.

[21] M. Kathalewar, A. Sabnis, *Journal of Coatings Technology and Research*, 2014, 11, 601–618.

[22] J.-M. Raquez, M. Deléglise, M.-F. Lacrampe, P. Krawczak, *Progress in Polymer Science*, 2010, 35, 487–509.

[23] F. Hu, J.J. La Scala, J.M. Sadler, G.R. Palmese, *Macromolecules*, 2014, 47, 3332−3342.

[24] J. Qin, H. Liu, P. Zhang, M. Wolcott, J. Zhang, *Polymer International*, 2014, 63, 760–765.

[25] L. Rojo, B. Vazquez, J. Parra, A. López Bravo, S. Deb, J. San Roman, *Biomacromolecules*, 2006, 7, 2751-2761.

[26] P. Prakash, N. Gupta, *Indian Journal of Physiology and Pharmacology*, 2005, 49, 125–131.

[27] V.E. Tyler, L. R. Brady, J. E. Robbers, *Pharmacognosy*, Lea & Febiger, 7ª ed., Philadelphia, USA, 1976.

[28] B.R. Donovan, J.S. Cobb, E.F. T. Hoff, D.L. Patton, *RSC Advances*, 2014, 4, 61927–61935.

[29] T. Yoshimura, T. Shimasaki, N. Teramoto, M. Shibata, *European Polymer Journal*, 2015, 67, 397-408.

[30] P.T. Anastas, J.B. Zimmerman, *Environmental Science and Technology*, 2003, 37, 94A-101A.

[31] D. Guzmán, X. Ramis, X. Fernández-Francos, A. Serra, *RSC Advances*, 2015, 5, 101623–101633.

[32] D. Fourcade, B. S. Ritter, P. Walter, R. Schönfeld, R. Mülhaupt, *Green Chemistry*, 2013, 15, 910-918.

[33] R. Acosta Ortiz, E.A. Obregón Blandón, R. Guerrero Santos, *Green and Sustainable Chemistry*, 2012, 2, 62-70.

[34] D. Guzmán, B. Mateu, X. Fernández-Francos, X. Ramis, A. Serra, *Polymer International*, In press.

[35] S.P.S. Koo, M.M. Stamenovic, R.A. Prasath, A.J. Inglis, F.E. Du Prez, C. Barner-Kowollik, W Van Camp, T. Junkers, *Journal of Polymer Science Part A: Polymer Chemistry*, 2010, 48, 1699–1713.

[36] X. Fernández-Francos, A-O. Konuray, A. Belmonte, S. De la Flor, A. Serra, X. Ramis, *Polymer. Chemistry*, 2016, 7, 2280-2290.

[37] C. Acebo, X. Fernández-Francos, X. Ramis, A Serra, *Reactive and Functional Polymers*, 2016, 99, 17-25.

Supporting information

- Synthesis of the triallyl compound from eugenol (3A-EU)

Synthesis of 1-allyl-4-allyloxy-3-methoxybenzene (2A-EU)

16.4 g of eugenol (100 mmol) and 4.40 g of pulverized NaOH (110 mmol) were dissolved in 120 mL of dry DMF in a 500 mL three necked round bottomed flask under inert atmosphere. The mixture was stirred for 10 min and then allyl bromide (13.30 g, 110 mmol) was added dropwise over 1 h at 40 °C, once the addition was finished the solution was maintained at 40 °C for 3 h and then half an hour at 70 °C. The solvent was eliminated in the rotavap and the oil was dissolved in $CHCl_3$ and filtered to eliminate the precipitate of inorganic salts. The organic phase was washed twice with distilled water, dried over anhydrous $MgSO_4$ and the solvent eliminated to obtain 96% yield of 2A-EU as a yellowish oil. ^{1}H NMR ($CDCl_3$, δ in ppm): 6.7 d (Ar, 1H), 6.6 m (Ar, 2H), 6.1 m (-CH=,1H), 5.9 m (-CH=,1H), 5.3 dd (CH_2=, 1H), 5.2 dd (CH_2=, 1H), 5.0 m (CH_2=, 2H), 4.50 d (-CH_2-O-, 2H), 3.8 s (CH_3-O-, 3H) and 3.3 d (-CH_2-Ar, 2H). ^{13}C NMR ($CDCl_3$, δ in ppm): 149.2 (Ar), 146.2 (Ar), 137.8 (-CH=CH_2), 133.7 (-CH=CH_2), 133.0 (Ar), 120.2 (Ar), 118.0 (=CH_2), 115.8 (=CH_2), 113.5 (Ar), 112.0 (Ar), 70.0 (-CH_2-O), 56.0 (CH_3-O-) and 40.0 (-CH_2-). FT-IR (ATR): 3070, 3015, 2970, 2830, 1680, 1630, 1592, 1505, 1460, 1423, 1250, 1225, 1145, 1023, 997, 910, 850, 803 and 749 cm^{-1}.

Pyrolysis of 1-allyl-4-allyloxy-3-methoxybenzene (r2A-EU)

In a glass tube provided with a gas outlet 19.48 g (95.5 mmol) of 2A-EU were stirred at 200 °C for 3 h to obtain a 98% yield of a yellowish oil. ^{1}H NMR ($CDCl_3$, δ in ppm): 6.59 s (Ar, 2H), 5.91 m (-CH=, 2H), 5.6 s (-OH, 1H), 5.1 m (CH_2=, 4H), 3.9 s (CH_3-O-, 3H), 3.4 dd (-CH_2-Ar, 2H) and 3.3 dd (-CH_2-Ar, 2H). ^{13}C NMR ($CDCl_3$, δ in ppm): 146.4 (Ar), 141.6 (Ar), 138.0 (-CH=CH_2) 136.8 (-CH=CH_2, 131.1 (Ar), 125.5 (Ar), 122.0 (Ar), 115.5 (=CH_2), 115.4 (=CH_2), 108.9 (Ar), 56.0 (CH_3-O-), 40.0 (-CH_2-) and 34.0 (-CH_2-). FT-IR (ATR) 3540, 3075, 3012, 2970, 2900, 2845, 1630, 1605, 1442, 1498, 1293, 1227, 1205, 1146, 1070, 993, 910, 848 and 750 cm^{-1}.

Synthesis of 1,3-diallyl-4-allyloxy-5-methoxybenzene (3A-EU)

19.14 g of the previously obtained r2A-EU (94 mmol), 4.13 g (103 mmol) of pulverized NaOH and 120 mL of DMF were placed in a three necked round bottomed flask under inert atmosphere. The mixture was stirred for 10 min and then allyl bromide (12.49 g, 105 mmol) was added dropwise over 1 h at 40 °C. Once the addition was completed the mixture was kept at 40 °C for 3 h and then half an hour at 70 °C. The reaction product was treated with distilled water to dissolve the NaBr formed and extracted with chloroform. The organic phase was washed twice with distilled water, dried with anhydrous $MgSO_4$ and concentrated on a rotary evaporator to obtain 97% yield of 3A-EU as a yellowish oil. ^{1}H NMR ($CDCl_3$, δ in ppm): 6.7 s (Ar, 2H), 6.05 m (-CH=, 1H), 5.90 m (-CH=, 2H), 5.34 dd (CH_2=, 1H), 5.19 dd (CH_2=, 1H), 5.15-5.0 m (CH_2=, 4H), 4.46 d (-CH_2-O-, 2H), 3.87 s (CH_3-O-, 3H), 3.38 d (-CH_2-Ar, 2H), 3.31 d (-CH_2-Ar, 2H). ^{13}C NMR ($CDCl_3$, δ in ppm): 152.6 (Ar), 144.1 (Ar), 137.5 (-CH=CH_2), 137.3 (-CH=CH_2), 135.7 (Ar),

134.5 (Ar), 133.7 (-CH=CH_2), 121.7 (Ar), 117.0 (=CH_2), 115.8 (=CH_2), 115.5 (=CH_2), 110.5 (Ar), 73.7 (-CH_2-O-), 55.7 (CH_3-O-), 40.1 (-CH_2-) and 34.3 (-CH_2-). FT-IR (ATR) 3072, 3018, 2901, 2825, 1637, 1583, 1510, 1451, 1418, 1256, 1230, 1141, 1026, 986, 907, 804 and 752 cm^{-1}.

- Synthesis of the hexathiol derived from squalene (6SH-SQ)

Photochemical thiol-ene reaction (6STA-SQ)

A mixture of 5 g (12.2 mmol) of SQ, 11.1 g (146 mmol) of TAA and 0.062 g (0.24 mmol) of DMPA were photoirradiated with a UV lamp at 356 nm for 30 min. The product was dissolved in $CHCl_3$ and extracted with a 10% NaOH solution and then washed with water and dried over anhydrous $MgSO_4$. The solvent was removed on a rotary evaporator. A clear viscous liquid was obtained with 87% yield. ^{1}H NMR ($CDCl_3$, δ in ppm), 3.3 broad (CH-S, 6H), 2.3 s (CH_3-CO-, 18H), 1.1-2.0 broad (-CH2- and –CH-, 26H) and 0.8-0.9 broad (CH_3-, 24H). FT-IR (ATR): 2960, 2925, 1680, 1450, 1380, 1365, 1110, 1140, 950, 752 and 620 cm^{-1}.

Hydrolysis of 6STA-SQ (6SH-SQ)

9 g (10.4 mmol) of the 6STA-SQ were put in a round-bottomed flask with 60 mL of methanol and 1.8 g (45 mmol) of pulverized NaOH and vigorously stirred for 5.5 h at reflux temperature and inert atmosphere. The solution was allowed to cool and the solvent was removed. The product obtained was dissolved in water and acidified with 0.1 M HCl solution and then extracted with $CHCl_3$. The organic phase was washed with distilled water and dried over anhydrous $MgSO_4$. After solvent evaporation the purification of 6SH-SQ was carried out by silica gel column chromatography using hexane/ethyl acetate 8/2 mixture as eluent. The purified product was a pale yellow viscous liquid with a 71% yield. ^{1}H NMR ($CDCl_3$, δ in ppm), 2.60 broad (-CH-S-, 6H), 1.10-1.95 unresolved broad signals (-CH_2-, -CH- and -SH, 32H) and 0.8-1.05 broad (CH_3-, 24H). FT-IR (ATR): 2955, 2923, 2570, 1450, 1378, 1350 and 752 cm^{-1}. Spectra are fully coincident to those reported in the literature.[22]

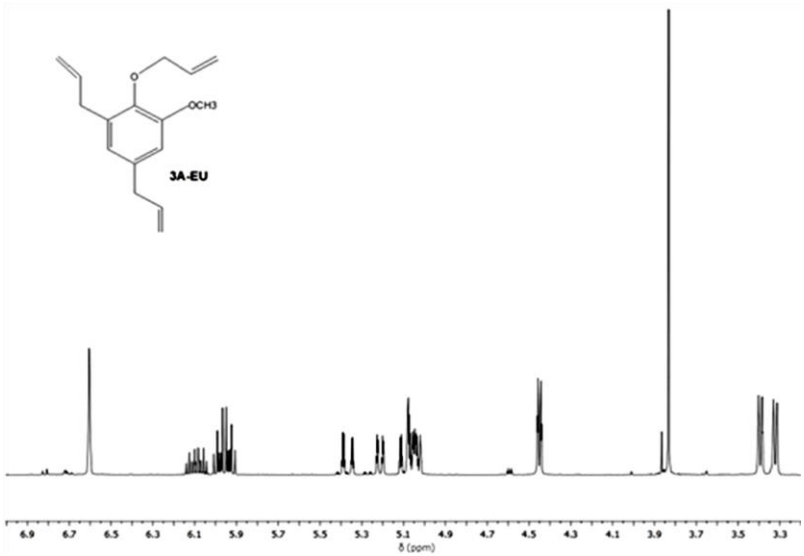

Figure A. ^{1}H NMR spectrum of the triallyl (3A-EU) derived from eugenol registered in $CDCl_3$

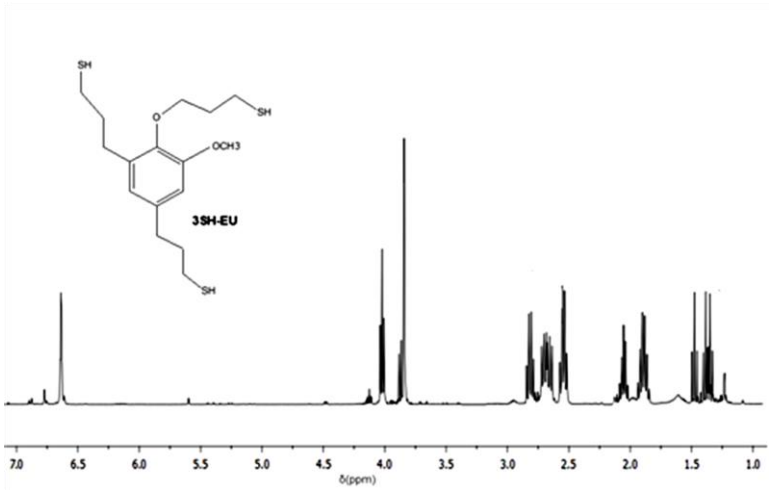

Figure B. ^{1}H NMR spectrum of the trithiol (3SH-EU) derived from eugenol registered in $CDCl_3$

UNIVERSITAT ROVIRA I VIRGILI
NUEVOS PROCESOS DE CURADO CLICK CON TIOLES Y SU APLICACIÓN A LA PREPARACIÓN DE MATERIALES BASADOS EN EUGENOL
Dailyn Guzmán Meneses

UNIVERSITAT ROVIRA I VIRGILI
NUEVOS PROCESOS DE CURADO CLICK CON TIOLES Y SU APLICACIÓN A LA PREPARACIÓN DE MATERIALES BASADOS EN EUGENOL
Dailyn Guzmán Meneses

UNIVERSITAT ROVIRA I VIRGILI
NUEVOS PROCESOS DE CURADO CLICK CON TIOLES Y SU APLICACIÓN A LA PREPARACIÓN DE MATERIALES BASADOS EN EUGENOL
Dailyn Guzmán Meneses

CAPÍTULO 8

Progress in Organic Coatings, enviado

Preparation of new biobased materials from a triglycidyl eugenol derivative through thiol-epoxy click reaction

Dailyn Guzmán, Xavier Ramis, Xavier Fernández-Francos, Silvia De la Flor, Angels Serra

UNIVERSITAT ROVIRA I VIRGILI
NUEVOS PROCESOS DE CURADO CLICK CON TIOLES Y SU APLICACIÓN A LA PREPARACIÓN DE MATERIALES BASADOS EN EUGENOL
Dailyn Guzmán Meneses

Preparation of new biobased materials from a triglycidyl eugenol derivative through thiol-epoxy click reaction

Abstract

A new triglycidyl eugenol derivative (3EPO-EU) was synthesized and characterized by spectroscopic techniques, and used as starting monomer in the preparation of novel bio-based thiol-epoxy thermosets. As thiols, commercially available tetrathiol derived from pentaerythritol (PETMP), a trithiol derived from eugenol (3SH-EU) and the hexathiol derived from squalene (6SH-SQ) were used in the presence of 4-(N,N-dimethylamino)pyridine as the basic catalyst. A flexible diglycidyl ether derived from hexanediol (2EPO-HEX) was also introduced in order to enhance conversion in formulations containing 6SH-SQ. The evolution of the curing was monitored by differential scanning calorimetry. The materials obtained are rigid at room temperature and showed Tgs up to 103 °C. The thermal stability, thermomechanical and mechanical properties were evaluated and discussed in terms of the structural characteristics of the resulting materials.

Keywords: Biopolymers, crosslinking, renewable resources, thermosets, structure-property relation.

Introduction

Epoxy thermosets have been extensively used due to their great number of advantages ranging from excellent thermal resistance, mechanical performance and chemical and environmental stability, among others.[1,2]

The most popular starting compound in the production of industrial epoxy resins is bisphenol A which is used in the preparation of coatings, adhesives, encapsulants, etc.[3,4] However, excessive exposure to this compound causes serious damage to health and a lot of research is currently done to find out more convenient alternatives.[5,6]

Nowadays, there is a great demand for products from renewable sources with the aim of reducing dependence on petrochemical compounds and finding safer alternatives to existing ones. In the last years, many investigations have been focused in the development of greener materials prepared from sustainable, friendly resources with safe behaviour from the point of view of health and environment.[7,8,9,10] In this respect, many studies have been performed in the preparation of epoxy thermosets from renewable sources with different structure,[11,12,13,14] but many of them from vegetable oils.[15,16,17,18]

Vegetable oils, although produced in huge quantities, cheap and easy to be transformed into pure epoxydated starting materials, have the drawback of their long aliphatic chains that leads to an excessive flexibility and too low Tg of the crosslinked materials, which limits their technological application.[18,19] For this reason, more rigid

structures such as phenols approaching the bisphenol A molecule could be interesting as a green alternative to prepare epoxy thermosets with improved characteristics.[20]

Eugenol (4-allyl-2-methoxyphenol) is a simple and aromatic compound, which is the main component (80-90%) of clove oil, the essential oil extracted of the clove plant (Eugenia caryophyllata). It has two functional groups, OH and allyl that can be further modified to form epoxy compounds with the adequate functionality and for this reason, it seems very attractive as starting material for the preparation of epoxy thermosets. This phenolic compound is a yellowish liquid-oil with its most important application in the medical field because it has great properties as analgesic, antibiotic, antiseptic, anti-oxidant, etc.[21,22,23,24] It has also been used in perfumery and in manufacturing stabilizers and antioxidants for the plastics industry. As a better advantage, it should be noted that it can be used in foods at low concentrations and therefore is safe as starting material for the preparation of green thermosets.[25]

Several authors reported on the preparation of epoxy thermosets starting from eugenol based structures. Wang et al.[26] prepared a new epoxy material with a bio-based content of 70.2%wt from an eugenol derivative cured by 4,4'-diamino diphenyl methane. The new material had a Tg of 114 °C, 40 °C lower than the DGEBA based material. Nevertheless, the new epoxy-eugenol material had higher Young´s modulus and hardness than DGEBA thermoset.

In another study,[27] eugenol was transformed into a diepoxyde and cured with methyl tetrahydrophthalic anhydride or with an anhydride derived from rosine (MPA) in the presence of an imidazole as the catalyst. The use of MPA as anhydride allowed to reach Tgs of 155 °C and the cured resins exhibited comparable performance to their petrochemical counterparts.

A highly stiff epoxy thermoset derived from eugenol with a triazine core structure and three epoxy groups per molecule was described in the literature.[28] This eugenol derivative was cured by using 3,3'-diamino diphenylsulfone. Compared with DGEBA materials cured under the same conditions, the new eugenol-based material led to improved thermomechanical properties (33 °C higher in Tg, 39% higher in Young's modulus and 55% improvement in hardness).

In a previous study of our group we put into evidence that thiol-epoxy reaction is highly advantageous in front of thiol-ene processes to obtain crosslinked materials from eugenol derivatives.[29] Yoshimura et al. proposed the preparation of networks from triallyl eugenol by thiol-ene processes but the maximum Tgs reached for the materials were not higher than 9.1 °C.[7] On substituting an allyl by a glycidyl group we increased the Tg in more than 25 °C by the higher efficiency of the thiol-epoxy process compared to the thiol-ene.

The present study proposes the preparation of a new eugenol epoxy compound with three glycidyl groups with a compact structure (3EPO-EU), which will later be cured

by a thiol-epoxy click reaction. According to our experience in thiol-epoxy curing systems a high functionality and rigid structures are needed to reach good thermomechanical characteristics.[30] As the thiol curing agent, we synthesized an eugenol derivative (3SH-EU) and we also prepared the hexathiol derived from squalene (6SH-SQ) previously reported.[31] We also selected as thiol the commercially available tetrathiol derived from renewable pentaerythritol (PETMP).[20] Scheme 1 represents the structure of the starting monomers used in this study.

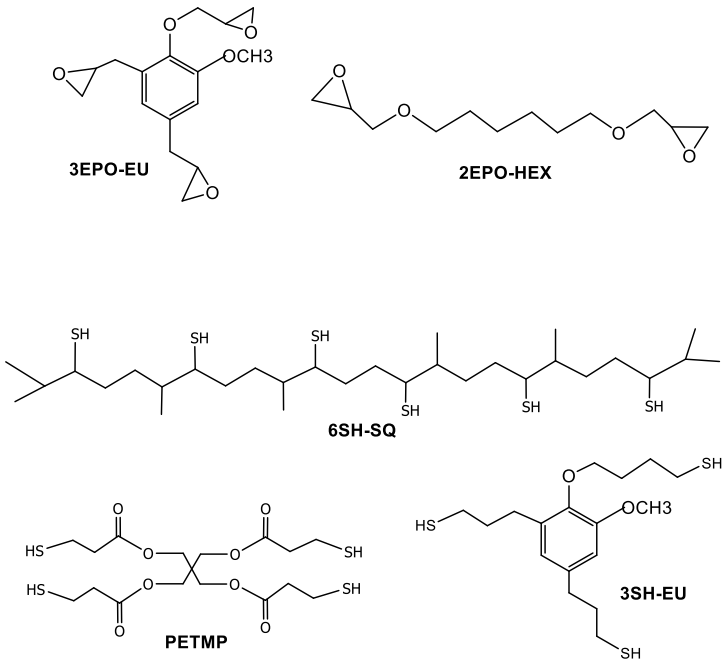

Scheme 1. Chemical structures of the monomers selected

Through thiol-epoxy curing process, fully bio-based epoxy thermosets with different characteristics have been obtained. It should be mentioned that, depending on the basic catalyst used, the latent character of thiol-epoxy curing allows the formulations to be maintained at room temperature during storage.[32] This fact, together with the easy control of the polymerization reaction, enhances the green character of this type of materials, due to the lower amount of waste material produced.

For the epoxidation of the compound derived from eugenol we followed the concept of green chemistry[33,34] and the epoxy compound was synthesized using the oxone methodology[35,36,37] instead of epoxidation by peracid (MCPBA),[38] because the former offers many advantages. Oxone is cheaper than MCPBA and the separation and purification processes are much easier and employs non-toxic organic compounds. MCPBA is non-stoichiometric and acts preferentially in chlorinated solvents. In addition, the thiols were also synthesized by a clean methodology, consisting in the

photoinitiated thiol-ene click addition of thioacetic acid to olefins in the absence of any solvent and further saponification by base.[31]

The study of the thermal curing of different thiol-epoxy formulations was performed by calorimetry and the materials prepared were characterized by thermogravimetry, thermomechanical analysis and mechanical tests. To improve the curing of some formulations and reach their complete curing, the addition of a linear renewable diglycidyl compound derived from 1,6-hexanediol (2EPO-HEX) was tested. This compound acts as flexible chain extender when the compactness of the monomers derived from eugenol and squalene limits the complete reaction that is caused by topological restrictions.

Experimental part

Materials

Eugenol (EU), allyl bromide, thioacetic acid (TAA), 2,2-dimethoxy-2-phenylacetophenone (DMPA), 4-(N,N-dimethylamino)pyridine (DMAP), pentaerytritol tetrakis (3-mercaptopropionate) (PETMP), squalene (SQ) and oxone (potassium peroxomonosulphate) were purchased from Sigma-Aldrich and were used without further purification. 1,6-hexanediol diglycidylether (2EPO-HEX from EPOTEC RD 107 Aditya Birla Chemicals, Thailand) was used as received. Benzyl triethyl ammonium chloride (TEBAC) was purchased from Alfa Aesar. Inorganic salts and bases were purchased from Scharlab. Methanol from Carlo Erba was used as received. Acetone, ethyl acetate and N,N-dimethylformamide (DMF) from VWR were purified by standard procedures.

Preparation of starting products

- *Synthesis of the diallyl and triallyl derivatives from eugenol (2A-EU, r2A-EU and 3A-EU)*

Diallyl and triallyl eugenol were prepared following a previously reported procedure.[7] The synthesis includes the allylation of eugenol in basic medium to obtain O-allyl eugenol (2A-EU) and then a Claisen rearrangement on heating to obtain 6-allyleugenol (r2A-UE). This product was allylated and the triallyl eugenol (3A-EU) was obtained (see Scheme 2). The spectra of these compounds were coincident with those reported.

- *Synthesis of triepoxy derivative from eugenol (3EPO-EU)*

In a 1000 mL three necked flask equipped with magnetic stirrer, thermometer and addition funnel, 1 g (4.1 mmol) of 3A-EU was dissolved into 120 mL of acetone and 100 mL of ethyl acetate. To this mixture, 0.2 g (0.8 mmol) of TEBAC, 43.0 g (511.8 mmol) of $NaHCO_3$ and 60 mL of water were added. The flask was cooled at 5 °C and then 56.7 g of oxone (equivalent to 93.0 mmol of $KHSO_5$) dissolved in 190 mL of H_2O were added

dropwise over 3 h at 5 °C under vigorous stirring. The mixture was kept at room temperature for 48 h. The organic layer was separated and washed with a solution of 20%wt NaCl in water. After drying with Mg_2SO_4, the solvent was eliminated at vacuum and the residue purified by silica gel chromatography (n-hexane/ethyl acetate (4:6), as eluent). The product 3EPO-EU was a viscous yellow liquid, 50% yield. 1H NMR ($CDCl_3$, δ in ppm), 6.72 m (Ar, 2H), 4.24 and 3.90 m (-CH_2-O-, 2H), 3.84 s (CH_3-O-, 3H), 3.34 m (CH of glycidyl ether, 1H), 3.18 and 3.4 m (CH of glycidyl groups attached to phenyl, 2H), 2.93-2.77 m (-CH_2- of oxirane rings, 6H) and 2.76, 2.68, 2.58 and 2.56 four dd (-CH_2- of glycidyl groups directly attached to Ph, 4H) (see Figure 1).^{13}C NMR ($CDCl_3$, δ in ppm): 32.6 (-CH_2-), 38.2 (-CH_2-), 44.1 (-CH2- oxirane), 46.5 (-CH_2- oxirane), 46.8 (-CH_2- oxirane), 50.3 (-CH- oxirane), 51.6 (-CH- oxirane), 52.1 (-CH- oxirane), 55.4 (-OCH_3), 73.5 (-CH_2-O-), 111.4 (C-3), 122.4 (C-5), 130.6 (C-6), 133.0 (C-4), 144.2 (C-1) and 152.0 (C-2) (see Figure 2). FT-IR (ATR): 3050, 2996, 2918, 2847, 1589, 1489, 1464, 1430, 1403, 1336, 1290, 1010, 968, 908, 831, 804, 754 cm^{-1}

- *Synthesis of trithiol compound from triallyl eugenol (3SH-EU)*

The synthesis was performed as previously reported by us.[29] The synthetic procedure starts from triallyleugenol (3A-EU) that was irradiated with thioacetic acid (TAA) in the presence of DMPA. The thioacetate was saponified with a methanol solution of NaOH.

- *Synthesis of hexathiol from squalene (6SH-SQ)*

The product was prepared following a two-step procedure previously reported, based on the photochemical thiol-ene of thioacetate on squalene in the presence of DMPA and saponification with methanolic NaOH.[31]

Preparation of the curing mixtures

Different formulations of the triepoxy derived from eugenol (3EPO-EU) with several thiols as PETMP, 3SH-EU and 6SH-SQ were prepared. The homogeneous mixtures were obtained by mixing with a spatula stoichiometric amounts of epoxy/SH groups (1:1), and adding 2 phr (2 parts per hundred of epoxy) of DMAP as basic catalyst. The formulations prepared were named as 3EPO-EU/PETMP, 3EPO-EU/3SH-EU and 3EPO-EU/6SH-SQ. A fourth mixture was prepared named as 3EPO-EU/6SH-SQ/2EPO-HEX which consist of a mixture of 80 %wt of 3EPO-EU and 20 %wt of 1,6-hexanediol diglycidyl ether (2EPO-HEX) with the stoichiometric amount of 6SH-SQ and 2 phr of DMAP. An equivalent formulation with 3SH-EU instead of 6SH-SQ, named as 3EPO-EU/3SH-EU/2EPO-HEX, was also tested but later discarded by its low properties.

Characterization techniques

^{1}H NMR and ^{13}C NMR spectra were registered in a Varian Gemini 400 spectrometer. $CDCl_3$ was used as the solvent. For internal calibration the solvent signal corresponding to $CDCl_3$ was used: δ (^{1}H) = 7.26 ppm, δ (^{13}C) = 77.16 ppm.

The study of the curing was performed by differential scanning calorimetry (DSC) in a Mettler DSC-821e calorimeter calibrated using an indium standard (heat flow calibration) and an indium-lead-zinc standard (temperature calibration). For dynamic studies, a flow of N_2 at 100mL/min was used and the weight of the samples for the analysis was 10 mg. The studies were performed in the temperature range of 30-250 °C, with a heating rate of 10 K/min.

The glass transition temperatures (Tgs) of the sample once cured were determined in dynamic scans at 20 °C/min from -20 °C to 100 °C. The Tgs of the final thermosets were evaluated after two consecutive heating dynamic scans at 20 °C/min starting at -20 °C in a Mettler DSC-822e device to delete the thermal history. The Tg value was taken as the middle point in the heat capacity step of the glass transition.

The thermal stability of cured samples was studied by thermogravimetric analysis (TGA), using a Mettler TGA/SDTA 851e thermobalance. All experiments were performed under inert atmosphere (N_2 at 100 mL/min). Pieces of the cured samples with an approximate mass of 8 mg were degraded between 30 and 600 °C at a heating rate of 10 K/min.

A Jasco FTIR spectrometer equipment (resolution of 4 cm^{-1}) with an attenuated-total-reflectance accessory with a diamond crystal (Golden Gate heated single-reflection diamond ATR, Specac-Teknokroma). All the measurements were performed at room temperature. IR was used to follow the diminution of thiol band at 2570 cm^{-1} and the evolution of the curing process of the different formulations. In this case, the spectra were collect before and after thermal process.

Dynamic mechanical thermal analyses (DMTA) were carried out with a TA Instruments DMA Q800 analyzer. The samples were isothermally cured in a mould at 80 °C for 1 h with a post curing at 120 °C for 30 min with the exception of 3EPO-EU/6SH-SQ and 3EPO-EU/6SH-SQ/2EPO-HEX which was cured at 100 °C for 1 h with a post curing at 140 °C for 1 h. Three point bending clamp was used on the prismatic rectangular samples (30 × 6.5 × 1.5 mm^3). The apparatus operated dynamically at 5 K/min from 30 to 170 °C for deleting the thermal history and then at 3 K/min from 30 to 170 °C at a frequency of 1 Hz with and oscillation amplitude of 10 µm.

Young's modulus was determined under flexural conditions at 30 °C, with the same clamp and geometry samples, applying a force ramp at constant load rate of 3 N/min, from 0.001 N to 18 N. Three samples of each material were analyzed and the results were averaged. Stress-strain at break tests were performed with the film-tension clamp in force controlled mode. Dogbone samples were used at a force rate of 1 N/min and the averaged value of at least three different samples were reported.

Microindentation hardness was measured with a Wilson Wolpert 401 MAV device following the ASTM E384-16 standard procedure. For each material at least 10

determinations were made with a confidence level of 95%. The Vickers hardness number *(HV)* was calculated from the following equation:

$$HV = \frac{1.8544 \cdot F}{d^2}$$

Where, *F* is the load applied to the indenter in kgf (0.025 kgf) and d is the arithmetic mean of the length of the two diagonals of the surface area of the indentation measured after load removal in mm.

Results and discussion

Synthesis and characterization of the starting monomers

The synthesis of the triepoxy derivative of eugenol was addressed by different synthetic procedures, all of them starting from diallyl phenol (r2A-EU), which was synthesized following a previous paper,[7] as represented in Scheme 2. The first step consists in the allylation of eugenol and the second is a pericyclic Claisen rearrangement at 200ºC with practically quantitative yields. These products showed a high purity by NMR spectroscopy and no further purification was required.

The first synthetic methodology selected for the preparation of the triglycidyl derivative from r2A-EU was the one inspired in the synthesis of eugenol epoxy resins proposed by Qin et al.[27] These authors started from eugenol, which was acetylated, and then the allyl group epoxidated with m-chloroperbenzoic. The product obtained was finally reacted with epichlorohydrin in the presence of NaOH and the substitution of acetyl group by glycidyl was accomplished with about 60% yield. Although both synthetic steps, epoxidation and glycidation, were well-established procedures, the application of this methodology to the dially derivative (r2A-EU) did not produced the desired 3EPO-EU, but a complex mixture of compounds. The presence of a glycidyl group in ortho position to the phenol group, which is the only difference in comparison to the synthesis proposed by Qin,[27] could be the responsible of the unexpected side-reactions. Since NaOH catalyses the reaction of the acetate with EPC, the alkoxides formed could attack intramolecularly the epoxy in this ortho position or even could lead to oligomeric products by intermolecular attack. As an alternative, we proposed another general synthetic pathway, which is represented in Scheme 2.

This procedure goes through the formation of the triallyl derivative of eugenol, following the methodology proposed by Yoshimura et al.[7] This methodology allowed the preparation of 3A-EU with excellent yield and purity. ^{1}H and ^{13}C NMR spectra of the di- and triallylic compounds prepared were coincident with those reported in the literature.[7]

The last step in the synthetic procedure was the epoxidation of 3A-EU. The first epoxidation methodology attempted was the classical epoxidation with peracid (MCPBA). The application of this method did not produce the triepoxy compound in

good yield but only in small quantity, although a great excess of peracid (9:1 mol/mol) was added and the reaction time was extended for as long as 10 days. In view of these results, the oxone method[35,36] was tested. This method can be considered as more environmentally friendly than epoxidation with MCPBA, especially when it was performed in a two-phase system (ethyl acetate/water) using benzyl triethyl ammonium chloride as the phase transfer catalyst (PTC). In these conditions acetone and the formed dimethyldioxirane, which is the true epoxidation agent, are more soluble in the organic phase, which contains the triallyl eugenol derivative, and this method was described to lead to the highest yield of epoxy compound.[35] By this methodology, we obtained the pure triglycidyl derivative of eugenol (3EPO-EU) in a 50% of yield after purification by column chromatography.

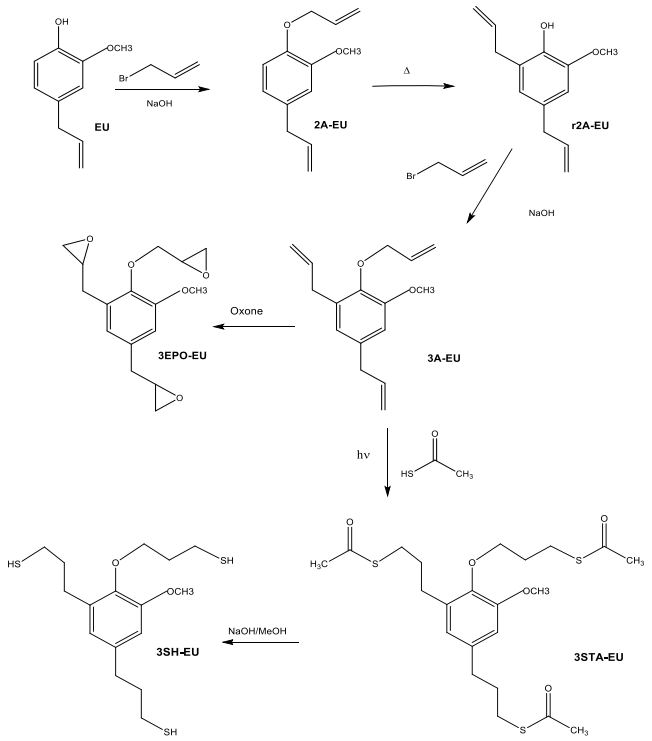

Scheme 2. Synthetic pathway for the synthesis of the triglycidyl derivative of eugenol (3EPO-EU) and trithiol (3SH-EU)

Aouf et al.[39] prepared a tetraglycidyl derivative of gallic acid by allylation and further epoxidation. They also proved the advantages of using the oxone method in front of the epoxidation with m-chloroperbenzoic acid, since a great proportion of peracid was required to get an only moderate yield of the desired epoxy compound. The epoxidated eugenol derivative prepared was characterized by NMR spectroscopy and Figure 1 presents its ^{1}H NMR spectrum.

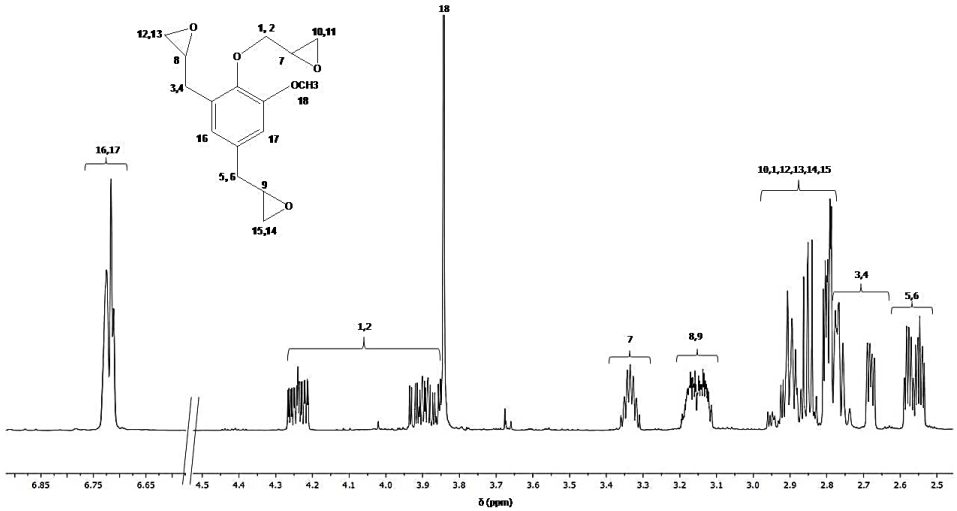

Figure 1. ^{1}H NMR spectrum of 3EPO-EU in $CDCl_3$

As we can see, the spectrum is rather complex because of the presence of three different glycidyl groups, two of them directly attached to the aromatic ring, but with different electronic environments and the other, more deshielded because of its attachment to the oxygen atom. Each glycidyl group presents five unequivalent protons due to the presence of the asymmetric carbon that leads to the methylene protons to be diastereotopic among them. Therefore, five different signals are expected for each glycidyl group with a complex coupling pattern. The integration of the signals and the chemical shifts support the structure for 3EPO-EU. Moreover, the purity of the product is put in evidence.

Figure 2 shows the ^{13}C NMR spectrum of the epoxy derivative with the corresponding assignments, which were mainly done by comparison with similar structures.[7] The spectrum also shows a great number of signals, because of the total absence of symmetry.

The triallyl derivative of eugenol (3A-EU) was also the starting material for the synthesis of the trithiol derived from eugenol (3SH-EU), which was prepared by a two-step synthetic procedure as represented in Scheme 2. This consist in a first photochemical thiol-ene reaction followed by the saponification of the thioester formed. This compound was described in a previous publication.[29] The viscous liquid product was obtained with high yield and purity and its structure confirmed by spectroscopic measurements. The hexathiol derived from squalene (6SH-SQ) was prepared by the same synthetic methodology (thiol-ene/saponification) as reported before.[31,29]

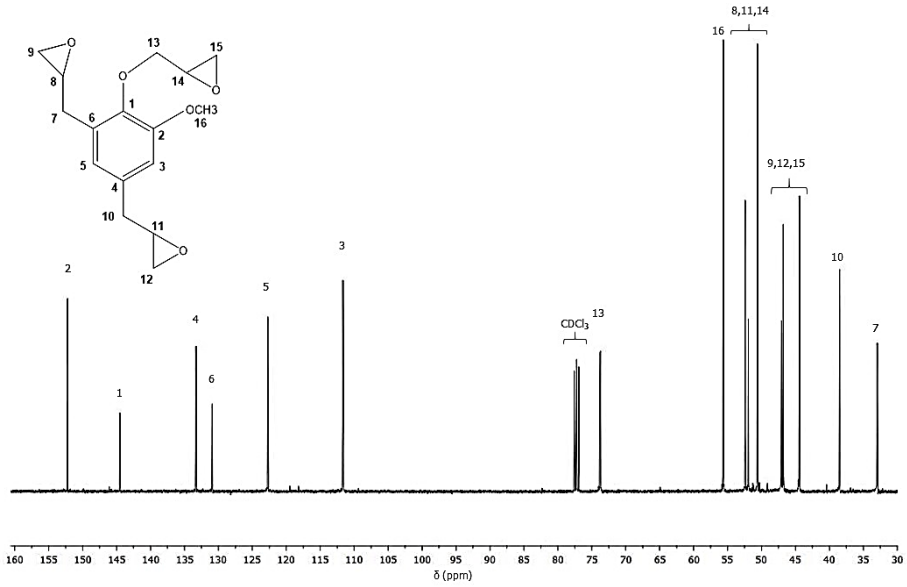

Figure 2. ^{13}C NMR spectrum of 3EPO-EU in $CDCl_3$

Calorimetric study of the curing process

Calorimetric studies were performed to see the evolution of the curing process for the different mixtures studied. In a first study, stoichiometric mixtures of 3EPO-EU with three thiols (PETMP, 3SH-EU and 6SH-SQ) and 2 phr of DMAP were cured at 10 °C/min in the calorimeter. The resulting curves are collected in Figure 3.

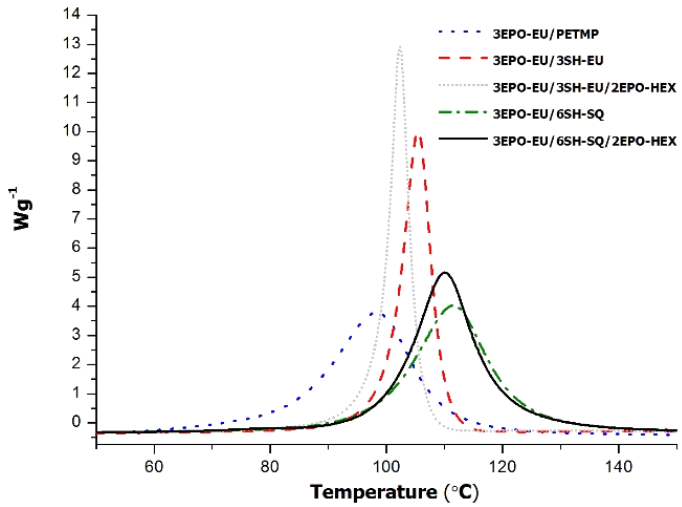

Figure 3. DSC thermograms corresponding to the dynamic curing at 10 °C/min of the mixtures eugenol resin/thiols and with a proportion of 2 phr of the DMAP

As we can see, the mixture containing PETMP begins to react at lower temperatures, indicating its higher reactivity, whereas the thiol derived from squalene is the one that reacts at the highest temperature. The main data obtained from the calorimetric study are collected in Table 1.

Table1. Calorimetric data of the mixture epoxy with thiols using a proportion of DMAP as catalyst

Sample	ΔH^a (J/g)	ΔH^b (kJ/ee)	Tg^c (◦C)
3EPO-EU/ PETMP	518.7	115.0	60
3EPO/3SH-EU	439.9	94.1	70
3EPO/6SH-SQ	333.7	69.9	103
3EPO/3SH-EU/2EPO-HEX	443.8	96.6	47
3EPO/6SH-SQ/2EPO-HEX	430.0	90.0	87

a. Enthalpy evolved by gram of sample in a dynamic curing
b. Enthalpy by equivalent epoxy of sample in a dynamic curing
c. Glass transition temperature of the material after thermal curing

The degree of curing achieved for the formulation is mainly related to the enthalpy released by epoxy equivalent. From these values, it is inferred that 6SH-SQ reacts only partially, since the enthalpy released is about 70 kJ/ee, much less than the one obtained from the curing of 3EPO-EU/PETMP formulations. Also in the case of using 3SH-EU as the thiol, the enthalpy evolved was a little lower than expected. According to that, we investigated if a higher degree of curing could be achieved, by adding a linear flexible diepoxy compound to the formulation to reduce steric and topological restrictions in the network formation. 1,6-Hexanediol diglycidylether (2EPO-HEX) was selected as reactive diluent, since this compound is a derivative of adipic acid, which is a natural product. A 20%wt of 2EPO-HEX and an 80% of 3EPO-EU were mixed and the stoichiometric amount of the selected thiol was added. The curves for 3EPO-EU/3SH-EU/2EPO-HEX and 3EPO-EU/6SH-SQ/2EPO-HEX are also included in Figure 3 and the main data collected in Table 1. As we can see, the curing exotherms are slightly shifted to lower temperatures by adding 2EPO-HEX to the formulation and the reaction occurs more quickly. The curing enthalpies increased but only a little in case of mixtures with 3SH-EU.

To confirm that the curing process has been completed, FTIR-ATR spectra were registered. Figure 4 shows, as an example, the most significant regions of the spectra before and after curing of the formulation cured with 3SH-EU.

The initial spectrum shows the typical absorptions of S-H st. at 2570 cm^{-1} and the band at 908 and 831 cm^{-1} corresponding to the epoxy ring. Both absorptions have disappeared completely in the spectrum of the cured material, whereas a new broad absorption at 3500 cm^{-1} appears due to the formation of the β-hydroxy thioether group in the network structure. The small size of the thiol absorption and the partial overlapping of epoxide band with others in the region make difficult the monitoring of the evolution of the curing process.

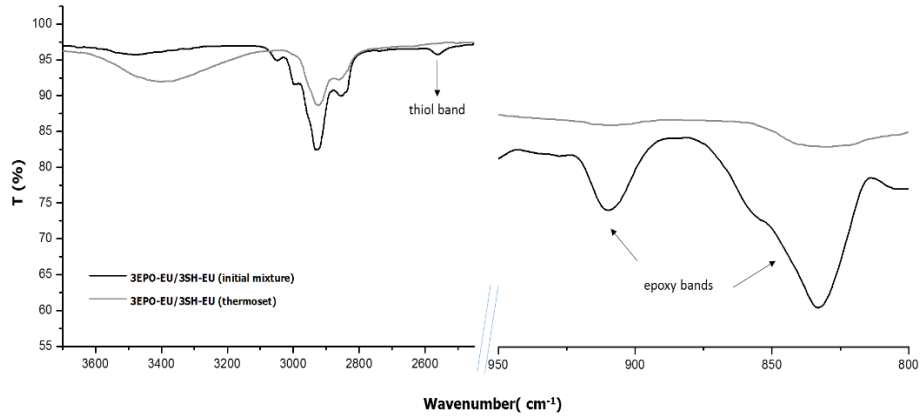

Figure 4. FTIR spectra of a mixture 3EPO-EU/3SH-EU catalyzed by 2 phr of DMAP before and after curing

Characterization of the materials

The Tg of the materials after dynamic curing were determined by DSC and the values are included in Table 1. We can comment that although the 3EPO-EU/6SH-SQ mixture was not completely reacted, the Tg of the material obtained is higher than 100 °C due to the multifunctionality of the thiol and is also much higher than the materials obtained from PETMP and 3SH-EU as the thiols. In a previous study on the curing of cycloaliphatic epoxy resins with several thiols, a Tg of 116 °C was reached when using 6SH-SQ as the thiol, which was also much higher than in similar materials prepared from PETMP or 3SH-EU. Despite of the flexible aliphatic structure of the squalene derivative, the high functionality and short distance between reactive groups leads to materials with a tightly crosslinked network structure.

We can also observe that the addition of 2EPO-HEX to the reactive mixture reduces notably the Tg and therefore, an increase in its proportion in the formulation, although possibly beneficial from the point of view of the degree of curing attained, is detrimental for this characteristic. The low Tg of the material derived from 3EPO-EU/3SH-EU/2EPO-HEX led us to discard this material for the following characterization studies.

In a previous study,[29] triallyl eugenol (3A-EU) was photocured through thiol-ene reaction with the same thiols selected in the present study and the Tgs of the materials obtained were very low, between 1 and 14 °C. In the same study, the combination of thiol-ene and thiol-epoxy reaction of the diallyl glycidyl eugenol with the same tiols allowed to increase the Tgs up to 28-57 °C, which was attributed to the better behavior of thiol-epoxy processes. In the present study, in which the thiol-ene reaction has been changed to thiol-epoxy, higher Tgs have been reached, confirming that thiol-ene

processes in eugenol derivatives had not the expected click characteristics than thiol-epoxy reaction has. Thiol-ene is accompanied by side-reactions like radical-radical coupling that limits the achievement of high crosslinking densities.

The materials prepared were characterized by thermogravimetry to investigate their stability at high temperatures. Figure 5 shows the weight loss curves against temperature in inert atmosphere and Table 2 collects the main data obtained from these studies.

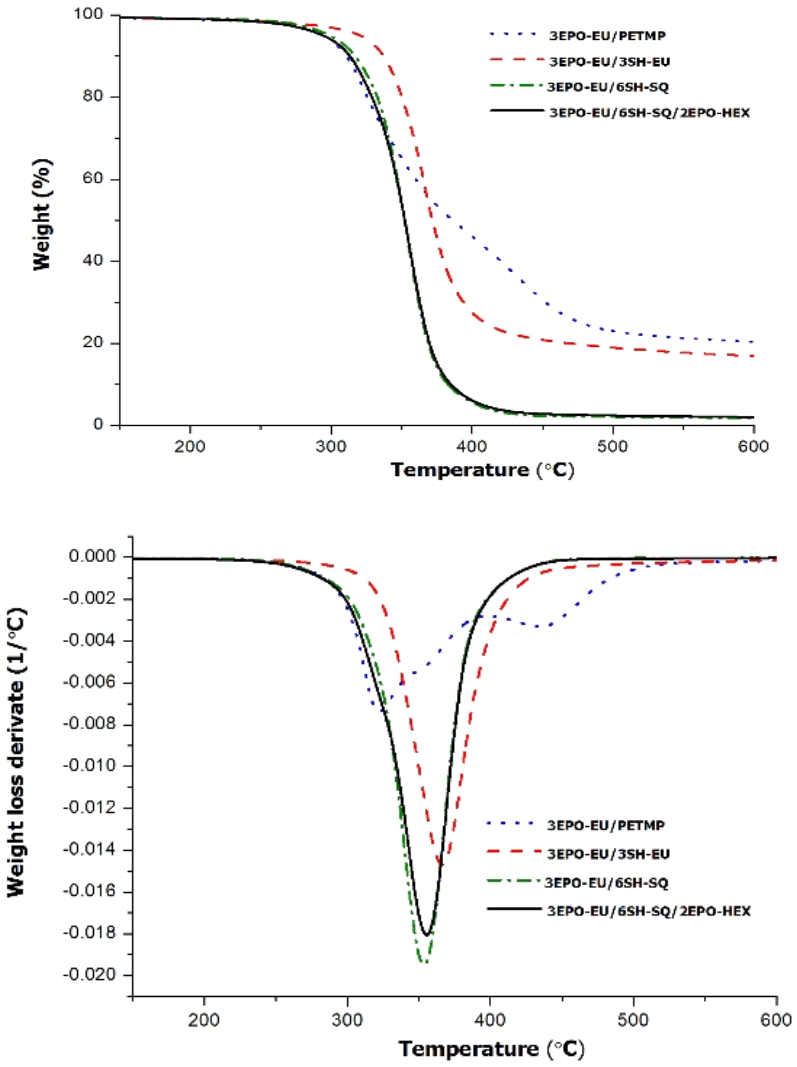

Figure 5. TGA curves under N_2 atmosphere at 10 K/min of the materials obtained from triglycidyl eugenol with different formulations

Table 2. Thermal and thermomechanical data of the materials obtained from the different formulations selected

Sample	$T_{5\%}$[a] (°C)	T_{max}[b] (°C)	Residue[c] (%)	$T_{tan\delta}$[d] (°C)	E_r[e] (MPa)	E^f (MPa)
3EPO-EU/PETMP	295	322	20	76	23.5	1014
3EPO-EU/3SH-EU	320	366	22	86	25.4	1526
3EPO-EU/6SH-SQ	299	353	2	108	28.5	1619
3EPO-EU/6SH-SQ/2EPO-HEX	295	355	2	98	18.6	1187

a. Temperature of 5% of weight loss in N_2 atmosphere
b. Temperature of the maximum rate of degradation in N_2 atmosphere
c. Yield chart after degradation in N_2 atmosphere
d. Temperature of maximum of tan δ determined by DMTA
e. Storage modulus in the rubbery state determined at tan δ + 50 °C
f. Young's modulus at 30 °C under flexural conditions

From the values of temperatures of initial weight loss (5%) and the temperature of maximum degradation rate, we can see that the material with a lower thermal stability is the one obtained from PETMP, probably due to the presence of ester groups that can break by pyrolytic β-elimination processes. It has been reported that ester groups begins to degrade at temperatures above 250 °C but weight loss is influenced by the global network structure.[40] According to that, the degradation curve and specially the derivative curve of this material show a more complex degradation pattern. The material obtained from 3EPO-EU/3SH-EU formulation presents the highest initial degradation temperature and seems to have the simplest degradation mechanism. This can be explained because of its aromatic character. In contrast, in the previously studied thiol-ene formulations,[29] the use of 3SH-EU as thiol led to materials with the worst characteristics. Its eugenol-derived structure can justify the occurrence of side-reactions in the thiol-ene crosslinking, limiting the effectiveness of the process and preventing the formation of highly dense crosslinked structures.

The thermomechanical characteristics of the thermosets prepared were studied by DMTA and Table 2 collects the most significant data extracted. The temperature of the maximum of the relaxation shows values according to the Tg determined by DSC but a little higher, as expected from this technique. Figure 6 shows the tan δ evolution against temperature. The materials obtained from PETMP and 3SH-EU show high and quite narrow curves, which are an indication of homogeneous materials, with the relaxation taking place at moderate temperatures. The materials prepared from 6SH-SQ show a broader relaxation curve at higher temperature evidencing the formation of a more heterogeneous network structure, typical of more densely crosslinked materials. This difference can be explained by the multifunctionality of the hexathiol and the difficulty of all groups to react. The relaxation of the network occurs at lower temperature and in a narrower range on adding 2EPO-HEX to the formulation, due to the flexibilizing effect of 2EPO-HEX, as expected.

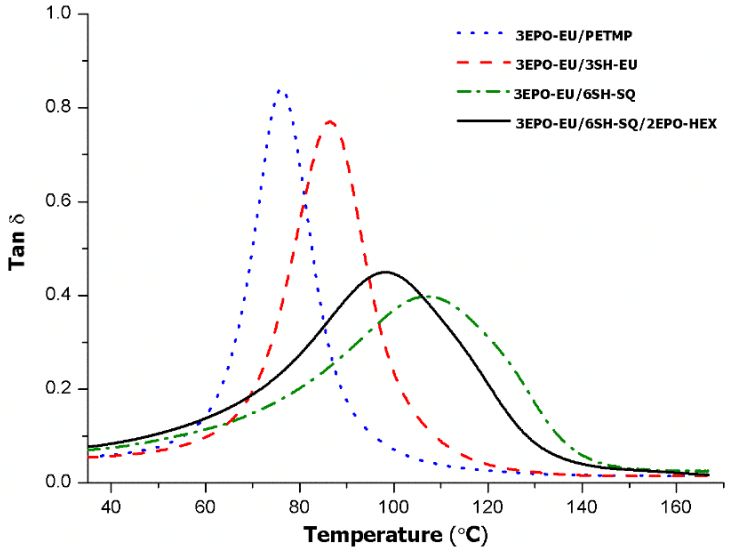

Figure 6. Plot of tan δ against temperature for the different materials prepared

The dependence of the storage modulus against temperature is represented in Figure 7 for all the materials and the main values are listed in Table 2.

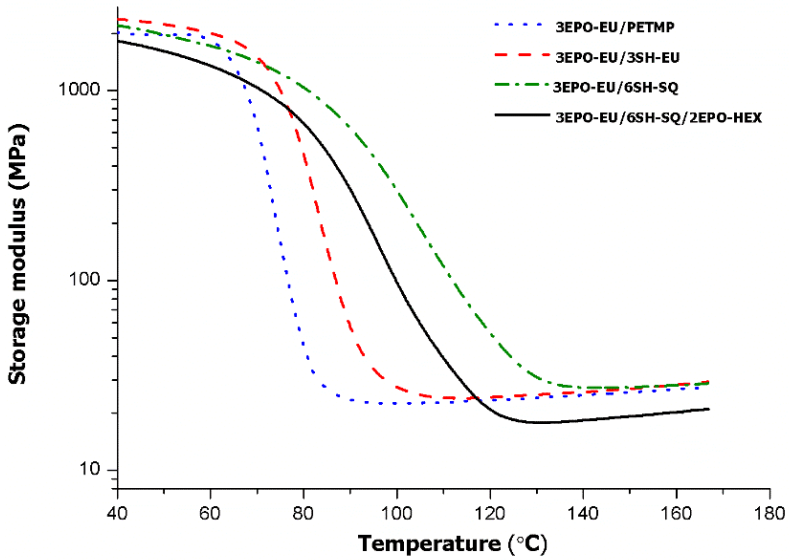

Figure 7. Plot of storage modulus against temperature for the different materials prepared

From the values of the table, we can see that the Young's moduli of the materials at 30 °C, determined under flexural conditions, are higher when the thiol with the highest functionality (6SH-SQ) was used, although quite similar to the value of the material prepared from the thiol with aromatic structure (3SH-EU). The addition of the

flexible diglycidyl compound to the formulation with 6SH-SQ leads to a reduction in the modulus, as expected. The moduli in the rubbery region also present similar tendencies, but it decreases notably on adding the linear diglycidyl ether to the formulation.

Dogbone samples of the different materials were prepared and studied with the tension clamp in the DMTA to obtain the stress-strain relationships. Table 3 shows the values obtained by this technique together with the values of microindentation hardness measured.

Table 3. Mechanical data of the materials obtained by dual curing by stress-strain at break and microindentation hardness testing. Coefficients of variation less than 8% for stress and strain, and less than 5% for microindentation hardness

Sample	Strain at break (%)	Stress at break (MPa)	Microindentation hardness[a] (HV)
3EPO-EU/PETMP	3.0	27.2	12.8
3EPO-EU/3SH-EU	2.2	30.1	14.1
3EPO-EU/6SH-SQ	2.3	50.4	20.3
3EPO-EU/6SH-SQ/2EPO-HEX	4.1	48.5	18.4

a. Coefficient of variation less than 8% for3EPO-EU/6SH-SQ/2EPO-HEX

Results from microindentation hardness are in accordance with the tensile behaviour and their results presented in Table 3. From the values of the table, we can state that the material obtained from 6SH-SQ alone shows low strain at break and the highest stress at break and elastic stiffness, due to the multifunctionality of the thiol and to the smaller size of the structural unit between crosslinks. In addition, the value of microindentation hardness in this material is higher than that determined for the materials obtained from other thiols. The addition of the reactive diluent to the formulation slightly reduces the stress at break but reduces the elastic stiffness and clearly enhances the strain at break, due to the flexibility introduced by the 2EPO-HEX structure, making it a more ductile material. May seem quite unexpected the slight decrease in microindentation hardness on adding this modifier, but this result is in accordance with the similar yield behaviour of both materials. It is also worth noting that microindentation hardness values for the sample 3EPO-EU/6SH-SQ/2EPO-HEX were more difficult to obtain due to their higher ductile nature, hence the higher deviation in the results. A partial plastic deformation occurred in some parts of the indentation mark, which allowed some elastic recovery to take place along the sides, causing the face of the mark to curve inwards and form a star-shaped indentation. However, as the elastic recovery in the direction of the diagonals is very small (because of intense stress concentration) the measurement of diagonal lengths gives valid hardness values but with greater deviation.

Finally, the material prepared from PETMP shows the lower mechanical performance of all the thermosets prepared in terms of stress at break and Young's modulus (see Table 2). Because this product is commercially available, the material

obtained could have broad application where the mechanical requirements were not so high.

The materials prepared from 3EPO-EU by the thiol-epoxy crosslinking process shows better mechanical performance than similar materials obtained by thiol-ene or dual thiol-ene/thiol-epoxy processes.[29] This confirms the goodness of the thermal thiol-epoxy reaction in front of the radical thiol-ene process, when applied to eugenol derivatives.

Conclusions

A triepoxy compound derived from eugenol has been obtained by a four step procedure that included allylation, Claisen rearrangement and epoxidation by oxone. The structure and purity of this compound was confirmed by ^{1}H and ^{13}C NMR spectroscopy.

The curing of this compound was performed by thiol-epoxy click reaction using three different thiols derived from renewable resources in the presence of a base as catalyst. When the hexathiol derived from squalene was used, an uncomplete reaction was detected. The addition of a reactive diluent as 1,6-hexanediol diglycidylether allowed a higher curing degree to be attained because of the reduction of steric and topological constrains.

The thermosets obtained showed Tg values higher than room temperature, and the maximum value was reached in case of the material obtained from the squalene thiol derivative, with a Tg higher than 100 °C. This material also displayed a good mechanical performance, with the highest Young's modulus and stress at break. The addition of the diglycidylic flexible derivative, 2EP-HEX, reduced the Tg value and the Young modulus, but does not affect much to the stress at break and microhardness.

The thermomechanical data displayed by the thermosets prepared confirms the goodness of the thiol-epoxy process in the preparation of thermosets from eugenol and the possibility of preparation of fully bio-based thermosets with good characteristics. These characteristics also show the adequacy of the triglycidyl eugenol derivative as epoxy monomer for the preparation of biobased thermosets. The adequate selection of the structure of thiols and epoxy monomers allows preparing biobased materials with tuned properties.

Acknowledgments

The authors would like to thank MINECO (MAT2014-53706-C03-01, MAT2014-53706-C03-02) and Generalitat de Catalunya (2014-SGR-67) for the financial support. Xavier F-F. acknowledges the Serra-Húnter programme (Generalitat de Catalunya).

References

[1] C.A. May. Ed, *Epoxy resins. Chemistry and Technology*, Marcel Dekker,USA, New York, 1988.

[2] J. H. Hodgkin, G. P. Simon, R. J. Varley, *Polymers Advances Technologies*, 1998, 9, 3-10.

[3] I. Hamerton, *Recent Developments in Epoxy Resins*, in Rapra Review Reports, Rapra Technology Limited, Shrewsbury, UK, 1996.

[4] E. Petrie, *Epoxy Adhesive Formulations*, McGraw-Hill, New York, USA, 2006.

[5] Material safety data sheet-Canada colors and chemicals limited, *http://doc.ccc-group.com/msds/english/236407.pdf*. Accessed in May. 15th 2017

[6] F. Ng, G. Couture, C. Philippe, B. Boutevin, S. Caillol, *Molecules*, 2017, 22, 149.

[7] T. Yoshimura, T. Shimasaki, N. Teramoto, M. Shibata, *European Polymer Journal*, 2015, 67, 397-408.

[8] S. Benyahya, C. Aouf, S. Caillol, B. Boutevin, J. P. Pascault, H. Fulcrand, *Industrial Crops and Products*, 2014, 53, 296-307.

[9] I. Bechtold, K. H. Bretz, S. Kabasci, R. Kopitzky and A. Springer, *Chemical Engineering & Technology*, 2008, 31, 647-654.

[10] M. Fache, B. Boutevin, S. Caillol, *Sustainable Chemistry and Engineering*, 2016, 4, 35-46.

[11] S. Ma, X. Liu, Y. Jiang, Z. Tang, C. Zhang, J. Zhu, *Green Chemistry*, 2013, 15, 245-254.

[12] M. Fache, A. Viola, R. Auvergne, B. Boutevin, S. Caillol, *European Polymer Journal*, 2015, 68, 526-535.

[13] R. Auvergne, S. Caillol, G. David, B. Boutevin, J. P. Pascault, *Chemical Reviews*, 2014, 114, 1082-1115.

[14] F. Hu, J. J. La Scala, J. M. Sadler, G. R. Palmese, *Macromolecules*, 2014, 47, 3332-3342.

[15] M. Stemmelen, V. Lapinte, J.P. Habas, J.J. Robin, *European Polymer Journal*, 2015, 68, 536-545.

[16] F. L. Jin, S.J. Park, *Polymer International*, 2008, 57, 577-583.

[17] M.A.R. Meier, J.O. Metzger, U.S. Schubert, *Chemical Society Reviews*, 2007, 36, 1788-1802.

[18] A. Llevot, *Journal of the American Oil Chemists' Society*, 2017, 94, 169-186.

[19] S. G. Tan, W. S. Chow, *Polymer-Plastics Technology and Engineering*, 2010, 49, 1581-1590.

[20] D. Fourcade, B.S. Ritter, P. Walter, R. Schönfeld, R. Mülhaupt, *Green Chemistry*, 2013, 15, 910-918.

[21] K. Pramod, S.H. Ansari, J. Ali, *Natural Product Communications*, 2010, 5, 1999-2006.

[22] E. Nagababu, J.M. Rifkind, S. Boindala, L. Nakka, *Methods in Molecular Biology*, 2010, 610, 165-180.

[23] S.F. Hamed, Z. Sadek and A. Edris, *Journal of Oleo Science*, 2012, 61, 641-648.

[24] T. F. Bachiega, J.P. Barreto de Sousa, J. K. Bastos, J. M. Sforcin, *Journal of Pharmacy and Pharmacology*, 2012, 64, 610-616.

[25] H. Nam, M.M. Kim, *Food and Chemical Toxicology*, 2013, 55, 106-112.

[26] J. Wan, B. Gan, C. Li, J. Molina-Aldareguia, E.N. Kalali, X. Wang, D. Y. Wang, *Chemical Engineering Journal*, 2016, 284, 1080-1093.

[27] J. Qin, H. Liu, P. Zhang, M. Wolcott, J. Zhang, *Polymer International*, 2014, 63, 760-765.

[28] J. Wan, J. Zhao, B. Gan, C. Li, J. Molina Aldareguia, Y. Zhao, Y.-T. Pan, D. Y. Wang, *ACS Sustainable Chemistry and Engineering*, 2016, 4, 2869-2880.

[29] D. Guzmán, X. Ramis, X. Fernández-Francos, S. De la Flor, A. Serra, *European Polymer Journal*, Send to revision.

[30] D. Guzmán, X. Fernández-Francos, X. Ramis, A. Serra, *Polymers*, 2015, 7, 680-694.

[31] R. Acosta Ortiz, E. A. Obregón Blandón, R. Guerrero Santos, *Green and Sustainable Chemistry*, 2012, 2, 62-70.

[32] D. Guzmán, X. Ramis, X. Fernández-Francos, A. Serra, *European Polymer Journal*, 2014, 59, 377-386.

[33] S.K. Sharma, A. Mudhoo, *Green Chemistry for Environmental Sustainability*, CRC press, Florida, USA, 2011.

[34] M. Lancaster, *Green Chemistry: An Introductory Text*, RSC publishing, 2nd ed, London, UK, 2010.

[35] N. Hashimoto and A. Kanda, *Organic Process Research and Development*, 2002, 6, 405-406.

[36] S. E. Denmark, D. C. Forbes, D. S. Hays, J. S. DePue, R. G. Wilde, *The Journal of Organic Chemistry*, 1995, 60, 1391-1407.

[37] R. Curci, M. Fiorentino, L. Troisi, *The Journal of Organic Chemistry*, 1980, 45, 4758-4760.

[38] K.A. JØrgensen*, Chemical Reviews*, 1989, 89, 431-458.

[39] C. Aouf, H. Nouailhas, M. Fache, S. Caillol, B. Boutevin, H. Fulcrand, *European Polymer Journal*, 2013, 49, 1185-1195.

[40] M. Arasa, X. Ramis, J.M. Salla, A. Mantecón, A. Serra, *Polymer Degradation and Stability,* 2007, 92, 2214-2222.

UNIVERSITAT ROVIRA I VIRGILI
NUEVOS PROCESOS DE CURADO CLICK CON TIOLES Y SU APLICACIÓN A LA PREPARACIÓN DE MATERIALES BASADOS EN EUGENOL
Dailyn Guzmán Meneses

UNIVERSITAT ROVIRA I VIRGILI
NUEVOS PROCESOS DE CURADO CLICK CON TIOLES Y SU APLICACIÓN A LA PREPARACIÓN DE MATERIALES BASADOS EN EUGENOL
Dailyn Guzmán Meneses

UNIVERSITAT ROVIRA I VIRGILI
NUEVOS PROCESOS DE CURADO CLICK CON TIOLES Y SU APLICACIÓN A LA PREPARACIÓN DE MATERIALES BASADOS EN EUGENOL
Dailyn Guzmán Meneses

CAPÍTULO 9

Bis-eugenol based thermosets prepared by thiol-click chemistry

Dailyn Guzmán, Silvia De la Flor, Xavier Fernández-Francos, Xavier Ramis, Angels Serra

UNIVERSITAT ROVIRA I VIRGILI
NUEVOS PROCESOS DE CURADO CLICK CON TIOLES Y SU APLICACIÓN A LA PREPARACIÓN DE MATERIALES BASADOS EN EUGENOL
Dailyn Guzmán Meneses

Bis-eugenol based thermosets prepared by thiol-click chemistry

Abstract

Thiol-ene photocuring and thiol-epoxy thermal curing have been applied to prepare new thermosets from renewable materials. As monomers, a tetrallyl and a tetraepoxy derivative of bis-eugenol were prepared by dimerization of eugenol, allylation and further epoxidation. These compounds were reacted with a commercially available tetrathiol, PETMP, and a synthesized hexathiol obtained from squalene in photoinitiated and thermal conditions. The reaction process was studied by calorimetry, and the materials obtained were characterized by thermogravimetry, thermomechanical studies and mechanical testing. Thiol-epoxy materials showed a better mechanical performance than thiol-ene photocured thermosets. These last materials showed a lower Tg and had elastomeric characteristics, whereas the thiol-epoxy thermosets reached much higher Tg, higher Young's moduli, strain-stress properties and microindentation hardness.

Keywords: Green chemistry, bis-eugenol, click reaction, thiol-epoxy, thiol-ene.

Introduction

The declining oil reserves, global warming, and littering problems threat the future of polymeric materials. Moreover, the amount of plastics produced during the first decade of our century is almost as large as the amount produced throughout the entire last century. For all these reasons, we need to transform the petrochemical era into a new era of green technology with new polymeric materials derived from renewable resources that fulfil all the requirements of the petrochemical counterparts.[1]

Within the polymeric materials, thermosets find a broad use in the field of adhesives, coatings, encapsulants, etc., being the group of epoxy resins one of the most appreciated for high demanding applications, especially when high thermal and chemical stability are required.[2] Most of these epoxy thermosets derive from bisphenol A (BPA) that is a substance, which can act as chemical oestrogen and therefore presents serious toxicity issues.[3] Moreover, BPA is obtained from fossil resources and therefore its substitution by other environmentally friendly bisphenol alternatives is one of the most approached challenges in recent times from the academic and industrial sides in this field.[4,5]

Amongst renewable starting materials, vegetable natural oils have been widely used to prepare thermosetting materials. This is because of they are cheap, they present double bonds that can be epoxidated and they have no toxicological nor environmental issues. However, their flexible aliphatic structure limit their range of application since the materials obtained usually present too low Tgs and their reactivity is quite different from the observed for glycidylic epoxides.[6,7,8]

Some authors reported on the use of renewable alternatives to plant oils for obtaining thermosets, this is the case of vainillin,[9] itaconic acid,[10] cardanol,[11] furan derivatives[12] or sugars[13] between natural starting substances. From them, different materials with good mechanical performances were obtained because of the more rigid structure of the network formed. Therefore, the proper selection of the monomer structure is of special interest to reach the desired characteristics.

Eugenol (EU, 4-allyl-2-methoxyphenol), the main component (80-90%) of clove oil is usually obtained by steam distillation or Soxhlet extraction from leaves, buds and stems of clove trees.[14] Eugenol has pharmaceutical applications, since it can act as antimicrobial, analgesic, antioxidant, anti-inflammatory, antispasmodic, antigenotoxic, anticarcinogenic and antidepressant.[15,16,17] In dentistry, it is applied in combination with zinc oxide, to form a polymerized cement used for surgical dressings, temporary fillings, pulp capping agents and cavity liners.[18] It is also used as flavor and fragrance in cosmetics and food industry.[19] Eugenol was classified as "generally recognized as safe (GRAS)" by the US Food and Drug Administration.[20] However, several adverse effects, when used at high concentrations, have been reported specially when enters in contact with the skin.[19]

Structurally, eugenol is an aromatic compound with two functional groups, phenol and allyl that can be further modified to prepare a great variety of derivatives.[21] Some researchers have selected several eugenol-based compounds for preparing three-dimensional structures. An epoxy derivative of eugenol was crosslinked by an anhydride derived from rosin and the thermosets prepared have similar reactivity, dynamic mechanical properties and thermal stability than commercial materials.[22] Wan et al.[23] prepared a new epoxy material with a bio-based content of 70.2%wt from an eugenol derivative cured by 4,4'-diamino diphenyl methane. The new material had a Tg of 114 °C, 40 °C lower than the DGEBA based material. Nevertheless, the new epoxy-eugenol thermoset had higher Young's modulus and hardness than the petrochemical analogous. In another study, highly stiff epoxy thermosets derived from eugenol with a triazine core structure and three epoxy groups per molecule was prepared and then cured by using 3,3'-diamino diphenylsulfone.[24] In comparison with DGEBA thermosets cured under the same conditions, the new eugenol based material led to improved thermomechanical properties (33 °C in Tg, 39% in Young's modulus and 55% enhancement in hardness).

In addition to the transformation of eugenol to epoxy monomers, the presence of allyl groups and phenol opens the possibility of using eugenol derivatives as monomers in the preparation of three-dimensional structures by thiol-ene processes. Yoshimura et al.[25] prepared triallyl eugenol, which was crosslinked by a photochemical thiol-ene process leading to adhesives with a limited Tg of 9.1 °C. This result was explained by the occurrence of side-reactions during the thiol-ene process, such as thiol-thiol coupling that hinders the complete reaction to occur. In a previous work of our group, we could

prove that the substitution of an allyl group of triallyleugenol by a glycidyl group allowed to increase the Tg value and enhanced the mechanical performance in reference to the thiol-ene material.[26]

The possibility of dimerization of eugenol[27] opens the possibility to prepare phenols that approach the structure of the bisphenol A molecule.[28] From bis-eugenol derivatives, thermosets with higher thermomechanical performance could be prepared as green alternative to petrochemical materials, following two different methodologies: a) photoinitiated thiol-ene and b) thermal thiol-epoxy curing processes. This is because of bis-eugenol can be allylated to get tetrallyl bis-eugenol (4A-BEU)[29] and subsequently allyl groups can be transformed into glycidylic groups by epoxidation to obtain a tetra-glycidyl bis-eugenol (4EPO-BEU). In the present work, both tetrafunctional compounds have been prepared and then crosslinked with thiols of different structural characteristics to get three-dimensional network structures. As the thiols, we selected pentaerytritol tetrakis (3-mercaptopropionate) (PETMP) and the hexathiol derived from squalene (SQ), both compounds with the possibility to be obtained from renewable resources. All the starting materials are represented in Scheme 1.

The curing procedure has been monitored by calorimetry (DSC) and infrared spectroscopy (FTIR) to find out the best reaction conditions. The fully bio-based thermosets obtained have been characterized by thermogravimetry, thermomechanical analysis and mechanical tests.

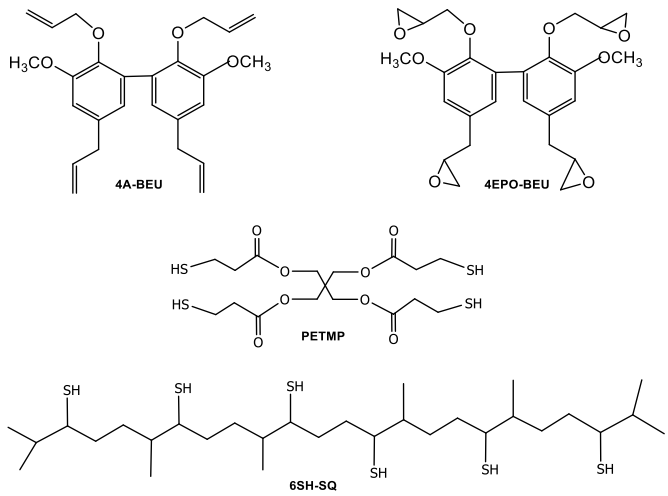

Scheme 1. Chemical structures of the starting compounds

Experimental part

Materials

Eugenol (EU), allyl bromide, thioacetic acid (TAA), 2,2-dimethoxy-2-phenylacetophenone (DMPA), 4-(N,N-dimethylamino)pyridine (DMAP),

1-methylimidazole (1-MI), pentaerytritol tetrakis (3-mercaptopropionate) (PETMP), squalene (SQ) and oxone (potassium peroxomonosulphate) were purchased from Sigma-Aldrich and were used without further purification. Potassium hexa ferricyanide, ammonium hydroxide and inorganic salts from Scharlab were used as received. Benzyl triethyl ammonium chloride (TEBAC) was purchased from Alfa Aesar. Methanol, acetone, ethyl acetate and N,N-dimethylformamide (DMF) from VWR were purified by standard procedures.

Preparation of starting products

- *Synthesis of bis-eugenol (BEU)*

The synthesis of bis-eugenol was based on a previous reported procedure.[27] In a 500 mL flask, 10.5 g (64 mmol) of eugenol were dissolved in a mixture of 100 mL of acetone and 50 mL of water and then 70 mL of NH_4OH at 25% were added under magnetic stirring. The mixture was maintained for 10 min while a green-yellow colour appeared. To this mixture a saturated aqueous solution of $K_3[Fe(CN)_6]$ (21.1 g, 64 mmol) was added dropwise during 5 h. When finished, 70 mL of NH_4OH at 25% were added to keep the alkalinity of the reaction medium and the mixture was kept on stirring overnight. The solution was neutralized by adding diluted HCl at room temperature and a solid precipitated which was filtered, washed three times with distilled water and then dried in the vacuum oven at 60 °C. The product was purified by column chromatography using a mixture of ethyl acetate/hexane (40/60). (m.p. 104 °C by DSC) (yield 98%). ^{1}H NMR ($CDCl_3$, δ in ppm): 3.33 (d, 4H, J=6.5 Hz, -CH_2-), 3.79 (s, 6H, -OCH_3), 4.96-5.18 (m, 4H, =CH_2), 6.14 (m, 2H, =CH-) and 6.69-6.75 (m, 4H, aromatic). ^{13}C NMR ($CDCl_3$, δ in ppm): 40.0 (-CH_2-), 56.0 (-OCH_3), 110.8 (C-6), 115.6 (=CH2), 123.3 (C-2), 124.7 (C-3), 131.8 (C-1), 137.8 (=CH-), 141.2 (C-4) and 147.4 (C-5).

- *Synthesis of tetrallyl derivative of bis-eugenol (4A-BEU)*

The synthesis of tetrallyl biseugenol was based on a previous reported procedure.[29] In a 100 mL three necked flask equipped with magnetic stirrer, thermometer and addition funnel, 5.71 g (17.5 mmol) of BEU and 1.54 g (38.5 mmol) of NaOH were dissolved into 50 mL of DMF. The solution was stirred for 10 min and 4.67 g (38.5 mol) of allyl bromide was added drop by drop during 1 h at 40 °C. The mixture was maintained at 40 °C for 3 h and at 70 °C for 30 min. Distilled water was added to dissolve the NaBr formed and then the organic product was extracted with chloroform. The organic layer was washed twice with water and then dried over $MgSO_4$. The product was concentrated in the rotavap and then dried at high vacuum. The product obtained was a brown coloured oil in a 94% of yield. ^{1}H NMR ($CDCl_3$, δ in ppm): 3.3 (d, 4H, J=6.5 Hz, -CH_2-), 3.87 (s, 6H, -OCH_3), 4.29 (d, 4H, J=6.3 Hz, -CH_2-O-), 4.99-5.12 (m, 8H, =CH_2), 5.75-5.85 (m, 2H, =CH-), 5.92-6.02 (m, 2H, =CH-), 6.71 (d, 2H, J=2 Hz, aromatic) and 6.75 (d, 2H, J=2 Hz, aromatic). ^{13}C NMR ($CDCl_3$, δ in ppm): 39.8 (-CH_2-), 55.6 (-OCH_3), 73.7 (-CH_2-O-), 111.5 (C-3), 115.6 (=CH_2), 116.4 (=CH_2), 123.2 (C-5), 132.5 (C-4), 134.4 (=CH-), 134.7

(=CH-), 137.2 (C-6), 143.8 (C-1) and 152.4 (C-2). FTIR-ATR: 3076, 3000, 2976, 2837, 1680, 1638, 1580, 1484, 1460, 1417, 1355, 1267, 1218, 1142, 1100, 1047, 988, 912, 844, 814, 748 and 722 cm^{-1}. (Spectra are collected in supporting information).

- *Synthesis of tetraglycidyl derivative of bis-eugenol (4EPO-BEU)*

In a three necked 1000 mL flask equipped with magnetic stirrer and addition funnel, 1 g of 4A-BEU (2.5 mmol) was dissolved in 100 mL of ethyl acetate and 100 mL of acetone. Then, a solution of 34.14 g of $NaHCO_3$ (0.41 mol) and 0.12 g (0.53 mmol) of benzyl triethyl ammonium chloride in 70 mL of water was added. The mixture was cooled down at 5-8 °C under vigorous stirring and a solution of oxone (45 g, 73.8 mmol) in 150 mL of water was added drop by drop during 2 h, approximately. The mixture was kept at room temperature under stirring for 3 days. Once finished, the phases were separated and the organic layer washed twice with water. After drying over $MgSO_4$, the solvent was evaporated in the rotavap. The product was purified by column chromatography using as eluent ethyl acetate/hexane mixture (60/40). A viscous yellow liquid was obtained with a yield of 86 %. ^{1}H NMR ($CDCl_3$, δ in ppm), 6.81-6.77 m (Ar, 4H), 3.95 and 3.92 m (-CH_2-O-, 4H), 3.89 s (CH_3-O-, 6H), 3.16 m (CH of glycidyl ether, 2H), 3.04 m (CH of glycidyl groups attached to Ph, 2H), 2.81-2.55 m (-CH_2- of oxirane rings, 8H) and 2.4 m (-CH_2- of glycidyl groups directly attached to Ph, 4H).^{13}C NMR ($CDCl_3$, δ in ppm): 38.1 (-CH_2-), 44.0 (-CH_2- oxirane), 46.4 (-CH_2- oxirane), 50.1 (CH- oxirane), 52.0 (CH- oxirane), 55.5 (-OCH3), 73.5 (-CH_2-O-), 112.2 (C-3), 123.1 (C-5), 132.0 (C-4), 132.4 (C-6), 1-43.9 (C-1) and 152.0 (C-2). FTIR-ATR: 3052, 2996, 2935, 2841, 1719, 1581, 1484, 1460, 1417, 1359, 1255, 1220, 1146, 1096, 1046, 1011, 965, 909, 833 and 732 cm^{-1}.

- *2.2.4. Synthesis of hexathiol from squalene (6SH-SQ)*

The product was obtained following a two-step procedure previously reported, based on the photochemical thiol-ene of thioacetate on squalene in the presence of DMPA and saponification with methanolic NaOH (shown in supporting information).[30]

Preparation of the curing mixtures

Two different types of formulations were prepared. Thiol-ene formulations named as 4A-BEU/thiol and thiol-epoxy formulations named as 4EPO-BEU/thiol. The mixtures were prepared by mixing with a spatula stoichiometric amounts of allyl/SH and epoxy/SH groups, respectively, until reaching homogenous mixtures.

Two different thiol-ene formulations were prepared from 4A-BEU as allyl monomer and two different thiols: PETMP and 6SH-SQ in equimolecular proportion. The photochemical reaction was catalyzed by adding a 4% of a mixture of Irgacure 184 and Irgacure 819 in weight ratio 3:1 in some drops of acetone to obtain a homogeneous mixture. Then, acetone was eliminated at vacuum for 30 minutes. These formulations were named as 4A-BEU/PETMP y 4A-BEU/6SH-SQ.

Two different thiol-epoxy formulations were prepared from tetraepoxy (4EPO-BEU) with the same thiols, PETMP and 6SH-SQ. The homogeneous mixtures were obtained by mixing with a spatula stoichiometric amounts of epoxy/SH groups (1:1), and adding 2 phr (2 parts per hundred of epoxy) of 1-MI as basic catalyst. These formulations were named as 4EPO-BEU/PETMP y 4EPO-BEU/6SH-SQ.

Characterization techniques

^{1}H NMR and ^{13}C NMR spectra were registered in a Varian Gemini 400 spectrometer. $CDCl_3$ was used as the solvent. For internal calibration the solvent signal corresponding to $CDCl_3$ was used: δ (^{1}H) = 7.26 ppm, δ (^{13}C) = 77.16 ppm.

Samples of the different compositions were photocured at 30 °C, in a Mettler DSC-821e calorimeter appropriately modified with a Hamamatsu Lightning cure LC5 (Hg–Xe lamp) with two beams, one for the sample side and the other for the reference side. 5 mg samples were cured in open aluminium pans in nitrogen atmosphere. Two scans were performed on each sample to subtract the thermal effect of the radiation. The method used was 2 min to stabilize the temperature, 10 min irradiation and 2 min at rest. The intensity of light used was 15 mW/cm^2.

The study of the thermal curing was performed by differential scanning calorimetry (DSC) in a Mettler DSC-821e apparatus. For dynamic studies, a flow of N_2 at 100 mL/min was used and the weight of the samples for the analysis was 10 mg. The calorimeter was calibrated using an indium standard (heat flow calibration) and an indium-lead-zinc standard (temperature calibration). The studies were performed in the temperature range of 30-250 °C, with a heating rate of 10 K/min.

The glass transition temperatures (Tgs) of the samples after irradiation were determined in dynamic scans at 20 °C/min from -20 °C to 150 °C. The Tgs of the final thermosets were determined after two consecutive heating dynamic scans at 20 °C/min starting at -20 °C in a Mettler DSC-822e device to delete the thermal history. The Tg value was taken as the middle point in the heat capacity step of the glass transition.

A Bruker Vertex 70 FTIR spectrometer equipped with an attenuated total reflection accessory (ATR) (Golden Gate, Specac Ltd. Teknokroma) which is temperature controlled (heated single-reflection diamond ATR crystal) equipped with a liquid nitrogen-cooled mercury-cadmium-telluride (MCT) detector was used to register the FTIR spectra of the mixtures during UV irradiation and fully cured samples. The spectra were registered in the wave number range between 4000 and 600 cm^{-1} with a resolution of 4 cm^{-1} and averaged over 20 scans. UV-curing was performed using a Hamamatsu Lightning cure LC5 (Hg-Xe lamp) with one beam conveniently adapted to the ATR accessory. A wire-wound rod was used to set a sample thickness of 50 μm. OPUS software was used for the analysis of the spectra. The spectra were corrected for the dependence of the penetration depth on the wavelength and normalized with respect to the absorbance of C=C aromatic peaks at 1587 cm^{-1} (neglecting the contribution of the overlapping tiny

signal associated with the allyl group). The normalized thiol band at 2576 cm^{-1} and the allyl band at 1639 cm^{-1} were integrated and the thiol and allyl conversions after the photocuring (X_{uv}) and after thermal curing (X_{final}) were determined as:

$$X_{UV} = 1 - \frac{A'_{UV}}{A'_0} \quad (1)$$

$$X_{final} = 1 - \frac{A'_{final}}{A'_0} \quad (2)$$

Where A'_{UV}, A'_{final} and A'_0 are the normalized area of thiol or allyl bands after photocuring and thermal curing and at the beginning of the curing, respectively.

A Jasco FTIR spectrometer equipment (resolution of 4 cm^{-1}) with an attenuated-total-reflectance accessory with a diamond crystal (Golden Gate heated single-reflection diamond ATR, Specac-Teknokroma). All the measurements were performed at room temperature. IR was used to follow the disappearance of thiol band at 2570 cm^{-1} and the evolution of the curing process of the different formulations. In this case, the spectra were collect before and after thermal process.

The thermal stability of cured samples was studied by thermogravimetric analysis (TGA), using a Mettler TGA/SDTA 851e thermobalance. All experiments were conducted under inert atmosphere (N_2 at 100 mL/min). Pieces of the cured samples with an approximate mass of 8 mg were degraded between 30 and 600 °C at a heating rate of 10 K/min.

Dynamic mechanical thermal analyses (DMTA) were carried out with a TA Instruments DMA Q800 analyzer. The preparation of rectangular samples (40 mm x 6.7 mm x 1.6 mm) of the thiol-ene formulations was done by putting the mixtures in silicone moulds, which were photoirradiated in an ultraviolet camera (320-390 nm), DymaxECE 2000 UV model systems. The samples were irradiated with an intensity of 105 mW/cm^2 for a period of 60 seconds each face 14 times, waiting for 60 seconds min between irradiations, to c ontrol the temperature of the sample. The thiol-epoxy cured samples from the selected formulations based on 4EPO-BEU were isothermally cured in a mould at 90 °C for 1 h with a post curing at 130 °C for 30 min for 4EPO-BEU/PETMP and 110 °C for 1 h and 140 °C with a post curing at 160 °C for half hour for 4EPO-BEU/6SH-SQ. Three point bending clamp was used on the prismatic rectangular samples. The apparatus operated dynamically at 5 K/min from 30 to 190 °C for deleting the thermal history and then at 3 K/min from 30 to 190 °C at a frequency of 1 Hz with and oscillation amplitude of 10 µm.

Young's modulus was determined under flexural conditions at 30 °C, with the same clamp and geometry samples, applying a force ramp at constant load rate of 3 N/min, from 0.001 N to 18 N. Three samples of each material were analyzed and the results

were averaged. Stress strain at break tests were performed with the film-tension clamp in force controlled mode. Dog-bone samples were used at a force rate of 1 N/min and the mean value of at least three different samples were reported.

Microindentation hardness was measured with a Wilson Wolpert 401 MAV device following the ASTM E384-16 standard procedure. For each material 10 determinations were made with a confidence level of 95%. The Vickers microindentation hardness number (*HV*) was calculated from the following equation:

$$HV = \frac{1.8544 \cdot F}{d^2} \qquad (3)$$

where, *F* is the load applied to the indenter in kgf and *d* is the arithmetic mean of the length of the two diagonals of the surface area of the indentation measured after load removal in mm.

Results and discussion

Synthesis and characterization of monomers

In the present study, we firstly prepared bis-eugenol (BEU) by a previously published procedure,[27] which is based on the oxidative coupling of eugenol produced by the redox ferricyanide-ferrocyanide system. It should be commented that apart from the chemical synthesis, a biological synthesis for BEU using Kalopanax pictus callus culture has been published, which leads to a pure product without any side-reaction.[31] Although advantageous, the biological synthesis falls out of our field of expertise and consequently the classical oxidative coupling of EU has been selected to prepare BEU.

The synthesis of the tetra allyl derivative of bis-eugenol was addressed by the procedure depicted in Scheme 2 that consists in the reaction of BEU with allyl bromide. The same compound was obtained by Neda et al.[29] in DMSO solution, but in our case DMF was selected as the reaction solvent and a higher yield was obtained. The structure and purity of the products were determined by NMR spectroscopy. The ^{1}H NMR spectrum is similar to the one reported in the Neda's publication. The ^{1}H and ^{13}C NMR spectra of 4A-BEU are collected in the supporting information.

From the tetra allyl derivative the corresponding tetra epoxy compound (4EPO-BEU) was prepared. The methodology for the epoxidation of the allyl derived from the bis-eugenol, was based on the use of oxone in a biphasic system acetyl acetate/water.[32] The oxone method was chosen instead of epoxidation with m-chloroperbenzoic acid, because of its better environmental character.[33]

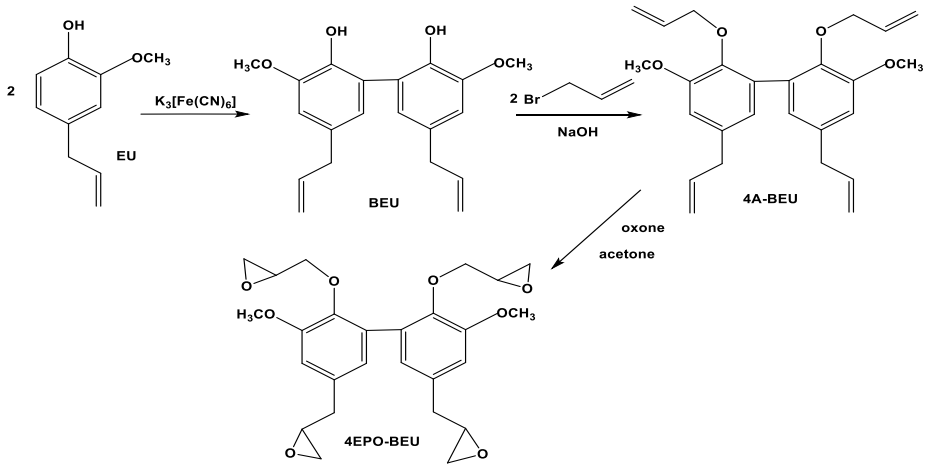

Scheme 2. Synthetic procedure to access the starting monomers

The epoxidation with oxone requires the use of acetone, since it allows the formation of dioxirane, which is the true epoxidation agent. Applying this method, we obtained the pure tetra epoxy derivative of eugenol (4EPO-BEU) in a 86% of yield after purification by column chromatography.

The epoxidated bis-eugenol derivative prepared was characterized by NMR spectroscopy. Figure 1 and 2 present their ^{1}H NMR and ^{13}C NMR spectra with the corresponding assignments.

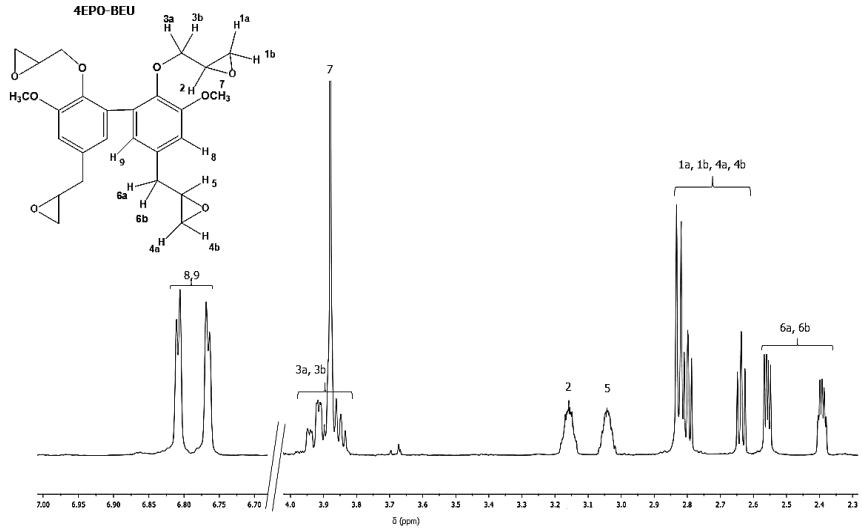

Figure 1. ^{1}H NMR spectrum of 4EPO-BEU in $CDCl_3$

Figure 1 shows a complex spectrum due to the presence of four glycidyl groups, two of them directly linked to the aromatic ring, and two others, which appear more

deshielded due to their attachment to oxygen. Each glycidyl group has five non-equivalent protons due to the presence of the asymmetric carbon that leads to the methylene protons to be diastereotopic to each other. Thus, five different signals are expected for each glycidyl group with a complex coupling pattern. The integration of signals and chemical shifts support the structure for 4EPO-BEU.

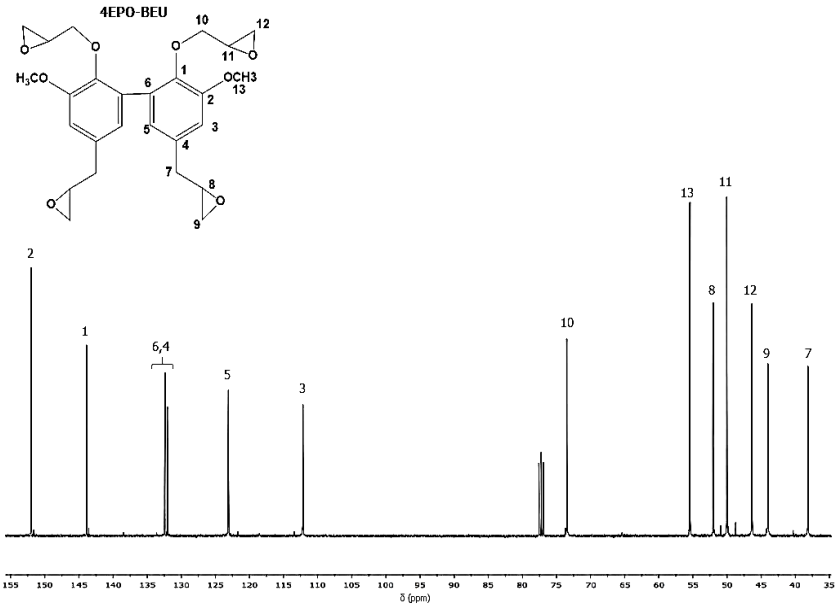

Figure 2. ^{13}C NMR spectrum of 4EPO-BEU in $CDCl_3$

Figure 2 shows the ^{13}C NMR spectrum of the epoxy derivative with the corresponding assignments, which were performed by comparison with the spectrum of the allylic starting product, and the chemical shifts of a previously synthesized glycidylic compound.[34]

The characterization of compounds derived from bis-eugenol by FTIR spectroscopy showed some characteristic absorptions corresponding to their chemical structures. Among the most relevant bands for the 4A-BEU, the vinyl stretching signal at 1638 cm^{-1} can be observed, and for 4EPO-BEU, the absorptions at 909 and 833 cm^{-1} confirms the presence of the epoxy group.

The hexathiol derived from squalene (6SH-SQ) was synthesized by a two-step synthetic procedure, which consist in a first photochemical thiol-ene reaction followed by the saponification of thioester formed. The viscous liquid product was obtained with high yield and purity and its structure confirmed by spectroscopic measurements.[30]

Preparation of materials based on 4A-BEU by thiol-ene reaction

The compound 4A-BEU was used as starting monomer in the preparation of thermosets by thiol-ene reaction using a 3:1 mixture of Irgacure 184/Irgacure 819

photoinitiators, following a similar study carried out by Yoshimura et al.[25] using a triallyl derivative of eugenol.

The curing process of the thiol-ene formulations was followed by photoDSC and infrared spectroscopy. Figure 3 shows the exothermic curves corresponding to the photocuring of the formulations studied.

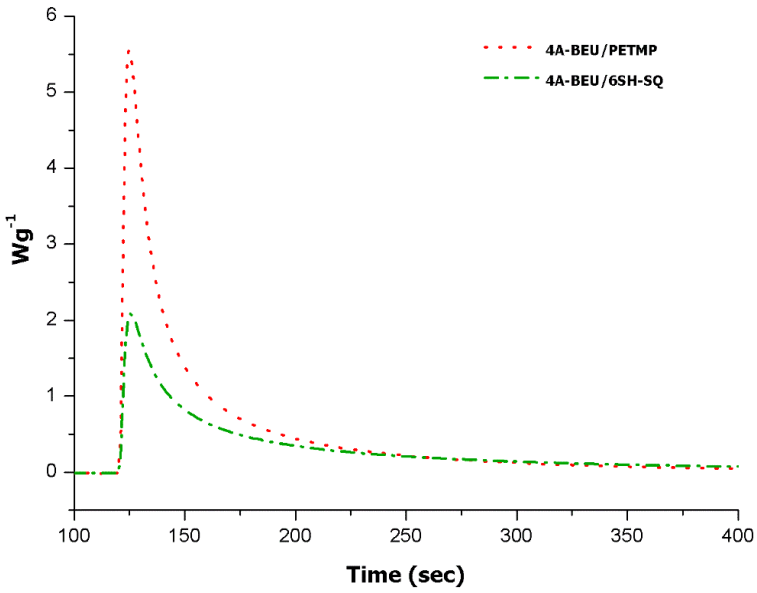

Figure 3. DSC thermograms corresponding to the photocuring at 30 °C of the mixtures of 4A-BEU with both thiols

In the photoDSC plots it can be seen how the formulation 4A-BEU/ PETMP seems to be cured much faster than the formulation prepared with 6SH-SQ. This may be due to the different reactivity of primary and secondary thiol groups and to the fact that the hexathiol generates some topological problems that prevent the reaction from occur properly. The shape of the curves does not allow an exact measurement of the reaction heat involved in this thiol-ene reaction. However, Table 1 shows the approximate heat evolved and the Tgs of the resulting materials.

Table 1. Photocalorimetric and conversion data, obtained by FTIR spectroscopy of the curing of both formulations with 4% of the photoinitiator

Formulation	Δh[a] (J/g)	Δh[b] (kJ/eq)	Tg[c] (°C)	Allyl conversion[d] (%)	Thiol conversion[d] (%)
4A-BEU/PETMP	170	39.4	39	0.96	1.00
4A-BEU/6SH-SQ	118	25.1	38	0.81	0.81

a. Enthalpy released per gram on irradiating the initial mixture
b. Enthalpy released per epoxy equivalent on irradiating the initial mixture
c. Glass transition temperature of the final cured material
d. Conversion of both reactive groups determined by FTIR-ATR

Table 1 reveals that the heat evolved in the photocuring of both formulations is a little lower than the reported by us in previous studies for thiol-ene processes, which were of about 50 kJ/eq.[35] In the case of the 6SH-SQ formulation, the enthalpy released per reactive group is lower than in the formulation with the tetrathiol. This indicates that the reaction does not proceed completely, probably due to the above mentioned topological restrictions produced by its multifunctionality and compact structure. A similar behaviour was reported in other curing systems in which 6SH-SQ was involved.[26] The Tg for the material obtained from 4A-BEU/PETMP formulations is similar than that of 4A-BEU/6SH-SQ, which confirms the incomplete reaction of the squalene formulation, taking into account the higher functionality of 6SH-SQ.

The thiol-ene reaction was also studied by FTIR spectroscopy in order to evaluate the real chemical transformation that is carried out during the curing process. The evolution of the most significant bands of the starting monomers was followed by FTIR spectroscopy during irradiation of a film of the sample in the ATR. The evolution of the thiol groups was monitored by the band at 2570 cm^{-1} corresponding to S-H st and the decrease of the allyl groups by the band at 1638 cm^{-1} of the C=C st. As the reference band, we used the typical of the aromatic ring at 1580-1600 cm^{-1}. The conversion was calculated as explained in the experimental part. Table 1 shows the final conversion reached of allyl and thiol groups in the cured material. As we can see, in the photochemical reaction of 4A-BEU/PETMP mixtures, allyl and thiol groups are consumed quasi completely in a similar way. The slightly lower ally conversion reached can be rationalized by the existence of thiol-thiol coupling, in short extension, during thiol-ene reaction, as reported by some authors.[36] Yoshimura et al.[25] prepared materials from triallyl eugenol and tetrathiol (PETMP) by the same procedure and obtained a material with a Tg of 9.1 °C and very poor thermomechanical properties, similarly to that described by us.[26] They attribute the low curing degree achieved to undesired parallel reactions such as thiol-thiol coupling, which leads to a reduction of the crosslinking densities. Moreover, eugenol derivatives seem to present additional problems when used in photochemical reactions. Its chemical structure, with two allyl groups directly connected to an aromatic ring allows to stabilize radical species by means of resonance, reducing the reactivity of these allyl groups.

Table 1 also shows that for the 4A-BEU/6SH-SQ formulation allyl and thiol groups are consumed in a parallel way, but reaching a low conversion of 81%. Thus, thiol-thiol coupling seems not to proceed but the thiol-ene reaction can be limited by the lower reactivity and topological restrictions of squalene derivative, according to the lower enthalpy evolved during photocuring.

Preparation of the materials derived from 4EPO-BEU by thiol-epoxy curing

In previous studies based in eugenol derivatives, we proved the greatest suitability of thermal thiol-epoxy click processes in front of the photochemical thiol-ene reaction

to obtain thermosets with good thermomechanical characteristics.[26] Moreover, the tetrafunctionality of 4EPO-BEU allows us to hope to achieve improved performances.

The thiol-epoxy curing was studied by calorimetry to evaluate the evolution of the process with both thiols and to find out the most adequate amine to initiate the curing and the reaction temperatures range. In previous studies we used both 1-MI and DMAP as base, being both adequate depending on the substrates used.[26,34,35,37] The calorimetric curves obtained for the curing process of the different formulations are represented in Figure 4.

As it can be seen in Figure 4, PTEMP show the highest reactivity and the curing is produced at lower temperatures and with a high curing rate. Differently, the formulation with 6SH-SQ reacts much slower, showing a very broad and bimodal curve that accounts for a lower reactivity, similarly as observed before for the photochemical thiol-ene curing.

In reference to the basic catalysts, DMAP is more effective than 1-MI, with both thiols and initiate the curing at lower temperature. Taking into account that we aim a certain stability of the initial mixture, in order to apply it safely, we selected 1-MI as the catalyst. It should be also commented that 1-MI, which is liquid, is advantageous in front of the solid DMAP, to prepare homogeneous mixtures from the 4EPO-BEU based formulations, which are quite viscous.

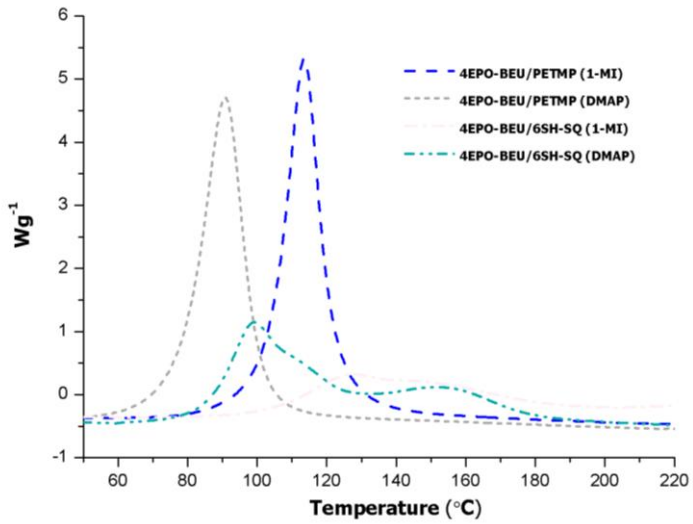

Figure 4. Calorimetric curves of the initial mixture 4EPO-BEU formulations with the thiols tested with 2 phr of the different catalysts

To improve the curing process in the 4EPO-6SH-SQ formulations it was necessary to increase the amount of 1-MI so that the curing process could be carried out in a higher extent. Figure 5 shows the effect of the increasing amount of catalyst on the curing exotherms for the 4EPO-BEU/6SH-SQ formulation.

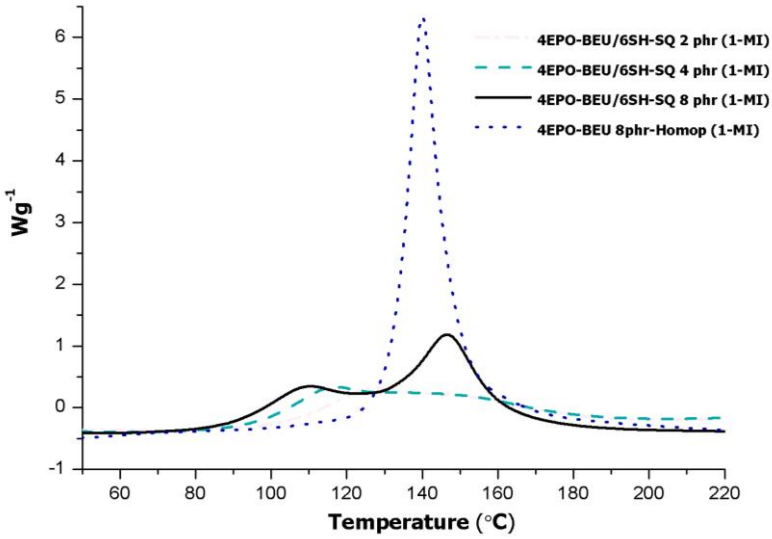

Figure 5. Calorimetric curves of the 4EPO-BEU/6SH-SQ formulations catalyzed by different proportions of 1-MI

As can be seen in the figure, the amount of 1-MI markedly affects the curing process. As the amount of catalyst in the system increases, the presence of two polymerization processes becomes clearer. In the formulation with 8 phr of catalyst a bimodal curve with a maximum at about 110 °C and a second peak, more intense, at 145 °C are easily observable. The first process can be attributed to the thiol-epoxy reaction, whereas the second peak, which perfectly matches with the resin homopolymerization, also represented in Figure 5, can be attributed to this process. The occurrence of epoxy homopolymerization in stoichiometric epoxy/thiol mixtures account for a low reactivity of 6SH-SQ with topological restrictions that limits the thiol-epoxy reaction and therefore some epoxy groups remain unreacted. These groups are able to homopolymerize by an anionic ring-opening mechanism, initiated by 1-MI, as occurred in non-stoichiometric thiol-epoxy formulations.[38]

In the figure we can also see that on increasing the amount of catalyst the area under the exotherm is enhanced. In Table 2 the enthalpies evolved for all formulations are collected. Although on adding a higher proportion of 1-MI to the formulation the heat released by epoxy equivalent clearly increases, even with 8 phr of catalyst this value does not reach the one measured for 4EPO-BEU/PETMP formulations catalyzed by 2 phr of catalyst. The increase of the heat released on increasing the catalyst proportion is due to the occurrence of the homopolymerization process. However, the homopolymerization of 4EPO-BEU did not rend the expected enthalpy per epoxy equivalent, which for DGEBA anionic homopolymerization was about 76 kJ/eq.[39] This could be explained by the rigidity and the multifunctionality of BEU epoxy derivative.

The measured curing enthalpy in PETMP formulations, 126 kJ/eq, suggests that the reaction is complete, according to previously reported values.[40]

Table 2. Reaction enthalpies and Tgs of the different formulations with 2 phr of the 1-MI determined by DSC

Formulation	1-MI (phr)	Δh[a] (J/g)	Δh[b] (kJ/eq)	Tg[c] (°C)
4EPO-BEU/PETMP	2	532	126.7	70
4EPO-BEU/6SH-SQ	2	187	42.0	47
4EPO-BEU/6SH-SQ	4	223	50.3	53
4EPO-BEU/6SH-SQ	8	378	86.2	57
4EPO-BEU	8	579	68.0	91

a. Enthalpy released per gram on heating the initial mixture
b. Enthalpy released per epoxy equivalent on heating the initial mixture
c. Glass transition temperature of the final cured material

Table 2 collects the Tgs of the cured materials. Although PETMP introduces flexibility to the network structure, the rigidity of biseugenol core allows to reach a quite high Tg value. In a previous work,[40] we determined the Tg of the material obtained from DGEBA/PETMP formulations, which resulted to be 55 °C. Thus, from this point of view, biseugenol derived epoxy monomer can be a perfect bio-based substitute for DGEBA resins. As expected, the increase in the proportion of 1-MI in the formulation leads to increase the Tg of the materials obtained, due to the homopolymerization that takes place. Although not fully reacted, the thermoset obtained by the only homopolymerization of 4EPO-BEU reached the highest Tg vale.

To confirm that the curing process has been completed in 4EPO-BEU/PETMP formulations, FTIR spectra were recorded before and after curing on the ATR device. Figure 6 shows the most significant regions of the spectra.

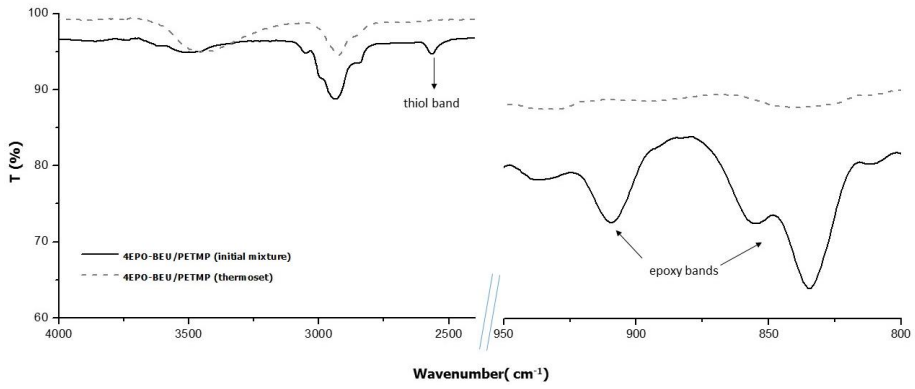

Figure 6. FTIR spectra of a mixture 4EPO-BEU/PETMP catalyzed by 2 phr of 1-MI before and after curing

The initial spectrum shows the typical absorptions of S-H st. at 2570 cm^{-1} and the band at 908 and 835 cm^{-1} corresponding to the epoxy ring. These absorptions have disappeared completely in the spectrum of the cured material, whereas a new broad absorption at 3454 cm^{-1} appears because of the formation of the β-hydroxy thioether groups in the network structure. The small intensity of the thiol absorption and the overlapping of epoxide band with others in the region make difficult the monitoring of the evolution of the curing process.

Characterization of materials based on 4A-BEU and 4EPO-BEU monomers

The materials prepared by thiol-ene and thiol-epoxy were characterized by different techniques to determine their thermal and mechanical characteristics.

The range of stability at high temperatures of the thermosets prepared was determined by thermogravimetry. Figure 7 shows the derivatives of weight loss curves against temperature in inert atmosphere and Table 3 collects the most significant data obtained by this technique.

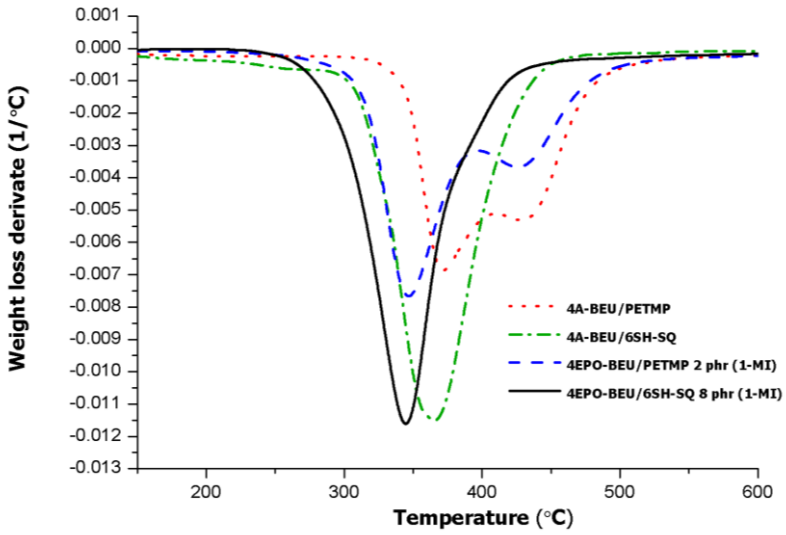

Figure 7. DTG curves under N_2 at 10 K/min of the materials obtained from bis-eugenol derivatives with different formulations.

First of all, we can see that the thermosets prepared from PETMP show a more complex degradation mechanism, regardless of the type of curing performed, since curves with a bimodal shape can be clearly observed, with a first and faster degradative process followed by a defined shoulder at temperatures above 400 °C. In contrast, the 6SH-SQ containing materials show well-defined degradation curves that begin at lower temperatures than those previously commented. The higher complexity of degradation of the PETMP thermosets has been observed in similar materials obtained from 3EPO-EU.[34]

Table 3. Thermal data of the materials obtained after curing processes from bis-eugenol derivatives

Sample	$T_{5\%}$[a] (°C)	T_{max}[b] (°C)	Residue[c] (%)	$T_{tan\delta}$[d] (°C)	E_r[e] (MPa)	E[f] (MPa)
4A-BEU/PETMP	327	372	27	64	24.4	758
4A-BEU/6SH-SQ	248	365	9	46	7.2	133
4EPO-BEU/PETMP	311	347	26	83	26.0	1385
4EPO-BEU/6SH-SQ	295	345	8	140	47.0	1606

a. Temperature of 5% of weight loss in N_2 atmosphere
b. Temperature of the maximum rate of degradation in N_2 atmosphere
c. Residue after thermal degradation in N_2 atmosphere
d. Glass transition temperature determined by DMTA
e. Storage modulus in the rubbery state determined at δ + 50 °C
f. Young's modulus at 30 °C under flexural conditions

The values in the table show that the thermosets prepared from 6SH-SQ begin their degradation at lower temperatures than PETMP containing materials and lead to a lower proportion of char when heated at 600 °C. However, the highest difference in T5% between materials obtained from both thiols is observable in the thiol-ene materials, in which the degree of curing achieved by the use of 6SH-SQ is much less than that of PETMP. The temperature of the maximum rate of degradation depends more on the curing procedure than on the thiol structure, being Tmax higher for the photocured materials. Although structurally both type of materials are quite similar, thiol-ene thermosets have thioether bonds, whereas thiol-epoxy networks present β-hydroxy thioether units, which can contribute to produce different degradation patterns.

Table 3 collects the most typical thermomechanical data obtained for the materials prepared by thiol-ene and thiol-epoxy processes. Between both photocured materials, 4A-BEU/6SH-SQ shows the lowest performance, as expected from the low reactivity observed in the photocuring process. The material obtained from 4A-BEU/PETMP formulation shows better thermomechanical characteristics and even higher than previously reported materials obtained by photocuring of triallyl eugenol.[26] In this previous work, we reported that the photocured materials obtained from mixtures of triallyl eugenol (3A-EU) with PETMP and 6SH-SQ, the best thermomechanical characteristics were reached when 6SH-SQ was the thiol selected, thanks to its multifunctionality that leads to a tighter network. The different behaviour in 4A-BEU materials can be rationalized on the basis of the high rigidity and voluminous structure of the bis-eugenol core with a functionality of four that exacerbates the topological restrictions of the densely functionalized squalene hexathiol, leading to lower thiol-ene conversion that reduces the crosslinking density.

On comparing the data of the thermally cured epoxy-thiol materials, it can be stated that the sample 4EPO-BEU/6SH-SQ presents the best thermomechanical properties. Since we have demonstrated that the thiol-epoxy reaction could not be adequately carried out in this formulation due to topological restrictions, the

enhancements in the final properties should be attributed to the contribution of the network formed by homopolymerization, which is tighter, leading to higher values of tan δ temperature and Young's modulus. However. on comparing the thermomechanical data obtained for 4EPO-BEU/PETMP and DGEBA/PETMP thermosets[40] we can confirm that the bis-eugenol derivative is a good alternative for replacing the oil-derived DGEBA resin.

In addition to the values obtained from thermomechanical tests it is interesting to inspect the α relaxation curves of the materials prepared. Figure 8 shows the curves in two different graphics, to clearly visualize the different shapes for each material.

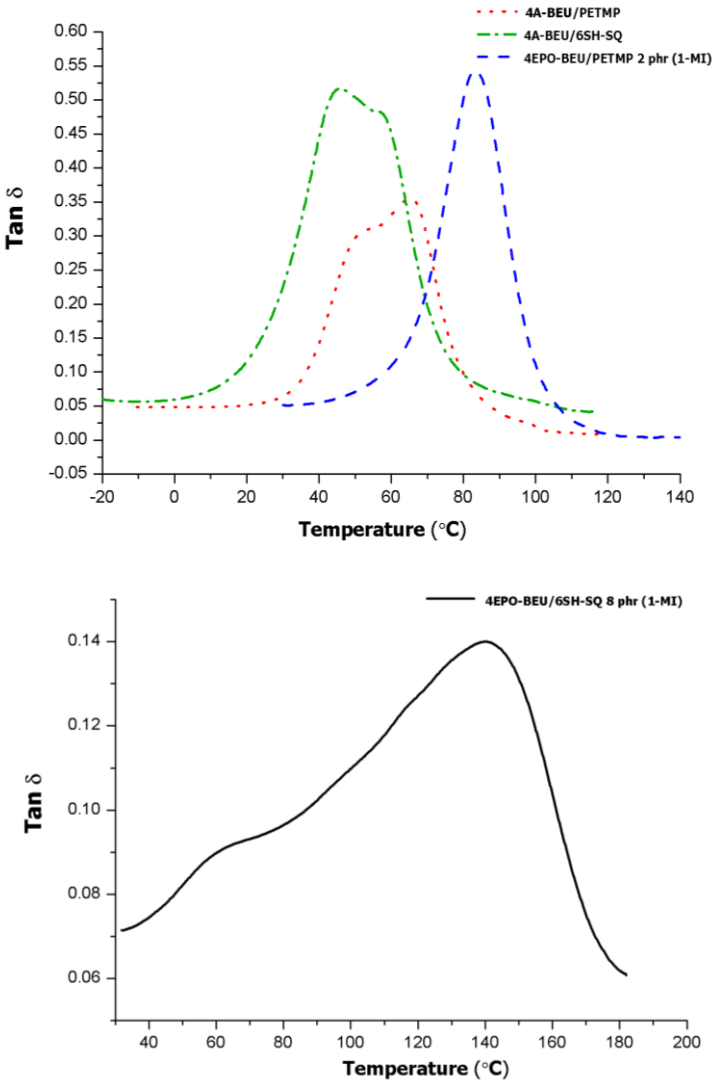

Figure 8. Plots of tan δ against temperature for the various materials prepared

Whereas the shape of the curve of 4EPO-BEU/PETMP sample is unimodal and narrow, the materials obtained by photopolymerization are broader and slightly split. This agrees with the concurrence of side-reactions in the thiol-ene process and to the uncomplete curing achieved as has been demonstrated in the photocuring study, both facts leading to heterogeneous materials. It is worth to note, the broad and bimodal shape of the tan δ curve obtained for 4EPO-BEU/6SHSQ (right plot). The height of the curve, much lower than the others, indicates a high crosslinking density and low damping characteristics. Moreover, the material is heterogeneous as reflected in the broadness and complexity of the curve, which confirms the coexistence of two different network structures in the material, one thiol-epoxy and another of polyether. The thiol-epoxy network presents an α relaxation at approximately 60 °C whereas the tight polyether structure increases the Tg of the material, which reaches a value of 140 °C.

The values of Young's modulus and the storage modulus in the rubbery state collected in Table 3 reflect the network characteristics. Thus, the more rigid material is the one obtained from squalene in thermal conditions, because of the polyether formation. On the other hand, squalene leads to the softer and less crosslinked material in photocuring conditions, because of the lower reactivity of 6SH-SQ and the coexistence of undesired side-reactions. Thus, for bis-eugenol structures, thermal thiol-epoxy processes are more effective than photochemical thiol-ene reactions to get materials with better mechanical performance. This observation agrees well with the results obtained in simple eugenol derivatives[26] and confirms that the eugenol structure is not adequate for radical type thiol-ene reactions.

The strain-stress and microindentation hardness testing were performed on dog-bone samples to evaluate the mechanical characteristics of the materials prepared. Table 4 collects the main data extracted from these tests.

Table 4. Mechanical data of the materials obtained by stress-strain and microindentation hardness testing. Coefficients of variation less than 8% for stress, strain and tensile modulus, and less than 5% for microindentation hardness.

Sample	Strain at break (%)	Stress at break (MPa)	Microindentation hardness[a] (HV)
4A-BEU/PETMP	8.8	6.6	9.8
4A-BEU/6SH-SQ	8.5	5.4	6.3
4EPO-BEU/PETMP	2.3	23.2	11.5
4EPO-BEU/6SH-SQ	1.6	29.9	14-20

a. Indentation test load of 25 g for all formulations

As can be seen, the materials obtained by photochemical curing have poor tensile strength and high elongation at break, showing an elastomeric behaviour. In the case of thermosets obtained by thermal curing, a significant increase in tensile strength and a decrease in the elongation of the materials were observed. These materials exhibited higher hardness values than the materials derived from the allyl derivative of bis-

eugenol. As in the case of simple eugenol derivatives,[26] the thermoset prepared from 4EPO-BEU/6SH-SQ presented the best mechanical performance, due to the contribution of the homopolymerization to generate a more resistant material.

For the material from squalene hexathiol, different values of hardness were measured, due to the inhomogeneous character of the material. Values between 14 and 20 could be found, being 20 the most predominant in the material.

Conclusions

Two different tetrafunctional compounds, 4A-BEU and 4EPO-BEU, were prepared from bis-eugenol, previously obtained by dimerization of eugenol as starting renewable material. The synthetic procedure consisted in an allylation reaction and further epoxidation using oxone to obtain the epoxy derivative.

The tetraallyl derivative of bis-eugenol, 4A-BEU, was used as the monomer in the thiol-ene reaction using two thiols of different functionalities, PETMP and 6SH-SQ, the last one derived from squalene. It was observed that the mixtures presented incomplete curing reactions and possible side-reactions that limits the degree of curing achieved. PETMP showed a better reactivity in these systems than 6SH-SQ due to topological problems.

The tetraepoxy derivative of bis-eugenol, 4EPO-BEU, was the monomer in the thiol-epoxy reaction using the same thiols selected for the photocuring, catalyzed by 1-methylimidazole as the base. We could prove that the curing with PETMP was complete, but when 6SH-SQ was selected as the thiol, the degree of curing achieved was limited. On increasing the proportion of base, homopolymerization of epoxide at high temperature also occurred. This was attributed to the topological restrictions of squalene thiol to react because of its multifunctionality and compact structure.

The materials prepared from the thiol-epoxy curing had better thermal and mechanical characteristics than the materials obtained by photochemical thiol-ene reaction, but the squalene derived thermoset has an heterogeneous network due to the different processes occurring during curing.

The use of bis-eugenol derivatives as renewable starting material for the preparation of thermosets has been demonstrated advantageous in front of eugenol derivatives, especially in thermomechanical characteristics.

The bis-eugenol tetraepoxy derivative is a good alternative for replacing the oil-derived DGEBA resin according to their thermomechanical characteristics.

Acknowledgments

The authors would like to thank MINECO (MAT2014-53706-C03-01, MAT2014-53706-C03-02) and Generalitat de Catalunya (2014-SGR-67) for the financial support.

References

[1] R. Mülhaupt, *Macromolecular Chemistry and Physics*, 2013, 214, 159−174

[2] C.A. May, (ed.), *Epoxy resins. Chemistry and technology*, Marcel Dekker, USA, New York, 1988

[3] F. Ng, G. Couture, C. Philippe, B. Boutevin, S. Caillol, *Molecules*, 2017, 22, 149-197.

[4] S. Ma, T. Li, X. Liu, J. Zhu, *Polymer International*, 2016; 65, 164–173.

[5] E. A. Baroncini, S. Kumar Yadav, G. R. Palmese, J. F. Stanzione, *Journal of Applied Polymer Science*, 2016, DOI: 10.1002/APP.44103.

[6] R. Auvergne, S. Caillol, G. David, B. Boutevin, *Chemical Reviews*, 2014, 114, 1082−1115.

[7] M. Stemmelen, V. Lapinte, J-P Habas, J-J Robin, *European Polymer Journal*, 2015, 68, 536–545.

[8] C. Ding, P. S. Shuttleworth, S.Makin, J. H. Clark, A. S. Matharu, *Green Chemistry*, 2015, 17, 4000-4008.

[9] M. Fache, B. Boutevin, S. Caillol, *Sustainable Chemistry & Engineering*, 2016, 4, 35−46.

[10] S. Ma, X. Liu, Y. Jiang, Z. Tang, C. Zhang, J. Zhu, *Green Chemistry*, 2013, 15, 245–254.

[11] E. Darroman, N. Durand, B. Boutevin, S. Caillol, *Progress in Organic Coatings*, 2016, 91, 9–16.

[12] F. Hu, J. J. La Scala, J. M. Sadler, G. R. Palmese, *Macromolecules*, 2014, 47, 3332−3342.

[13] P. Niedermann, G. Szebényi, A. Toldy, *eXPRESS Polymer Letters*, 2015, 9, 85–94.

[14] G. Wenqiang, L. Shufen, Y. Ruixiang, T. Shaokun, Q. Can, *Food Chemistry*, 2007, 101, 1558–1564.

[15] B. Yogalakshmi, P. Viswanathan, C.V. Anuradha, *Toxicology*, 2010, 268, 204–212.

[16] A. Garg, S. Singh, *Colloid Surface B*, 2011, 87, 280–288.

[17] H. J. Bohnert, H. R. Nguyen, N.G. Lewis, *Bioengineering and Molecular Biology of Plant Pathways*, Elsevier, CA, USA, San Diego, 2008.

[18] S. Fujisawa, Y. Kashiwagi, T. Atsumi, I. Iwakura, T. Ueha, Y. Hibino, I. Yokoe, *Journal of Dentistry*, 1999, 27, 291-295.

[19] G. P. Kamatou, I. Vermaak, A. M. Viljoen, *Molecules*, 2012, 17, 6953-6981.

[20] Expert Committee on Food Additives, *Evaluation of Certain Food Additives and Contaminants*, WHO Technical Report Series 683, WHO Press: Geneva, Suiza, Ginebra, 1982.

[21] T. S. Kaufman, *Journal of the Brazilian Chemical Society*, 2015, 26, 1055-1085.

[22] J. Qin, H. Liu, P. Zhang, M. Wolcott, J. Zhang, Polymer International, 2014, 63, 760-765.

[23] J. Wan, B. Gan, C. Li, J. Molina-Aldareguia, E. Naderi Kalali, X. Wang, D-Y Wang, *Chemical Engineering Journal*, 2016, 284, 1080–1093.

[24] J. Wan, J. Zhao, B. Gan, C. Li, J. Molina-Aldareguia, Y. Zhao, Y-T Pan, D-Y Wang, *ACS Sustainable Chemistry & Engineering*. 2016, 4, 2869−2880.

[25] T. Yoshimura, T. Shimasaki, N. Teramoto, M. Shibata, *European Polymer Journal*, 2015, 67, 397–408.

[26] D. Guzmán, X. Ramis, X. Fernández-Francos, S. De la Flor, A. Serra, *European Polymer Journal*, doi:10.1016/j.eurpolymj.2017.06.026.

[27] A. De Farias Dias, *Phytochemistry*, 1988, 27, 3008-3009.

[28] D. Fourcade, B. Sebastian Ritter, P. Walter, R. Schönfeld, R. Mülhaupt, *Green Chemistry*, 2013, 15, 910-918.

[29] M. Neda, k. Okinaga, M. Shibata, *Materials Chemistry and Physics,* 2014, 148, 319-327.

[30] R. Acosta Ortiz, E.A. Obregón Blandón, R. Guerrero Santos, *Green and Sustainable Chemistry*, 2012, 2, 62-70.

[31] B. Kim, J. Young Kim, Y. Yi, Y. Lim, *Journal of the Korean Society for Applied Biological*, 2012, 55, 677-680.

[32] N. Hashimoto, A. Kanda, *Organic Process Research & Development*, 2002, 6, 405-406.

[33] C. Aouf, H. Nouailhas, M. Fache, S. Caillol, B. Boutevin, H. Fulcrand, *European Polymer Journal*, 2013, 49, 1185.

[34] D. Guzmán, X. Ramis, X. Fernández-Francos, S. De la Flor, A. Serra, *Progress in Organic Coatings*, Send to revision.

[35] D. Guzmán, X. Ramis, X. Fernández-Francos, A. Serra, *RSC Advances*, 2015, 5, 101623-101633.

[36] S.P.S. Koo, M.M. Stamenovic, R.A. Prasath, A.J. Inglis, F.E. Du Prez, C. Barner-Kowollik, W. Van Camp, T. Junkers, *Journal of Polymer Science Part A: Polymer Chemistry*, 2010, 48, 1699–1713.

[37] D. Guzmán, B. Mateu, X. Fernández-Francos, X. Ramis, A. Serra, *Polymer International*, 2017, DOI 10.1002/pi.5336.

[38] X. Fernández-Francos, A-O Konuray, A. Belmonte, S. De la Flor, A. Serra, X. Ramis, *Polymer Chemistry*, 2016, 7, 2280-2290.

[39] X. Fernández-Francos, W. D. Cook, A. Serra, X. Ramis, G. G. Liang, J. M. Salla, *Polymer*, 2010, 51, 26-34.

[40] D. Guzmán, X. Ramis, X. Fernández-Francos, A. Serra, *Polymer*, 2015, 7, 680-694.

Supporting information

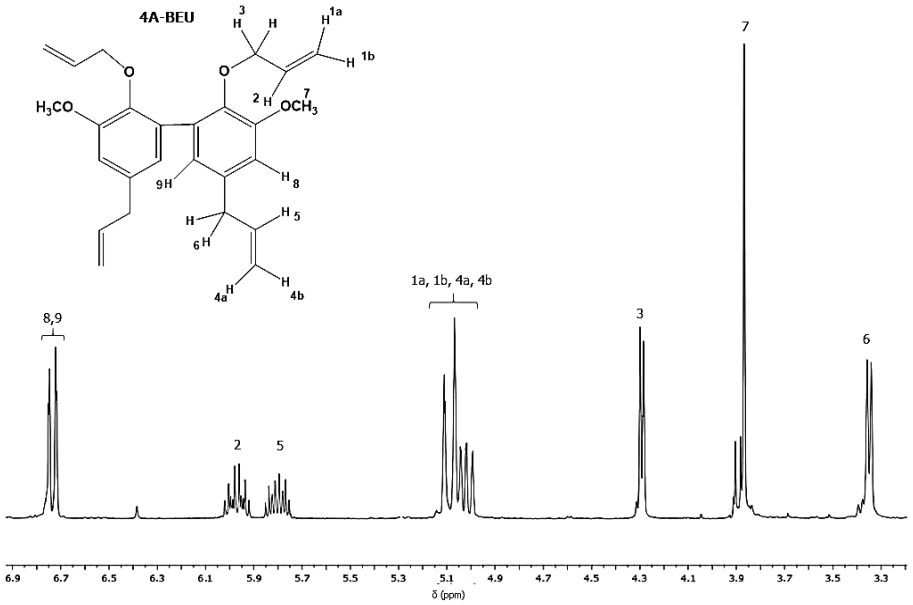

Figure A. ^{1}H NMR spectrum of the tetra allyl (4A-BEU) derived from eugenol registered in $CDCl_3$

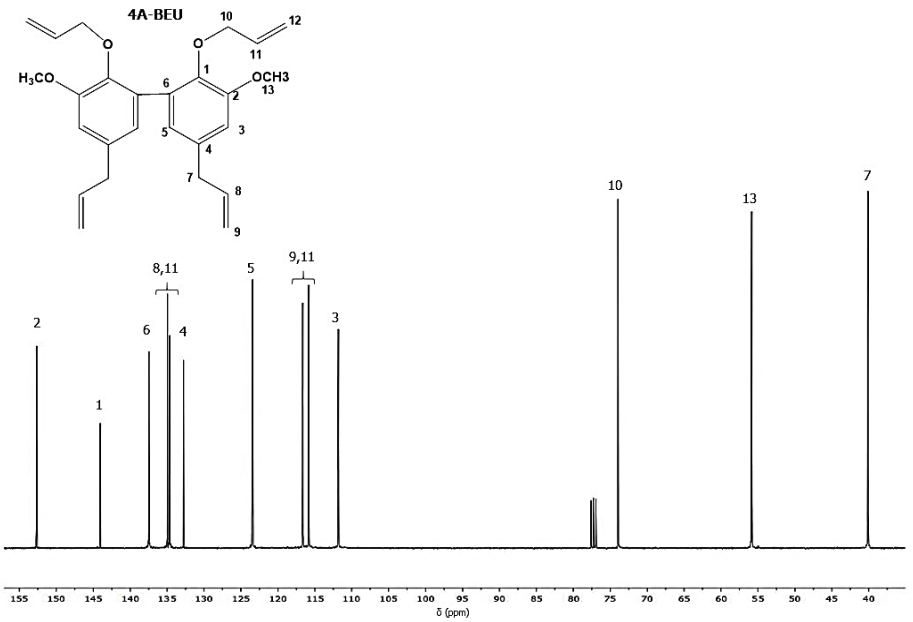

Figure B. ^{13}C NMR spectrum of the tetra allyl (4A-BEU) derived from eugenol registered in $CDCl_3$

UNIVERSITAT ROVIRA I VIRGILI
NUEVOS PROCESOS DE CURADO CLICK CON TIOLES Y SU APLICACIÓN A LA PREPARACIÓN DE MATERIALES BASADOS EN EUGENOL
Dailyn Guzmán Meneses

UNIVERSITAT ROVIRA I VIRGILI
NUEVOS PROCESOS DE CURADO CLICK CON TIOLES Y SU APLICACIÓN A LA PREPARACIÓN DE MATERIALES BASADOS EN EUGENOL
Dailyn Guzmán Meneses

UNIVERSITAT ROVIRA I VIRGILI
NUEVOS PROCESOS DE CURADO CLICK CON TIOLES Y SU APLICACIÓN A LA PREPARACIÓN DE MATERIALES BASADOS EN EUGENOL
Dailyn Guzmán Meneses

CAPÍTULO 10

Conclusiones

UNIVERSITAT ROVIRA I VIRGILI
NUEVOS PROCESOS DE CURADO CLICK CON TIOLES Y SU APLICACIÓN A LA PREPARACIÓN DE MATERIALES BASADOS EN EUGENOL
Dailyn Guzmán Meneses

1. La utilización de tioles reactivos mediante reacciones *click*, tiol-eno y tiol-epoxi, ha resultado ser una estrategia adecuada para la obtención de nuevos termoestables duales y no duales, basados en monómeros comerciales o bien de origen natural, como el eugenol y el escualeno.

2. El empleo de catalizadores latentes precursores de aminas terciarias, inactivos a baja temperatura y activos a alta temperatura, ha permitido obtener mezclas tiol/epoxi con una elevada estabilidad durante su almacenamiento a temperatura ambiente. Los termoestables obtenidos empleando estos sistemas catalíticos han presentado una excelente estabilidad térmica y alta transparencia.

3. La incorporación de triglicidil isocianurato a sistemas latentes tiol-epoxi, junto con el aumento de la funcionalidad del tiol utilizado, ejercen un efecto cooperativo beneficioso, observándose un aumento significativo de las propiedades térmicas y mecánicas finales de los termoestables obtenidos, respecto a sistemas equivalentes donde no se ha realizado esta incorporación.

4. La utilización de precursores latentes de aminas terciarias en cantidades adecuadas ha permitido establecer una nueva metodología para la preparación de termoestables duales secuenciales por medio de una primera etapa de curado tiol-eno fotoactivada y una segunda tiol-epoxi activada térmicamente. Los materiales obtenidos son estables al final de la primera etapa de curado y las propiedades al final de ambas etapas de curado pueden moldearse modificando la cantidad relativa entre monómeros vinílicos y epoxídicos.

5. Se han sintetizado nuevos tioles multifuncionales, algunos de ellos derivados de fuentes renovables como el eugenol y el escualeno, mediante reacción tiol-eno fotoinducida del correspondiente compuesto vinílico con ácido tioacético seguida de la saponificación del acetil tioester formado y se ha comprobado la bondad del método para diferentes substratos sin grupos saponificables.

6. Los tioles empleados en las reacciones de curado *click* presentaron diferentes reactividades. El PETMP resultó ser el más reactivo en todas las reacciones tiol-*click*, ya sean térmicas o fotoquímicas. Sin embargo, su estructura flexible conlleva a materiales con menor Tg que los obtenidos mediante el empleo de otros tioles estudiados. El tiol derivado del eugenol, 3SH-EU, es muy efectivo para ser empleado en reacciones tiol-epoxi, pero no es aconsejable su empleo en procesos de fotocurado. El hexatiol derivado del escualeno, es apto para ser empleado en cualquier tipo de reaccion tiol-*click*, aunque genera problemas topológicos debido a su estructura química y alta multifuncionalidad, los termoestables obtenidos mediante 6SH-SQ presentan muy buenas propiedades físicas y mecánicas.

7. Se ha establecido un nuevo método de curado térmico de resinas epoxi cicloalifáticas con tioles en presencia de una base, obteniéndose termoestables altamente entrecruzados. Los materiales obtenidos presentan propiedades que

dependen de la rigidez y funcionalidad del tiol utilizado, siendo el material preparado con el derivado hexafuncional del escualeno el que presenta mayor valor de temperatura de transición vítrea y módulo de Young.

8. La estructura química del eugenol, altamente versátil, ha permitido la síntesis de sus derivados tritiol, trialil, dialil glicidil y triglicidil, mediante procedimientos sintéticos bien establecidos. El camino sintético incluye alilación, transposición de Claisen y en el caso de los glicidil derivados, epoxidación mediante oxona, que es un procedimiento que sigue los principios de química verde, y que ha demostrado ser ventajoso respecto a la epoxidación con perácido.

9. El derivado trialílico del eugenol ha sido curado mediante un procedimiento fotoiniciado tiol-eno con diferentes tioles. Las reacciones de acoplamiento tiol-tiol así como la estabilización por resonancia de las especies radicalarias de eugenol no permiten que la reacción tiol-eno tenga lugar de forma completa, corroborando así algunos resultados descritos en la literatura para sistemas similares.

10. El derivado dialil glicidil del eugenol ha podido ser curado mediante una metodología tipo *click* dual, con un tiol comercial o tioles procedentes de fuentes renovables, consistente en una primera etapa tiol-eno fotoinducida seguida de una segunda etapa tiol-epoxi térmica. La presencia de grupos glicidílicos, que reaccionan en la segunda etapa térmica, ha permitido obtener unos materiales finales con mayor dureza y resistencia a la rotura que los obtenidos en una sola etapa de curado tiol-eno.

11. El triepóxido sintetizado se ha utilizado para la preparación de termoestables mediante curado tiol-epoxi, catalizado por una base, con diferentes tioles de origen natural. La adecuada selección de los tioles y monómeros epoxi permite preparar materiales con unas propiedades finales hechas a medida, aunque la multifuncionalidad del hexatiol derivado del escualeno ha requerido la adición de un diepóxido lineal flexible, para reducir las restricciones topológicas producidas y alcanzar un curado completo. Los materiales obtenidos a partir del triepóxido del eugenol presentaron propiedades térmicas y mecánicas muy superiores a materiales equivalentes preparados a partir de los derivados trialil y dialil glicidil eugenol. En consecuencia, la sustitución total de los grupos alilo por grupos epóxido en el eugenol aporta importantes ventajas en la preparación de esta familia de termoestables.

12. El bis-eugenol, sintetizado mediante la dimerización del eugenol ha sido utilizado como compuesto de partida para obtener los respectivos monómeros alílicos y glicidílicos tetrafuncionales mediante procedimientos análogos a los anteriormente citados. Al igual que en el caso de los derivados sencillos del eugenol, se prepararon materiales por entrecruzamiento con diferentes tioles mediante procedimientos *click* tiol-eno fotoiniciados, o *click* tiol-epoxi térmicos. Los materiales obtenido

mediante procedimiento de curado térmico tiol-epoxi mostraron mejores cualidades térmicas y mecánicas. Los materiales obtenidos a partir de bis-eugenol presentaron mejores propiedades térmicas y mecánicas que los derivados del eugenol sencillo, debido a su estructura rígida y su mayor funcionalidad.

13. De manera general, los resultados expuestos en este trabajo abren una nueva vía de curado dual para obtención de materiales termoestables hechos a medida y que permiten su uso en metodologías de fabricación avanzadas. La utilización de precursores de amina latente permite la preparación de formulaciones estables, con excelente procesabilidad que pueden originar un material intermedio, manipulable aunque estable, que mediante una segunda etapa térmica lleva al material final con las características requeridas, aunque es necesaria una optimización de las condiciones de reacción.

14. La segunda aportación del trabajo ha sido la utilización de los principios de la química e ingeniería verde en la preparación de nuevos materiales termoestables. Este proceder abarca tanto la preparación de monómeros de origen natural, como la utilización de la química *click* en la síntesis de estos monómeros y en el curado de los mismos.

UNIVERSITAT ROVIRA I VIRGILI
NUEVOS PROCESOS DE CURADO CLICK CON TIOLES Y SU APLICACIÓN A LA PREPARACIÓN DE MATERIALES BASADOS EN EUGENOL
Dailyn Guzmán Meneses

UNIVERSITAT ROVIRA I VIRGILI
NUEVOS PROCESOS DE CURADO CLICK CON TIOLES Y SU APLICACIÓN A LA PREPARACIÓN DE MATERIALES BASADOS EN EUGENOL
Dailyn Guzmán Meneses

UNIVERSITAT ROVIRA I VIRGILI
NUEVOS PROCESOS DE CURADO CLICK CON TIOLES Y SU APLICACIÓN A LA PREPARACIÓN DE MATERIALES BASADOS EN EUGENOL
Dailyn Guzmán Meneses

CAPÍTULO 11

Apéndices

UNIVERSITAT ROVIRA I VIRGILI
NUEVOS PROCESOS DE CURADO CLICK CON TIOLES Y SU APLICACIÓN A LA PREPARACIÓN DE MATERIALES BASADOS EN EUGENOL
Dailyn Guzmán Meneses

Lista de abreviaturas

1-MI	1-metilimidazol
2-MI	2-metilimidazol
2AG-EU	Dialilglicidil derivado del eugenol
2EPO-HEX	Diglicidiléter del 1,6-hexanodiol
3A-EU	Trialil derivado del eugenol
3EPO-EU	Triglicidil derivado del eugenol
3SH-EU	Tritiol derivado del eugenol
3SH-ISO	Tritiol derivado del trialilisocianurato
4A-BEU	Tetraalil derivado del bis-eugenol
4EPO-BEU	Tetraglicidilderivado del bis-eugenol
6SH-SQ	Hexatiol derivado del escualeno
%wt	Porcentaje en peso
α	Grado de conversión
δ	Desplazamiento químico (ppm)
ε	Coeficiente de absorbitividad
|η*|	Viscosidad compleja
ΔCp	Capacidad calorífica
Δh_t	Calor liberado
Δh_{res}	Calor liberado en el barrido de post-curado
Δh_{total}	Valor de referencia del calor liberado en un curado completo
A	Absorbancia o factor pre-exponencial
$\overline{A^t}$	Absorbancia normalizada a un tiempo t
$\overline{A^o}$	Absorbancia normalizada inicial
A'_{UV}	Absorbancia normalizada después del fotocurado
A'_{final}	Absorbancia normalizada después del curado térmico
BDMA	N, N-bencildimetilamina
BEU	Bis-eugenol
C	Concentración

DGEBA	Diglicidiléter del bisfenol A
DMAP	4-(N,N-dimetilamino)piridina
DMF	N,N-Dimetilformamida
DMPA	2,2-dimetoxi-2-fenilacetofenona
DMTA	Análisis térmico dinamomecánico
DGT	Derivada de la curva termogravimétrica
DSC	Calorimetría diferencial de barrido
E	Energía de activación o módulo de Young
ECC	3',4'-epoxiciclohexanocarboxilato de 3,4-epoxiciclohexilo
EPC	Epiclorhidrina
eq	Equivalente
E_r	Módulo relajado
EU	Eugenol
FT-IR	Espectroscopía de infrarrojo con transformada de Fourier
Irgacure 184	1-hidroxiciclohexilfenilcetona
Irgacure 819	Óxido de fenil bis(2,4,6-trimetilbenzoil) fosfina
LC-80	Imidazol encapsulado
phr	Partes por cien de resina o mezcla reactiva
PI	Fotoiniciador
PETMP	Pentaeritritol tetrakis (3-mercaptopropionato)
PDU-250	N,N-dimetil-N'-fenilurea
R	Constante de los gases
RMN	Resonancia magnética nuclear
SQ	Escualeno
T	Temperatura
t	Tiempo
$T_{5\%}$	Temperatura correspondiente a la pérdida de masa del 5%
T_{max}	Temperatura correspondiente a la máxima velocidad de pérdida de masa
TAA	Ácido tioacético

TAIC	Trialilisocianurato
TEBAC	Cloruro de benciltrietilamonio
Tg	Temperatura de transición vítrea
TGA	Análisis termogravimétrico
TGIC	Triglicidilisocianurato
TTMP	Trimetilolpropano tris(3-mercaptopropionato)
TMS	Tetrametilsilano
UV	Ultravioleta

UNIVERSITAT ROVIRA I VIRGILI
NUEVOS PROCESOS DE CURADO CLICK CON TIOLES Y SU APLICACIÓN A LA PREPARACIÓN DE MATERIALES BASADOS EN EUGENOL
Dailyn Guzmán Meneses

Lista de publicaciones

Artículos de la tesis

Dailyn Guzmán, Xavier Ramis, Xavier Fernández-Francos, Angels Serra. New catalysts for diglycidyl ether of bisphenol A curing based on thiol-epoxy click reaction. *European Polymer Journal* **2014**, 59, 377-386.

Dailyn Guzmán, Xavier Ramis, Xavier Fernández-Francos, Angels Serra. Enhancement in the glass transition temperature in latent thiol-epoxy click cured thermosets. *Polymers* **2015**, 7, 680-694.

Dailyn Guzmán, Xavier Ramis, Xavier Fernández-Francos, Angels Serra. Preparation of click thiol-ene/thiol-epoxy thermosets by controlled photo/thermal dual curing sequence. *RSC Advances* **2015**, 5, 101623-101633.

Dailyn Guzmán, Blai Mateu, Xavier Fernández-Francos, Xavier Ramis, Angels Serra. Novel thermal curing of cycloaliphatic resins by thiol–epoxy click process with several multifunctional thiols. *Polymer International* **2017**, DOI 10.1002/pi.5336.

Dailyn Guzmán, Xavier Ramis, Xavier Fernández-Francos, Silvia De la Flor, Angels Serra. New bio-based materials obtained by thiol-ene/thiol-epoxy dual curing click procedures from eugenol derivates. *European Polymer Journal* **2017**, in press.

Dailyn Guzmán, Xavier Ramis, Xavier Fernández-Francos, Silvia De la Flor, Angels Serra. Preparation of new biobased materials from a triglycidyl eugenol derivative through thiol-epoxy click reaction *Progress in Organic Coatings* **2017**, Enviado.

Dailyn Guzmán, Silvia De la Flor, Xavier Fernández-Francos, Xavier Ramis, Angels Serra. Bis-Eugenol Based-Thermosets Prepared by Thiol Chemistry. En preparación.

Artículos en colaboración

Alberto Belmonte, **Dailyn Guzmán**, Xavier Fernández-Francos, Silvia De la Flor. Effect of the network structure and programming temperature on the shape-memory response of thiol-epoxy “click” systems. *Polymers* **2015**, 7, 2146–2164.

Oleksandra Korychenska, **Dailyn Guzmán**, Angels Serra, Xavier Ramis, Juozas V. Grazulevicius. Fluorescent thiol-epoxy thermosets obtained from diglycidylether of bisphenol A and carbazole based diepoxy monomer. *Reactive and Functional Polymers* **2017**, 116, 107-113.

UNIVERSITAT ROVIRA I VIRGILI
NUEVOS PROCESOS DE CURADO CLICK CON TIOLES Y SU APLICACIÓN A LA PREPARACIÓN DE MATERIALES BASADOS EN EUGENOL
Dailyn Guzmán Meneses

Comunicaciones a congresos

Dailyn Guzmán, Angels Serra, Xavier Fernández-Francos, Xavier Ramis. Nuevo sistema latente para el curado de resinas epoxi con tioles. XIII Reunión del Grupo Especializado de Polímeros (GEP) de la RSEQ y RSEF, Girona (España) 2014. Oral.

Dailyn Guzmán, Xavier Ramis, Xavier Fernández-Francos, Angels Serra Increase in the glass transition temperature of thermosets obtained by DGEBA/thiol click reactions. European Polymer Federation Congress 2015, Dresden (Alemania). Póster.

Alberto Belmonte, **Dailyn Guzmán**, Xavier Fernández-Francos, Silvia De La Flor. Thiol-epoxy thermosets with enhanced shape-memory performance. European Polymer Federation Congress 2015, Dresden (Alemania). Oral.

Angels Serra, Xavier Ramis, Cristina Acebo, **Dailyn Guzmán**, Alberto Belmonte, Xavier Fernández-Francos, Silvia De la Flor. Nuevos termoestables obtenidos mediante procesos duales basados en reacciones tipo "click" con tioles. XIV Reunión del Grupo Especializado de Polímeros. Real Sociedad Española de Física y Química, Burgos (España) 2016. Oral.

Xavier Fernández Francos, Ali Osman Konuray, **Dailyn Guzmán**, Alberto Belmonte, Silvia De La Flor, Angels Serra, Xavier Ramis. Sequential dual-curing processes based on thiol-click reactions. MACRO 2016. 46th World Polymer Congress, Istanbul (Turquía). Oral.

Dailyn Guzmán, Blai Mateu, Xavier Fernández-Francos, Xavier Ramis, Angels Serra. New thermosets from cycloaliphatic epoxy resin by thiol-epoxy click reaction. IXth ECNP International Conference on Nanostructured Polymers and Nanocomposites. Roma (Italia). 2016. Póster.

Dailyn Guzmán, Xavier Ramis, Xavier Fernández-Francos, Angels Serra. New fully biobased materials from eugenol derivatives obtained by thiol-epoxy click reaction. APME 2017 Advanced Polymers via Macromolecular Engineering. Ghent (Belgium), 2017. Póster.

Dailyn Guzmán, Xavier Ramis, Xavier Fernández-Francos, Silvia De la Flor, Angels Serra. New bio-based materials obtained by thiol-ene/thiol-epoxy dual curing click procedures from eugenol derivates. European Polymer Federation Congress 2017, Lyon (Francia). Póster.

UNIVERSITAT ROVIRA I VIRGILI
NUEVOS PROCESOS DE CURADO CLICK CON TIOLES Y SU APLICACIÓN A LA PREPARACIÓN DE MATERIALES BASADOS EN EUGENOL
Dailyn Guzmán Meneses